

ATTACHMENT 2: SEISMIC HAZARD CHARACTERIZATION AND GROUND MOTION ANALYSES



**NTP 6 Seismic Studies
Technical Memorandum No. 4
v0**

**Seismic Hazard Characterization and Ground Motion Analyses
for the Susitna-Watana Dam Site Area**

AEA11-022



Prepared for:

Alaska Energy Authority
813 West Northern Lights Blvd.
Anchorage, AK 99503

Prepared by:

Fugro Consultants, Inc. for MWH
1777 Botelho Drive, Suite 262
Walnut Creek, CA 94596

February 24, 2012

The following individuals have been directly responsible for the preparation, review and approval of this Technical Memorandum.

Fugro Consultants, Inc.

Prepared by: Justin Pearce, Dean Ostenaa, Roland LaForge
Seth Dee, Jason Altekruise

QC Review by: Keith Kelson

Approved by:


Justin Pearce, Project Manager
P.G. 7752 (CA); C.E.G. 2421 (CA)

MWH:

Technical Reviewers: Norman Abrahamson, Consultant; Peter Dickson and
Michael Bruen, MWH; Rich Koehler, ADGGS

Approved by:


Michael Bruen, Design Manager

Approved by:


Brian Sadden, Project Manager

Disclaimer

This document was prepared for the exclusive use of AEA and MWH as part of the engineering studies for the Susitna-Watana Hydroelectric Project, FERC Project No. 14241, and contains information from MWH which may be confidential or proprietary. Any unauthorized use of the information contained herein is strictly prohibited and MWH shall not be liable for any use outside the intended and approved purpose.

Table of Contents

| | |
|-----------------------------------------------------|-----------|
| 1.0 EXECUTIVE SUMMARY..... | 1 |
| 2.0 INTRODUCTION | 5 |
| 2.1 Scope of Work | 5 |
| 2.2 Regulatory Guidance | 6 |
| 2.3 Approach and Goals | 7 |
| 2.4 Previous Studies | 7 |
| 2.4.1 Woodward-Clyde (1980, 1982) | 8 |
| 3.0 GEOLOGIC AND SEISMOTECTONIC SETTING..... | 12 |
| 3.1 Tectonics and Regional Stratigraphy | 12 |
| 3.2 Significant Historical Earthquakes..... | 16 |
| 3.2.1 2002 Denali fault earthquake | 17 |
| 3.2.2 1964 Great Alaskan earthquake..... | 17 |
| 3.2.3 1912 Delta River earthquake..... | 18 |
| 3.3 Quaternary Geology..... | 18 |
| 3.3.1 Previous work..... | 19 |
| 3.3.2 Quaternary geologic setting | 20 |
| 3.3.3 Quaternary geology in the site vicinity..... | 21 |
| 3.3.4 Relevance to seismic hazard evaluation | 23 |
| 3.3.5 Surficial geology at the dam site area | 23 |
| 3.4 Dam Site Area Geology | 24 |
| 3.5 Site Bedrock Velocity | 25 |
| 4.0 SEISMIC SOURCE CHARACTERIZATION..... | 27 |
| 4.1 Subduction Related Sources..... | 27 |
| 4.1.1 Plate interface | 27 |
| 4.1.2 Intraslab | 28 |
| 4.2 Quaternary Crustal Faults..... | 28 |
| 4.2.1 Denali fault | 31 |
| 4.2.2 Castle Mountain fault | 33 |
| 4.2.3 Pass Creek – Dutch Creek fault..... | 34 |
| 4.2.4 East Boulder Creek fault | 34 |
| 4.2.5 Matanuska Glacier fault | 35 |

| | | |
|------------|---------------------------------------------------------------------|-----------|
| 4.2.6 | Sonona Creek fault | 35 |
| 4.3 | Zones of Distributed Deformation | 35 |
| 4.3.1 | Northern foothills fold and thrust belt zone | 35 |
| 4.3.2 | Southern Denali faults | 36 |
| 4.4 | Talkeetna Block Structures | 38 |
| 4.4.1 | Talkeetna thrust fault / Talkeetna suture | 38 |
| 4.4.2 | Susitna lineament..... | 39 |
| 4.4.3 | Shorter structures proximal to the dam site..... | 40 |
| 4.5 | Crustal Seismicity | 41 |
| 4.5.1 | Earthquake catalog | 41 |
| 4.5.2 | Stress data | 42 |
| 4.5.3 | Crustal source zones | 42 |
| 4.6 | Earthquake Recurrence from Seismicity | 43 |
| 5.0 | PROBABILISTIC SEISMIC HAZARD ANALYSIS METHODS AND INPUTS ... | 44 |
| 5.1 | PSHA Code and Methodology | 44 |
| 5.2 | GMPEs | 44 |
| 5.3 | Sensitivity Evaluations | 45 |
| 5.3.1 | Time dependence | 46 |
| 5.3.2 | Relative contributions of sources and distance | 46 |
| 5.4 | PSHA Inputs | 47 |
| 5.4.1 | Subduction related sources..... | 47 |
| 5.4.2 | Interslab sources..... | 48 |
| 5.4.3 | Crustal faults | 48 |
| 6.0 | PSHA RESULTS..... | 54 |
| 6.1 | Hazard Curves | 54 |
| 6.2 | UHS | 54 |
| 6.3 | Deaggregations..... | 54 |
| 7.0 | CONDITIONAL MEAN SPECTRA..... | 57 |
| 7.1 | Methodology | 57 |
| 7.2 | CMS Results..... | 61 |
| 8.0 | DETERMINISTIC EVALUATIONS..... | 62 |
| 8.1 | Selection and Evaluation of Critical Sources..... | 62 |
| 8.2 | Deterministic Ground Motion Estimates..... | 66 |
| 8.3 | Comparison to Previous Studies..... | 67 |
| 9.0 | INITIAL SURFACE FAULTING AND GEOHAZARD IDENTIFICATION | 71 |

| | | |
|-------------|---------------------------------------------------------|-----------|
| 9.1 | Watana Lineament..... | 71 |
| 9.2 | Northwest-striking Structures in the Site Vicinity..... | 72 |
| 9.3 | The Talkeetna Thrust Fault / Talkeetna Suture Zone..... | 72 |
| 9.4 | Other Potential Seismic Hazards | 74 |
| 10.0 | SUMMARY | 76 |
| 11.0 | REFERENCES..... | 78 |

List of Tables

| | |
|-----------------------------------------------------------------------------------------------|----|
| Table 1. Summary of Site Bedrock Seismic Velocity Data | 26 |
| Table 2A. Fault Characterization | 30 |
| Table 2B. Northern Foothills Fold and Thrust Belt (NFFTB) Fault Data | 31 |
| Table 3. Ground Motion Prediction Equations Used in PSHA | 45 |
| Table 4. Site Region Faults Excluded from the PSHA Source Model | 50 |
| Table 5. Geometric Fault Parameters for Susitna Source Model, as Modeled for PSHA | 52 |
| Table 6. Fault slip rate and magnitude parameters, as modeled for PSHA | 53 |
| Table 7. Areal Zone Discrete Depth Distributions | 53 |
| Table 8. Total Hazard, Mean Probabilistic Acceleration Amplitudes (g) | 55 |
| Table 10. Megathrust - Deaggregation Results for BCH11T | 59 |
| Table 11. Megathrust - Deaggregation Results for ZH06T | 59 |
| Table 12. Intraslab- Deaggregation Results for AB03Ib | 60 |
| Table 13. Intraslab - Deaggregation Results for BCH11I | 60 |
| Table 14. Intraslab - Deaggregation Results for ZH06I | 61 |
| Table 15. Deterministic Hazard Input Parameters | 64 |
| Table 16. Crustal Seismicity (10,000 yr) Period-Dependent Deaggregation Results Summary | 64 |
| Table 17. Deaggregation Results, Crustal Seismicity (10,000 yr) | 65 |
| Table 18. Crustal Seismicity (10,000 yr) Single-Earthquake Deterministic Parameters | 65 |
| Table 19. Deterministic Result Comparison between Woodward-Clyde (1982) and this study | 69 |
| Table 20. Comparison of WCC (1982) and FCL (this study) hazard results | 70 |

List of Figures

- Figure 1. Major Physiographic Provinces
- Figure 2. Tectonic Overview of Central Interior Alaska
- Figure 3. Site Region Faults
- Figure 4. Tectonostratigraphic Terrane Map of the Talkeetna Block
- Figure 5. Rupture Areas for Historical Alaskan Subduction Zone Earthquakes
- Figure 6. Denali Fault Characterization
- Figure 7. Northern Foothills Fold and Thrust Belt
- Figure 8. Castle Mountain Fault
- Figure 9. Generalized Cross Section of Quaternary Deposits and Surfaces
- Figure 10. Site Vicinity Quaternary Geology
- Figure 11. Site Geology
- Figure 12. Watana Dam Site Top of Bedrock and Surficial Geologic Map
- Figure 13a. Site Region Geology
- Figure 13b. Site Region Geology Legend
- Figure 14. Map and Cross Section of Subduction-Zone Earthquakes
- Figure 15. Subduction Interface Model
- Figure 16. USGS Intraslab Model, 31-50 Mi (50-80 Km)
- Figure 17. USGS Intraslab Model, 50-75 Mi (80-120 Km)
- Figure 18. Denali Fault Slip Rates
- Figure 19. Sonona Creek Fault Trace
- Figure 20. Sonona Creek Fault Scarp
- Figure 21. Site Vicinity Tectonic Features
- Figure 22. Simplified Geologic Map and Cross Section
- Figure 23. Unfiltered Earthquake Catalog
- Figure 24. Declustered Earthquake Catalog

- Figure 25. Stress Tensor Inversion Results from Crustal Earthquake Focal Mechanisms
- Figure 26. Stress Tensors Inversion Results for Individual Crustal Data Volumes in South Central Alaska
- Figure 27. Areal Zone Latitude Vs. Depth Earthquake Plots
- Figure 28. Areal Zone Seismicity Depth Histograms
- Figure 29. Final Recurrence Catalogs
- Figure 30. Magnitude Vs. Time Prior to 2011
- Figure 31. Maximum Likelihood Recurrence Curves for SAB Areal Zones
- Figure 32. Maximum Likelihood Recurrence Curves for NFFTB Areal Zones
- Figure 33. Crustal Fault Model
- Figure 34. Hazard Curves for Peak Horizontal Acceleration
- Figure 35. Hazard Curves for 0.5-Second Spectral Acceleration
- Figure 36. Hazard Curves for 1.0-Second Spectral Acceleration
- Figure 37. Hazard Curves for 3.0-Second Spectral Acceleration
- Figure 38. Mean Uniform Hazard Spectra, Total Hazard
- Figure 39. Relative Contributions, Peak Horizontal Acceleration
- Figure 40. Relative Contributions, 0.5-Second Spectral Acceleration
- Figure 41. Relative Contributions, 1.0-Second Spectral Acceleration
- Figure 42. Relative Contributions, 3.0-Second Spectral Acceleration
- Figure 43. Deaggregation for the Megathrust, Peak Horizontal Acceleration, 2500-Year Return Period
- Figure 44. Deaggregation for the Megathrust, 1.0-Second Spectral Acceleration, 10,000-Year Return Period
- Figure 45. Deaggregation for the Intraslab, 0.5-Second Spectral Acceleration, 2500-Year Return Period
- Figure 46. Deaggregation for the Intraslab, 3.0-Second Spectral Acceleration, 10,000-Year Return Period
- Figure 47. UHS and CMS, Megathrust, 10,000-Year Return Period
-

Figure 48. UHS and CMS, Intraslab, 10,000-Year Return Period

Figure 49. UHS and Extended CMS, Megathrust, 10,000-Year Return Period, Alternative 1

Figure 50. UHS and Extended CMS, Megathrust, 10,000-Year Return Period, Alternative 2

Figure 51. UHS and Extended CMS, Intraslab, 10,000-Year Return Period, Alternative 1

Figure 52. UHS And Extended CMS, Intraslab, 10,000-Year Return Period, Alternative 2

Figure 53. Intraslab Deterministic Hazard Compared to the Total Hazard UHS

Figure 54. Megathrust Deterministic Hazard Compared to the Total Hazard UHS

Figure 55. Denali Fault Deterministic Hazard Compared to the Total Hazard UHS

Figure 56. Castle Mountain Fault Deterministic Hazard Compared to the Total Hazard UHS

Figure 57. Fog Lake Graben Deterministic Hazard Compared to the Total Hazard UHS

Figure 58. Southern Alaska Block Central Period-Dependent Deterministic Hazard Compared to the Total Hazard UHS

Figure 59. Southern Alaska Block Central Single-Earthquake Deterministic Hazard Compared to the Total Hazard UHS

List of Appendices

- APPENDIX A. TIME-DEPENDENT CALCULATIONS
- APPENDIX B. DEAGGREGATION STACK PLOTS
- APPENDIX C. CONDITIONAL MEAN SPECTRA RESULTS
- APPENDIX D. MERCALLI EARTHQUAKE INTENSITY SCALE

Explanation of Abbreviations

| | |
|-------|------------------------------------------|
| AEA | Alaska Energy Authority |
| AEIC | Alaska Earthquake Information Center |
| ASZ | Alaska subduction zone |
| BPT | Brownian passage time |
| CMS | Conditional mean spectra |
| CRB | Copper River basin |
| FCL | Fugro Consultants, Inc. |
| FERC | Federal Energy Regulatory Commission |
| g | gravitational acceleration |
| GMPE | Ground motion prediction equation |
| GPS | Global positioning system |
| ka | Thousands of years ago (kiloannum) |
| M | Earthquake magnitude, moment scale |
| MCE | Maximum credible earthquake |
| Ms | Earthquake magnitude, surface-wave scale |
| MWH | MWH Americas, Inc. |
| NFFTB | Northern foothills fold and thrust belt |
| NGA | Next generation of attenuation equations |
| PHA | Peak horizontal acceleration |
| PSHA | Probabilistic seismic hazard analysis |
| RTS | Reservoir-triggered seismicity |
| SA | Spectral acceleration |
| SAB | Southern Alaska block |

| | |
|------|--------------------------------------------------------------------|
| UHS | Uniform hazard spectra |
| USGS | United States Geological Survey |
| Vs30 | Average shear wave velocity in the top 30 meters of ground surface |
| WCC | Woodward-Clyde Consultants |

1.0 EXECUTIVE SUMMARY

The proposed Susitna-Watana Dam is a hydroelectric power development project being planned by the Alaska Energy Authority (AEA). This site-specific seismic hazard update and probabilistic seismic hazard analysis (PSHA) is developed to support MWH Americas (MWH) analysis of conceptual dam design alternatives, selection of the preferred dam type, and preparation of the Pre-Application Document submittal to Federal Energy Regulatory Commission (FERC).

This report reviews the previous studies, develops an updated site-specific seismic source model, and presents initial ground motion parameters (based on FERC guidelines). As part of the hazard update, a new seismic source characterization model of the dam region and site was constructed. Most recent ground motion prediction equations (GMPEs) including next generation attenuation (NGA) relationships for shallow crustal sources, and a recently developed GMPE for the Cascadia subduction zone, are used in the probabilistic and deterministic seismic hazard analysis for the Susitna-Watana Dam.

Site specific seismic hazard studies for the dam site were undertaken previously by Woodward-Clyde Consultants (WCC, 1980, 1982). This technical memorandum is based on review of these previous studies, syntheses of existing geologic maps and reports, field geotechnical investigations, as well as new regional geologic and seismologic information including data developed from recent, large earthquakes that have occurred since the early 1980s.

Since the previous seismic hazard study (WCC, 1982), new geologic and seismic hazard information has been developed from field work and research, observations and investigations of large earthquake events, and development of new numerical relationships, most recently for subduction zone earthquakes. These include Quaternary geologic mapping (Williams and Galloway, 1986), new stratigraphic models based on geologic map data (Carter et al., 1989); regional fault activity mapping by Plafker et al. (1994), the occurrence of the 2002 Denali earthquake, recent investigations by Alaska Geologic Survey (e.g., Hauessler, 2008), and the 2010 Chile and 2011 Japan subduction earthquakes. Some newly developing information, such as the new Alaska Quaternary fault and fold database (Koehler et al., 2011a), were not fully available at the time of this report.

The regulatory process for seismic hazard evaluation defined by FERC specifies that both probabilistic and deterministic evaluations be conducted. In accordance with these

requirements, this seismic hazard assessment includes: an updated seismic source model (Section 4); updated probabilistic seismic hazard analysis (Sections 5 and 6); Conditional Mean Spectrum analysis (Section 7); deterministic seismic hazard analysis informed by PSHA (Section 8); and an initial assessment of potential surface fault rupture hazards and identification of other potential seismic hazards (Section 9).

An updated seismicity catalog was developed from data available from the U.S. Geological Survey (USGS) and Alaska Earthquake Information Center (AEIC). These data include nearly three decades of additional seismicity, and following a declustering procedure, are the basis for the earthquake recurrence analysis.

The updated seismic source model includes structural elements that are relatively consistent with previous studies, such as the Denali fault, Castle Mountain fault, subduction-related sources, and “background” sources. New data and observations from tectonic, geologic, paleoseismic, and seismologic studies, as well as data from recent large earthquakes, are incorporated into the new source model. Based on these data, the new seismic source model also considers the potential implications of newly recognized zones of distributed tectonic deformation within the region, potentially active structures within the Talkeetna block, time-dependent scenarios for the subduction interface to consider the effects of the Great Alaskan 1964 earthquake, and time-dependent scenarios for the Denali fault based on the 2002 earthquake.

A probabilistic seismic hazard analysis (PSHA) was completed using an initial seismic source model that includes a limited number of weighted scenarios to capture uncertainty in the source characterization for elements such as slip rates, and time-dependent behavior for well-studied faults. Other elements of the source model, many of which have limited available data (such as the Fog Lake graben source), are included with preliminary source characterizations that may be conservative, as sensitivity tests to gauge impacts on the computed total hazard. Uncertainty in the selection of appropriate attenuation parameters is considered through use of multiple GMPE’s for each class of seismic source in the PSHA model.

The results of the PSHA are portrayed as hazard curves showing the total model results and contributions of each seismic source. Uniform hazard spectra (UHS) are computed for the 100, 250, 1,000, 2,500, 5,000, and 10,000 year return periods. Deaggregation of total UHS was performed for peak horizontal acceleration (PHA), 0.5 second, 1.0 second, and 3.0 second periods. The deaggregation results indicate that the primary seismic source contributors are the subduction-related plate interface source (megathrust), and the intraslab source down dip of the megathrust. These sources

dominate the ground motions for the PHA and 0.5-, 1.0-, and 3.0-second spectral accelerations (SA), with the subduction interface source becoming increasingly dominant at longer periods. Although assigned a conservative probability of activity of 1.0, the Fog Lake graben source does not contribute significantly in the PSHA, because of its relatively low slip rate.

Conditional mean spectra (CMS) were developed from the UHS for the above mentioned spectral response periods, for return periods of 2,500, 5,000, and 10,000 years. These were modified so that the envelope of the ensemble spectral response periods, for a given return period, matched the UHS.

Deterministic ground motion estimates were developed for six critical seismic sources based on maximum magnitude estimates, site to source distances, and the weighted GMPE's used for each source in the PSHA analyses. The deterministic sources are the subduction interface, subduction intraslab, Denali fault, Castle Mountain fault, Fog Lake graben faults, and a 10,000-year return period earthquake for the background source derived from deaggregation of the PSHA results. The 84th percentile deterministic results are compared to total UHS, except for the Fog Lake graben source, in which the median values are compared following FERC guidance for low slip rate faults.

The seismic source characterization and ground motion results from this study include most elements from the prior Woodward-Clyde (1980, 1982) studies but are not directly comparable due to many changes in practice and methodologies. The major fault sources represented in the prior Woodward-Clyde studies are included with updated seismic source characterizations. The detection level earthquake (Woodward-Clyde, 1982) concept is superseded by the use of probabilistic analyses of the background seismicity in the site and region. In addition, this present study includes seismic sources (e.g., subduction intraslab source) not characterized in the prior Woodward-Clyde studies. Notably, conventions for use of earthquake magnitude scales have changed, as have data and practice for use of ground motion predictive equations. There are general similarities between results of this study with the prior results, but also significant differences due to differing seismic source characterizations, methodologies, and ground motion attenuation parameters.

Mean PHA from the deterministic fault sources included in this study are generally lower than values for the same deterministic fault sources as listed in Woodward-Clyde (1982). This difference is mostly a result of the different GMPE's used in the current study. However, the current study includes an additional deterministic source, the subduction intraslab source that was not included in Woodward-Clyde (1982), but

results in the largest deterministic mean PHA among the present study deterministic sources, and is slightly larger than any deterministic values presented in the previous Woodward-Clyde reports.

The probabilistic methodologies used in the previous Woodward-Clyde studies are not described in detail, so it is not possible to identify specific reasons for differences in the results. In general, in the present study, mean PHA for return periods less than 2500 years is slightly smaller than estimates from Woodward-Clyde. For a return period of 10,000 years, the mean PHA from the present study is significantly higher than the previous Woodward-Clyde estimates.

A review of the previous surface fault rupture hazard assessments indicates lineaments that are very near to, or project beneath, the proposed dam facilities or toward the anticipated reservoir. Specifically, these include the Watana lineament, the northwest-striking shear zones near the Watana site area, i.e., the “Fins” feature of earlier studies, and the Talkeetna thrust fault. The previous Woodward-Clyde studies concluded that these lineament features were either: (a) not a tectonic fault, or (b) not a “recently active” fault, but presented limited direct geologic evidence demonstrating fault inactivity.

This scope of this seismic hazard characterization study excluded an evaluation of fault activity, assessment of the potential for generating seismically-induced seiche (a large wave) within the reservoir, nor an assessment of potential for reservoir-triggered seismicity. These potential seismic hazards are planned be analyzed as part of future studies.

2.0 INTRODUCTION

The proposed Susitna-Watana Dam is a hydroelectric power development project planned to be constructed on the upper Susitna River under the auspices of the Alaska Energy Authority (AEA). The proposed dam would be constructed near about River Mile 184 on the Susitna River, north of the Talkeetna Mountains near the Fog Lake area (Figure 1). Current concepts envision a dam approximately 700 feet high, impounding a reservoir with a maximum water surface elevation at about 2000 feet. At this elevation, the dam would impound a reservoir of approximately 8,900 acre-feet. This configuration would allow for development of a powerhouse with installed hydroelectric capacity of about 600 MW.

MWH Americas (MWH) is the prime contractor providing engineering and geotechnical services to AEA for the project development and submittal of licensing documents to the Federal Energy Regulatory Commission (FERC).

Under subcontract to MWH, Fugro Consultants, Inc. (FCL) prepared this seismic hazard characterization and ground motion analyses in support of MWH's development of conceptual dam design alternatives, selection of the preferred dam type, and preparation of the Pre-Application Document.

2.1 Scope of Work

The scope of work for this investigation is defined under Task Order T1011562-96192-OM dated June 29, 2011 (NTP-6), and amendments thereafter. In general, the scope of services under this task order is to complete an updated seismic hazard characterization and preliminary ground motion analysis for the proposed Susitna-Watana Dam. Specific technical activities within the scope of work include literature review and research, compilation of an updated seismicity catalog, identification and characterization of the seismic sources that may influence the project, initial evaluation of surface faulting and other geohazards, and estimation of the expected ground motions at the dam site based on probabilistic seismic hazard analysis (PSHA) and deterministic analyses. Other activities specified in the task order include coordination and documentation of the study results in this technical memorandum.

At the time of this report, LiDAR-based topographic data were not available for the study area and, therefore, an update to the previous lineament analysis (WCC, 1980; 1982) was not included as part of this scope. By extension, detailed assessment of fault activity, including geologic mapping or trenching, was excluded from this current scope

of work. Development of time histories for the critical seismic sources, analysis of potential reservoir-triggered seismicity, and assessment of potential seismically-induced seiche in the reservoir also were not included as part of this scope. Future studies are planned during licensing and design to address fault mapping and fault activity issues, as well as these other potential seismic hazards.

2.2 Regulatory Guidance

The proposed project will be licensed by FERC and evaluated under the FERC Engineering Guidelines for the Evaluation of Hydropower Projects (FERC, 2011). Guidance for the evaluation of seismic hazards is provided under a Draft version of Chapter 13, Evaluation of Earthquake Ground Motions (Idriss and Archuleta, 2007). These guidelines were put forward for review and further development by FERC, but have been used for several years on an interim basis.

The Chapter 13 draft guidelines are intended to provide FERC with a basis for evaluating the adequacy of the seismic hazard evaluation of the site, which is ultimately the basis for establishment of seismic design criteria for the project. The guidelines identify required geologic and seismologic studies including:

- Identification of faults and seismic sources in the region that may be significant to the dam site. This includes characterization of the degree of activity, style of faulting, maximum magnitudes, and recurrence information for each seismic source.
- Development of maps and tables that depict the spatial and geometric relations of the faults and seismic source zones to the site along with specific distance parameters needed to evaluate ground motions from each source.
- Collection of historical and instrumental seismicity data for the region, including information on the maximum and minimum depth of events.

The draft FERC guidelines describe requirements for both deterministic and probabilistic development of ground motions for rock conditions at the site. Under both approaches, use of the most recent and multiple attenuation or Ground Motion Prediction Equations (GMPEs) is recommended. Use of site-specific results are recommended for analyses and design; USGS website (<http://earthquake.usgs.gov/hazmaps/>) values are to be used only for comparison.

2.3 Approach and Goals

The goal of the seismic hazard evaluation is to provide a technical basis for dam alternatives analysis by using recent historical and instrumental seismicity data to raise the level of understanding to the current state-of-the-practice by using new methods that result in a defensible, up-to-date seismic hazard characterization for the dam site.

The overall approach was to update and re-evaluate the existing site seismic hazard and ground motion studies based on a new seismotectonic model that identifies and characterizes seismic sources of potential significance to the project. This model synthesizes new and available data for the Alaskan subduction zone, the Denali fault, the Castle Mountain fault, and other potential seismogenic sources in the site region. The seismic source characterization provides updated delineation of possible extent and locations for seismic sources, along with estimates of maximum earthquake magnitude, fault type, style of faulting, geometry and seismogenic depth, and recurrence. For this evaluation, the seismic source characterization will identify uncertainties and data gaps that may contribute to uncertainties or may require further evaluations for design.

2.4 Previous Studies

This section identifies the relevant inventory of Susitna-specific seismic hazard investigations and regional tectonic studies known to this seismic hazard update and assessment. These existing data and reports are the basis for this office-based seismic hazard update. Previous seismic hazard studies used both deterministic and probabilistic approaches to estimate ground motion hazard (WCC, 1980, 1982). The site investigation prepared by WCC (1980, 1982) included micro-seismicity network installation and monitoring, surficial geologic mapping, lineament analysis, and paleoseismic trenching to assess fault activity and potential surface fault rupture in the dam site vicinity. Review of the WCC ground motion analysis was completed by R&M Consultants (R&M, 2009), which used U.S. Geological Survey (USGS) regional probabilistic seismic hazard maps to estimate peak horizontal ground motions near the dam site, and compare to the WCC results. To date, the WCC (1980, 1982) reports are the most detailed investigation of seismic hazards for the site that included field geologic data collection, lineament analysis, Quaternary geologic mapping, and paleoseismic trenching.

In addition to the WCC (1980, 1982) analyses, two other previous studies provide relevant information to this project. First, the USGS regional hazard maps (Wesson et

al., 2007) prepared for Alaska show ground motion values (peak ground acceleration and spectral amplitude at periods of 0.2, 0.3 and 1.0 seconds) at probabilities of exceedance of 2 percent and 10 percent in 50 years, and ground conditions of NEHRP B/C ($V_{s30} = 2,493$ ft/s [760 m/s]). Second, a probabilistic seismic hazard analysis for the Port of Anchorage was prepared by URS (2008) to estimate the levels of ground motions at the site in Anchorage (about 120 miles southwest of the dam site) at probabilities of exceedance of 50 percent, 10 percent, and 2 percent in 50 years. Available geologic and seismologic data were used to evaluate and characterize potential seismic sources, the likelihood of earthquakes of various magnitudes occurring on those sources, and the likelihood of the earthquakes producing ground motions over a specified level. A deterministic analysis was also performed to compare with the PSHA results and to generate target spectra for development of time histories.

2.4.1 Woodward-Clyde (1980, 1982)

WCC (1980, 1982) summarized a multi-year, multi-task study evaluating the seismic hazards and development of seismic design parameters for the Susitna Hydroelectric Project. The technical evaluation considered:

- Evaluation of geologic framework and tectonic setting
- Geologic evaluation of faults and lineaments, and recency of fault activity
- Evaluation of historical seismicity
- Detection level earthquake and estimating the maximum credible earthquake
- Estimation of ground motion parameters
- Assessment of potential for reservoir-triggered seismicity

2.4.1.1 Geologic evaluation of faults and lineaments, and recency of fault activity

To assess the presence or absence of potentially significant faults, WCC (1980) defined a framework and approach to identify features of potential importance (e.g., structural lineaments, topographic lineaments, alignment of geomorphic features) that may represent near-surface expression of faulting. The approach used office-based techniques to identify potential candidate features. Criteria based on length of feature

and distance of feature from the site (>62 mi [100 km]) were used to screen those candidate features. Thirteen significant features were identified by WCC (1980) for more detailed evaluation, including field geologic investigations.

Subsequently, WCC (1982) completed additional investigations operating under the definition that faults with “recent displacement” would be considered capable of generating earthquakes that may cause ground motions of potential significance to the project. WCC (1980) defined faults with surface rupture in the past 100,000 years have “recent displacement” and should be considered in seismic design. Faults with no evidence of “recent displacement” were not considered further as seismic sources, although direct geologic evidence demonstrating inactivity was lacking.

Based on those data and analysis, WCC (1980, 1982), concluded there was no evidence of “recent” activity on these thirteen significant features. None of the thirteen features were considered as potential seismic sources, and none were considered capable of surface fault rupture. Separately, the “detection level earthquake” was considered as an independent seismic source of potential significance to the project.

2.4.1.2 Detection level earthquake and estimating the maximum credible earthquake

A “detection level earthquake” was defined as the largest earthquake that might have occurred without leaving any detectable geologic evidence (e.g. surface geomorphic expression or a rupture scarp) (WCC, 1982). This event was considered a separate potential seismic source; a crustal earthquake of unknown fault location, but in proximity to the dam site. The goal was to assess what lower-bound earthquake magnitude could occur that may not necessarily be detected by geologic investigations. Inclusion of the detection level earthquake accounted for potential faults along which no geologic evidence of surface rupture was observed by the investigation. This concept is not used explicitly in the current study. Unknown locations or sources of future earthquakes are accounted for in the present study through the characterization of background zones of crustal seismicity.

The WCC (1982) evaluation included assessing the dimensions of surface faulting associated with worldwide earthquakes in similar tectonic environments, comparison to threshold of surface faulting for well-studied California earthquakes, and analyzing the potential degree of preservation of fault-related geomorphic features in the Talkeetna Terrane (generally corresponding to the Talkeetna block of this study, see Section 3.1). Based on this evaluation, the detection level earthquake, a crustal earthquake occurring

within the Talkeetna Terrane was defined. WCC (1982) study provided estimates of the maximum credible earthquake (MCE) with ground motions for selected seismic sources, based on the attenuation relationships existing at that time. The potential seismic sources identified by WCC (1980) are: the Castle Mountain fault, the Denali fault, Benioff zone interplate (megathrust) region, Benioff zone intraplate region (slab), and the “detection level” source (within the Talkeetna Terrane).

The MCE estimates for the two crustal faults were as follows: the Denali fault was estimated capable of a magnitude (Ms) 8 at 44 mi (70 km) distance; and the Castle Mountain fault was estimated capable of a magnitude (Ms) 7½ at 65 mi (105 km) distance.

For the two Benioff zone sources, the subduction interface (interplate) was estimated capable of magnitude (Ms) 8½ (Mw 9.2) at 40 mi (64 km) distance from the site and the intraplate zone was estimated capable of magnitude (Ms) 7½ at 31 mi (50 km) distance.

The detection level earthquake (or, regional background crustal source) was estimated to be a magnitude (Ms) 6 within 6 mi (10 km) from the site.

2.4.1.3 Estimation of ground motion parameters

Based on the potential seismic sources identified, WCC (1982) estimated ground motion parameters for design using deterministic and probabilistic methods. WCC (1982) list seven of GMPEs that were considered in the selection of attenuation relationships. While it is stated that one group of relations was selected for crustal earthquakes and another for subduction zone earthquakes, it is not stated which were used for each, nor what weighting, if any, was applied. Some are published and readily available, while some are contained in conference proceedings and difficult to obtain. However, all are for peak horizontal acceleration (PHA) only, as WCC (1980) applied spectral shapes tied to the PHA value. The results of the WCC (1982) deterministic estimates of ground motions and parameters were:

- Benioff zone (interplate) source produced 0.35 g acceleration for 45-second duration
- Denali fault produced 0.2 g acceleration for 35-second duration
- Detection level earthquake produced 0.5 g acceleration for 6-sec duration

The detection level earthquake yields very high accelerations because of the close source-to-site distance (6 mi [10 km]).

The results of the WCC (1982) probabilistic estimates of ground motions and parameters were:

- The 50% probability of exceedance in 100 years yielded 0.28 g
- 10% probability of exceedance in 100 years yielded 0.41 g
- 1% probability of exceedance in 100 years yielded 0.64 g

The Benioff zone interplate (megathrust) source dominated the probabilistic estimates.

2.4.1.4 Reservoir-triggered seismicity

The proposed Susitna-Watana reservoir will be very large (~8,900 acre-feet) and very deep (~650 feet). WCC (1982) assessed the potential effects of the proposed reservoir with respect to potential for generating reservoir-triggered seismicity (RTS). The assessment was based on a comparison to similar reservoirs worldwide. The estimated RTS magnitude was assumed to be limited by “natural” events independent of RTS. The probability of RTS was estimated to be 0.46. However, the RTS was considered to be of limited impact due in large part to the concluded absence of faults with recent displacement within the hydrologic regime of the reservoir (WCC, 1982).

3.0 GEOLOGIC AND SEISMOTECTONIC SETTING

South-central Alaska experiences rapid rates of tectonic deformation driven by the obliquely convergent northwestward motion of the Pacific Plate relative to the North American Plate. In southern and southeastern Alaska, the convergent and oblique relative plate motion is accommodated by subduction of the Pacific Plate at the Alaska-Aleutian megathrust and dextral (right-lateral) transform faulting along the Queen Charlotte and Fairweather fault zones. In the interior of south-central Alaska, transpressional deformation primarily is accommodated by dextral slip along the Denali and Castle Mountain faults, as well as by horizontal crustal shortening to the north of the Denali fault (Figure 2).

3.1 Tectonics and Regional Stratigraphy

The Susitna-Watana Dam site is located within a distinct crustal and geologic domain referred to in this report as the Talkeetna block. The Talkeetna block is bounded by the Denali fault system to the north, the Castle Mountain fault to the south, the Wrangell Mountains to the east and the northern Aleutians and Tordrillo Mountains volcanic ranges to the west (Figure 1). The Talkeetna block encompasses the north-central portion of the Southern Alaska block (SAB) of Haeussler (2008) (Figure 2). Major strain release occurs on northern and southern block boundaries (i.e., Denali and Castle Mountains bounding faults), but mechanisms of strain accommodation are less well defined to the east and west. There is a relative absence of large historical earthquakes within the Talkeetna block (Section 4.5), as well as a lack of mapped faults with documented Quaternary displacement within the Talkeetna block (Figure 3).

The Talkeetna block is comprised of three principal physiographic provinces: the Susitna basin, Talkeetna Mountains, and the Copper River basin (Figure 1). The Susitna-Watana dam site is located within the Talkeetna Mountains province. The Copper River basin is an intermontane basin surrounded by the Alaska, Talkeetna, Chugach and Wrangell mountains. The basin is characterized by flat lying to hummocky topography and is overlain by extensive glacial, glacio-fluvial, and glacial-lacustrine deposits. The Susitna basin is a north south-trending basin and is the principal depocenter for alluvium transported by numerous major river systems which originate in the surrounding mountains. Talkeetna Mountains are an elevated block which lies between the Copper River and Susitna basins, with glaciated peaks between 6560 feet and 9840 feet (2000 and 3000 m) in elevation. The Susitna River heads in the ranges north of the Copper River basin and flows westward through the northern Copper River basin and through the Talkeetna Range following a deeply incised

canyon. Downstream, sediments from the river contribute to alluvial deposition in the Susitna basin.

The Talkeetna Mountains consist of an assemblage of northeast trending tectonostratigraphic terranes including the North Talkeetna Flysch basin, the Wrangellia Terrane, and the Peninsular Terrane (Glen et al., 2007b). The Wrangellia and Peninsular Terranes are comprised of largely late-Paleozoic to early Mesozoic metavolcanic and metasedimentary rocks that originated well south of their current (~30° latitude) position, and likely were sutured together in the Late Jurassic (Csejtey et al., 1982). The terranes were accreted onto North America in the mid- to late-Cretaceous and translated northward to approximately their current location via strike-slip faults on the continental margin (i.e. Fairweather fault) (Ridgeway et al., 2002). The North Talkeetna Flysch basin is part of the Kahiltna Assemblage, which consists of strata deposited in an oceanic basin between the Wrangellia Terrane and North America prior to and during the early stages of accretion. The North Talkeetna flysch basin consists of sediments shed to the northwest from the Wrangellia Terrane (Glen et al., 2007a). Following deposition, the basin sediments were obducted on to the continent during Wrangellia emplacement. The northeast striking Talkeetna thrust fault/Talkeetna suture zone is the principal terrane-bounding structure in the region, separating the North Talkeetna flysch basin in the northwest from the Wrangellia Terrane in the southeast (Figure 3 and 4). In addition to the three principal tectonostratigraphic terranes, numerous narrow, fault-bounded terranes are tectonically intermixed within the Kahiltna Assemblage between the Denali fault and the Talkeetna suture zone (i.e. Chulitna Terrane) (Nokleberg et al., 1994). Late Cretaceous through Tertiary volcanic and hypabyssal intrusions are found throughout the Talkeetna Mountains, and often intrude or overlie the Cretaceous accretionary structures.

Early tectonic studies of the Talkeetna Mountains described the Talkeetna thrust fault as a southeast-dipping thrust that accommodated the middle to late Cretaceous emplacement of the Wrangellia Terrane (Csejtey et al., 1982; Nokleberg et al., 1994). The thrust trace is recognized by the juxtaposition of the Triassic and Permian metavolcanic and metasedimentary Wrangellia Terrane rocks on the south and Late Jurassic through Cretaceous sedimentary rocks of the Kahiltna Assemblage on the north. The approximate fault trace follows a broad topographic lineament striking northeast across the Talkeetna Mountains (Figure 3). On older maps, the southwestern margin of the fault is mapped as overlain or terminated by Tertiary intrusive and volcanic rocks (Csejtey et al., 1978); to the northeast, the fault is interpreted to terminate or merge against the younger, north-dipping Broxson Gulch fault (Nokleberg et al., 1994).

Mapping by O'Neill et al. (2003a) along the northeastern reaches of the Talkeetna fault found little evidence for penetrative deformation adjacent to the fault and stratigraphic relationships, which suggest limited displacement along the fault. Based on these observations, they concluded that major contractional displacement has not occurred along the Talkeetna thrust fault. O'Neill et al. (2003a) further propose that the principal suture zone is located to the northwest near Broad Pass where mini-terrane of uplifted Wrangellia Terrane basement rocks are exposed. They characterize the Talkeetna suture zone as a deep crustal structure bounding the northwestern edge of the Wrangellia Terrane, overlain by a wide zone (0.5-12 mi [1-20 km]) of Tertiary or younger faults. Glen et al. (2007b) use tectonic analysis of gravity and magnetic data to propose replacement of the term Talkeetna thrust fault with the Talkeetna suture zone. Glen et al. (2007b) and O'Neill et al. (2003b) propose that the surface fault structures may have been reactivated in the late Tertiary as a broad dextral shear zone associated with movement along the Denali fault. Geologic constraints on the most recent movements within the Talkeetna suture zone are further discussed in Section 4 and Section 9.

The Alaska-Aleutian subduction zone is one of the longest and most tectonically active plate boundaries in the world. It extends for nearly 2,485 mi (4,000 km) from south central Alaska to the Kamchatka peninsula, and has produced some of the world's largest earthquakes, such as the 1964 M 9.2 Good Friday (or, Great Alaskan) earthquake (Figure 5). The subduction zone has three tectonic regimes: continental subduction in the east, an island arc along the central Aleutian volcanic chain and oblique subduction and transform tectonics in the west (Nishenko and Jacob, 1990). The eastern continental subduction zone, in the vicinity of Prince William Sound, is significant in the evaluation of the seismic hazards at the Watana dam site. In this region, the Pacific Plate is converging with North American Plate at a rate of 54 mm/yr (2.1 in/yr) at a slightly oblique angle (DeMets and Dixon, 1999; Carver and Plafker, 2008). The subducting slab has a shallow, 10° or less, dip (Carver and Plafker, 2008) and a typical forearc basin. Transform motion along the eastern edge of the subducting slab is accommodated by the Queen Charlotte and Fairweather fault zones.

The transition from subduction to transform tectonics is complicated by the allochthonous Yakutat microplate which is colliding with southern Alaska along the eastern edge of the subducting slab (Figure 2). The collision of the Yakutat microplate is considered to have substantial influence on the deformation and counterclockwise rotation in the interior of south-central Alaska (Haeussler, 2008). GPS velocity measurements show that the microplate is moving northwest at ~50 mm/yr (2.0 in/yr), a velocity that is similar in magnitude to the subducting Pacific Plate. The similarity in motion vectors suggests substantial coupling between the two plates (Elliott et al., 2010). Block modeling by

Elliott et al. (2010) indicates that Yakutat is converging with southern Alaska at a rate of ~45 mm/yr (1.7 in/yr).

Dextral crustal stress in the region primarily is accommodated by the Denali fault to the north and the Castle Mountain fault to the south. The Denali fault predominantly shows right-lateral, strike-slip fault motion, and in map view has an arcuate shape (Figure 6). Along its eastern extent, the fault strikes northwest. The fault trace turns increasingly to a westerly to southwesterly strike toward its western extent.

The Denali fault defines the northern margin of the Southern Alaska block of Haeussler (2008) (Figure 2) and has been a major structural component of Alaska since it formed as a crustal suture during the Late Jurassic to early Cretaceous (Ridgeway et al., 2002). Offset of 56 Ma metamorphic and intrusive rocks suggests at least 249 mi (400 km) of total right lateral displacement along the fault (Nokleberg et al., 1985). Offset is further constrained in the Denali region where the 38 million year old Mt. Foraker pluton is displaced 24 mi (38 km) from the McGonagal Pluton (Reed and Lamphere, 1974). In 2002, the Denali fault produced a M 7.9 earthquake, the largest strike-slip earthquake to occur in North America in almost 150 years (Eberhart-Phillips et al., 2003). Detailed studies of offset glacial features along the fault following the 2002 earthquake have demonstrated a clear westward decrease in the Quaternary slip rate along the fault (Matmon et al., 2006; Meriaux et al., 2009) (Figure 6).

Along the north and south sides of the Denali fault are two zones of deformation. To the north of the fault is the Northern foothills fold and thrust belt (NFFTB), a zone of variably dipping, but generally north-vergent Quaternary thrust faults and folds that accommodates transpressional deformation along the north side of the Alaska Range (Figure 7). Surface structures likely sole with depth into a master detachment with a surface trace along the northern margin of the fold and thrust belt (Bemis et al., in press). The westward reduction in Denali fault slip rate (Figure 6) is considered to be largely the result of strain partitioning onto the NFFTB (Haeussler, 2008; Meriaux et al., 2009).

South of the Denali fault are several south-vergent thrust faults that splay off from the central section of the Denali fault (Figure 6). Most of these faults are recognized as Tertiary terrane-bounding features where Mesozoic or Paleozoic rocks are thrust over Tertiary sediments and volcanics (Haeussler, 2008). Rupture along the previously unmapped Susitna Glacier thrust fault during the 2002 Denali fault earthquake highlighted the potential for seismogenic activity in this area, in contrast to the relatively sparse mapping of Quaternary faults south of the Denali fault. This concept is well

expressed in the Neotectonic Map of Alaska fault explanatory note (Plafker et al., 1994; back panel):

The map represents an analysis of data from published or publically available unpublished material, supplemented by reconnaissance field investigations of most of the younger onshore faults. Additional faults undoubtedly exist but have not yet been recognized because of the reconnaissance nature of much of the geologic mapping or because they are concealed beneath unconsolidated deposits or water. Future geologic and seismologic investigations will undoubtedly identify many more faults and will provide evidence, requiring changes...for faults shown on this map.

The geometry of the NFFTB and the thrust faults south of the Denali fault form a positive flower structure within the Alaska Range (Haeussler, 2008). Positive flower structures are common in transpressional orogens where strain is partitioned between a master strike slip faults and thrust faults that dip towards, and sole into the strike slip fault at depth (Sylvester, 1988). Spatial distributions of aftershocks from the 2002 Denali fault earthquake are consistent with the flower structure hypothesis (Ratchkovski et al., 2004).

The Castle Mountain fault is a dextral oblique strike-slip fault whose western segment is defined by a 39-mi (62-km) long Holocene fault scarp; the eastern section primarily is recognized only in bedrock (Figure 8). Paleoseismic studies of the western section demonstrate four earthquakes on the fault in the past 2800 years, with a recurrence interval of approximately 700 years (Haeussler et al., 2002).

3.2 Significant Historical Earthquakes

The region within the 124-mi (200-km) radius of the Susitna-Watana dam site, is seismically active as indicated by the occurrence of earthquakes with a magnitude greater than or equal to M 5 (AEIC seismicity catalog). The greatest number of these are deep (> 25-mi (40-km) depth) events with magnitudes up to M 7.1, that likely are associated with the subducting Pacific Plate, and a smaller number of events to the southeast that likely are associated with tectonic under-plating of the Yakutat block. The remaining events are crustal earthquakes occurring at depths of about 19 mi (30 km) or less. The largest of those crustal earthquakes is the 2002 M 7.9 Denali fault earthquake (initiated on the Susitna Glacier fault), with an epicenter approximately 59 mi (95 km) from the dam site. Several of the $M \geq 5$ events are associated with the

Denali fault including: the M 6.7 foreshock of the 2002 earthquake (Nenana Mountain earthquake), several 2002-2003 aftershocks up to M 5.8, and six additional events up to M 6.4.

Events up to M 7.2 are located in the Northern foothills fold and thrust belt and the Minto Flats seismic zone. The Northern foothills fold and thrust belt includes the Kantishna seismic cluster, the Northern foothills thrust, and the Molybdenum Ridge fault (Figure 7). An M 5.7 event in 1984 is associated with the Castle Mountain fault (Lahr et al., 1986). Many events cannot be spatially correlated with a documented Quaternary fault, including an M 7.2 earthquake in 1912.

Seven historical earthquakes are documented within 31 mile (50 kilometers) of the site (AEIC catalog). Four of these earthquakes have depths between 30 to 60 mi (49 to 97 km), which places them within the subducting slab. The largest slab event within 31 mi (50 km) of the site has a magnitude of M 5.4. Three earthquakes are located at upper crustal depths (13-22 mi [21-36 km]), the largest of which has a magnitude of M 6.2. These three earthquakes occurred between 1929 and 1933, and spatially are not associated with any known Quaternary fault, though they may be inaccurately located, or have poor depth control, due to the lack of regional seismograph stations at that time.

3.2.1 2002 Denali fault earthquake

The M 7.9 2002 Denali fault earthquake is the largest onshore strike-slip earthquake in North America in the past 150 years (Eberhart-Phillips et al., 2003). The earthquake initiated on the previously unmapped Susitna Glacier thrust fault (Figure 6) with a 30-mi (48-km) surface rupture and up to 36 feet (11 m) of displacement (Crone et al., 2004). The earthquake then propagated eastward rupturing 140 mi (226 km) of the central Denali fault and 41 mi (66 km) of the Totschunda fault. Average slip along the Denali fault was approximately 16 feet (5 m), with a maximum slip of 29 feet (8.8 m) west of the junction with the Totschunda fault (Haeussler et al., 2004). The earthquake caused no fatalities and minimal damage to infrastructure, likely due to the sparse population density near the fault. The estimated intensity of the earthquake at the Watana Dam site was Modified Mercalli scale VI (USGS, 2003).

3.2.2 1964 Great Alaskan earthquake

The M 9.2, March 28, 1964 Great Alaskan earthquake had an epicenter directly south of the 124-mile (200-km) radius site region; however, the subsurface rupture area extends nearly beneath the site region (Figure 5). The isoseismal map of the event shows the

Watana Dam site experienced ground shaking with Modified Mercalli scale VII intensity (Stover and Coffman, 1993). The earthquake is the second largest recorded in the world since instrumental recordings began in the late 1800s (the one larger event was the 1960 M9.5 Chilean earthquake).

The 1964 earthquake ruptured approximately 500 mi (800 km) of the Aleutian megathrust with left-lateral reverse-slip motion, and produced approximately 66 feet (20 m) of maximum displacement (Christensen and Beck, 1994). The earthquake was felt over 700,000 square miles in Alaska and Canada (Hake and Cloud, 1966) with an intensity of MM VII estimated at the Watana Dam site (Stover and Coffman, 1993). Coseismic vertical displacements affected an area of about 200,000 square miles. Prince William Sound experienced up to 38 feet (11.5 meters) of uplift, and 7.5 feet (2.3 meters) of inland subsidence (relative to sea level) occurred (Plafker, 1969). Fifteen fatalities were attributed to the earthquake, and 113 fatalities from the ensuing tsunami. In Anchorage, the earthquake destroyed structures up to 6-stories high and triggered numerous destructive landslides.

3.2.3 1912 Delta River earthquake

A widely felt 1912 earthquake, commonly referred to as the Delta River earthquake, was relocated by Doser (2004) to a location within 6 miles (10 km) of the Denali fault, though with 95% error bounds of about 62 mi (100 km) in the east-west direction and 44 mi (70 km) north to south. Carver et al. (2004) interpreted healed tree damage as having resulted from surface deformation during the 1912 event. However, paleoseismic studies at several sites along the Denali fault do not show any evidence for a surface rupturing 1912 event (Schwartz et al., 2003; Plafker et al., 2006; Koehler et al., 2011b). Therefore, the event is considered as being unassociated with a particular known crustal fault.

3.3 Quaternary Geology

Quaternary geologic information is relevant to understanding the geomorphic processes, resultant surficial geologic deposits as well as relationships amongst deposits, both stratigraphically and chronologically. Quaternary stratigraphy and chronology are used to establish geologic datum for evaluating tectonic (fault) activity during and since the late Quaternary.

For this office-based seismic hazard update, assessing late Quaternary fault activity via existing data and literature helps provide a basis for including (or not including)

particular faults in the seismic source model, and helps screen for the potential of surface fault rupture hazard. Synthesis and evaluation of existing Quaternary geologic mapping and related scientific publications are therefore crucial data for this assessment.

3.3.1 Previous work

Quaternary geologic mapping has been completed for some of the Talkeetna Mountains region, as well as locally near the proposed Watana Dam site area. There is substantial variability in the scale, completeness, coverage, and level of detail across the existing geologic maps. The following paragraphs present a very brief summary of the available previous Quaternary studies and data relevant to the seismic hazard update.

In the 1970s the U.S. Geological Survey (USGS) developed a key geologic map of the Talkeetna Mountains (Csejtey et al., 1978). Among other features, this map depicts a trace of the Talkeetna fault, labeled and symbolized as a thrust fault, but lacks detailed mapping of Quaternary deposits. Several scales of maps and Quaternary geologic field investigations were completed near the dam site by consultants in the early 1980s (e.g., WCC, 1980; Appendix A in WCC, 1982,). Some detailed, but aerially limited, geologic mapping of surficial deposits (e.g. lacustrine clay) were preliminarily prepared for the proposed project (WCC, 1980), but were not finalized. There is reference to detailed mapping of deposits and moraines in WCC (Appendix A in 1982) but final maps were apparently not produced for, or included in, the final report. Project consultants completed detailed geomorphic mapping of terrain units based on air photo interpretation (Acres, 1980; Geotechnical Report, Volume 2; Appendix G-K). The terrain maps were not synthesized into a geologic framework as developed in the WCC report. Limited mapping of Quaternary deposits also was developed near the site by Acres (1981, 1982) and Harza-Ebasco (1984) as part of detailed geotechnical investigations for the Susitna-Watana Dam site.

Additional, detailed Quaternary geological mapping of surficial deposits directly east of the site in the mid-1980s (with radiocarbon age data) was published by the USGS (Williams and Galloway, 1986). Several publications after Williams and Galloway (1986) offer regional geologic and geomorphic conceptual models for explaining the distributions and relationships between different surficial deposits, based on evidence of large late Pleistocene inland ice-dammed lakes in the Copper River basin.

The following sections provide an overview of the regional Quaternary geologic setting, briefly summarizes and evaluates the Quaternary stratigraphy and chronology

presented in WCC (1982), for the general dam site vicinity, and the relevance of the existing Quaternary geologic studies to the seismic hazard update for the Susitna Dam site evaluation.

3.3.2 Quaternary geologic setting

Glacial ice fields and ice lobes spread over much of south central Alaska during the late Cenozoic. The Alaskan glaciations waxed and waned during the Quaternary period, and the repeated ice advances sculpted and formed much of the existing surficial deposits and geomorphic landforms. The dynamic fluctuations of ice created several depositional environments as well as various landforms, such as: outwash plains, proglacial lakes, ice-dammed lakes, bogs, kame terraces, moraines, till, drift, eolian loess, and localized glaciofluvial channels and deltas (Hamilton, 1994).

3.3.2.1 Glaciations

Late Cenozoic glaciations in Alaska usually are recognized as chronologic events that have relatively diffuse time boundaries because of the time-transgressive nature, and the variability in ice extent and timings of ice movement from place to place. Four main glacial episodes are identified in the south central Alaska region in the Quaternary. From young to older, these Pleistocene events are: Late Wisconsin glaciation (~24 ka¹ to ~11 ka), Early Wisconsin glaciation (~75 ka to ~40 ka), Illinoian glaciation (>125 ka), and pre-Illinoian glaciation (~300 ka) (Hamilton, 1994). The main glacial episodes may be further subdivided into “phases” or “stades,” based on local geologic relationships correlated to relatively regional deposits. Individual ice lobe advances in specific regions may be identified based on detailed mapping and age-dating of surficial deposits (e.g., Williams and Galloway, 1986).

Numerous ice fields and glacial lobes existed in the Talkeetna Mountains as well as the Chugach Mountains to the south (Williams and Ferrans, 1961). Mid to Late Wisconsin glacial advances in the Talkeetna Mountains region directly east of the Susitna-Watana Dam site are well documented by Williams and Galloway (1986). These mountainous regions developed alpine glacial lobes that flowed down their respective valleys and extended onto the Copper River basin floor to various lengths. As glaciers filled the Copper River basin, they created an ice dam which formed at least two, and probably more, aerially extensive ice-dammed lakes (Nichols, *in* Carter et al., eds., 1989).

¹ Ka abbreviates “kiloannum;” thousands of years ago. For example, 24 ka is read as 24,000 years ago.

Glaciers emanating from the ice fields in the Chugach, Wrangell, and the Alaska Range flowed down their valleys and terminated in the lake. The lake (i.e., Lake Ahtna) may have episodically drained at different elevations and times during the late Wisconsin (Williams and Galloway, 1986; Williams, *in* Carter et al., eds., 1989; Ferrians *in* Carter et al., eds. 1989; Wiedmer et al., 2010). At their greatest extents, these glaciers coalesced and extended across the Susitna-Watana Dam site area; as the glaciers receded, the dam site was inundated by glacial Lake Ahtna.

3.3.3 Quaternary geology in the site vicinity

The most extensive investigations of the Quaternary geologic deposits and history were completed in the late 1970s and early 1980s for the proposed hydroelectric project. Many of these studies were instrumental in providing data which later lead to the full recognition of the extent of Quaternary glaciation and glacial lakes in the region, but at the time of these studies, that framework had not been fully integrated. For the seismic hazard evaluation of the proposed hydroelectric project, the primary source of Quaternary geologic data in the site vicinity was developed for WCC (1980, 1982) (Section 2.4). From their studies and mapping, a site vicinity stratigraphic and chronologic framework was developed (WCC, 1982). The following paragraphs briefly examine and evaluate this stratigraphic and chronologic framework.

3.3.3.1 Stratigraphy

Based on the Quaternary geologic mapping (Figures 9 through 11) and field work, the principal Quaternary deposits near the site vicinity include: Glacial drift and differing-age tills, re-worked till, well-sorted and stratified coarse-grained deposits from glaciofluvial outwash, well-sorted sands with sedimentary structures indicative of fluvial deltaic origin, and fine-grained deposits with massive to laminated structures indicative of lacustrine deposition. These deposits were identified at field exposures in outcrop, as shown on a cross sectional diagram (WCC, 1982) (Figure 9). The cross section illustrates variable stratigraphy both laterally and vertically, with thick sections of lacustrine deposits overlain by oxidized till or highly oxidized reddish glaciofluvial deposits. The cross section also illustrates the elevational positions of the deposits. Terraced sands are shown stranded on topographic high points, and deltaic sands are shown at lower elevations that laterally grade into lacustrine deposits. No attempt was made to conceptually link the deposits together into a site-specific geologic model. The proposed conceptual geologic model of WCC (1982) involved assuming a particular geomorphic relationship of deposits in which, presumably younger deposits, are at

lower elevations and nested within (or, “inset into”), elevationally higher, presumably older, deposits (Figure 10); and that each subsequent ice lobe advance phase was of diminished aerial and vertical extent relative to the previous phase. Neither assumption was rigorously tested.

WCC (1982) identifies thick lacustrine beds as owing to the formation of lakes by glacial ice damming (p 3-18). However, the data (WCC, 1980; 1982) as well as subsequent geological research (Williams and Galloway, 1986; Carter et al., 1989; Hamilton, 1994; Weidmer et al., 2010) more favor the presence of two or more large ice-dammed paleolakes that existed in the Copper River basin sometime during the late Pleistocene and perhaps into the early Holocene (Lake Susitna, older; Lake Ahnta, younger). These ice-dammed paleolakes may have occupied several elevations through time identified by abandoned shorelines and potential geologic “spillways” near the dam site area (Williams and Galloway, 1986). Based on radiocarbon dating, the younger lake, Lake Ahnta, may have drained by at least $9,400 \pm 300$ ka. The large and potentially youthful paleolake and lake-draining deposits may have key linkages to the stratigraphy near the dam site vicinity.

3.3.3.2 Chronology

The WCC (1982) cross section illustrates presumed estimated maximum ice elevations for different Late Wisconsin glacial phases (Figure 9), as a partial basis for correlating deposits and assigning chronology. The other bases were relative and absolute dating techniques. The relative dating technique largely was indiscriminant and unsuccessful. For absolute dating, WCC (1982) obtained eleven radiocarbon dates in the surficial geologic deposits near the dam site vicinity. Of these eleven, five exceeded the method limit (i.e., minimum age); four were early Holocene (circa 9,500 ybp); two were early Holocene (circa 3,000 ybp). None of the samples dated presumed Late Wisconsin deposits (~24 ka to ~11 ka) – an important age window for evaluating fault activity for critical engineered structures.

Moreover, the WCC (1982) geologic map indicates that a substantial amount of the surficial deposits are greater than 11,000 years old (Figure 10). This gap or disparity between presumed deposit age based on elevation (i.e. the geologic map) and the results of the eleven age-dates implies that an adequate site stratigraphic chronology that directly links the surficial and subsurface deposits to their correct age (as well as sequence and genesis) was not established.

3.3.4 Relevance to seismic hazard evaluation

Overall, the geologic and chrono-stratigraphic model of WCC (1982) largely is based on presumed maximum Late Wisconsin ice elevations, assumed inset geomorphic relations, and regional correlation of deposits based on these presumed elevations of ice and positional relationships of deposits (e.g. Figure 10). This conceptual framework largely is based on inference and tenuous correlation of deposits based on elevation. Further, the model does not account for geomorphic process, sequence stratigraphy, variability of stratigraphy, or site-specific event chronology. This implies that the chrono-stratigraphic framework of WCC (1982) is inappropriate for evaluating seismic hazard, because a consistent stratigraphic or geomorphic datum for evaluating late Pleistocene fault activity was not established.

Importantly, WCC (1982) absolute age data are not available for the time interval appropriate for seismic hazard evaluation. While the ages, timings, and extents of the ice-dammed paleolakes have been broadly estimated (e.g. Williams and Galloway, 1986), they have not been defined clearly or conclusive regionally and at the site level. The age and timing of lacustrine and paleolake-related deposits is relevant to this seismic hazard analysis because, based on the date and research published after 1982, the surficial deposits near the site vicinity may, in places, be younger than implied by the geologic map of WCC (1982). This has direct bearing on the presumed datum for assessing “recency” of fault activity in terms of: (1) potential near-field seismogenic sources, and, (2) evaluating potential surface fault rupture hazard (Section 9.1).

3.3.5 Surficial geology at the dam site area

The surficial deposits at the dam site were mapped and correlated based on drill samples of the thick overburden on the north abutment during the geotechnical studies for the dam and construction materials (USACE, 1979; Acres 1981, 1982; Harza-Ebasco, 1984).

The Acres studies’ geologic mapping at the site is presented in Figure 11, and top of bedrock contour mapping is presented in Figure 12. These studies subdivided the deposits into three distinct zones: top of slope deposits from approximate elevation of 2200 ft to 1900 ft), slope deposits from 1900 ft down to the river channel, and riverbed deposits (Acres, 1981 and 1982). The top of slope marks the topographic transition from the “V” shaped canyon below and the relatively flat upland plateau above. Surficial deposits in this zone consist of till, alluvium and talus and are generally 20 to 50 feet thick with isolated bedrock outcrops. The slope deposits occur where the valley profile

changes from a “U” shape to a “V” shape and consist of up to 40 feet of dominantly talus and rock avalanche deposits with abundant bedrock outcrop in cliff faces (Acres, 1981 and 1982).

Geophysical surveys and borings above the Susitna River channel by Harza-Ebasco (1983) found that the channel is underlain by alluvial deposits with relatively uniform thickness up to approximately 80 feet (Harza-Ebasco, 1984). The deposits are comprised primarily of well-graded coarse-grained gravels, sandy gravels and gravelly sands with cobbles and boulders. The underlying bedrock channel is generally symmetrical and nearly flat-bottomed with the exception of two pronounced depressions upstream of the dam site that have alluvial overburden up to 140-feet-thick. The depressions are not on strike with the principal bedrock shear zones identified in previous studies (Acres, 1981 and 1982), however, the features are presumed to be located in areas of weaker, erodible bedrock.

Deposits on flat uplands reach up to 550-foot thickness on the north abutment area, and 350 feet thick on the south abutment. Additional field investigations to the north of the dam site for construction material sources identified a relict channel incised into the bedrock and obscured by flat lying surficial deposits (Acres, 1981 and Harza-Ebasco, 1984). The relict channel is comprised of two bedrock thalwegs up to 500 feet deep, filled with fluvial, glacial and lacustrine deposits. The channel is interpreted to have been a paleo-channel of the Susitna River in pre-glacial times. The channel may follow less resistive rock to the north of the massive diorite pluton that underlies the dam site and continued into the current lower reaches of Tsusena Creek. Subsequent glacial advance from Tsusena Creek would have diverted the channel into approximately its current alignment (Acres, 1981).

3.4 Dam Site Area Geology

The dam site area was first mapped by Csejtey et al. (1978) whose mapping of the Talkeetna Mountains Quadrangle was later incorporated into regional mapping compilations by Wilson et al. (1998 and 2009) (Figure 13). The Wilson et al. (2009) compilation includes previously unpublished lineaments and bedrock faults near the dam site. Detailed bedrock mapping at or near the dam site was performed in conjunction with the previous Watana Dam site investigations in the late 1970s and early 1980s (USACE, 1975, 1979; WCC, 1980, 1982; Acres, 1981, 1982; Harza-Ebasco, 1984).

The oldest bedrock unit proximal to the dam site is a flysch sequence comprised of Cretaceous shales (regionally altered to argillite) and lithic greywacke sandstone of the Kahiltna assemblage (Csejtey et al., 1978). These sediments were shed from sources in the east and northeast into a basin between the Wrangalia Terrane and North America during the Cretaceous orogeny (Glen et al., 2007a). Small bodies of Paleocene granite units with interfingering migmatite and pelitic schists, and granodiorites with minor diorite (Csejtey et al., 1978), regionally intrude the Kahiltna assemblage. The intrusive rocks are part of a large suite of largely granitic and granodioritic rocks which intruded between 53.2 Ma to 64 Ma during the late stages of accretionary tectonics. Diorite and quartz diorite bedrock underlies much of the dam site and is likely part of this regional intrusive suite (Acres, 1981). The youngest bedrock units in the site vicinity are Paleocene to Miocene subaerial volcanic rocks and related shallow intrusives that may be related to the Paleocene plutons (WCC, 1980). At the dam site these young volcanic rocks include andesite porphyry and numerous felsic through mafic dikes (Acres, 1981). Basalt flows outcropping in Deadman Creek, to the east of the dam site have an early-mid Eocene age (approximately 48 Ma, based on Argon isotope analyses) (Schmidt et al., 2002).

3.5 Site Bedrock Velocity

P-wave seismic velocities from seismic refraction surveys were measured during the earlier geotechnical evaluation of the dam site area and presented in Acres (1981, 1982). The velocity measurements from those studies are presented in cross sections in the Acres reports. The reports also present interpreted velocity ranges used to classify the various bedrock materials in the subsurface. Table 1 summarizes the estimated bedrock seismic maximum and minimum velocity ranges. The P-wave velocities (feet per second) have been converted to S-wave velocities (meters per second) using the conversion calculation of Aki and Richards (1980). These conversions suggest that S-wave velocities at the site range from about 3,950 ft/s to 12,800 ft/s (1,200 m/s to 3,900 m/s), and are further categorized by degree of rock weathering and alteration (Table 1).

S-wave velocity for the site is a key input for the ground motion prediction equations (GMPE) as discussed in Section 5.2. Ground motion estimates developed for this study are intended as inputs to base models, in which effects of soils and structures are separately computed. For these types of analyses, ground motion estimates are input at the rock foundation interface or deep in the modeled foundation. Although specific details of foundation excavations have not been developed for dam alternatives, and no

site-specific shear wave velocity measurements have been obtained for the site, the existing data provides a preliminary indication of the potential foundation conditions. Based on available data, it appears that S-wave velocities at the site for unweathered to lightly weathered rock which may form the majority of the structure foundation may well exceed 7,875 ft/s (2,400 m/s) (Table 1).

Table 1. Summary of Site Bedrock Seismic Velocity Data

| Watana Dam Site and Vicinity Seismic Velocity Correlations | | | | |
|----------------------------------------------------------------------------------------------------|------------------------------------|----------------|-----------------------------------|----------------|
| Material | P wave (ft/sec)¹ | | S wave (m/sec)² | |
| | Minimum | Maximum | Minimum | Maximum |
| Highly sheared weathered or altered bedrock | 7,000 | 10,600 | 1,232 | 1,865 |
| Sheared, fractured weathered or altered bedrock | 10,600 | 13,500 | 1,865 | 2,376 |
| Bedrock, surface weathering or stress relief jointing to moderate depths, generally very competent | 13,500 | 16,200 | 2,376 | 2,851 |
| Bedrock, fresh, extremely competent, minimal fracturing | 16,200 | 22,200 | 2,851 | 3,907 |

Notes: (1) Data from Acres (1982) report, Table 5.1. (2) P wave (ft/sec) to S wave (m/sec) conversion = (P wave x 0.3048)/1.732 after Aki and Richards (1980).

4.0 SEISMIC SOURCE CHARACTERIZATION

4.1 Subduction Related Sources

The Alaska subduction zone (ASZ) is one of the world's most seismically active subduction zones. Relative plate motion between the Pacific and North American Plates increases from about 5.4 cm/yr (2 in/yr) at its eastern end near the Talkeetna Mountains to about 7.8 cm/yr (3 in/yr) at the west end of the Aleutian arc (Figure 5). The ASZ is also termed the Alaska-Aleutian Arc. East of longitude 170 degrees West, the Pacific Plate is subducting beneath continental crust, while to the west it subducts beneath oceanic crust that was trapped after initiation of the arc in the middle Eocene. This results in a more shallow-dipping plate interface to the east than to the west.

Earthquakes associated with the ASZ are of two main types: large “megathrust” events due to accumulated frictional strain between the two plates (most notable being the 1964 M 9.2 earthquake, described in section 3.2.2), and those occurring within the down going Pacific Plate as it descends into the mantle. These “intraslab” earthquakes, considered capable of reaching magnitudes of M 7.5, are due to factors such as spreading ridge push, gravitational pull of the plate due to density contrasts between it and the mantle, and metamorphic reactions due to increasing temperature and pressure within the down going plate. In this study, we model these two types of subduction earthquakes from the ASZ, termed *interface* (or *megathrust*), and *intraslab*.

The dam site area lies at the eastern end of the ASZ. At this location the plate interface has an extremely low dip, almost flat (Figure 14B). The northern boundary of the interface is at a depth of about 22 mi (35 km) and lies about 50 mi (80 km) southeast of the site. To the northwest of this line intraslab earthquakes are produced as the plate dips more steeply as it descends into the mantle. Beneath the site the top of the plate is at a depth of about 31 mi (50 km) (Figure 14).

4.1.1 Plate interface

The interface between the North American and Pacific Plates is the source of the largest magnitude earthquakes in the source model. Due to studies of the 1964 M 9.2 earthquake, seismic refraction/reflection surveys (e.g. Brocher et al., 1994), and research results from a regional seismograph network operated by the Alaska Earthquake Information Center (AEIC) (Ratchkovski and Hansen, 2002), the geometry of the down going plate within a few hundred km of the site is fairly well known.

In this region, Wesson et al. (2007) following cross sections of relocated seismicity shown in Ratchkovski and Hansen (2002), modeled the interface as shown in Figure 15. In this figure the up-dip 20 km (12 mi) contour is seen to the southeast. The contour representing the down-dip boundary of the plate interface is seen to the northwest. To the southwest its depth is 40 km (25 mi), reflecting the steeper interface dip to the west, and at longitude 151 degrees West, it begins to shoal from 40 km (25 mi) to 33 km (20 mi) to the end of the interface at the northeast end. This reflects the slightly tilted interface seen in Figure 14 (Figure 6b of Ratchkovski and Hansen, 2002).

4.1.2 Intraslab

Intraslab earthquakes occur within the down going Pacific plate, after it breaks contact with the North American Plate in the megathrust zone, and assumes a steeper dip as it descends into the upper mantle. Notable earthquakes of this type include the M 6.5 1965 and M 6.8 2001 Nisqually, Washington earthquakes associated with the Cascadia subduction zone. As seen in Figure 14, in the site region this zone consists of two parts: an intermediate zone dipping about 25 degrees between depths of 31 and 50 mi (50 and 80 km), and a deeper zone from 50 to 93 mi (80 to 150 km) that dips more steeply. The physical sources of these earthquakes include ridge push from oceanic spreading ridges, gravitational pull of the slab due to density contrasts between it and the surrounding mantle, and chemical reactions due to increasing pressure and temperature.

4.2 Quaternary Crustal Faults

The following section discusses all faults within 125 mi (200 km) of the dam site with evidence of historical or Quaternary activity, as well as suspicious faults that may or may not be active structures (Figure 3, Table 2A). (The activity term “suspicious” is from Plafker et al. (1994)). Fault parameters obtained from peer-reviewed references are summarized in Tables 3A and 3B. The primary compilation of faults in Alaska, and the initial basis for the model included is the “Neotectonic Map of Alaska” by Plafker et al. (1994). Quaternary faults identified after the Plafker et al. (1994) map and presented in published literature have also been included in the model. A Quaternary fault and fold database of Alaska is currently being compiled by the Alaska Division of Geological & Geophysical Surveys (Koehler et al., 2011a), however, final publication of the database is not expected until 2012. Table 5 numerates the closest distance from the site area to the faults listed in Tables 2A and 2B. In Table 5, “JB distance” is the closest

distance to the horizontal projection of the fault plane, and “Rupture Distance” is the closest distance to the fault plane.

Table 2A. Fault Characterization

| Fault Name | Section | Age from Plafker et al. (1994) | Age from Other Sources | Sense of Slip | Dip | Seismogenic Depth (km) | Slip Rate (mm/yr) | Recurrence (years) |
|--------------------------------|-----------------------------------------|-----------------------------------------------------------|--------------------------------------------------------|---------------|--------------------------------------------------------|-------------------------------------------------------|-------------------------------------------------------------------------------------------------------------------------------------------------------------------------------------------------------------|---------------------------------------------------------------------------------------|
| Castle Mountain fault | Eastern Castle Mountain - Caribou fault | Eastern Castle Mountain = Historic; Caribou = Pleistocene | Historic based on 1984 seismicity (Lahr et al., 1986) | RL - Reverse | 76° N (Lahr et al., 1986); 80°-90° (Fuchs, 1980) | ? | lateral: 0.5 - 0.6 (Fuchs, 1980) thrust: ? | N/A |
| | Western Castle Mountain | Holocene | Holocene (Haeussler et al., 2002; Willis et al., 2007) | RL - Reverse | 70°-90° N (Haeussler et al 2000) | 20 [based on 1984 EQ (Lahr et al., 1986)] | lateral: 2.8-3.6, [preferred rate of 3.0 -3.2] (Willis et al., 2007); 2.9 mm/yr (Wesson et al. 2007); 0.45-0.63 (Koehler and Reger, 2011) thrust: 0.07-0.14 | 700 (Haeussler et al., 2002) |
| Denali fault | Eastern | Holocene | Holocene (Matmon et al., 2006) | RL | ? | ? | 8.4 +- 2.2 mm/yr (Matmon et al., 2006) | 380 (mean ages from Plafker et al., 2006 and DFWG summarized in Koehler et al., 2011) |
| | Central | Holocene/ Suspicious | Historic - 2002 M7.9 (Eberhart-Phillips et al., 2003). | RL | 75°-90° (Haeussler et al., 2004). | 12 [from 2002 aftershocks (Ratchkovski et al., 2003)] | 14.4 +- 2.5 mm/yr (Matmon et al., 2006), 85 km W = 13.0 +- 2.9 mm/yr 255-283 km W = 9.4 +- 1.6 mm/yr 323 km W = 6.7 +- 1.2 mm/yr (Meriaux et al., 2009) (distance relative to Totschunda junction) | 400 (mean age from DFWG summarized in Koehler et al., 2011) |
| | Western | Holocene/ suspicious | N/A | RL | ? | ? | ? | ? |
| Pass Creek - Dutch Creek fault | N/A | Late Pleistocene | Holocene (Haeussler et al., 2008) | Normal | ? | ? | 1.72 mm/yr min slip rate based on scarp height of Willis and Bruhn (2006) | 1340 max (Willis and Bruhn, 2006) |
| Sonona Creek fault | N/A | N/A | Holocene (Williams and Galloway, 1986) | ? | ? | ? | ? | ? |
| East Boulder Creek fault | N/A | Late Pleistocene | Holocene (Plafker et al, 1994) | ? | ? | ? | ? | ? |
| Matanuska Glacier fault | N/A | N/A | Holocene (Haeussler and Anderson, 1995) | Right normal | ? | ? | ? | ? |
| Susitna Glacier fault | N/A | N/A | Historic 2002 M7.9 (Eberhart-Phillips et al., 2003). | Reverse | 19-48 (Crone et al., 2004 and Ratchovski et al., 2003) | ? | ? | ~4000 (Crone et al. (2004) |
| Broxson Gulch fault | N/A | Neogene | Cenozoic (Ridgeway et al., 2002) | Reverse | 5-40 (Stout and Chase, 1980) | ? | ? | ? |
| McCallum-Slate Creek fault | N/A | Late Pleistocene | Early Pliocene (Weber and Turner, 1977) | Reverse ? | ? | ? | ? | ? |
| Bull River fault | N/A | suspicious | N/A | Reverse | ? | ? | ? | ? |
| Foraker fault | N/A | ? | N/A | Reverse | ? | ? | ? | ? |
| Broad Pass fault | N/A | ? | N/A | Reverse | ? | ? | ? | ? |

Notes: See Table 2B for Northern foothills fold and thrust belt faults

Table 2B. Northern Foothills Fold and Thrust Belt (NFFTB) Fault Data

| Fault Name | Age from Plafker et al. (1994) | Age from Bemis et al. (in press) | Sense of Slip | Dip (direction) |
|-----------------------------|---------------------------------------|-----------------------------------------|----------------------|------------------------|
| Billy Creek fault | suspicious | Holocene | LL - Reverse (NW up) | >60 (?) |
| Canteen fault | Late Pleistocene | Holocene | LL - Reverse (NW up) | >60 (direction?) |
| Cathedral Rapids fault | N/A | Holocene | Reverse (S up) | 15-60 (S) |
| Ditch Creek fault | N/A | Quaternary | Reverse (SW up) | >60? (SW?) |
| Donnelly Dome fault | Late Pleistocene | Holocene | Reverse (S up) | 45-90 (S) |
| Dot "T" Johnson fault | N/A | Holocene | Reverse (S up) | 15-45 (S) |
| East Fork fault | Holocene | Holocene | Reverse (N up) | >60 (S?) |
| Eva Creek fault | N/A | Quaternary | Reverse (N up) | >60 (direction?) |
| Glacier Creek fault | N/A | Quaternary | Reverse (S up) | 30-60 (S) |
| Gold King fault - Section A | N/A | Late Pleistocene | Reverse (S up) | 15-30 (S) |
| Gold King fault - Section B | N/A | Quaternary | Reverse (S up) | 10-30 (N) |
| Granite Mountain fault A | Late Pleistocene | Holocene | LL - Reverse (NE up) | >60 (direction?) |
| Granite Mountain fault B | Late Pleistocene | Quaternary | Reverse (S up) | 30-60 (SW) |
| Healy Creek fault | Late Pleistocene | Late Pleistocene | Reverse (N up) | 60-90 (N) |
| Kansas Creek fault | N/A | Quaternary | RL - Reverse (S up) | >30 (S) |
| Macomb Plateau fault | N/A | Quaternary | Reverse (S up) | 15-60 (S) |
| McGinnis Glacier fault | | Holocene | Reverse (SW up) | >45 (SW?) |
| Molybdenum Ridge Fault | N/A | Holocene | Reverse (S up) | 15-45 (S) |
| Mystic Mountain fault | Neogene | Late Pleistocene | RL - Reverse (S up) | >30 (S) |
| Nern Foothills thrust | N/A | Late Pleistocene | Reverse (S up) | 15-45 (S) |
| Panoramic fault | N/A | Late Pleistocene | Reverse (NE up) | >60 (?) |
| Park Road fault | N/A | Late Pleistocene | Reverse (N up) | 30-90 (N) |
| Peters Dome Fault | N/A | Quaternary | Reverse (S up) | 15-45 (S) |
| Potts fault | N/A | Quaternary | Reverse (NE up) | >60? (?) |
| Red Mountain fault | N/A | Late Pleistocene | Reverse (S up) | 30-60 (?) |
| Rex fault | N/A | Late Pleistocene | Reverse (S up) | >30 |
| Stampede fault | N/A | Late Pleistocene | Reverse (N up) | 15-30 (N) |
| Trident fault | N/A | Late Pleistocene | Reverse (SE up) | >30 (SE) |
| Trident Glacier fault | N/A | Quaternary | Reverse (S up) | 30-60? (S) |

Notes: (1) Fault Data from the NFFTB summarized from Bemis et al. (in press). (2) LL = left lateral, RL = right lateral.

4.2.1 Denali fault

The Denali fault is a right-lateral fault with an arcuate shape striking to the northwest in the east, and an increasingly westerly and southwesterly strike to the west (Figure 6). A

typical geometry evoked for the fault includes an eastern section located east of the junction with the Totschunda fault, a central section between the Totschunda junction and an asperity in the fault strike near Denali, and a western section west of Denali. The western termination of active faulting is considered in the source model to be at latitude 154.7°W based on Wesson et al. (2007), who propose that slip tapers to 0 mm/yr at this location. Western continuation of the fault beyond this point would not be expected to have significant impact on the site ground motions due to the large distance, ~202 mi (~324 km), to the western end of the Denali fault. The fault sections outlined above serve solely for geographic reference, as there is no evidence that the section boundaries would inhibit seismic rupture.

The largest historical earthquake on the fault is the 2002 M7.9 Denali fault earthquake, which had 211 mi (340 km) of total surface rupture. The earthquake initiating in the west and ruptured a 30-mi (48-km) long section of the previously unrecognized Susitna Glacier thrust fault. Slip propagated primarily eastward rupturing 140 mi (226 km) of the Central Denali fault. At the eastward limit of slip on the Central Denali fault the rupture stepped southeastward rupturing 66 km of the Totschunda fault (Haeussler et al., 2004).

Subsequent studies of Quaternary slip rates along the fault using cosmogenic exposure dating of offset moraines and other glacial features show a westward reduction in slip rate on the Denali fault (Figure 6). Slip rates are summarized in Figures 6 and 18. Matmon et al. (2006) calculate an 8.4 ± 2.2 mm/yr slip rate for the eastern Denali fault, and a 6.0 ± 1.2 mm/yr on the Totschunda fault. The slip rates of the Totschunda and Eastern Denali faults sum to 14.4 ± 2.5 mm/yr at the eastern part of the Central Denali fault section. The preferred slip rates on the central Denali fault west of the Totschunda fault junction are: 85 km west of the site is 13.0 ± 2.9 mm/yr (Meriaux et al., 2009), 255-283 km west is 9.4 ± 1.6 mm/yr (Matmon et al. 2006), 323 km west is 6.7 ± 1.2 mm/yr (Meriaux et al., 2009), and 626 km west is 0 mm/yr (Wesson et al., 2007). The westward reduction in slip rate is widely considered to be the result of the partitioning of slip onto the Northern foothills fold and thrust belt (Figure 7) (Bemis et al., in press; Haeussler, 2008; Matmon et al., 2006; Meriaux et al., 2009). These slip rates are in line with measurements of strain accumulation via geodetics, 6.5 to 9 mm/yr (Fletcher, 2002), and InSAR, 10 mm/yr (Biggs et al., 2007). The westward reduction in slip rate is also consistent with the westward decrease in displacement during the 2002 earthquake (Haeussler et al., 2004).

Paleoseismic studies performed by the Denali Fault Working Group after the 2002 earthquake found that the penultimate slip events were of similar magnitude to the 2002 event (Schwartz et al., 2003). Carver et al. (2004) used tree ring counts from damaged trees near the Delta River to propose that the penultimate event was a M7.2 earthquake

on July 6, 1912. Results from test pits adjacent to the Delta River by Plafker et al. (2006) suggest two paleo-events at 310 to 460 years before present, and 650 to 780 years before present. Trenching by the Denali Fault Working Group produced the following Denali fault earthquake chronology:

- The 2002 rupture trace had earthquakes between 350 and 600 years before present, and between 715 and 1,080 years before present;
- West of the 2002 earthquake the fault ruptured between 110 and 380 years before present, and between 560 and 670 years before present;
- East of the Totschunda – Denali fault junction the fault experienced three events between 110 and 356 years before present; ≥ 560 and 690 years before present; and $\leq 1,020$ and 1,230 years before present (summarized in Koehler et al., 2011b).

Koehler et al. (2011b) trenched a site along the 2002 rupture trace and found that the penultimate event at this location was after 560 to 670 years before present. None of the paleoseismic trenching studies found evidence for the 1912 Delta River earthquake discussed in Carver et al. (2004) and Doser (2004).

4.2.2 Castle Mountain fault

The Castle Mountain fault is an active, oblique strike-slip fault with a western and eastern section (Figure 8). The eastern section is combined with the Caribou fault of Plafker et al. (1994) due to their parallel geometry and the designation by Plafker et al. (1994) that both sections have evidence for Quaternary displacement. The eastern section-Caribou fault is primarily recognized in bedrock, has no evidence for Holocene surface rupture, and has historic seismicity to Mb 5.7 (1984 EQ documented in Lahr et al. 1986). The western section is defined by a 39-mi (62-km) Holocene fault scarp (north side up); and has no known historic seismicity greater than M5 (Flores and Doser, 2005). The fault trace was mapped in detail by Detterman et al. (1974 and 1976), and also by Haeusler (1998). Detterman et al. (1974) document a near surface fault dip of 75 degrees northward and seismic reflection data shows the fault to be steeply dipping (70 to 90 degrees) at depth (Haeussler et al., 2000).

Paleoseismic investigations of the Castle Mountain fault have yielded varying Quaternary slip rates and interpretations of deformational style. Detterman et al. (1974) proposed a maximum age for the most recent event of 1860 ± 250 years based on a radiocarbon ages of a displaced soil horizon exposed in a trench across a 2.1 m (6.9 ft)

high scarp. Detterman et al. (1974) also document 7 meters (23 feet) of horizontal displacement of a linear sand ridge across the fault. Trenching by Haeussler et al. (2002) on the western section identified 4 earthquakes on the fault (including one event on an adjacent fault strand) in the past 2800 years with a recurrence interval of approximately 700 years. The most recent rupture occurred 730-610 years before present. Haeussler et al. (2002) determined a shortening rate of 0.07 to 0.14 mm/yr (< 0.01 in/yr) but no lateral offset was observed in the trenches. Willis et al. (2007) use an offset post-glacial outwash channel on the western section to constrain a lateral slip rate of 2.8 mm/yr to 3.6 mm/yr (0.11 in/yr to 0.14 in/yr), with a preferred rate of 3.0 mm/yr to 3.2 mm/yr (0.12 in/yr to 0.13 in/yr). Koehler and Reger (2011) propose that a lateral slip rate of 0.45 to 0.63 mm/yr (0.018 to 0.025 in/yr) may be more appropriate for the western section. Fuchs (1980) proposed a post-Eocene slip rate of 0.5 to 0.6 mm/yr (0.020 to 0.024 in/yr) for the eastern section.

4.2.3 Pass Creek – Dutch Creek fault

The Pass Creek – Dutch Creek fault is a northeast-striking, south side down, normal fault bounding the northern edge of the Peters Hills Basin (Haeussler et al., 2008) (Figure 3). The Peters Hills basin is a small Neogene basin that may be a piggyback basin in the hanging wall of a “Broad Pass fault” (see discussion on the Southern Denali fault zone below) (Haeussler et al., 2008). The Pass Creek – Dutch Creek fault forms a 21-ft (6.5-m) tall scarp that displaces Holocene sediments, and creates a vegetation lineament on the north side of the Skwetna River. The last significant rupture on the fault had > 6.5 ft (>2 m) of uplift and cut a moraine with a radiocarbon age of 1340 ± 60 years before present (Willis and Bruhn, 2006).

4.2.4 East Boulder Creek fault

The East Boulder Creek fault is 14 mi (22 km) long, northeast striking and located south of and parallel to the Caribou fault section of the Eastern Castle Mountain fault system. Detterman et al. (1976) first mapped the trace of the fault based on surface features including notches, benches, saddles, linear gullies and scarps, but make no estimation of the fault's age. They document evidence for south side up relative displacement along the fault. Plafker et al. (1994) depict the fault as having Late Pleistocene activity. Because of the fault's proximity and parallel orientation to the Castle Mountain fault, it is considered a potentially active right-lateral fault.

4.2.5 Matanuska Glacier fault

The Matanuska Glacier fault is classified as having Holocene activity in Plafker et al. (1994), based on mapping by Burns et al. (1983) and oral communication with Gar Pessel (2011). Haeussler and Anderson (1995) write that the fault is a "4-km long east-west-striking fault [that] apparently offsets tundra 30 cm vertically with a right normal sense of offset."

4.2.6 Sonona Creek fault

The Sonona Creek fault is located in the western Copper River basin (Figures 19 and 20). The structure is mapped by Williams and Galloway (1986) as a 4-mi (7-km) long, active, northeast-striking fault with north side down sense of displacement, offsetting Late Pleistocene glaciolacustrine sediments. No information is provided to indicate further the age, sense or amount of displacement on this fault. This mapped feature is evident in Google Earth images (Figure 20). Although resolution is low, topographic height of the scarp appears limited, suggesting that at least the vertical slip rate is relatively low. As a singular surface rupture along a potentially active fault, the length of the scarp is relatively short. The presently available images in Google Earth are permissive of extensions and certainly do not rule out extensions of this fault in either direction.

4.3 Zones of Distributed Deformation

Zones of distributed deformation are regions with poorly characterized or suspected active faults; where the Quaternary geologic and fault mapping may be incomplete, and/or the slip-rate and recurrence of individual faults is poorly understood. The site region includes two areas classified as zones of distributed deformation: the Northern foothills fold and thrust belt, and the Southern Denali faults.

4.3.1 Northern foothills fold and thrust belt zone

The Northern foothills fold and thrust belt (NFFTB) is a zone of Quaternary faults and folds along the north side of the Alaska Range (Bemis and Wallace, 2007; Bemis et al., in press) (Figure 7, Table 2B). The zone is primarily comprised of variably dipping thrust faults with dominantly north vergent deformation. Bemis and Wallace (2007) propose that much of the NFFTB is underlain by a gently south-dipping basal detachment that may daylight at the Northern foothills thrust along the northern margin of the NFFTB in the vicinity of the Nenana River. The surface trace of the basal detachment is not identified in the western and eastern margins of the NFFTB. The

western margin of the NFFTB is marked by the termination of uplifted topography northwest of the Peters Dome fault and the Kantishna Hills anticline. The eastern margin is constrained by the paleoseismic investigation by Carver et al. (2010) which found no evidence for Quaternary deformation east of the Cathedral Rapids fault in the vicinity of Tok, Alaska. Quaternary deformation is presumed across the uplifted region within the NFFTB; however, rates of Quaternary deformation along individual faults are still poorly constrained (Bemis et al., in press). Mapping of deformation in Pleistocene gravels by Bemis (2010) suggests that the region west of the Nenana River has a maximum shortening rate of 3 mm/yr. Bemis et al. (in press) used offset Nenana gravel along the Granite Mountain fault to suggest horizontal shortening 1-4 mm/yr (0.04-0.16 in/yr) of in the eastern NFFTB. Meriaux et al. (2009) proposes that the partitioning of slip from the Denali fault onto the NFFTB could produce convergence rates up to about 4 mm/yr (0.16 in/yr) in the eastern NFFTB end, and about 12 mm/yr (0.47 in/yr) to the west. Due to the apparent variability in slip rates longitudinally across the NFFTB the zone is divided into a western and eastern zone.

4.3.2 Southern Denali faults

The southern Alaska Range is characterized by numerous northeast- and east-trending, generally south vergent, thrust and reverse faults that splay off from the southern side of the Denali fault (Figure 6). Most of these faults have evidence for Tertiary activity and several bound disparate tectonostratigraphic terranes (Haeussler, 2008; Glen, 2004). Glen (2004) proposed that these faults are linked to dextral transport along the arcuate Denali fault and may accommodate compressional deformation as crustal blocks migrate around the restraining fault geometry. The only fault in the area with clear evidence for Quaternary activity is the previously unrecognized Susitna Glacier fault, which ruptured in the 2002 M7.9 Denali fault earthquake. The similar orientation and tectonic setting of the Tertiary faults to the Susitna Glacier fault suggests that these structures have the potential for Quaternary activity. Furthermore, many of these faults are located in glaciated remote regions where evidence for Quaternary activity may have been obscured or gone unrecognized. It is also likely that the current inventory of thrust faults splaying off the south side of the Denali fault is incomplete. The Southern Denali fault zone is a zone of distributed deformation that extends 16 mi (25 km) south of the trace of the Central Denali fault and includes the following six structures.

4.3.2.1 Foraker thrust

The Foraker thrust is mapped as a northeast-striking, northwest-dipping thrust fault running through predominantly glaciated terrain between Mt. Foraker and Mt. McKinley

(Wilson et al., 1998). It is considered one of the principal thrust faults responsible for uplift of the high terrain in the Denali region and likely is kinematically linked to the nearby restraining bend in the Denali fault (Haeussler et al., 2008; Haeussler, 2005). Haeussler (2005) states that the Foraker thrust is “difficult to constrain, but is likely young and possibly active.”

4.3.2.2 Bull River fault

The Bull River fault is mapped as a northeast-striking, southeast-dipping thrust fault located between the Denali and Broad Pass regions (Wilson et al., 1998). The fault juxtaposes Cretaceous Kahiltna flysch sequence rocks in the hanging wall against Tertiary Tyonek Formation sedimentary rocks and Eocene Granites and granodiorites in the footwall. Plafker et al. (1994) classify the fault as having Neogene activity.

4.3.2.3 Broad Pass fault

The Broad Pass fault is a poorly understood structure defined by a northeast-striking topographic lineament, Mesozoic rocks topographically above Neogene rocks in the Susitna basin, and scattered shallow thrust earthquakes northwest of Broad Pass (Haeussler, 2008). The thrust has been evoked by Haeussler et al. (2008) as a possible master thrust underlying the Peter Hills piggyback basin.

4.3.2.4 Susitna Glacier fault

The Susitna Glacier thrust fault was unrecognized prior to the 2002 Denali fault earthquake when 30 mi (48 km) of the fault ruptured with 13 ft (4 m) of average displacement (Crone et al., 2004). The fault has a northeast strike and a northwest dip of approximately 19° near the ground surface. Focal mechanisms from the 2002 earthquake found that the fault ruptured on a 48° dipping plane at 2.6 mi (4.2 km) depth (Ratchovski et al., 2003), which suggests that the fault steepens at depth. Crone et al. (2004) identified a pre-2002 fault scarp exposing volcanic ash in the hanging wall, indicating a penultimate earthquake that post-dates deposition of the ash. The offset ash is considered to be either the Jarvis Creek ash (3.6 ka) or the Hayes Tephra (upper Holocene), suggesting at least one additional Holocene earthquake on the fault. Recent, uninterpreted trenching data from the fault presented by Personius et al. (2010) shows a single paleoevent that ruptures a peat layer with radiocarbon ages ranging from 660-4570 calendar years before present.

4.3.2.5 *Broxson Gulch fault*

The Broxson Gulch fault is an east- and northeast-striking and north-dipping thrust fault located in the eastern Alaska Range, north of the Copper River basin. Plafker et al. (1994) classify the fault as having Neogene activity and Ridgeway et al. (2002) suggest the fault is late Cenozoic in age. The thrust separates Maclaren Terrane rocks on the north from Wrangalia rocks in the south, and is typically mapped as cutting the Talkeetna thrust fault to the southwest (Ridgeway et al., 2002; Wilson et al. 1998) Stout and Chase (1980) found the fault to have a 5-40° dip along its eastern edge. Both Haeussler (2008) and Glen (2004) note the likely kinematic connection between the Broxson Gulch fault and the Denali fault.

4.3.2.6 *McCallum-Slate Creek fault*

The McCallum-Slate Creek fault is a southeast-striking, north-dipping thrust fault that parallels the Denali fault immediately east of the Broxson Gulch fault. The fault does not splay off the Denali fault with a counterclockwise orientation like the other thrusts in the region, but its geometry suggests that they connect at depth (Haeussler, 2008). Plafker et al. (1994) classify the fault as having late-Pleistocene activity. Weber and Turner (1977) document offset in a 5.25 Ma tephra layer along the fault suggesting early Pliocene activity.

4.4 **Talkeetna Block Structures**

The region is characterized by bedrock faults and distributed deformation associated with Cretaceous accretion of the Wrangellia Terrane (Csejtey et al., 1978 and 1982; Ridgeway et al., 2002) and post-accretionary right-lateral bulk shear in the Tertiary (O'Neil et al. 2005, Glen et al. 2007b). To date, no direct geologic evidence to conclusively evaluate the late Quaternary fault activity in the Talkeetna Block exists. The proximity of the Talkeetna block structures to the Watana Dam site area requires a thorough discussion of the previously mapped faults with respect to the seismic hazard characterization.

4.4.1 Talkeetna thrust fault / Talkeetna suture

A mapped through-going structure within the Talkeetna block is the Talkeetna thrust fault or Talkeetna suture. The Talkeetna thrust is mapped as a northeast-striking, southeast-dipping fault by Csejtey et al. (1978), WCC (1981), and Wilson et al. (1998) (Figure 13A and 21). The fault juxtaposes Triassic and Permian metavolcanic and metasedimentary Wrangellia terrane rocks on the south against late Jurassic through

Cretaceous sedimentary rocks of the Kahiltna Assemblage on the north. The mapped trace of the fault terminates in the northeast against the younger Broxson Gulch thrust and is mapped as being obscured in the southwest by Tertiary igneous rocks (Figure 13A). The approximate fault trace follows a broad topographic lineament striking northeast across the Talkeetna Mountains; however, the precise location of the fault (expressed as a lineament) is obscured along much of its length by Tertiary igneous rocks and Quaternary sediments. Well-documented exposures of the fault are located at Talkeetna Hill in the southwest near the Talkeetna River, Butte Creek in the northeastern Talkeetna Mountains. (WCC, 1981) (locations 1 and 4 respectively in Figure 21), and in the Clearwater Mountains (O'Neill et al., 2003a). The investigation by WCC (1982) found indeterminate geologic evidence for conclusively evaluating Quaternary activity along the fault.

O'Neill et al. (2003a) mapped structural and stratigraphic relationships at Butte Creek (location 4 in Figure 21) and Pass Creek along the northeastern reaches of the fault. They found that the Kahiltna Assemblage sedimentary rocks in the footwall of the fault were derived from relatively proximal Wrangalia Terrane rocks. O'Neill et al. (2003a) also found no evidence for penetrative deformation associated with the fault. Based on these observations, O'Neill et al. (2003a) concluded that major contractional displacement has not occurred along the Talkeetna thrust. They conclude that the tens of kilometers of tectonic transport during emplacement of the Wrangellia Terrane are expected to be localized on structures to the northwest.

Glen et al. (2007b) use tectonic analysis of gravity and magnetic data to propose replacement of the term *Talkeetna thrust fault* with the Talkeetna suture zone. They describe the Talkeetna suture zone as a deep crustal structure bounding the northwestern edge of the Wrangellia Terrane. Surface structures near and overlying the Talkeetna suture zone occupy a wide zone of complex faulting that includes the Susitna lineament and a range front fault along the south side of the Fog Lakes lowland (Figure 22).

Modeling of geophysical anomalies across the suture zone by Glen et al. (2007a) show the suture zone as dipping steeply both to the northwest and to the southeast. They propose that this indicates either variations in dip along strike, or that the modeled anomalies are offset by individual segments within a fault zone with varying orientations.

4.4.2 Susitna lineament

The Susitna lineament is a pronounced northeast-southwest trending lineament located near the dam site area (Figure 21). Gedney and Shapiro (1975) described the feature

as a fault based on differential K-Ar cooling data in the Talkeetna Mountains and seismicity. However, subsequent mapping by Csejtey et al. (1978) found no evidence for a major fault in the location of the Susitna lineament. The lineament is mapped near Butte Lake by Smith et al. (1988) and through the central Talkeetna Mountains near the dam site by Clautice (1990). Fault and lineament mapping by Wilson et al. (2009) shown no northeast trending faults in the vicinity of the Susitna lineament but do show several short lineament segments (5-7.5 mi [8-12 km]) that are adjacent to, and parallel with, the previously mapped lineament trace (Figure 13). WCC (1982) found the Susitna lineament to be a bedrock feature not related to faulting, except for possible erosion along a minor shear zone parallel to the fault. This conclusion was based on bedrock and surficial mapping, a magnetometer survey, and paleoseismic trenching along the trace of the lineament.

Glen et al. (2007b) describes the Susitna lineament as a series of 6-12 mi (10-20 km) long en echelon segments stepping eastward along strike to the north. They report east side down motion on the lineament which exposes Eocene volcanic rocks and Miocene and Oligocene sedimentary rocks in the Fog Lakes and Watana basins. O'Neill et al. (2003b and 2005) suggest that the en echelon pattern of the lineament may be the result dextral motion during post-accretion right-lateral bulk shear.

4.4.3 Shorter structures proximal to the dam site

In addition to the Talkeetna suture and the Susitna lineament, there are numerous northeast- and northwest-striking bedrock faults and lineaments in the Talkeetna block. Several of these structures, proximal to the Watana Dam site area (i.e. the northwest-striking shear zones ("Fins" feature and the Watana lineament)), were studied in detail by WCC (1982) and are discussed further in Section 9. Additional faults and lineaments are shown in mapping by Wilson et al. (2009) (Figure 13).

The northeast-southwest structures likely originated during Cretaceous accretionary deformation (Csejtey et al., 1978 and 1982; Ridgeway et al., 2002). Post-accretionary deformation driven by Tertiary right lateral bulk shear in the Talkeetna block has been proposed by several studies (O'Neil et al. 2005, Glen et al., 2007a and 2007b). These studies suggest that Tertiary transtensional deformation reactivated northeast-southwest oriented structures and produced several prominent grabens and half grabens including the Watana Creek lowland, and Fog Lakes lowland. Glen et al. (2007a) propose that the Fog Lakes lowland is bounded on the west by the Susitna lineament, and to the east by a series of range front normal faults (e.g. Talkeetna fault) defining a Fog Lakes graben (Figure 21 and 22).

4.5 Crustal Seismicity

4.5.1 Earthquake catalog

4.5.1.1 Earthquake data source and magnitudes

A catalog of earthquakes for the study area was compiled starting with the Alaska Earthquake Information Center (AEIC) earthquake catalog. The catalog contains earthquakes of magnitude 3.0 and above, down to a depth of 62 miles (100 km), and from 1899 through December 31, 2010. The base AEIC catalog was supplemented with the undeclustered (includes aftershock earthquakes) USGS catalog from the 2007 Alaska hazard maps (Wesson et al., 2007). In addition, the earthquake locations, depths, and/or magnitudes were updated using the results of relocation studies by Doser (2004), Doser and Brown (2002), Doser et al. (2002), Doser et al. (1999), and Ratchkovski et al. (2003). The AEIC catalog mb, ML, and MS magnitudes were converted to moment magnitude (M_w) following the relations of Ruppert and Hansen (2010), which apply to earthquakes from 1971 to the present. Earthquakes prior to 1971 were assigned M_w magnitudes according to: (1) the relocation studies noted above, (2) the 2007 USGS Alaska catalog, or (3) following the relation which agrees with the magnitudes used by the USGS. The updated catalog (Figure 23) was declustered (remove aftershocks) using the Gardner-Knopoff algorithm (Gardner and Knopoff, 1974). An aftershock exclusion zone was used to identify likely aftershocks of the 2002 Denali earthquake (Figure 24). Earthquakes within the exclusion zone, post-dating the 2002 event were removed from the catalog. The 2002 Denali earthquake itself is also removed from the catalog as it is directly associated with the Denali fault, and, therefore, is inappropriate to remain in the catalog database used to derive aerial source zone earthquake recurrence. This event is accounted for in hazard calculations through the characterization of the Denali fault discussed later in the report in Sections 5.3.1 and 5.4.3.

4.5.1.2 Earthquake magnitude completeness

In order to analyze catalog completeness as a function of magnitude, a “Stepp” plot was constructed which shows the event rate per year as a function of time since the present. This is shown in Figure 30 using 5-year bins, and indicates completeness for M 3 since 1970, M 4 and 5 since 1965, and M 6 since 1930. M 7 events are few, thus, completeness for these should rely on population density and reporting. Wesson et al. (2007) estimated completeness for M 4.5 since 1964, M 6 since 1932, and M 6.9 since

1898 for their Alaska catalog. Because the results shown in Figure 30 are consistent with Wesson et al. (2007) completeness estimates, the Wesson et al. (2007) completeness estimates are adopted for this study. The M 3 completeness since 1970 is consistent with seismic network information in Ruppert and Hansen (2010).

4.5.2 Stress data

The evaluation of crustal stresses can aid in the understanding of faulting styles in areas of limited fault data. Ruppert (2008) generated Alaskan stress maps and stress tensor inversions derived from earthquake focal mechanisms (Figures 25 and 26). The crustal stress data in the site region, south of the Denali fault and north of the Castle Mountain fault, is heterogeneous but largely consistent with a transpressional tectonic setting and dominantly reverse and strike-slip faulting. The best fitting maximum stress for the crustal data surrounding the dam site is near horizontal and oriented west-northwest, and the minimum and intermediate stresses are steeply plunging (Figure 26). This stress orientation is consistent with right-lateral oblique faulting on northeast-oriented structures such as the faults bounding the Fog Lakes graben.

4.5.3 Crustal source zones

Crustal thickness in the southern Alaska block (SAB) source zones is estimated to be 16 mi (25 km) in the West and Central zones, and 31 mi (50 km) in the East zone. However, the West and Central zones experience earthquakes associated with the subducting slab below 14 mi (23 km) depth (see Figure 27). The maximum depth for earthquakes in the recurrence catalog in the West and Central zones is reduced to 14 mi (23 km) to exclude these apparent slab events, but the source model for these zones allows earthquakes down to 16 mi (25 km), reflecting the uncertainty in crustal thickness. In comparison, WCC (1982) apparently used a seismogenic crustal thickness in their Talkeetna terrane of 12 mi (20 km). The Eastern zone is located off the northwest edge of the subducting slab so events as deep as 31 mi (50 km) are included in the recurrence catalog, and the source model allows for earthquakes down to 31 mi (50 km) as well.

The majority of seismicity in NFFTB zones is located above 12-mi (20-km) depth, and most events below 12 mi (20 km) have high vertical location errors (> 3 mi [5 km]) (see Figure 28), thus seismicity in the recurrence calculations is constrained to a maximum depth of 12 mi (20 km).

4.6 Earthquake Recurrence from Seismicity

Earthquake catalogs used for SAB and NFFTb areal source zone recurrence calculations are shown in Figure 29. Fewer earthquakes are shown in Figure 29 than in Figure 24 because of removal of some events after filtering for the completeness periods discussed in Section 4.5.1. The location of the 1912 Denali earthquake, as relocated by Doser (2004), is directly north of the Denali fault. Considering the large location error, the 1912 event conservatively is included in the SAB Central zone recurrence catalog instead of the NFFTb West zone. Figures 31 and 32 present the maximum likelihood recurrence curves for the SAB and NFFTb areal zones, respectively.

5.0 PROBABILISTIC SEISMIC HAZARD ANALYSIS METHODS AND INPUTS

5.1 PSHA Code and Methodology

The basic PSHA methodology employed here follows the precepts of Cornell (1968). The programs used were Fugro Consultants, Inc. codes *faultsource_31 version 3.1.228* for fault sources, *mrs5.2 version 5.2.228* for areal sources, and *agrid1.1 version 1.1.228* for gridded seismicity sources. Earlier versions of these codes were vetted under the PEER PSHA Code Verification Workshop (Wong et al., 2004).

5.2 GMPEs

Ground motion prediction equations (GMPEs) transform magnitude, distance, and other ground motion-related parameters into ground motion amplitude distributions for a wide range of vibrational frequencies. Such equations are continually being developed and refined as more strong motion accelerograms become available. For this project, three types of GMPEs were drawn upon: those for crustal sources, those for plate interface sources, and those for intraslab sources. The GMPEs and their weights for the three source categories were selected and are shown in Table 3.

For the megathrust and intraslab GMPEs BCH11 is preferred model because it is based on a much larger data set that includes all of the data used by Zhao et al. (2006), and uses the Atkinson and Macias (2009) simulation result to constrain the break in the magnitude scaling at high magnitudes. The Atkinson and Boore (2003) relation uses the “global” version, as opposed to the Cascadia version. The crustal source GMPEs consist of four NGA GMPEs, each weighted equally.

All of the GMPEs in Table 3 employ V_{s30} (average shear-wave velocity in the top 30 meters) as a site condition parameter for linear and non-linear site response, either explicitly or as a site category indicator. Based on the initial data review, the hazard is computed using a reference V_{s30} of 2,625 ft/s (800 m/s), as this is the range that is constrained by the empirical data, and adjustments to the site rock conditions value may be made after site characterization is complete. The 2,625 ft/s (800 m/s) is less than the estimates derived from measured P-wave velocities presented in the Acres (1982) report and summarized in Section 3.5. The P-wave derived velocity data from these reports are not included for the V_{s30} parameter in the GMPE’s due to the significant ambiguity in interpreting the velocity data from cross sections, and the potential error resulting from converting P-wave to S-wave velocity. The adopted value of 2,625 ft/s

(800 m/s) is considered a somewhat conservative velocity value that may be refined at a future date based on site-specific shear-wave data.

Table 3. Ground Motion Prediction Equations Used in PSHA

| Sources | GMPE | Abbreviation | Weight |
|------------|-------------------------------|--------------|--------|
| Megathrust | BC Hydro, 2011 ¹ | BCH11 | 0.50 |
| | Zhao et al., 2006 | ZH06 | 0.25 |
| | Atkinson and Macias, 2009 | AM09 | 0.25 |
| Intraslab | BC Hydro, 2011 ¹ | BCH11 | 0.50 |
| | Zhao et al., 2006 | ZH06 | 0.25 |
| | Atkinson and Boore, 2003 | AB03 | 0.25 |
| Crustal | Abrahamson and Silva (2008) | AS08 | 0.25 |
| | Chiou and Youngs (2008) | CY08 | 0.25 |
| | Campbell and Bozorgnia (2008) | CB08 | 0.25 |
| | Boore and Atkinson (2008) | BA08 | 0.25 |

Note: (1) as provided by N. Abrahamson, August 2011.

5.3 Sensitivity Evaluations

Initial development of the source model and discussions with the project reviewers identified several topics for sensitivity analyses or additional consideration at the early phase of the ground motion analysis in order to assess their implementation in the PSHA. The objective of these evaluations was to focus resources and efforts on issues that have the most direct implications for the site hazard evaluations. Topics identified were:

- Time dependent models for Alaska (Prince William Sound) megathrust Mw 9.2 and the 2002 Denali Mw 7.9 events
- Relative importance of crustal areal and fault zones vs. megathrust, (as shown by hazard curves for PHA and 1.0 sec)
 - Relative contributions of distant crustal sources
 - Implications of additional seismic sources within the Southern Alaska block and Talkeetna Terrane
- Sensitivity to depth in NGA GMPEs, implications

-
- Deterministic megathrust response spectra

5.3.1 Time dependence

Models compared for the time-dependent vs. time-independent sensitivity include: Poissonian (time independent model - needs only return period, rate always the same); Lognormal distribution of inter-event times (time-dependent) model - needs median and standard deviation values; Brownian passage time (BPT) (time-dependent) – model needs median and aperiodicity parameter, similar to lognormal standard deviation. These are described more in Appendix A.

The results of the time-dependent vs. time-independent calculations show that the probability of occurrence of a repeat of the 1964 M 9.2 event in the 150 year time window is less than 0.05 for the time-dependent models, while for the Poissonian rate it is 0.24. Similarly, for a repeat of the 2002 Denali fault rupture, time-dependent probabilities of occurrence are less than 0.06, while the Poissonian probability is 0.31.

Conversely, the western Denali fault that did not rupture in 2002 has a time-dependent probability of occurrence in 150 years of 0.5 to 0.6, while under the time-independent assumption the probability would be 0.33. The time-dependent models are assigned a weight of 0.67, and the non-time-dependent model 0.33.

5.3.2 Relative contributions of sources and distance

Initial evaluations, completed as part of this study, confirmed by the PSHA results (Section 6.1), indicate that the dominant seismic sources for the Susitna-Watana Dam site area are the two subduction related sources: subduction interface, and intraslab. Crustal sources are less significant. These initial evaluations also indicate that, given the relatively high slip rates and magnitudes associated with the Denali and Castle Mountain fault sources, crustal fault sources at greater distances with similar or smaller magnitudes would not provide significant contributions to the hazard for the site. Thus, fault sources more distant than the Denali and Castle Mountain faults were not considered further for the PSHA calculations.

Although initial evaluation suggested that dominant hazard contributions would be from the subduction related sources, the potential impacts of crustal fault sources in the Talkeetna Terrain region near the site were considered as well. The potential impacts of additional crustal sources in this region can be evaluated through comparisons of the contributions of fault sources in this region such as the Sonoma Creek fault and Fog Lakes graben faults to background crustal seismicity and the subduction-related

sources. These crustal sources were included in the PSHA to illustrate this sensitivity as discussed in Section 5.4 below.

5.4 PSHA Inputs

5.4.1 Subduction related sources

For the purposes of this study, the megathrust, or plate interface, geometry is modeled as a single plane (seen as the rectangle in Figure 15) dipping 2.6 degrees to the northwest with upper (southeast) and lower (northwest) depth bounds of 12 and 22 mi (20 and 35 km). This geometry also roughly corresponds to the estimated rupture extent of the 1964 event (Figure 5). The geometric parameters of this plane, including distances to the site, are listed in Table 5.

Following Wesson et al. (2007), the largest megathrust event is modeled as a repeat of the M 9.2 1964 event. A time-independent (Poissonian) annual rate of 1/560 is assigned, based on paleoseismic investigations (Carver and Plafker, 2008). The final rate of this magnitude event has been ultimately decreased due to inclusion of time-dependent models, described in Appendix A.

Also following Wesson et al. (2007), the M 7-8 interface earthquakes are modeled as being exponentially distributed according to rates calculated from the Wesson et al. (2007) earthquake catalog. This catalog resulted from a hierarchical compilation of several catalogs, resolution of magnitudes to the Mw scale, and declustering to remove dependent events. The a and b Gutenberg-Richter recurrence values for this source were taken from Wesson et al. (2007). Earthquakes in this magnitude range were modeled as occurring on the fault plane shown in Figure 15. The interface earthquakes in the M 5-7 range are modeled as “gridded, smoothed seismicity.” As described in Wesson et al. (2007), this model is created by sorting this seismicity into 0.1 degree bins, and performing Gaussian smoothing with a correlation distance (Frankel et al., 1995) of 46 mi (75 km) (Figures 16 and 17). The grid sources were placed at a depth of 3 mi (5 km), as in Wesson et al. (2007). Although this depth is not realistic, given that the megathrust lies 12 to 19 miles (20 to 30 km) beneath the site, this depth was retained to maintain consistency with the Wesson et al. (2007) model. The geometry is modeled as a single plane (seen as the rectangle in Figure 15) dipping 2.6 degrees to the northwest with upper (southeast) and lower (northwest) depth bounds of 12 and 22 mi (20 and 35 km). This geometry also roughly corresponds to the estimated rupture extent of the 1964 event (Figure 5). The geometric parameters of this plane, including

distances to the site, are listed in Table 5. Time-dependent models and their usage for this source are described in Appendix A.

5.4.2 Interslab sources

For the intraslab source we have used the Wesson et al. (2007) model, which consists of gridded seismicity for two depth levels, 31 to 50 mi (50-80 km), and 50 to 75 mi (80-120 km), and a magnitude range of M 5 to M 7.5. Following Wesson et al. (2007), the depth for the 31 to 50 mi (50-80 km) sources was set to 37 mi (60 km), and 56 mi (90 km) for the 50 to 75 mi (80-120 km) points.

5.4.3 Crustal faults

Five crustal faults are included in the PSHA with the source characterization parameters contained in Table 6. Two of these faults, the Denali and Castle Mountain, have been included in the previous USGS source model (Wesson et al., 2007). Based on data discussed in Section 4.2, the source characterizations for these faults have been updated, and include time-dependent alternatives for the Denali fault, as well. The Pass Creek-Dutch Creek fault was not included in the USGS source model, but previously was identified as a Quaternary fault in Plafker et al. (1994). A conservative slip rate distribution is included for this fault based on the data discussed in Section 4.2.3. The Sonona Creek and Fog Lakes graben are potential sources within the Southern Alaska block newly considered in this evaluation because of their potential proximity to the Susitna-Watana Dam site. Evidence to support full seismic source characterization for both sources is incomplete. There are no published estimates for Quaternary displacement on either of these faults. However, the structures are included in this evaluation with a full probability of activity, to test the sensitivity of their inclusion to the hazard estimates for the site. Thus, slip rate distributions for these sources span about 2 orders of magnitude, and range from 0.01 to 0.3 mm/yr to test a range of values that would reflect relative inactivity to an activity rate which is similar to the lower range of slip rates on the Castle Mountain fault.

The Sonona Creek fault was identified based on mapping by Williams and Galloway (1986), and a simplified source trace extended from that mapping based on limited evaluation of Google Earth imagery (Figure 20). The source characterization assumes a relatively low slip rate based on the limited extent and apparently small height of the scarp shown on the Williams and Galloway (1986) map. Fault length was extended to provide sufficient length for fault rupture consistent with the M 7 assumed for the initial maximum event.

The Fog Lake graben structures also are included as a sensitivity test to the potential reactivation of existing structures within the vicinity of the Talkeetna thrust/Susitna lineament region near the site. An M 7 is assumed as a maximum event for this test, and fault-element length was chosen to accommodate rupture for this size event. The fault-element locations are based on the geomorphic expression along the ranges bounding the Fog Lakes graben, as generally outlined by Glen et al. (2007a). Slip rates are considered low, with the assumption that rates in excess of about 0.5 – 1 mm/yr would produce readily identifiable geomorphic evidence of faulting.

Several additional sources discussed in Section 4, including faults at distances greater than about 56 mi (90 km) from the site, were not included as seismic elements in the source model (Table 4). These crustal faults were not included based on initial evaluations (Section 5.3.2) that indicated that inclusion into the seismic source model and PSHA would have negligible impact on the computed hazard at the site. Existing data suggests all of the excluded faults would have contributions that were no greater than those of the Castle Mountain fault, because maximum magnitudes and slip rates are generally lower, and closest distances to the site are greater. The Castle Mountain fault does not appear on Figures 39 – 42 because its contribution is less than 5 percent, even with inclusion of potentially conservative slip-rate scenarios as discussed in Section 5.4.3.2. Thus, other faults in the region, including subsidiary faults to the Denali fault similar to the Susitna Glacier fault, would not be expected to have significant contributions to the ground motions at the Susitna-Watana site area unless slip rates on these faults were comparable or higher than those used in the present model for the Castle Mountain fault.

Fault sources are modeled as one or more planar segments. The faults as modeled for the PSHA are shown in map view on Figure 33.

Table 4. Site Region Faults Excluded from the PSHA Source Model

| Fault Name | Distance from Site (km) | Distance from Site (miles) |
|----------------------------------------------------------------------------|-------------------------|----------------------------|
| Faults in the Southern Alaska Block – South of Denali fault | | |
| Broad Pass fault | 63.8 | 39.6 |
| Broxson Gulch fault | 62.6 | 38.9 |
| Bull River fault | 78.2 | 48.6 |
| Cathedral Rapids fault | 244.1 | 151.7 |
| East Boulder Creek fault | 101.6 | 63.1 |
| Foraker fault | 135.5 | 84.2 |
| Matanuska Glacier fault | 136.4 | 84.8 |
| McCallum-Slate Creek fault | 153.9 | 95.6 |
| McGinnis Glacier fault | 147.0 | 91.3 |
| Susitna Glacier fault | 77.8 | 44.1 |
| Faults in the Northern fold and thrust belt – North of Denali fault | | |
| Billy Creek fault | > 70 | > 45 |
| Canteen fault | > 70 | > 45 |
| Ditch Creek fault | > 70 | > 45 |
| Donnelly Dome fault | > 70 | > 45 |
| Dot "T" Johnson fault | > 70 | > 45 |
| East Fork fault | > 70 | > 45 |
| Eva Creek fault | > 70 | > 45 |
| Glacier Creek fault | > 70 | > 45 |
| Gold King fault - Section A | > 70 | > 45 |
| Gold King fault - Section B | > 70 | > 45 |
| Granite Mountain fault A | > 70 | > 45 |
| Granite Mountain fault B | > 70 | > 45 |
| Healy Creek fault | > 70 | > 45 |
| Kansas Creek fault | > 70 | > 45 |
| Macomb Plateau fault | > 70 | > 45 |
| Molybdenum Ridge fault | > 70 | > 45 |
| Mystic Mountain fault | > 70 | > 45 |
| Northern Foothills thrust | > 70 | > 45 |
| Panoramic fault | > 70 | > 45 |
| Park Road fault | > 70 | > 45 |
| Peters Dome fault | > 70 | > 45 |
| Potts fault | > 70 | > 45 |
| Red Mountain fault | > 70 | > 45 |
| Rex fault | > 70 | > 45 |
| Stampede fault | > 70 | > 45 |
| Trident fault | > 70 | > 45 |
| Trident Glacier fault | > 70 | > 45 |

5.4.3.1 *Denali fault*

The occurrence of an M 7.9 earthquake on the Denali fault in 2002 (Section 3.2.1) led to a number of scientific investigations that greatly improved the characterization of this fault for seismic hazard studies.

As shown in Figure 33, two geometric models are considered for this study: one in which a repeat of the 2002 rupture occurs and the segment to the west ruptures independently; and another model in which the entire fault length ruptures. Each of these scenarios has a maximum magnitude of 7.9, and a maximum moment model is used for each (Table 6). The two scenarios are weighted equally.

Following Wesson et al. (2007), the modeled slip on the Denali fault decreases monotonically from 14.4 mm/yr at the east end to zero at the west end. The estimated slip rate as a function of distance along the fault is shown in Figure 18. This was accounted for in the PSHA as follows: In modeling ruptures on a fault, a rupture that has less area than the fault itself is assumed to occur at any location with equal probability. Such ruptures are modeled by placing them sequentially along strike and up and down dip with some spacing interval (0.6 mi [1 km] in this study). A rupture will consequently correspond to a portion of the fault along the x-axis in Figure 18. The slip rate assigned to that rupture will, therefore, be the average slip rate along that portion of the fault. Alternative models of the Denali fault in which the fault extends farther west are not considered, because these models would primarily extend the fault beyond 200 mi (320 km) from the site and the initial sensitivity evaluations (Section 4.3.2) indicate no significant change in the ground motion results from this type of change to the source model.

Time-dependent occurrence rate models also were employed for the Denali fault. The rationale is that since the 2002 rupture occurred so recently, another such event should be less likely than the average rate in the near future. By similar reasoning, an earthquake on the segment west of the 2002 rupture, which hasn't occurred for about 600 years, is more likely to occur in the near future than the average. Details and results of the time-dependent analysis are contained in Appendix A.

5.4.3.2 *Castle Mountain fault*

The Castle Mountain fault, described in Section 4.2.2, is modeled as two scenarios: a segmented model where the east and west segments rupture independently, and an unsegmented model where the entire fault length ruptures in one earthquake. The fault geometry and location are shown in Figure 33. These scenarios are weighted equally.

To account for the uncertainty of the western segment slip rate (ie. Haeussler et al., 2002; Koehler and Reger, 2011; Willis et al., 2007) two slip-rate scenarios are used (Table 6), also equally weighted. The higher slip-rate scenario reflects the rates used in prior USGS hazard models (Wesson et al., 2007), while the lower slip-rate scenario reflects more recent investigations (e.g., Koehler and Reger, 2011).

5.4.3.3 Pass Creek-Dutch Creek fault, Sonona fault, and Fog Lake Graben faults

The Pass Creek-Dutch Creek, Sonona, and Fog Lake graben faults are described in Sections 4.2.3, 4.2.6, and 4.4.3, respectively, and shown in map view in Figure 33. Their geometric properties are listed in Table 5, and maximum magnitudes and slip-rate distributions in Table 6. No alternative models were employed for these sources.

Table 5. Geometric Fault Parameters for Susitna Source Model, as Modeled for PSHA

| Fault | Length (km) | Area ¹ (km ²) | Depth Range (km) | Dip | Rupture Distance ² (km) | JB Distance ³ (km) | Farthest Distance (km) |
|----------------------------------|-------------|--------------------------------------|------------------|------|------------------------------------|-------------------------------|------------------------|
| ASZ - megathrust interface model | 319.9 | 102,500 | 20.0 to 35.0 | 2.6 | 78.4 | 70.2 | 529.4 |
| Denali - 2002 rupture | 307.5 | 4612 | 0.0 to 15.0 | 90.0 | 86.0 | 86.0 | 312.3 |
| Denali - West segment | 386.4 | 5795 | 0.0 to 15.0 | 90.0 | 71.2 | 71.2 | 324.0 |
| Denali - entire fault | 726.0 | 10,889 | 0.0 to 15.0 | 90.0 | 71.2 | 71.2 | 356.5 |
| Castle Mtn fault | 189.6 | 3856 | 0.0 to 20.0 | 80.0 | 99.8 | 97.8 | 186.1 |
| Castle Mtn West fault high | 61.4 | 1253 | 0.0 to 20.0 | 80.0 | 136.9 | 135.4 | 186.1 |
| Castle Mtn West fault low | 61.4 | 1253 | 0.0 to 20.0 | 80.0 | 136.9 | 135.4 | 186.1 |
| Castle Mtn East fault | 128.2 | 2602 | 0.0 to 20.0 | 80.0 | 99.8 | 97.8 | 138.0 |
| Pass Creek-Dutch Creek fault | 65.6 | 1552 | 0.0 to 20.0 | 60.0 | 106.8 | 104.9 | 170.4 |
| Sonona fault | 36.9 | 749 | 0.0 to 20.0 | 80.0 | 71.5 | 69.2 | 91.6 |
| Fog Lake graben north | 60.9 | 1230 | 0.0 to 20.0 | 80.0 | 6.9 | 3.5 | 49.4 |
| Fog Lake graben south | 47.7 | 969 | 0.0 to 20.0 | 80.0 | 9.5 | 6.1 | 34.3 |

Notes: (1) Magnitude-area formula for strike-slip faults from UCERF2 (Field et al., 2009), all others from Wells & Coppersmith (1994). (2) Rupture distance is the closest distance to the fault plane. (3) Joyner-Boore distance is the closest horizontal distance to surface projection of the fault plane.

Table 6. Fault Slip Rate and Magnitude Parameters, as Modeled for PSHA

| Fault | Slip Rate (mm/yr) | Mean (mm/yr) | Slip Rate Distribution Type | Maximum Magnitude |
|----------------------------------------|--------------------------------------------------|--------------|-----------------------------|-------------------|
| Denali System | | | | |
| Unsegmented | 0.0 – 14.4 | N/A | tapered ² | 7.9 |
| West of 2002 rupture segment | 9.8 – 0.0 | N/A | tapered ² | 7.9 |
| 2002 rupture segment ¹ | 14.4 – 9.8 | N/A | tapered ² | 7.9 |
| Eastern segment | Not modeled separately due to distance from site | | | |
| Southern Alaska Crustal faults | | | | |
| Sonona Creek | 0.1 – 0.5 | 0.3 | triangle,sym | 7.0 |
| Pass Creek – Dutch Creek | 0.5 – 1.5 | 1.0 | triangle,sym | 7.0 |
| Fog Lake graben north | 0.01 – 0.3 (0.1) ³ | 0.14 | triangle,asym ³ | 7.0 |
| Fog Lake graben south | 0.01 – 0.3 (0.1) ³ | 0.14 | triangle,asym ³ | 7.0 |
| Castle Mountain fault scenarios | | | | |
| Segmented Model (weight 0.5) | | | | |
| Castle Mtn east | 0.5 | 0.5 | none | 7.2 |
| Castle Mtn west (weight 0.5) | 0.4 – 0.6 | 0.5 | uniform | 7.2 |
| Castle Mtn west (weight 0.5) | 2.1 – 3.6 | 2.9 | uniform | 7.2 |
| Unsegmented Model (weight 0.5) | | | | |
| Castle Mtn combined | 0.4 – 0.6 | 0.5 | triangle,sym | 7.6 |

Notes: (1) 2002 rupture segment includes the 72 km of the Totschunda fault ruptured in 2002. (2) See Figure 18. (3) Apex value for asymmetric triangular distribution in parentheses.

Table 7. Areal Zone Discrete Depth Distributions

| Depth (km) | Southern Areal Background | | | | | | Northern Foothills Fold and Thrust Belt | | | |
|------------|---------------------------|--------|------------------|--------|---------------|-------------------|-----------------------------------------|--------|---------------|--------|
| | West (n = 72) | | Central (n = 81) | | East (n = 18) | | West (n = 233) | | East (n = 18) | |
| | Count | Weight | Count | Weight | Count | Weight | Count | Weight | Count | Weight |
| 2.5 | 22 | 0.31 | 17 | 0.21 | 1 | 0.06 | 13 | 0.06 | 8 | 0.44 |
| 7.5 | 22 | 0.31 | 19 | 0.23 | 3 | 0.16 ¹ | 64 | 0.27 | 6 | 0.33 |
| 12.5 | 18 | 0.25 | 25 | 0.31 | 2 | 0.10 ¹ | 109 | 0.47 | 3 | 0.17 |
| 17.5 | 9 | 0.12 | 15 | 0.19 | 9 | 0.50 | 47 | 0.20 | 1 | 0.06 |
| 22.5 | 1 | 0.01 | 5 | 0.06 | 1 | 0.06 | - | - | - | - |
| 27.5 | - | - | - | - | 1 | 0.06 | - | - | - | - |
| 32.5 | - | - | - | - | - | - | - | - | - | - |
| 37.5 | - | - | - | - | - | - | - | - | - | - |
| 42.5 | - | - | - | - | - | - | - | - | - | - |
| 47.5 | - | - | - | - | 1 | 0.06 | - | - | - | - |

Note: (1) weight reduced by 0.01 to account for rounding so the full weight = 1.0.

6.0 PSHA RESULTS

6.1 Hazard Curves

A hazard curve consists of a ground motion level (in g) on the x-axis, and the mean annual frequency of exceeding that ground motion on the y-axis. Mean hazard curves were developed for four spectral response periods, peak horizontal acceleration (PHA), and 0.5, 1.0, and 3.0 seconds acceleration response at 5% damping. These are shown in Figures 34 through 37. The major sources have been grouped together for purposes of presentation. For example, the interface curve contains the sum of the hazard from the three magnitude ranges described in Section 5.3.1, and the hazard from the M 9.2 scenario. Similarly, the combined hazard is shown for the Denali and Castle Mountain fault scenarios, the two Fog Lake graben fault elements, and the five areal sources.

6.2 UHS

A uniform hazard spectrum (UHS) is developed from the suite of total hazard curves, each of which is calculated for a specific spectral period (or its inverse, spectral frequency) at the specified damping level. The spectrum is keyed to a return period, which is the inverse of annual frequency of exceedance. For example, to construct a 10,000-year uniform hazard spectrum, the ground motion level for PHA (0.00 or 0.01 spectral period) at the 0.0001 (1/10,000) y-axis level of that hazard curve is tabulated. The same is done for the hazard for the other spectral periods. The spectral period is then plotted on the x-axis, and the tabulated ground motion level on the y-axis. These spectra, therefore, indicate the ground motion amplitudes across the entire range of periods for a common hazard level.

Mean uniform hazard spectra for the total hazard were developed for return periods of 100, 250, 1000, 2,500, 5,000, and 10,000 years. These results are shown in Figure 38, values are provided in Table 8, and also in Appendix C.

6.3 Deaggregations

A deaggregation of the ground motion hazard was performed, based on the principles outlined in McGuire (1995) and Bazzurro and Cornell (1999). Bazzurro and Cornell (1999) provide a comparative review of different techniques and their implications. They point out that there is a tradeoff between matching the target spectrum precisely, and identifying the most likely event to produce the target motions. McGuire's (1995) method of collecting contributions that *equal* the target motion for each GMPE was

applied here, and the deaggregation therefore is focused on matching the target spectrum.

Source deaggregation plots are shown in Figures 39 through 42, one for each of the four spectral response periods (PHA, 0.5 sec, 1.0 sec, 3.0 sec). Only sources contributing 5% or more at any ground motion level are plotted, so the minor sources are not shown. In Figures 39 through 42, the 100- and 10,000-year ground motion levels are shown, and in some cases, intermediate return periods. These values can be found in the appropriate cell in Table 8.

Table 8. Total Hazard, Mean Probabilistic Acceleration Amplitudes (g)

| Period (sec) | 100 yrs | 250 yrs | 1,000 yrs | 2,500 yrs | 5,000 yrs | 10,000 yrs |
|---------------------|----------------|----------------|------------------|------------------|------------------|-------------------|
| 0.01 | 0.1270 | 0.1991 | 0.3671 | 0.5222 | 0.6641 | 0.8271 |
| 0.02 | 0.1397 | 0.2184 | 0.3997 | 0.5662 | 0.7179 | 0.8918 |
| 0.03 | 0.1578 | 0.2467 | 0.4506 | 0.6370 | 0.8064 | 1.0004 |
| 0.05 | 0.1855 | 0.2898 | 0.5275 | 0.7437 | 0.9394 | 1.1631 |
| 0.075 | 0.2417 | 0.3784 | 0.6914 | 0.9807 | 1.2461 | 1.5527 |
| 0.10 | 0.2895 | 0.4545 | 0.8344 | 1.1897 | 1.5184 | 1.9008 |
| 0.15 | 0.3007 | 0.4732 | 0.8782 | 1.2609 | 1.6152 | 2.0264 |
| 0.20 | 0.2780 | 0.4383 | 0.8181 | 1.1764 | 1.5067 | 1.8874 |
| 0.25 | 0.2430 | 0.3837 | 0.7175 | 1.0325 | 1.3231 | 1.6586 |
| 0.30 | 0.2140 | 0.3391 | 0.6373 | 0.9200 | 1.1816 | 1.4844 |
| 0.40 | 0.1717 | 0.2746 | 0.5204 | 0.7540 | 0.9703 | 1.2201 |
| 0.50 | 0.1387 | 0.2233 | 0.4255 | 0.6179 | 0.7969 | 1.0038 |
| 0.75 | 0.0938 | 0.1532 | 0.2963 | 0.4351 | 0.5661 | 0.7209 |
| 1.0 | 0.0713 | 0.1179 | 0.2304 | 0.3421 | 0.4496 | 0.5791 |
| 1.5 | 0.0466 | 0.0774 | 0.1529 | 0.2305 | 0.3085 | 0.4054 |
| 2.0 | 0.0345 | 0.0569 | 0.1125 | 0.1709 | 0.2313 | 0.308 |
| 3.0 | 0.0221 | 0.0364 | 0.0713 | 0.1093 | 0.1490 | 0.1995 |

The PHA hazard is dominated by the Alaska subduction zone intraslab at all return periods (Figure 39). This reflects the high rate of M 5 – 7.5 events produced by this source. The results are mixed for the 0.5 spectral acceleration (SA), with intraslab seismicity dominating at return periods less than 2,500 years, and megathrust seismicity dominating at longer periods (Figure 40). A similar result occurs for the 1.0 second SA, but with megathrust activity dominating for the 1,000-year return period and longer (Figure 41). For 3.0-second response SA, the Alaska subduction zone sources, Denali fault, and areal sources contribute equally for the 100 year return period, but the Alaska subduction zone megathrust dominates at all longer return periods (Figure 42).

Plots showing magnitude, distance, and epsilon contributions to the total hazard were produced for the two major sources (the Alaska subduction zone interface and intraslab), for three return periods (2,500, 5,000, and 10,000 years). Epsilon is the number of standard deviations above or below the median, from which a ground motion amplitude (for a given magnitude and distance) is contributing. Three GMPEs for each source, combined with four spectral response periods, results in 24 total hazard plots. While all are contained in Appendix C, four plots are discussed in this report body for characterization purposes. The four plots are described below.

Figure 43 shows megathrust results for PHA, 2,500-year return period, and the BC Hydro 2011 GMPE. The plot shows the dominant contribution from the M 9.2 earthquake, with minor contributions from M 7 events. Figure 44 shows the same results, but for 1.0-second response and a return period of 10,000 years. For these results, the distance to the megathrust is evident, 48 mi (78 km) or greater. Figure 45 shows contributions to the total hazard from the intraslab source, for 0.5-second response, 2,500-year return period, and the Zhao et al. (2006) GMPE. Since the dam site lies above this source, an exponential-appearing decrease with distance is evident. An exponential-appearing decrease also is seen with magnitude, because the magnitudes have an exponential rate distribution. Figure 46 shows the same source and GMPE, but for 3.0-second response and a 10,000-year return period. This plot shows that the intraslab contributions are coming only from higher magnitude events near the site, at the extreme tails of the ground motion distributions.

7.0 CONDITIONAL MEAN SPECTRA

Conditional mean spectra (CMS) were generated for 3 return periods and 4 acceleration response spectral periods (5% damping). As described in the PSHA results (Section 6.3 Deaggregation), the two dominant sources for all spectral response periods and return periods of 2,500 years and greater are the megathrust and intraslab sources of the Alaska subduction zone. CMS were developed for those sources.

The following sections consist of a description of the methodology used to develop the CMS, and the results. The UHS and CMS data are shown on figures in Appendix C.

7.1 Methodology

The methodology of Baker (2011) was used to develop the CMS. CMS are generated from deterministic spectra based on the PSHA deaggregation results, which for each reference spectral period (T^*) and return period, consist of a magnitude, distance, and epsilon. Epsilon is the number of standard deviations from the median ground motion from the ground motion prediction equation (GMPE) required to match the target UHS value.

This combination of parameters should match the UHS target motion at T^* . In actual practice, however, the match is never exact, due to the fact that the deaggregation procedure requires establishment of bins that account for a range of parameter values, rather than exact ones. The deaggregation values are the modal bin averages (Bazzurro and Cornell, 1999). In addition, a seismic source often consists of a group of sources, and the deaggregation values represent the composite result of those sources. Therefore the epsilon for the CMS T^* must be adjusted so that the amplitude at T^* equals the UHS at T^* . This new epsilon is termed $\varepsilon(T^*)$ in Baker (2011). CMS are computed for each GMPE, and weighted in the same manner as for the UHS.

The deterministic spectrum is then modified by first multiplying the period and T^* dependent correlation coefficients by $\varepsilon(T^*)$:

$$\mu_{\varepsilon(T_i)\varepsilon(T^*)} = \rho(T_i, T^*)\varepsilon(T^*) \quad (\text{Equation 4, Baker (2011)})$$

This is called the “conditional mean epsilon.” This, multiplied by the period-dependent sigma, is then added to the log of the median deterministic ground motion:

$$\mu_{\ln Sa(T_i)|\ln Sa(T^*)} = \mu_{\ln Sa}(M, R, T_i) + \rho(T_i, T^*)\varepsilon(T^*)\sigma_{\ln Sa}(T_i)$$

It should be noted that the correlation coefficient formulation of Baker and Jayaram (2008), which was developed for the Next Generation Attenuation (NGA) GMPEs and based on the intra-event residuals, was used here. This assumes that the correlation coefficients for the total residuals for the GMPEs used for this study will be similar. Al Atik (2011) showed that the correlations developed by Baker and Jayaram (2008) are similar to the correlation coefficients for the intra-event residuals for the BC Hydro subduction model GMPE. Al Atik (2011) showed that the correlations of the intra-event residuals are reasonable approximations for the correlations of the total residuals.

The magnitude, distance, and epsilon values for the T* values (0, 0.5, 1.0 and 3.0 seconds) and the three return periods (2500, 5000, and 10,000 years) are shown in deaggregation Tables 9 through 11 for interface fault source, and Tables 12 through 14 for the intraslab source. There is one table for each of the GMPE used in this study. See Section 5.2 and Table 3 for discussion of the GMPE's and acronyms. The magnitude-distance-epsilon values used are the modal bin values in the "Mod_MDE" column, as recommended by Bazzurro and Cornell (1999). CMS results from the GMPEs were interpolated to a common period set, and weighted as in Table 8.

As recommended in the FERC guidance (Idriss and Archuleta, 2007), the CMS were "extended" so that the envelope of the CMS for a given return period equaled the UHS. This is to assure that there are no gaps in CMS replication of the UHS.

Because two of the critical response periods, PHA (T = 0.0 or 0.01) and 3.0 seconds, lie at the ends of the UHS range, the manner in which the CMS are "extended" to fill in the UHS is ambiguous. For example, the period range from 0 to 0.5 seconds can be accounted for by raising either the 0.0- or 0.5-second period CMS to the UHS level. On the long period end of the spectrum, the 1.0- to 3.0-second range can be "filled in" by either the 1.0- or 3.0-second CMS. Therefore, CMS were computed for both alternatives.

Table 9. Megathrust - Deaggregation Results for AM09

| GMPE | Period | RP | Mbar | Dbar | Epsbar | Mod_MD | Mod_MDE |
|------|--------|------|------|------|--------|-------------|--------------------|
| am09 | 0 | 2.5k | 9.2 | 78.4 | 1.81 | 9.25 - 77.5 | 9.25 - 77.5 - 1.90 |
| am09 | 0 | 5k | 9.2 | 78.4 | 2.25 | 9.25 - 77.5 | 9.25 - 77.5 - 2.30 |
| am09 | 0 | 10k | 9.2 | 78.4 | 2.65 | 9.25 - 77.5 | 9.25 - 77.5 - 2.70 |
| am09 | 0.5 | 2.5k | 9.16 | 78.8 | 1.12 | 9.25 - 77.5 | 9.25 - 77.5 - 1.10 |
| am09 | 0.5 | 5k | 9.19 | 78.4 | 1.5 | 9.25 - 77.5 | 9.25 - 77.5 - 1.50 |
| am09 | 0.5 | 10k | 9.2 | 78.4 | 1.86 | 9.25 - 77.5 | 9.25 - 77.5 - 1.90 |
| am09 | 1 | 2.5k | 9.06 | 81 | 0.67 | 9.25 - 77.5 | 9.25 - 77.5 - 0.50 |

| GMPE | Period | RP | Mbar | Dbar | Epsbar | Mod_MD | Mod_MDE |
|------|--------|------|------|------|--------|-------------|---------------------|
| am09 | 1 | 5k | 9.14 | 79.1 | 0.99 | 9.25 - 77.5 | 9.25 - 77.5 - 0.90 |
| am09 | 1 | 10k | 9.18 | 78.5 | 1.33 | 9.25 - 77.5 | 9.25 - 77.5 - 1.30 |
| am09 | 3 | 2.5k | 8.79 | 85.2 | -0.5 | 9.25 - 77.5 | 9.25 - 77.5 - -1.10 |
| am09 | 3 | 5k | 9.01 | 80.8 | -0.23 | 9.25 - 77.5 | 9.25 - 77.5 - -0.50 |
| am09 | 3 | 10k | 9.12 | 79.1 | 0.16 | 9.25 - 77.5 | 9.25 - 77.5 - 0.10 |

Table 10. Megathrust - Deaggregation Results for BCH11T

| GMPE | Period | RP | Mbar | Dbar | Epsbar | Mod_MD | Mod_MDE |
|--------|--------|------|------|------|--------|-------------|--------------------|
| bch11T | 0 | 2.5k | 9.16 | 79.2 | 1.03 | 9.25 - 77.5 | 9.25 - 77.5 - 0.90 |
| bch11T | 0 | 5k | 9.18 | 78.7 | 1.32 | 9.25 - 77.5 | 9.25 - 77.5 - 1.30 |
| bch11T | 0 | 10k | 9.19 | 78.5 | 1.6 | 9.25 - 77.5 | 9.25 - 77.5 - 1.50 |
| bch11T | 0.5 | 2.5k | 9.15 | 79.3 | 0.88 | 9.25 - 77.5 | 9.25 - 77.5 - 0.90 |
| bch11T | 0.5 | 5k | 9.17 | 78.7 | 1.19 | 9.25 - 77.5 | 9.25 - 77.5 - 1.10 |
| bch11T | 0.5 | 10k | 9.19 | 78.5 | 1.48 | 9.25 - 77.5 | 9.25 - 77.5 - 1.50 |
| bch11T | 1 | 2.5k | 9.15 | 79.3 | 0.8 | 9.25 - 77.5 | 9.25 - 77.5 - 0.70 |
| bch11T | 1 | 5k | 9.18 | 78.7 | 1.13 | 9.25 - 77.5 | 9.25 - 77.5 - 1.10 |
| bch11T | 1 | 10k | 9.19 | 78.5 | 1.45 | 9.25 - 77.5 | 9.25 - 77.5 - 1.50 |
| bch11T | 3 | 2.5k | 9.18 | 78.7 | 0.94 | 9.25 - 77.5 | 9.25 - 77.5 - 0.90 |
| bch11T | 3 | 5k | 9.19 | 78.4 | 1.33 | 9.25 - 77.5 | 9.25 - 77.5 - 1.30 |
| bch11T | 3 | 10k | 9.2 | 78.4 | 1.7 | 9.25 - 77.5 | 9.25 - 77.5 - 1.70 |

Table 11. Megathrust - Deaggregation Results for ZH06T

| GMPE | Period | RP | Mbar | Dbar | Epsbar | Mod_MD | Mod_MDE |
|-------|--------|------|------|------|--------|--------|--------------------|
| zh06T | 0 | 2.5k | 9.19 | 78.5 | 0.63 | 9.25 - | 9.25 - 77.5 - 0.70 |
| zh06T | 0 | 5k | 9.2 | 78.4 | 0.97 | 9.25 - | 9.25 - 77.5 - 0.90 |
| zh06T | 0 | 10k | 9.2 | 78.4 | 1.29 | 9.25 - | 9.25 - 77.5 - 1.30 |
| zh06T | 0.5 | 2.5k | 9.18 | 78.8 | 0.54 | 9.25 - | 9.25 - 77.5 - 0.50 |
| zh06T | 0.5 | 5k | 9.19 | 78.5 | 0.88 | 9.25 - | 9.25 - 77.5 - 0.90 |
| zh06T | 0.5 | 10k | 9.2 | 78.4 | 1.2 | 9.25 - | 9.25 - 77.5 - 1.10 |
| zh06T | 1 | 2.5k | 9.17 | 79 | 0.29 | 9.25 - | 9.25 - 77.5 - 0.30 |
| zh06T | 1 | 5k | 9.19 | 78.6 | 0.63 | 9.25 - | 9.25 - 77.5 - 0.70 |
| zh06T | 1 | 10k | 9.2 | 78.4 | 0.96 | 9.25 - | 9.25 - 77.5 - 0.90 |
| zh06T | 3 | 2.5k | 9.18 | 78.8 | 0.12 | 9.25 - | 9.25 - 77.5 - 0.10 |
| zh06T | 3 | 5k | 9.19 | 78.5 | 0.51 | 9.25 - | 9.25 - 77.5 - 0.50 |
| zh06T | 3 | 10k | 9.2 | 78.4 | 0.9 | 9.25 - | 9.25 - 77.5 - 0.90 |

Table 12. Intraslab- Deaggregation Results for AB03Ib

| GMPE | Period | RP | Mbar | Dbar | Epsbar | Mod_MD | Mod_MDE |
|--------|--------|------|------|------|--------|-------------|--------------------|
| ab03Ib | 0 | 2.5k | 7.33 | 84.9 | 1.8 | 7.55 - 62.5 | 7.55 - 62.5 - 1.10 |
| ab03Ib | 0 | 5k | 7.36 | 84.2 | 2 | 7.55 - 62.5 | 7.55 - 62.5 - 1.50 |
| ab03Ib | 0 | 10k | 7.38 | 83.7 | 2.18 | 7.55 - 62.5 | 7.55 - 62.5 - 1.70 |
| ab03Ib | 0.5 | 2.5k | 7.36 | 72 | 1.89 | 7.55 - 62.5 | 7.55 - 62.5 - 1.10 |
| ab03Ib | 0.5 | 5k | 7.39 | 70 | 2.1 | 7.55 - 62.5 | 7.55 - 62.5 - 1.50 |
| ab03Ib | 0.5 | 10k | 7.41 | 68.1 | 2.3 | 7.55 - 62.5 | 7.55 - 62.5 - 1.90 |
| ab03Ib | 1 | 2.5k | 7.37 | 73.6 | 1.77 | 7.55 - 62.5 | 7.55 - 62.5 - 0.90 |
| ab03Ib | 1 | 5k | 7.39 | 71.6 | 1.97 | 7.55 - 62.5 | 7.55 - 62.5 - 1.30 |
| ab03Ib | 1 | 10k | 7.41 | 69.6 | 2.18 | 7.55 - 62.5 | 7.55 - 62.5 - 1.50 |
| ab03Ib | 3 | 2.5k | 7.41 | 84.1 | 1.72 | 7.55 - 62.5 | 7.55 - 62.5 - 0.70 |
| ab03Ib | 3 | 5k | 7.43 | 81.1 | 1.98 | 7.55 - 62.5 | 7.55 - 62.5 - 1.30 |
| ab03Ib | 3 | 10k | 7.45 | 78.1 | 2.21 | 7.55 - 62.5 | 7.55 - 62.5 - 1.70 |
| ab03Ib | 0 | 2.5k | 7.33 | 84.9 | 1.8 | 7.55 - 62.5 | 7.55 - 62.5 - 1.10 |

Table 13. Intraslab - Deaggregation Results for BCH11I

| GMPE | Period | RP | Mbar | Dbar | Epsbar | Mod_MD | Mod_MDE |
|--------|--------|------|------|------|--------|-------------|--------------------|
| bch11I | 0 | 2.5k | 7.2 | 83.2 | 1.71 | 7.55 - 62.5 | 7.55 - 62.5 - 0.50 |
| bch11I | 0 | 5k | 7.24 | 81.1 | 1.86 | 7.55 - 62.5 | 7.45 - 62.5 - 0.90 |
| bch11I | 0 | 10k | 7.27 | 79.1 | 1.99 | 7.55 - 62.5 | 7.55 - 62.5 - 1.10 |
| bch11I | 0.5 | 2.5k | 7.25 | 83.7 | 1.79 | 7.55 - 62.5 | 7.55 - 62.5 - 0.70 |
| bch11I | 0.5 | 5k | 7.29 | 81.4 | 1.95 | 7.55 - 62.5 | 7.55 - 62.5 - 1.10 |
| bch11I | 0.5 | 10k | 7.33 | 79.2 | 2.1 | 7.55 - 62.5 | 7.55 - 62.5 - 1.30 |
| bch11I | 1 | 2.5k | 7.32 | 83.3 | 1.95 | 7.55 - 62.5 | 7.55 - 62.5 - 1.10 |
| bch11I | 1 | 5k | 7.35 | 80.8 | 2.12 | 7.55 - 62.5 | 7.55 - 62.5 - 1.30 |
| bch11I | 1 | 10k | 7.38 | 78 | 2.29 | 7.55 - 62.5 | 7.55 - 62.5 - 1.70 |
| bch11I | 3 | 2.5k | 7.39 | 81.4 | 2.15 | 7.55 - 62.5 | 7.55 - 62.5 - 1.50 |
| bch11I | 3 | 5k | 7.42 | 77 | 2.36 | 7.55 - 62.5 | 7.55 - 62.5 - 1.90 |
| bch11I | 3 | 10k | 7.45 | 72.6 | 2.54 | 7.55 - 62.5 | 7.55 - 62.5 - 2.30 |

Table 14. Intraslab - Deaggregation Results for ZH06I

| GMPE | Period | RP | Mbar | Dbar | Epsbar | Mod_MD | Mod_MDE |
|-------|--------|------|------|------|--------|-------------|--------------------|
| zh06I | 0 | 2.5k | 7.25 | 76 | 1.74 | 7.55 - 62.5 | 7.55 - 62.5 - 0.70 |
| zh06I | 0 | 5k | 7.3 | 74.2 | 1.91 | 7.55 - 62.5 | 7.55 - 62.5 - 0.90 |
| zh06I | 0 | 10k | 7.33 | 72.5 | 2.06 | 7.55 - 62.5 | 7.55 - 62.5 - 1.30 |
| zh06I | 0.5 | 2.5k | 7.3 | 76.4 | 1.78 | 7.55 - 62.5 | 7.55 - 62.5 - 0.70 |
| zh06I | 0.5 | 5k | 7.33 | 74.2 | 1.96 | 7.55 - 62.5 | 7.55 - 62.5 - 1.10 |
| zh06I | 0.5 | 10k | 7.36 | 72.2 | 2.12 | 7.55 - 62.5 | 7.55 - 62.5 - 1.50 |
| zh06I | 1 | 2.5k | 7.33 | 77 | 1.86 | 7.55 - 62.5 | 7.55 - 62.5 - 0.90 |
| zh06I | 1 | 5k | 7.36 | 74.6 | 2.04 | 7.55 - 62.5 | 7.55 - 62.5 - 1.30 |
| zh06I | 1 | 10k | 7.39 | 72 | 2.22 | 7.55 - 62.5 | 7.55 - 62.5 - 1.50 |
| zh06I | 3 | 2.5k | 7.4 | 76.3 | 2.14 | 7.55 - 62.5 | 7.55 - 67.5 - 1.50 |
| zh06I | 3 | 5k | 7.43 | 72.2 | 2.36 | 7.55 - 62.5 | 7.55 - 62.5 - 1.90 |
| zh06I | 3 | 10k | 7.46 | 68.2 | 2.55 | 7.55 - 62.5 | 7.55 - 62.5 - 2.30 |
| | | | | | | | |

7.2 CMS Results

Figures 47 and 48 show UHS and CMS results for the interface (megathrust) and intraslab, respectively, at a return period of 10,000 years. Figures 49 and 50 show interface UHS, the extended CMS, and the envelope of the extended CMS for the interface, for the two envelope procedures described above. In Figure 49, Alternative 1 shows the case where the period range 0.0 to 0.5 second is filled in by the 0.0 second CMS, and the 3.0-second CMS is unaltered. In Figure 50, for Alternative 2 the 0.0 second CMS is unaltered, the 0.0- to 0.5-second range is filled in by the 0.5 second CMS, and the 3.0 second CMS fills in the 1.0- to 3.0-second range.

Figures 51 and 52 show similar figures for the intraslab source. Which alternative extension procedure is selected should depend on the engineering application of the CMS. For all cases, the envelope of the extended CMS is seen to be equivalent to the UHS, which is the intended result of the extension procedure.

The UHS, CMS, and extended CMS data are shown on figures for all return periods contained in Appendix C.

8.0 DETERMINISTIC EVALUATIONS

The regulatory process for seismic hazard evaluation defined by FERC (Section 1.2) specifies that both probabilistic and deterministic evaluations be conducted. Draft guidance for the deterministic evaluation outlined in Section 5.1 of Idriss and Archuleta (2007) provides the general framework followed here.

8.1 Selection and Evaluation of Critical Sources

The seismic source characterization (Section 4) and the PSHA results (Section 6) provide a basis for selecting critical seismic sources for the deterministic evaluation. These critical sources are selected primarily based on consideration of magnitude, distance, and their relative contributions of each source in the PSHA analyses. Other seismic sources in the region may have smaller magnitudes at similar or comparable distances to this group of sources, and are therefore not included in the deterministic evaluation.

Four critical fault sources are identified: (1) subduction interface, (2) intraslab, (3) Denali fault, and, (4) Fog Lake graben (Table 15). For these fault sources, the same maximum magnitudes used in the both the probabilistic (Table 6) and deterministic evaluations (Table 15). Distances are measured from the site to the closest approach of the fault source as modeled in the PSHA model, except for the intraslab source. The intraslab source distance is estimated from cross sections which show seismicity associated with the down-going slab beneath southern Alaska and the site (Figure 14). Recurrence estimates associated with the largest events on the fault sources likely vary by more than an order of magnitude. Recurrence for the deterministic magnitudes on the Denali fault, subduction interface and intraslab sources are most likely less than 1000 years. Slip rates on these sources are high (greater than 0.1 mm/yr). Recurrence for an M 7 on the Fog Lake graben source is unknown, but potentially greater than 10,000 years. Slip rates on this source are also unknown (Section 4.4), but are included in the seismic source model as a range from 0.01 to 0.5 mm/yr. As a conservative approach and sensitivity test in the PSHA, a probability of activity of 1.0 is used for this source, but lack of data and evaluation of the Fog Lake graben source indicate that the present probability of activity should be considerably less than 1.0.

Diffuse seismicity occurring throughout the region is not associated with specific faults, but modeled in the PSHA as background source zones with a maximum magnitude of M 7.3. The site area location is near the center of the Southern Alaskan block (SAB) central zone and a deterministic evaluation for this seismic source zone is derived from the 10,000-yr return period deaggregation results from the PSHA (Section 6.1,

Appendix B, pages B73-B88), and Table 16. These results indicate that different magnitude and distance pairs result for each spectral period. Thus, a separate deterministic magnitude – distance pair could be selected for each of the four spectral periods of interest.

For consistency with the other deterministic evaluations, a single magnitude, distance, and epsilon were derived for this source. This was done by taking the average modal magnitude, distance, and epsilon for each GMPE over the four periods as shown in Table 17, and weighting those results equally. Table 18 gives the resulting parameters. In Table 18, the distance measure for BA08 is Rjb (closest distance to horizontal projection of the fault plane), and Rrup (closest distance to fault plane) for the other three. In the PSHA, point sources are modeled for the areal zone. For simplicity, this study assumes depth to top of rupture to be a single value, 10.8 km (6.7 mi), which is the mean of the distribution shown in Figure 28 (lower middle figure). In the averaging procedure, this depth was used to obtain Rrup for BA08, and Rjb for the other relations. All other parameters required, such as Vs30, are those used in the PSHA. For AS08, the depth to bottom of rupture is assumed to be the zone maximum, 25 km (12 mi).

Table 15. Deterministic Hazard Input Parameters

| Source | Magnitude (Mw) | Rupture Distance (km) | JB Distance (km) | Epsilon | Depth (km) ¹ | Ground Motion Prediction Equations [weight] |
|---------------------------------------------|----------------|-----------------------|------------------|---------|-------------------------|----------------------------------------------------------|
| Megathrust | 9.2 | 78 | n/a | n/a | 35 | ZH06 [0.25] AM09 [0.25] BCH11 [0.50] |
| Denali fault | 7.9 | 71 | 71 | n/a | 0 – 15 | BA08 [0.25] CY08 [0.25] CB08 [0.25] AS08 [0.25] |
| Intraslab | 7.5 | 50 | n/a | n/a | 45 | ZH06 [0.25] AB03 [0.25] BCH11 [0.50] |
| Fog Lake graben | 7.0 | 7.0 | 3.5 | n/a | 0 – 20 | BA08 [0.25] CY08 [0.25] CB08 [0.25] AS08 [0.25] |
| Castle Mtn. fault | 7.6 | 100 | 98 | n/a | 0 – 20 | BA08 [0.25] CY08 [0.25] CB08 [0.25] AS08 [0.25] |
| Crustal seismicity ² (10,000 yr) | 6.48 | 16.9 | 13.0 | 0.59 | 10.8 ³ | BA08 [0.25] CY08 [0.25] CB08 [0.25] AS08 [0.25] |

Notes: (1) Depth range indicates top and bottom of faults, individual depths indicate the rupture depth. (2) Based on weighted magnitude-distance-epsilon deaggregation for SAB Central source and 10,000-yr return period (Table 18). (3) Depth is the weighted average of the SAB Central depth distribution (see Table 7).

Table 16. Crustal Seismicity (10,000 yr) Period-Dependent Deaggregation Results Summary

| Period (sec) | Return Period | Mbar | Dbar | Epsbar | Mod_MD | Mod_MDE |
|--------------|---------------|------|-------|--------|-------------|--------------------|
| 0.0 | 10k | 6.14 | 17.00 | 1.20 | 5.38 - 10.0 | 5.63 - 12.5 - 1.20 |
| 0.5 | 10k | 6.44 | 21.70 | 1.23 | 6.25 - 11.3 | 6.50 - 18.8 - 0.90 |
| 1.0 | 10k | 6.61 | 23.98 | 1.29 | 6.48 - 11.3 | 6.65 - 17.5 - 0.90 |
| 3.0 | 10k | 6.84 | 24.10 | 1.48 | 6.95 - 11.3 | 7.13 - 18.8 - 0.90 |

Note: These inputs are the average of Next Generation ground motion prediction equations Abrahamson and Silva (2008), Boore and Atkinson (2008), Campbell and Borzorgnia (2008), and Chiou and Youngs (2008).

Table 17. Deaggregation Results, Crustal Seismicity (10,000 yr)

| GMPE | Period | RP | Mbar | Dbar | Epsbar | Mod_MD | Mod_MDE |
|------|--------|-----|------|------|--------|-------------|--------------------|
| BA08 | 0.0 | 10k | 6.29 | 12.8 | 1.20 | 5.55 - 2.5 | 6.65 - 12.5 - 1.10 |
| BA08 | 0.5 | 10k | 6.52 | 18.0 | 1.19 | 6.55 - 7.5 | 6.75 - 22.5 - 1.30 |
| BA08 | 1.0 | 10k | 6.60 | 22.2 | 1.21 | 6.55 - 7.5 | 6.85 - 17.5 - 0.90 |
| BA08 | 3.0 | 10k | 6.77 | 26.8 | 1.28 | 6.65 - 7.5 | 7.15 - 22.5 - 0.90 |
| CY08 | 0.0 | 10k | 6.06 | 18.1 | 1.02 | 5.35 - 12.5 | 5.25 - 12.5 - 1.10 |
| CY08 | 0.5 | 10k | 6.33 | 19.4 | 1.20 | 5.95 - 12.5 | 5.95 - 12.5 - 0.90 |
| CY08 | 1.0 | 10k | 6.52 | 22.1 | 1.18 | 6.25 - 12.5 | 6.25 - 12.5 - 0.70 |
| CY08 | 3.0 | 10k | 6.75 | 23.1 | 1.39 | 6.75 - 12.5 | 6.85 - 12.5 - 0.50 |
| CB08 | 0.0 | 10k | 6.17 | 15.0 | 1.58 | 5.55 - 12.5 | 5.55 - 12.5 - 1.50 |
| CB08 | 0.5 | 10k | 6.47 | 18.7 | 1.50 | 6.55 - 12.5 | 6.55 - 12.5 - 0.70 |
| CB08 | 1.0 | 10k | 6.65 | 20.1 | 1.61 | 6.55 - 12.5 | 6.45 - 12.5 - 1.30 |
| CB08 | 3.0 | 10k | 6.90 | 20.7 | 1.70 | 7.25 - 12.5 | 7.25 - 12.5 - 0.90 |
| AS08 | 0.0 | 10k | 6.05 | 22.1 | 0.99 | 5.05 - 12.5 | 5.05 - 12.5 - 1.10 |
| AS08 | 0.5 | 10k | 6.42 | 30.7 | 1.01 | 5.95 - 12.5 | 6.75 - 27.5 - 0.70 |
| AS08 | 1.0 | 10k | 6.68 | 31.5 | 1.14 | 6.55 - 12.5 | 7.05 - 27.5 - 0.70 |
| AS08 | 3.0 | 10k | 6.92 | 25.8 | 1.54 | 7.15 - 12.5 | 7.25 - 27.5 - 1.30 |

Table 18. Crustal Seismicity (10,000 yr) Single-Earthquake Deterministic Parameters

| Magnitude | Rupture Distance (km) | JB Distance (km) | Depth (km) | Epsilon |
|-----------|-----------------------|------------------|------------|---------|
| 6.48 | 16.9 | 13.0 | 10.8 | 0.59 |

Note: These inputs are the average of Next Generation ground motion prediction equations Abrahamson and Silva (2008), Boore and Atkinson (2008), Campbell and Borzorgnia (2008), and Chiou and Youngs (2008) over all periods.

8.2 Deterministic Ground Motion Estimates

Deterministic ground motion estimates were developed for six critical seismic sources based on maximum magnitude estimates, site to source distances, and the weighted GMPE's used for each source in the PSHA analyses. The deterministic sources are the subduction interface, subduction intraslab, Denali fault, Castle Mountain fault, Fog Lake graben faults, and a 10,000-year return period earthquake for the background source derived from deaggregation of the PSHA results.

The deterministic ground motion evaluation uses multiple GMPEs appropriate for each type of seismic source with weights shown in Table 15. The same weighting of GMPE's is used in the deterministic evaluation as was used in the PSHA (Section 5.2).

The FERC guidelines (FERC, 2011; Idriss and Archuleta, 2007) recommend comparison of the deterministic results to the total UHS from the probabilistic evaluation. The weighted deterministic results, both median and 84th percentile, are shown as individually for each critical source in comparison to the total UHS from the probabilistic evaluation (Figures 53 – 58). The guidelines recommend use of 84th percentile values for the highly active sources, but use of median values for sources with low average slip rates (Section 5.1 in Idriss and Archuleta, 2007), such as the Fog Lake graben source.

The deterministic evaluation indicates that the largest values of ground motions at the site are associated with the subduction interface and intraslab sources due to their large magnitude, relatively short distance, and GMPE's used for these sources. For the intraslab source, the deterministic results are generally similar to the 10,000-yr UHS, except at periods greater than 0.5 sec (Figure 53). At periods of about 3 sec, the intraslab source contribution corresponds to the 2500-yr UHS. In contrast, for the subduction interface source, the deterministic results are near the 2500-yr UHS for periods less than 0.2 sec, but are near the 10,000-yr UHS for periods greater than 2 sec (Figure 54).

The median and 84th percentile results for the crustal sources indicate that these sources are relatively less significant compared to the subduction zone sources. The Denali fault source 84th percentile results correspond to the 100-yr UHS for periods up to about 0.2 sec and are below 1000-yr UHS at periods up to 3 sec (Figure 55). The Castle Mountain fault 84th percentile results are lower than the Denali fault, and are below the 100-yr UHS for periods up to about 1 sec and below 250-yr UHS for periods up to 3 seconds (Figure 56).

Based on the low slip rate and a likely probability-of-activity that is less than 1, median motions are recommended for comparing the Fog Lake graben source to the UHS. For most periods, these motions fall between the 250-yr and 1000-yr UHS (Figure 57). Deterministic contributions from the seismicity in the SAB central source zone, including 84th percentile estimates, also plot between the 250-yr and 1000-yr UHS hazard (Figures 58 and 59).

For the areal zone representing background crustal seismicity (SAB Central zone), two deterministic results were produced. The first derives period-dependent magnitude-distance-epsilon values from the four GMPEs shown in Table 15. These results, shown in Tables 16 and 17, indicate that high frequencies (PHA) are dominated by smaller magnitudes, while longer periods are dominated by larger magnitudes. This would have considerable impact if time histories were to be derived to account for the deterministic results. Figure 57 shows the results for the four considered periods, along with the UHS. The median results are consistent with the 250-year UHS at most spectral periods, and the 84th fractiles are at the 1000-year UHS level or less.

The second areal zone deterministic analysis reduces the deaggregation information to a single magnitude and epsilon, and the two relevant distance measures. Figure 58 shows a similar result; the median deterministic values are roughly consistent with the 250 year UHS, and the 84th fractile with the 1000-year UHS.

If a single deterministic earthquake for the areal zone source is desired, the results in Table 18 and Figure 59 are recommended. If period-dependent earthquake scenarios are desired, the results in Table 16 and Figure 58 are recommended. Given the similarity of these results with those for the Fog Lake graben faults, the areal zone results should probably be classified as a “low average slip-rate” source under the FERC terminology.

8.3 Comparison to Previous Studies

This section compares and contrasts the results of this study to the previous WCC results, for deterministic and probabilistic approaches. The seismic source characterization and ground motion results from this study include most elements from the prior Woodward-Clyde (1980, 1982) studies, but are not directly comparable due to many changes in practice and methodologies. The major fault sources represented in the prior Woodward-Clyde studies are included with updated seismic source characterizations. The detection level earthquake (Woodward-Clyde, 1982) concept is superseded by the use of probabilistic analyses of the background seismicity in the site and region. In addition, this present study includes seismic sources (e.g., subduction

intraslab source) not characterized in the prior Woodward-Clyde studies. There are general similarities between results of this study with the prior results, but also significant differences due to differing seismic source characterizations, methodologies, and ground motion attenuation parameters.

Table 19 compares deterministic results presented by WCC (1982) to those computed in this study. Mean PGAs for the megathrust seismic source are practically identical: 0.35 g compared to 0.33 g. The WCC (1982) characterization is a smaller magnitude event but closer distance than in this study, so it is difficult to assess which set of GMPEs is more conservative. WCC (1982) did not present a PGA for the intraslab, because they assumed that a smaller magnitude at a greater distance would produce ground motions lower than the megathrust source. However, the ground motions for this source presented here show that these motions are actually higher, by a substantial amount.

However, the discrepancy between the Denali fault PGA in the WCC (1982) study (0.20 g) and the PGA in this study (0.09 g; Table 19), for the same magnitude and distance, indicates that the earlier GMPEs produced higher ground motions than those used herein. The GMPEs available in 1982 were derived from a limited set of ground motion recordings, in both number, quality, and sampling of tectonic environments, compared to what is available present-day.

Seven GMPEs were considered by WCC (1982) in the selection of attenuation relationships. While it is stated that one group of relations was selected for crustal earthquakes and another for subduction zone earthquakes, it is not stated which were used for each, nor what weighting, if any, was applied. Some are published and readily available, while some are contained in conference proceedings and difficult to obtain. However, all are for peak horizontal acceleration (PHA) only, as WCC (1980) applied spectral shapes tied to the PHA value, as was common practice at the time of the WCC study.

Table 19. Deterministic Result Comparison between Woodward-Clyde (1982) and This Study

| Source | Woodward-Clyde (1982) | | | FCL (this study) | | | |
|---------------------------------|-----------------------|------------------------------|---------------------------|------------------|-----------------------|------------------|---------------------------|
| | MCE (Ms) ¹ | Distance (km) ^{1,4} | Mean PGA (g) ³ | MCE (Mw) | Rupture Distance (km) | JB Distance (km) | Mean PGA (g) ⁵ |
| Megathrust (interplate) | 8.5 | 64 | 0.35 | 9.2 | 78 | 70 | 0.33 |
| Intraslab (intraplate) | 7.5 | 50 | <i>Unavailable</i> | 7.5 | 50 | 0 | 0.53 |
| Denali fault – entire fault | 8.0 | 70 | 0.20 | 7.9 | 71 | 71 | 0.09 |
| Denali fault – 2002 rupture | <i>Not considered</i> | | | 7.9 | 86 | 86 | - |
| Denali fault – west segment | <i>Not considered</i> | | | 7.9 | 71 | 71 | - |
| Castle Mtn fault – entire fault | 7.5 | 105 | <i>Unavailable</i> | 7.6 | 100 | 98 | - |
| Castle Mtn West fault high | <i>Not considered</i> | | | 7.2 | 137 | 135 | - |
| Castle Mtn West fault low | <i>Not considered</i> | | | 7.2 | 137 | 135 | - |
| Castle Mtn East fault | <i>Not considered</i> | | | 7.2 | 100 | 98 | - |
| Pass Creek-Dutch Creek fault | <i>Not considered</i> | | | 7.0 | 107 | 105 | - |
| Sonona fault | <i>Not considered</i> | | | 7.0 | 72 | 69 | - |
| Fog Lake graben north | <i>Not considered</i> | | | 7.0 | 7 | 3.5 | 0.34 |
| Fog Lake graben south | <i>Not considered</i> | | | 7.0 | 10 | 6 | - |
| Detection level earthquake | 6.0 | < 10 | 0.50 | n/a | | | |
| Crustal seismicity (10,000 yr) | n/a | | | 6.6 | 15.1 | 9.9 | 0.27 ⁶ |

Notes: (1) From Table 8.1 in Woodward-Clyde (1982). (2) From Table 8.2 in Woodward-Clyde (1982). (3) From Section 8.3.2, p. 8-8 in Woodward-Clyde (1982). (4) Distance assumed to be Rupture distance. (5) Mean PGA ground motions are the weighted sum of GMPE's listed in Table 15. (6) Magnitudes and distances for crustal seismicity are from Table 18.

Table 20 compares the probabilistic results presented by WCC (1982) to those derived by this study. The probabilistic approach used by WCC was not described in great detail, and as with the deterministic comparisons discussed above, the details of GMPE's used in the WCC evaluations are unclear. However, it appears that for return periods up to about 2500 years, the WCC (1982) estimates are somewhat higher than

the mean PGA values resulting from this current study. However, for a 10,000-year return period, the current study results are significantly higher (0.64 g compared to 0.83 g). For both deterministic and probabilistic evaluations, the significant differences in input data, methodologies, and practice between the WCC studies and the current study make direct comparisons tenuous, at best.

Table 20. Comparison of WCC (1982) and FCL (this study) hazard results

| WCC (1982) | | | FCL (this study) | | |
|----------------------------------------|----------------------------------|--------------|-----------------------|--------------|-------------------|
| Probability of Exceedance in 100 years | Equivalent Return Period (years) | Mean PGA (g) | Return Period (years) | Mean PGA (g) | Mean 1 sec SA (g) |
| | | | 100 | 0.13 | 0.07 |
| 0.50 | 144 | 0.28 | | | |
| | | | 250 | 0.20 | 0.12 |
| 0.30 | 280 | 0.32 | | | |
| 0.10 | 949 | 0.41 | 1,000 | 0.37 | 0.23 |
| 0.05 | 1,950 | 0.48 | | | |
| | | | 2,500 | 0.52 | 0.34 |
| | | | 5,000 | 0.66 | 0.45 |
| 0.01 | 9,950 | 0.64 | 10,000 | 0.83 | 0.58 |

9.0 INITIAL SURFACE FAULTING AND GEOHAZARD IDENTIFICATION

This section reviews the potential for surface fault rupture hazard at the site as characterized in the WCC (1982) study, based on desktop evaluations using updated literature evaluations and seismic source characterizations. WCC (1982) concluded that topographic lineaments near the dam site are either not tectonic faults, or are not “recently active” structures (within the past 100,000 years). However, recent earthquakes in the region have demonstrated the potential for fault rupture on poorly or un-characterized faults strands. Active or potentially active faults, or lineaments that underlie the proposed dam footprint or the upstream extent of the proposed reservoir must be evaluated for surface rupture hazard. Active faults have some potential for surface rupture during a seismic event, depending on strength of the earthquake and other factors. Suspected or known fault structures that underlie the facility footprint and have a poorly understood surface rupture history are considered potentially active. Faults classified as inactive have no potential for co-seismic surface fault rupture.

This preliminary surface fault rupture hazard assessment is based upon features identified and evaluated during previous work for the Susitna-Watana dam site (WCC, 1980; 1982; Harza-Ebasco, 1984), recent relevant geologic publications (e.g., O’Neill et al., 2005; Glen et al., 2007a), and preliminary office-based interpretation using new landscape assessment tools (Google Earth). This surface fault rupture hazard assessment is preliminary and intended as a review of the current state of understanding regarding these structures. Further investigation of the activity, and therefore, rupture hazard of each or some individual features, may be needed in the future to either confirm or update the WCC conclusions.

Three structural features that underlie the dam site area or proposed reservoir were identified during the WCC studies (WCC, 1980 and 1982) including: the Talkeetna thrust fault, the Watana lineament, and northwest-striking structures (Figure 21). The trace of the Susitna lineament as presented by WCC (1982) is located proximal to the dam site area, but does not appear to underlie the anticipated dam foundations or reservoir. Therefore, the Susitna lineament is not considered in this surface rupture hazard assessment. The Talkeetna thrust discussion below incorporates the recent reassessment of the structure by O’Neill et al. (2005) and Glen et al. (2007a).

9.1 Watana Lineament

The Watana lineament is an east-west trending lineament that passes through the dam site and approximately follows an east-west linear section of the Susitna River. The

lineament was first identified by Gedney and Shapiro (1975). WCC (1982) performed bedrock mapping, evaluated angle boring logs and interpreted aerial photos along the lineament and concluded that it is comprised of a series of disconnected, short lineaments that are unrelated to Quaternary faulting. No further paleoseismic evaluation has been performed on the lineament. The conclusion of short, discontinuous lineaments (WCC, 1982) does not necessarily demonstrate, nor preclude, fault inactivity, and no potential for surface fault rupture.

9.2 Northwest-striking Structures in the Site Vicinity

Early site investigations identified is a zone of fractured and highly disturbed rock, with a prominent exposure in the cliffs along the north side of the Susitna River adjacent to the dam site (Acres, 1981). The structure, termed the “Fins” feature in most early reports, strikes northwest-southeast between the Susitna River and Tsusena Creek and dips 70 to 75 degrees. The feature as mapped by WCC (1982) follows a morphological depression in the surficial units between the Susitna River and Tsusena creek, which is roughly coincident with a buried paleochannel. Along their southeastern edge, adjacent to the dam site, it is expressed morphologically as a series of northwest-striking gullies and ridges. The feature was judged to be a short (2-mile long) fault without “recent” displacement by WCC (1982). A subsequent geotechnical evaluation of the feature by Harza-Ebasco (1984) included detailed geologic mapping and geotechnical borings. This study concluded that the northwest-striking feature is not a “through-going structure,” but rather a zone of closely spaced fractures, some with slickensides and clay infilling suggestive of “minor shearing,” but with no evidence of “major faulting.” Borrow area and geotechnical evaluations in the Harza-Ebasco studies depict a sequence of Quaternary glacial deposits which would overlie the extensions of the northwest-striking feature and which appear to be unfaulted (also see Section 3.3). The northwest-trending topographic lineament identified by WCC (1982) is apparent in Google Earth. The topographic depression could be explained by differential erosion in a region of sheared bedrock. However, further field evaluation of the structure would be necessary to verify the conclusions of WCC (1982) and Harza-Ebasco (1984).

9.3 The Talkeetna Thrust Fault / Talkeetna Suture Zone

The Talkeetna thrust fault / Talkeetna suture zone is a major terrane-bounding structure associated with continental accretion in the late Cretaceous and early Tertiary. The traditional view of the Talkeetna thrust fault (i.e., Csejtey, et al. 1982; Nokleberg et al., 1994) has been questioned by Glen et al. (2007a; 2007b), who propose that the

structure is a deep crustal suture that branches upward into a wide (12-mi [20-km]) zone of Tertiary or younger faults.

WCC (1982) evaluated the paleoseismology and recency of activity of the Talkeetna thrust fault, based on the assumption that the fault is a discreet upper crustal structure. The WCC (1982) study considered the likely fault trace to be concealed by young Cenozoic deposits along much of its length, with the exception of Talkeetna Hill to the southwest near the Talkeetna River (Location 1 in Figure 21). WCC (1982) constrained the concealed sections of the fault to a 3-mile-wide band along much of its length, and a 1-mile-wide band at the Susitna River. The WCC (1982) study concluded the Talkeetna thrust fault showed no evidence of “recent” displacement, based on the following observations and judgment (see Figure 21 for study locations):

- Undeformed Tertiary volcanic rocks (50 Ma potassium-argon age) overlie the fault at location 1 (Figure 21).
- Paleoseismic trenching at location 1 (Figure 21) revealed the fault trace in bedrock, but did not have age-appropriate deposits overlying the bedrock to positively evaluate fault activity.
- Trenching of a geomorphic lineament near the Fog Lakes (location 2, Figure 21) revealed no evidence of faulting in units exposed with an approximate age of 15,000 to 25,000 years old. The lineament was judged to be of glacial origin.
- Fold axis in Oligocene strata near Watana Creek (location 3, Figure 21) are oriented northwest-southeast, which is inconsistent with compressional stresses capable of reactivating the Talkeetna thrust.
- Offset of the Talkeetna thrust by a younger unnamed fault near the Talkeetna River.
- The assessment that the Talkeetna thrust fault is a late Cretaceous through early Tertiary accretionary structure. The active continental accretion is currently located over 340 mi (550 km) to the south-southeast.

The recent geologic model of Glen et al. (2007a and 2007b) recasts the Talkeetna thrust fault / Talkeetna suture based on field mapping and assessment of gravity and magnetic data and suggests that the previous WCC (1982) be reconsidered in light of this new framework. In this new model, the dam site is located within the Fog Lakes

graben, which overlies the deep crustal Talkeetna suture. The Fog Lakes graben is a rhombohedral zone bounded on the northwest by faults associated with the Susitna lineament, to the southeast by a series of unnamed range-front normal faults (Figure 21 and 22). The graben is interpreted to have formed as a basin in a broad zone of dextral transtensional shear, with probable development in the Eocene, Oligocene and Miocene. The spatial overlap of the Fog Lakes graben and the Talkeetna suture zone suggests that the two structures may be associated as reactivation structures along crustal weakness at the suture zone. An additional component of the Glen et al. (2007a and 2007b) model is that previously mapped surface traces of the Talkeetna thrust are reinterpreted as individual upper crustal faults that are components of a wide zone of deformation associated with the Talkeetna suture (i.e. Butte Creek fault and Watana Creek fault). The WCC (1982) evaluations were more focused on a concept of a single fault trace, and a tectonic model mostly associated with the older deformational elements in the Glen et al. (2007a,b) model. Undeformed Tertiary rocks identified by WCC (1982) at location 1 (Figure 21) would lie beyond the extent of the Fog Lakes graben of Glen et al. (2007a, b).

The reassessment of the Talkeetna thrust by Glen et al. (2007a and 2007b) as a southeastern graben-bounding fault is a new model for a poorly documented structure. Glen et al. (2007a and 2007b) do not present a map trace for this structure, but describe it as a range-front fault along the southern edge of the Fog Lakes lowland, and depict the faults on an interpretive cross section offsetting Tertiary rocks at shallow crustal depths (Figure 22). The southwestern Fog Lakes graben fault shown in Figure 21 is interpreted based on the description of the fault as a range front structure. This interpreted fault trace strikes northeast and projects toward the upstream extent of the reservoir. Preliminary assessment in Google Earth confirms several tonal and topographic lineaments in the vicinity of, and parallel to the interpreted fault trace, which are distinct from those evaluated by WCC (1982). These lineaments may be the result of several possible geologic processes. Analysis of additional, more-detailed data (e.g. LiDAR) with respect to further evaluation of the Fog Lakes graben fault would help clarify the surface rupture hazard of the structure.

9.4 Other Potential Seismic Hazards

This section identifies potential seismically-induced geologic hazards (e.g. landslides, seiche) that may be significant to the project facilities. The scope of work for this current study did not include a comprehensive evaluation of all potential geologic or seismic hazards. Geologic and seismic hazards specifically not addressed in this initial phase of work include confirmation or verification of fault activity judgments in WCC (1982), evaluation of potential reservoir-triggered seismicity (RTS) and the potential for

seismically-induced seiche within the proposed reservoir. Additional studies will be needed to address significant seismic or geologic hazard issues, and future studies are planned during licensing and design to address these potential seismic hazards. Additional potential geologic hazards, e.g., potential co-seismic liquefaction, also may be identified during future phases of Project work.

10.0 SUMMARY

The developed seismic source model considers several seismogenic and potentially seismogenic structures. These are: subduction-related sources (plate interface [megathrust], and plate intraslab), the Denali fault, Castle Mountain fault, Pass Creek-Dutch Creek fault, Sonoma Creek fault, zones of distributed deformation north and south of the Denali fault, and Talkeetna block structures (Fog Lake graben).

Mean hazard curves were developed for four spectral response periods, peak horizontal acceleration (PHA), and 0.5, 1.0, and 3.0 seconds acceleration response at 5% damping. Mean uniform hazard spectra (UHS) were developed for return periods of 100, 250, 1000, 2,500, 5,000, and 10,000 years.

Source deaggregation plots are developed, one for each of the four spectral response periods (PHA, 0.5 sec, 1.0 sec, 3.0 sec). Only sources contributing 5% or more at any ground motion level are plotted on the de-aggregations. The PHA hazard is dominated by the Alaskan source zone intraslab at all return periods. This reflects the high rate of M 5 to M 7.5 events generated by this source.

The draft FERC guidelines (FERC, 2011; Idriss and Archuleta, 2007) recommend comparison of the deterministic results to the UHS from the probabilistic evaluation. The seismic source characterization (Section 4) and the PSHA results (Section 6) provide a basis for selecting critical seismic sources for the deterministic evaluation.

Four critical fault sources are identified: (1) Subduction interface, (2) Intraslab, (3) Denali fault, and, (4) Fog Lake graben. A deterministic evaluation for the southern Alaskan block (SAB) central zone seismic source zone is derived from the 10,000-yr return period deaggregation results from the PSHA. Deterministic evaluation of the Castle Mountain fault shows that it is less significant than the four critical fault sources or the SAB seismic source zone. The deterministic evaluation indicates that the largest values of ground motions at the site are associated with the subduction interface and intraslab sources, because of their large magnitude, relatively short distance, and GMPE's used for these sources. The deterministic results for the crustal sources (e.g. Denali fault, Fog Lakes graben, Castle Mountain fault, and 10,000-year crustal seismicity) indicate that these sources are relatively less significant, as compared to subduction megathrust and intraslab seismic sources.

Comparisons between the ground motion results of the present study to the results from the WCC (1982) study are complicated by the differences in approach, state of practice, analyses tools, and input parameters. For the deterministic results (Table 19), a major difference arises because WCC (1982) chose to not consider the intraslab component

of the Alaska Subduction Zone as a separate seismic source with different GMPE, consistent with practice of the time. In the current study, the deterministic evaluation finds that the intraslab source produces the largest PGA at the site. For the probabilistic evaluation (Table 20), the present study results are slightly lower than those from WCC (1982) for return periods less than 2,500 years, but are higher than those from WCC (1982) for return periods of 10,000 years. It is difficult to examine the differences in the results due to the vast differences in input data and methodologies between the two studies.

11.0 REFERENCES

- Abrahamson, N.A., and W.J. Silva (2008), Summary of the Abrahamson & Silva NGA ground-motion relations, *Earthquake Spectra*, v. 24, n. 1, 67-97.
- Acres American Incorporated, 1981, Susitna Hydroelectric Project, 1980-81 Geotechnical Report.
- Acres American Incorporated, 1982, 1982 Supplement to Susitna Hydroelectric Project, 1980-81 Geotechnical Report.
- Atkinson, G.M., and D.M. Boore (2003), Empirical ground-motion relations for subduction-zone earthquakes and their application to Cascadia and other regions, *Bulletin of the Seismological Society of America*, 93, 1703-1729.
- Aki, K., and P. Richards, 1980, *Quantitative Seismology, Theory and Methods*, W.H. Freeman and Co., New York, 557 pp.
- Atkinson, G.M., and M. Macias (2009), Predicted Ground Motions for Great Interface Earthquakes in the Cascadia Subduction Zone, *Bulletin of the Seismological Society of America*, 96, 1552–1578.
- Al Atik, L., 2011, Correlations of Epsilons (for CMS) from Subduction Earthquakes and Comparisons with Crustal Earthquake Models. Presentation at the 2011 Consortium of Organizations for Strong Motion Observation Systems (COSMOS) annual meeting. www.cosmos-eq.org
- Baker, J.W. (2011), Conditional mean spectrum: tool for ground motion selection, *Journal of Structural Engineering*, 137(3), 322-331.
- Bazzurro, P., and C.A. Cornell, 1999, Disaggregation of Seismic Hazard'. *Bulletin of Seismological Society of America (B.S.S.A.)*, Vol. 89, No. 2, April, pp. 501-520.
- Bemis, S.P., Carver, G.A., Koehler, R.D., In Press, The Quaternary Thrust System of the Northern Alaska Range. Accepted for publication *in Geosphere*.
- Bemis, S.P., 2010, Moletrack scarps to mountains: Quaternary tectonics of the central Alaska Range [Ph.D. dissertation]: University of Oregon, 121 p.
- Bemis, S. P., and Wallace, W.K., 2007, Neotectonic framework of the north-central Alaska Range foothills, in *Tectonic Growth of a Collisional Continental Margin: Crustal Evolution of Southern Alaska*, *Geol. Soc. Am. Spec. Pap.*, vol. 431, edited by K. D. Ridgway et al., pp. 549-572, GSA, Boulder, Colo.
- Biggs, J, Wright, T, Lu, Z, and Parsons, B, 2007, Multi-interferogram method for measuring interseismic deformation—Denali fault, Alaska: *Geophysical Journal International*, v. 170, p. 1,165–1,179.
- Brocher, T. M., G. S. Fuis, M. A. Fisher, G. Plafker, M. J. Moses, J. J. Taber, and N. I. Christensen, 1994, Mapping the megathrust beneath the northern Gulf of Alaska using wide-angle seismic data, *J. Geophys. Res.*, 99(B6), 11,663–11,685

-
- Burns, L.E., Little, T.A., Newberry, R.J., Decker, J.E., and Pessel, G.H., 1983, Preliminary geologic map of parts of the Anchorage C-2, C-3, D-2, and D-3 quadrangles, Alaska: Alaska Division of Geological & Geophysical Surveys Report of Investigation 83-10, 3 sheets, scale 1:25,000.
- Campbell, K.W. and Y. Bozorgnia (2008), NGA ground motion model for the geometric mean component of PGA, PGV, PGD, and 5% damped linear elastic damped response spectra for periods ranging from 0.01 s to 10 s, *Earthquake Spectra*, v. 24, n. 1, 139-171.
- Carter, L.D., Hamilton, T.D., and Galloway, J.P., eds., 1989, Late Cenozoic history of the interior basins of Alaska and the Yukon: U.S. Geological Survey Circular 1026, 114 p.
- Carver, G.A., Bemis, S.P., Solie, D.N., Castonguay, S., and Obermiller, K.E., 2010, Active and potentially active faults in or near the Alaska Highway corridor, Dot Lake to Tetlin Junction, Alaska: Alaska Division of Geological & Geophysical Surveys Preliminary Interpretive Report 2010-1, 42 p.
- Carver, G.A. and Plafker, G., 2008 Paleoseismicity and neotectonics of the Aleutian Subduction Zone - An overview, in Freymueller, J.T., Haeussler, P.J., Wesson, R.L., and Ekstrom, Goran, eds., 2008, Active tectonics and seismic potential of Alaska: American Geophysical Union, Geophysical Monograph 179, p. 83–108.
- Carver, G., Plafker, G., Metz, M., Cluff, L., Slemmons, B., Johnson, E., Roddick, J. and Sorensen, S., 2004, Surface Rupture on the Denali Fault Interpreted from Tree Damage during the 1912 Delta River Mw 7.2-7.4 Earthquake: Implications for the 2002 Denali Fault Earthquake Slip Distribution, *Bulletin of the Seismological Society of America*, 94(6B): S58 - S71.
- Chiou, B. and R.R. Youngs (2008), An NGA model for the average horizontal component of peak ground motion and response spectra, *Earthquake Spectra*, v. 24, n. 1, 173-215.
- Christensen D.H. and Beck, S.L., 1994, The rupture process and tectonic implications of the great 1964 Prince William Sound earthquake: *Pure and Applied Geophysics*, v. 142, p. 29-53.
- Clautice, K.H., 1990, Geologic map of the Valdez Creek mining district: Alaska Division of Geological & Geophysical Surveys Public Data File 90-30, 1 sheet, scale 1:250,000.
- Cornell, C.A. (1968), Engineering seismic risk analysis, *Bulletin of the Seismological Society of America*, 58, 1583-1606. Clautice, K.H., 1990, Geologic Map of the Valdez Creek Mining District: Alaska Division of Geological and Geophysical Surveys PDF 90–30, 1 sheet, 1:25,000.
- Crone, A.J., Personius, S.F., Craw, P.A., Haeussler, P.J., and Staff, L.A., 2004, The Susitna Glacier thrust fault—Characteristics of surface ruptures on the fault that initiated the 2002 Denali Fault earthquake: *Bulletin of the Seismological Society of America*, v. 94, no. 6, part B, p. 5–22.
-

-
- Csejtey, B., Jr., Nelson, W.H., Hones, D.L., Silberling, N.J., Dean, R.M., Morris, M.S., Lanphere, M.A., Smith, J.G., and Silberman, M.L., 1978, Reconnaissance geologic map and geochronology, Talkeetna Mountains quadrangle, northern part of Anchorage quadrangle, and southwest corner of Healy quadrangle: Alaska U.S. Geological Survey, Open-File Report 78-558A, 60 p.
- Csejtey, Béla, Jr., Cox, D.P., Evarts, R.C., Stricker, G.D., and Foster, H.L., 1982, The Cenozoic Denali fault system and the Cretaceous accretionary development of southern Alaska, *Journal of Geophysical Research*, v. 87, no. B5, p. 3741–3754.
- Demets, C., and Dixon, T.H., 1999, New kinematic models for Pacific-North America motions from 3 Ma to present, 1: Evidence for steady motion and biases in the NUVEL-1A model, *Geophysical Research Letters*, v. 26, p. 1921-1924.
- Detterman, R.L., Plafker, G., Hudson, T., Tysdal, R.G., and Pavoni, N., 1974, Surface geology and Holocene breaks along the Susitna segment of the Castle Mountain fault, Alaska: U.S. Geological Survey Miscellaneous Field Studies Map MF-618, 1 sheet, scale 1:63,360.
- Detterman, R. L., Plafker, G., Russell, G. T. and Hudson, T. ,1976, Features along part of the Talkeetna segment of the Castle Mountain-Caribou fault system, Alaska, U.S. Geol. Surv. MF Map 738, 1 sheet.
- Doser, D. I., 2004, Seismicity of the Denali-Totschunda fault zone in central Alaska (1912-2008) and its relation to the 2002 Denali fault earthquake sequence, *Bull. Seismol. Soc. Am.*, 94(6B), SI32-S144.
- Doser, D.I., Veilleux, A., and Velasquez, M., 1999, Seismicity of the Prince William Sound Region for Thirty-two years following the 1964 Great Alaskan Earthquake: *Pure and Applied Geop.*, v. 154, p. 593-632.
- Doser, D.I., Brown W.A., and Velasquez, M., 2002, Seismicity of the Kodiak Island region (1964-2001) and its relation to the 1964 great Alaska earthquake, *Bull. Seismol. Soc. Am.* V.92, no. 8, p.3269-3292.
- Elliott, J. L., C. F. Larsen, J. T. Freymueller, and R. J. Motyka, 2010, Tectonic block motion and glacial isostatic adjustment in southeast Alaska and adjacent Canada constrained by GPS measurements, *J. Geophys. Res.*, 115, B09407.
- Eberhart-Phillips, D., Haeussler, P.J., Freymueller, J.T., Frankel, A.D., Rubin, C.M, Craw, P., Ratchkovski, N.A., Anderson, G., Carver, G.A., Crone, A.J., Dawson, T.E., Fletcher, H., Hansen, R, Harp, E.L., Harris, R.A., Hill, D.P., Hreinsdóttir, S., Jibson, R.W., Jones, L.M., Kayen, R., Keefer, D.K., Larsen, C.F., Moran, S.C., Personius, S.F., Plafker, G., Sherrod, B., Sieh, K., N., and Wallace, W. K., 2003, The 2002 Denali fault earthquake, Alaska: A large magnitude, slip-partitioned event, *Science*, 300(5622), pp. 1113-1118.
- FERC, 2011, Engineering guidelines for the evaluation of hydropower projects: Federal Energy Regulatory Commission website: <http://www.ferc.gov/industries/hydropower/safety/guidelines/eng-guide/chap13-draft.asp> (last accessed 10/6/11).
-

-
- Fletcher, H.J., 2002, Crustal deformation in Alaska measured using the Global Positioning System: Fairbanks, Alaska, University of Alaska Fairbanks, Ph.D. dissertation, 135 p.
- Flores, C. F., and Doser, D.I., 2005, Shallow seismicity of the Anchorage, Alaska region (1964–1999), *Bull. Seism. Soc. Am.* 95, 1865–1879.
- Fuchs, W.A., 1980, Tertiary tectonic history of the Castle Mountain–Caribou fault system in the Talkeetna Mountains, Alaska: Salt Lake City, University of Utah, Department of Geology and Geophysics, Ph.D. dissertation, 150 p.
- Gardner, J.K., and L. Knopoff (1974), Is the sequence of earthquakes in southern California, with aftershocks removed, Poissonian?, *Bulletin of the Seismological Society of America*, 64, 1363-1367.
- Gedney, L., and Shapiro, L., 1975, Structural lineaments, seismicity and geology of the Talkeetna Mountains area, Alaska: Unpublished report prepared for the U.S. Army Corps of Engineers, Alaska Division, 18 p.
- Glen, J. M. G., 2004, A kinematic model for the southern Alaska orocline based on regional fault patterns, in *Orogenic Curvature: Integrating Paleomagnetic and Structural Analysis*, *Geol. Soc. Am. Spec. Pap.*, vol. 383, edited by A. J. Sussman and A. B. Weil, pp. 161-172.
- Glen, J.M.G., Schmidt, J., Pellerin, L., McPhee, D.K., and O'Neill, J.M., 2007a, Crustal structure of Wrangellia and adjacent terranes inferred from geophysical studies along a transect through the northern Talkeetna Mountains, *in* Ridgway, K.D., Trop, J.M., Glen, J.M.G., and O'Neill, J.M., eds., *Tectonic Growth of a Collisional Continental Margin: Crustal Evolution of Southern Alaska: Geological Society of America Special Paper 431*, p. 21–41.
- Glen, J.M.G., Schmidt, J., and Morin, R., 2007b, Gravity and magnetic character of south-central Alaska: Constraints on geologic and tectonic interpretations, and implications for mineral exploration, *in* Ridgway, K.D., Trop, J.M., Glen, J.M.G., and O'Neill, J.M., eds., *Tectonic Growth of a Collisional Continental Margin: Crustal Evolution of Southern Alaska: Geological Society of America Special Paper 431*, p. 593–622.
- Hake, C. A. and Cloud, W. K., 1966, United States Earthquakes 1964, Coast and Geodetic Survey, U.S. Government Printing Office, 91 p.
- Haeussler, P.J., 1998, Surficial geologic map along the Castle Mountain fault between Houston and Hatcher Pass Road, Alaska: U.S. Geological Survey Open-File Report OF-98-480, scale 1:25,000, 1 sheet.
- Haeussler, P. J., 2005, What made Denali so tall? Structural geology of the high peaks of the Alaska Range, *Geol. Soc. Am. Abstr. Programs*, 37(7), 79.
- Haeussler, P.J., 2008, An overview of the neotectonics of interior Alaska—Far-field deformation from the Yakutat Microplate collision, *in* Freymueller, J.T., Haeussler, P.J., Wesson, R.L., and Ekstrom, Goran, eds., 2008, *Active tectonics*
-

-
- and seismic potential of Alaska: American Geophysical Union, Geophysical Monograph 179, p. 83–108.
- Haeussler, P.J., and Anderson, R.S., 1995, The “Twin Peaks Fault”: Not a tectonic or seismogenic structure, in Dumoulin, J.A., and Gray, J.E., eds., Geologic studies in Alaska by the U.S. Geological Survey, 1995: U.S. Geological Survey Professional Paper 1574, p. 93–99.
- Haeussler, P.J., Saltus, R.W., Karl, S.M., and Ruppert, N., 2008, Evidence for Pliocene to present thrust faulting on the south side of the Alaska Range in the vicinity of the Peters Hills piggyback basin, *Eos Trans. AGU*, 89(53), Fall Meet. Suppl., Abstract T44A-08.
- Haeussler, P. J., Bruhn, R.L. and Pratt, T.L., 2000, Potential seismic hazards and tectonics of upper Cook Inlet basin, Alaska, based on analysis of Pliocene and younger deformation, *Geol. Soc. Am. Bull.*, 112,p 1414-1429.
- Haeussler, P. J., T. C. Best, and C. F. Waythomas, 2002, Paleoseismology at high latitudes: Seismic disturbance of late Quaternary deposits along the Castle Mountain fault near Houston, Alaska, *Geol. Soc. Am. Bull.*, 114, 1296-1310, 1 plate.
- Haeussler, P. J. , Schwartz, D.P., Dawson, T.E., Stenner, H.D., Lienkaemper, J.J., Sherrod, B., Cinti, F.R., Montone, P., Craw, P.A., Crone A.J., and Personius, S.F., 2004, Surface rupture and slip distribution of the Denali and Totschunda faults in the 3 November 2002 M_L9 earthquake, Alaska, *Bull. Seismol. Soc. Am.*, 94(6B), S23-S52.
- Hamilton, T.D., 1994, Late Cenozoic Glaciation of Alaska, *in* Plafker, G., and Berg, H.C., eds., *The Geology of North America*, Vol. G-1, Chapter 27: The Geology of Alaska, pp. 813-844. The Geological Society of America, Boulder, Colorado.
- Harza-Ebasco, 1984, Susitna Hydroelectric Project Watana Development Winter 1983 Geotechnical Exploration Program.
- Idriss, I.M., and Archuleta, R.J., 2007, Evaluation of earthquake ground motions, draft manuscript for FERC Chapter 13, draft 06.5, <http://www.ferc.gov/industries/hydropower/safety/guidelines/eng-guide/chap13-draft.pdf> (last accessed 10/6/11)
- Koehler, R.D., Farrell, Rebecca-Ellen, Burns, P.A.C., Combellick, R.A., and Weakland, J.R., 2011a, Digital release of the Alaska Quaternary fault and fold database, American Geophysical Union annual meeting.
- Koehler, R.D., Personius, S.F., Schwarz, D.P., Haeussler, P.J., and Seitz, G.G., 2011b, A Paleoseismic study along the central Denali Fault, Chistochina Glacier area, south-central Alaska: Alaska Division of Geological & Geophysical Surveys Report of Investigation 2011-1, 17 p.
-

-
- Koehler, R.D. and Reger, R.D., 2011, Reconnaissance Evaluation of the Lake Clark Fault, Tyonek Area, Alaska, Division of Geological & Geophysical Surveys Preliminary Interpretive Report 2011-1.
- Lahr, J. C., R. A. Page, C. D. Stephens, and K. A. Fogleman, 1986. Sutton, Alaska, earthquake of 1984: Evidence for activity on the Talkeetna segment of the Castle Mountain fault system, *Bull. Seism. Soc. Am.* 76, 967–983.
- Matmon, A., Schwartz, D.P., Haeussler, P.J., Finkel, R., Lienkaemper, J.J., Stenner, H.D., and Dawson, T.E., 2006, Denali fault slip rates and Holocene–late Pleistocene kinematics of central Alaska: *Geology*, v. 34, p. 645–648.
- McGuire, R. K., 1995, Probabilistic Seismic Hazard Analysis and Design Earthquakes: Closing the Loop. *Bulletin of the Seismological Society of America*, 85(5), 1275-1284.
- Mériaux, A.S, Sieh, K, Finkel, R.C., Rubin, C.M., Taylor, M.H., Meltzner, A.J., and Ryerson, F.J., 2009, Kinematic behavior of southern Alaska constrained by westward decreasing postglacial slip rates on the Denali Fault, Alaska: *Journal of Geophysical Research*, v. 114, B03404.
- Nichols, D.R., 1989, Pleistocene Glacial Events, Southeastern Cooper River Basin, Alaska. *In* Carter, L.D., Hamilton, T.D., and Galloway, J.P., eds., 1989, Late Cenozoic history of the interior basins of Alaska and the Yukon: U.S. Geological Survey Circular 1026, pages 78-80.
- Nishenko, S. P and Jacob, K. H., 1990, Seismic Potential of the Queen-Charlotte-Alaska-Aleutian Seismic Zone, *Journal of Geophysical Research-Solid Earth and Planets*, Volume 95, Issue B3, p.2511-2532.
- Nokleberg, W. J., D. L. Jones, and N. J. Silberling, 1985, Origin and tectonic evolution of the Maclaren and Wrangellia terranes, eastern Alaska Range, Alaska, *Geol. Soc. Am. Bull.*, 96, 1251-1270.
- Nokleberg, W.J., Plafker, G, and Wilson, F.H., 1994, Geology of south-central Alaska, in Plafker, G, and Berg, H.C., eds., *The geology of Alaska*, v. G–1 of *The geology of North America: Boulder, Colo., Geological Society of America*, p. 311–366.
- O’Neill, J.M., Ridgway, K.D., and Eastham, K.R., 2003a, Mesozoic sedimentation and deformation along the Talkeetna thrust fault, south-central Alaska: New insights and their regional tectonic significance, *in* Galloway, J.P., ed., *Studies by the U.S. Geological Survey in Alaska, 2001: U.S. Geological Survey Professional Paper 1678*, p. 83–92.
- O’Neill, J.M., Schmidt, J.M., Glen, J.M.G., and Pellerin, Louise, 2003b, Mesozoic and Tertiary structural history of the northern Talkeetna Mountains, Paper 230-11: *Geological Society of America Abstracts with Programs*, v. 35, no. 6, p. 560.
- O’Neill, M.J., Schmidt, J.M., and Cole, R.B., 2005, Cenozoic intraplate tectonics—lithospheric right-lateral bulk shear deformation in the northern Talkeetna
-

-
- Mountains, south-central Alaska, Geological Society of America Abstracts with Programs, v. 37, no. 7, p. 79.
- Personius, S.F., Crone, A.J., Burns, P.A., Begét, J.E., Seitz, G.G., and Bemis, S.P., 2010, Logs and geologic data from a paleo-seismic investigation of the Susitna Glacier fault, central Alaska Range, Alaska: U.S. Geological Survey Scientific Investigations Map 3114, 2 sheets, <http://pubs.usgs.gov/sim/3114/>.
- Plafker, G., 1969, Tectonics of the March 27, 1964, Alaska earthquake: U.S. Geological Survey Professional Paper 543-I, 74 p.
- Plafker, G., L. M. Gilpin, and J. C. Lahr, 1994, Neotectonic map of Alaska, in *The Geology of Alaska, The Geology of North America*, vol. G-f, plate 12, edited by G. Plafker, and H. C. Berg, GSA, Boulder, Colo.
- Plafker, G., Carver, G.A., Cluff, L., and Metz, M., 2006, Historic and paleo-seismic evidence for non-characteristic earthquakes and the seismic cycle at the Delta River crossing of the Denali fault, Alaska [abs.]: 102nd Annual Meeting of the Cordilleran Section, Geological Society of America, May 8–10, Anchorage, Alaska, v. 38, 96 p.
- R & M Consultants (R&M), 2009, Task 1- Seismic Setting Review, Susitna Hydroelectric Project. R&M No.1158.21. 2 July 2009
- Ratchkovski, N., and R. Hansen (2002), New evidence for segmentation of the Alaska subduction zone, *Bulletin of the Seismological Society of America*, 92, 1754-1765.
- Ratchkovski, N. A., Hansen, R., J. C. Stanching, T. Cox, O. Fox, L. Rio, E. Clark, M. Lafevers, S. Estes, J. B. MacCormack, and T. Williams, 2003, Aftershock sequence of the Mw 7.9 Denali fault, Alaska, earthquake of 3 November 2002 from regional seismic network data, *Seism. Res. Lett.* 74, 743–752.
- Ratchkovski, N. A., Wiemer, S. and Hansen, R.A., 2004, Seismotectonics of the Central Denali Fault, Alaska, and the 2002 Denali Fault Earthquake Sequence, *Bulletin of the Seismological Society of America*, Vol. 94, No. 6B, pp. S156–S174.
- Reed, B. L., and M. A. Lanphere, 1974, Offset plutons and history of movement along the McKinley segment of the Denali fault system, Alaska, *Geol. Soc. Am. Bull.*, 85, 1883-1892.
- Ridgway, K. D., J. M. Trop, W. J. Nokleberg, C. M. Davidson, and K. R. Eastham, 2002, Mesozoic and Cenozoic tectonics of the eastern and central Alaska Range: Progressive basin development and deformation in a suture zone, *Geol. Soc. Am. Bull.*, 114, 1480-1504.
- Ruppert, N., and R. Hansen (2010), Temporal and spatial variations of local magnitudes in Alaska and Aleutians and comparison with body-wave and moment magnitudes, *Bulletin of the Seismological Society of America*, 100, 1174-1183.
- Ruppert, N. A., K. D. Ridgway, J. T. Freymueller, R. S. Cross, and R. A. Hansen (2008), Active tectonics of interior Alaska: Seismicity, GPS geodesy, and local
-

-
- geomorphology, in *Active Tectonics and Seismic Potential in Alaska*, J. T. Freymueller, P. J. Haeussler, R. Wesson, and G. Ekstrom (Editors), *Geophysical Monograph Series 179*, 109–133.
- Schmidt, J.M., Oswald, P.J., and Snee, L.W., 2002, The Deadman and Clark Creek fields: Indicators of early Tertiary volcanism in an extensional tectonic setting in the northern Talkeetna Mountains, Alaska: *Geological Society of America Abstracts with Programs*, v. 34, no. 5, p. A-101.
- Schwartz, D.P., and the Denali Fault Earthquake Geology Working Group (DFEWG), 2003, Paleo-earthquakes on the Denali–Totschunda fault system—Preliminary observations of slip and timing: American Geophysical Union, fall meeting.
- Smith, T.E., Albanese, M.D., and Kline, G.L., 1988, Geologic map of the Healy A-2 quadrangle, Alaska: Alaska Division of Geological and Geophysical Surveys, Professional Report 95, 1 plate, 1:63,360.
- Stout, J.H., and Chase, C.G., 1980, Plate kinematics of the Denali fault system, *Canadian Journal of Earth Sciences*, v. 17, p. 1527–1537.
- Stover, C.W. and Coffman, J.L., 1993, Seismicity of the United States, 1568-1989 (Revised): U.S. Geological Survey Professional Paper 1527, 415 p. Weber, F. R., and D. L. Turner (1977). A late Tertiary thrust fault in the central Alaska Range, U.S. Geol. Surv. Circular 751-B, B66–B67.
- Sylvester, A. G. (1988), Strike-slip faults, *Geol. Soc. Am. Bull.*, 100, 1666-1703.
- URS Corporation, 2008, Site-specific probabilistic and deterministic hazard analyses and development of earthquake ground motions for the Port of Anchorage Expansion Project. Consultant report prepared for Terracon Consultants, Inc., North Carolina.
- USGS, 2003, online resource: http://earthquake.usgs.gov/earthquakes/eqinthenews/2002/uslbb1/images/AK_mi_new.jpg
- Utsu, T. (2002), Relationships between magnitude scales, in Lee, W.H.K, Kanamori, H., Jennings, P.C., and Kisslinger, C., editors, *International Handbook of Earthquake and Engineering Seismology*: Academic Press, a division of Elsevier, two volumes, *International Geophysics*, v. 81-A, p. 733–746.
- Weber, F. R., and Turner, D. L, 1977, A late Tertiary thrust fault in the central Alaska Range, *US. Geol. Surv. Circ.*, 751-B, B66-B67.
- Wesson, R. L., Boyd, O. S., Mueller, C. S., Bufe, C. G., Frankel, A. D., Petersen, M. D., 2007, Revision of time-Independent probabilistic seismic hazard maps for Alaska: U.S. Geological Survey Open-File Report 2007-1043.
- Wiedmer, M., Montgomery, D., Gillespie, A., Greenberg, H. 2010, Late Quaternary megafloods from Glacial Lake Atna, Southcentral Alaska, U.S.A.; *Quaternary Research*, 73, p413-424.
-

-
- Williams, J. R. and Ferrians, O. J., 1961, Late Wisconsin and recent history of the Matanuska Glacier, Alaska: *Arctic*, v. 14, p. 82-90.
- Williams, J.R., Galloway, J.P., 1986. Map of western Copper River basin, Alaska, showing lake sediments and shorelines, glacial moraines, and location of stratigraphic sections and radiocarbon-dated samples. U.S. Geological Survey Open File Report 86-390, 30 p., 1 sheet, scale 1:250,000.
- Williams, J.R., 1989, A Working Glacial Chronology for the Western Cooper River Basin, Alaska. *In* Carter, L.D., Hamilton, T.D., and Galloway, J.P., eds., 1989, Late Cenozoic history of the interior basins of Alaska and the Yukon: U.S. Geological Survey Circular 1026, pages 80-84.
- Willis, J. B., and R. L. Bruhn, 2006, Active tectonics of the Susitna River basin, Alaska-intraplate deformation driven by microplate collision and subduction, *Geol. Soc. Am. Abstr. Programs*, 38(5), 96.
- Willis, J. B., Haeussler, P.J., Bruhn, R.L., and Willis, G.C., 2007, Holocene slip rate for the western segment of the Castle Mountain fault, Alaska, *Bull. Seismol. Soc. Am.*, 97(3), 1019-1024.
- Wilson, F.H., Dover, J.H., Bradley, D.C., Weber, F.R., Bundtzen, T.K., and Haeussler, P.J., 1998, Geologic map of central (interior) Alaska: U.S. Geological Survey Open-File Report 98-0133-B, 63 p., 3 sheets.
- Wilson, F. H., Hults, C.P., Schmoll, H.R., Haeussler, P.J., Schmidt, J.M., Yehle, L.A. and Labay K.A., 2009, Preliminary Geologic Map of the Cook Inlet Region, Alaska U.S. Geological Survey Open-File Report 2009-1108, 54 p., 2 sheets.
- Wong, I.G., Thomas, P.A., and Abrahamson, N., 2004. The PEER-Lifelines validation of software used in probabilistic seismic hazard analysis, in 2004 Geotechnical Engineering for Transportation Projects, Proceedings, M. Yegian and E. Kavazanjian (Editor). American Society of Civil Engineers, Geotechnical Special Publication No. 126, 1, 807-815.
- Woodward-Clyde Consultants (WCC), 1980, Interim Report on Seismic Studies for Susitna Hydroelectric Project.
- Woodward-Clyde Consultants (WCC), 1982, Final Report on Seismic Studies for Susitna Hydroelectric Project.
- Zhao J.X., Zhang, J., Asano, A., Ohno, Y., Oouchi, T., Takahashi, T., Ogawa, H., Irikura, K., Thio, H., Somerville, P., Fukushima, Y., and Fukushima, Y., 2006, Attenuation relations of strong ground motion in Japan using site classification based on predominant period” *Bulletin of the Seismological Society of America*, v. 96, p. 898–913.



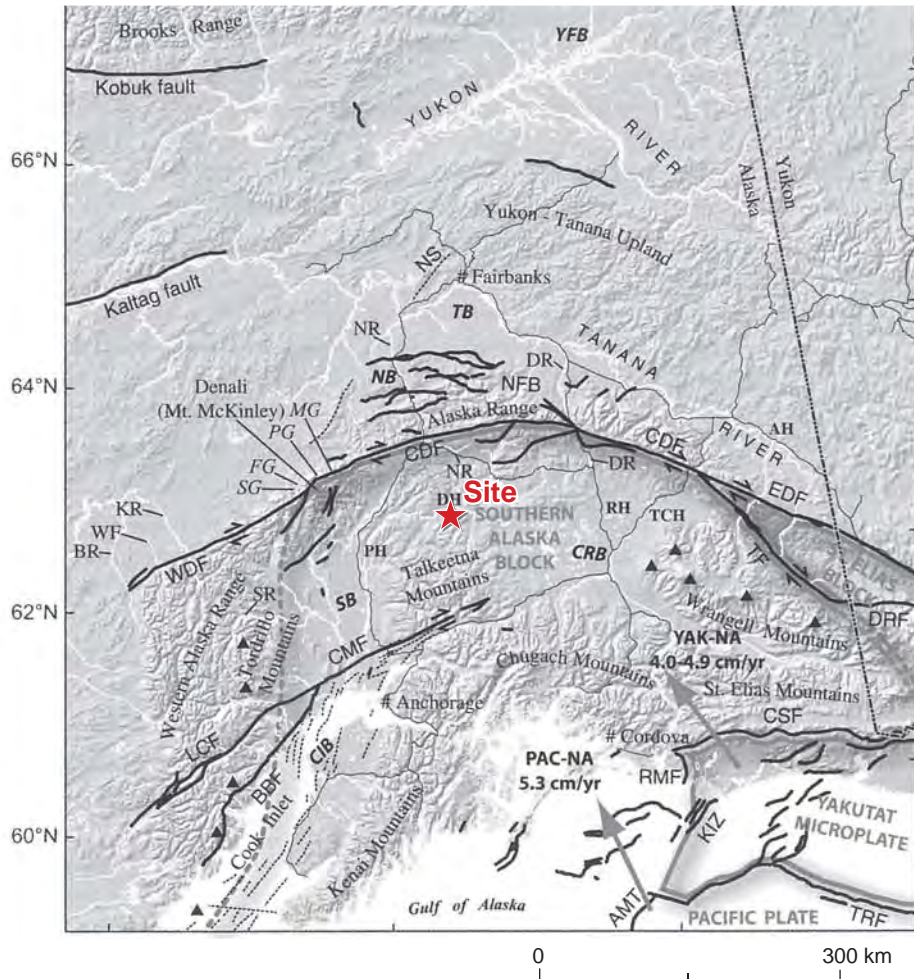
STATE OF ALASKA
ALASKA ENERGY AUTHORITY

SUSITNA-WATANA HYDROELECTRIC PROJECT

MAJOR
PHYSIOGRAPHIC
PROVINCES

02/02/12

FIGURE 1



Black lines are Neogene and active faults, dashed lines are anticlines. Triangles show active volcanoes. Crustal blocks are outlined in gray and are dashed where boundaries are uncertain. Faults: WDF, western Denali fault; CDF, central Denali fault; EDF, eastern Denali fault; NFB, northern foothills fold-and-thrust belt; NS, Nenana structure; TF, Totschunda fault; DRF, Duke River fault; LCF, Lake Clark fault; CMF, Castle Mountain fault; BBF, Bruin Bay fault; CSF, Chugach-St. Elias thrust fault; KIZ, Kayak Island fault zone; RMF, Ragged Mountain fault; AMT, Aleutian megathrust; TRF, Transition fault. Major roads are shown with thin black lines. AH, Alaska highway; PH, Parks highway; DH, Denali highway; RH, Richardson highway; DH, Denali highway; TCH, Tok cutoff highway. Abbreviated river names mentioned in text: NR, Nenana River, Delta River (both rivers flow north); BR, Big River; WF, Windy Fork; KR, Kuskokwim River; SR, Skwentna River. Glaciers: SG, Straightaway Glacier; FG, Foraker Glacier; PG, Peters Glacier; MG, Muldow Glacier. Sedimentary basins: cm, Cook Inlet basin; SB, Susitna basin; CRB, Copper River basin; NB, Nenana basin; TB, Tanana basin; YFB, Yukon Flats basin. From Haeussler (2008).



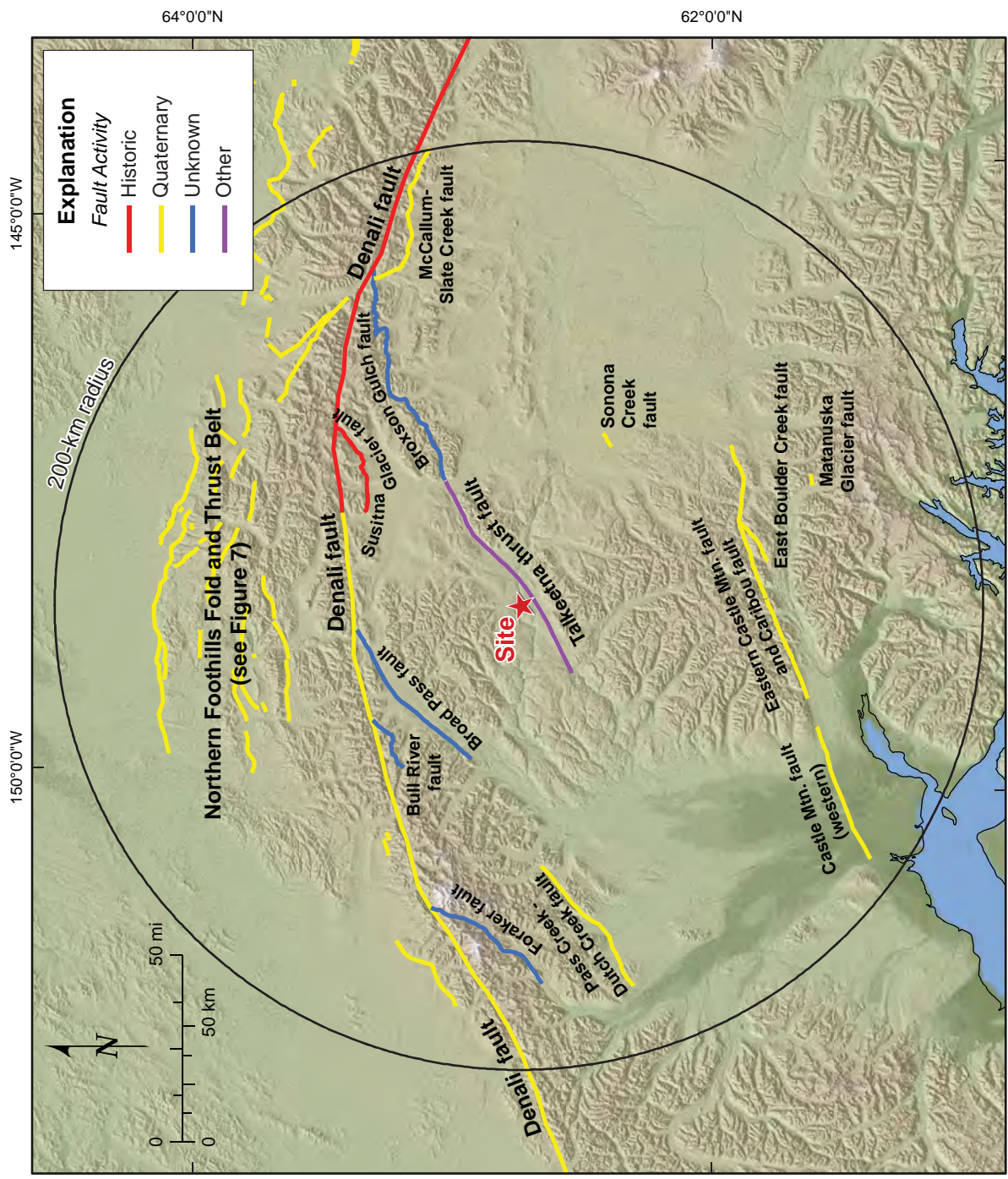
STATE OF ALASKA
ALASKA ENERGY AUTHORITY

ALASKA
ENERGY AUTHORITY

SUSITNA-WATANA HYDROELECTRIC PROJECT

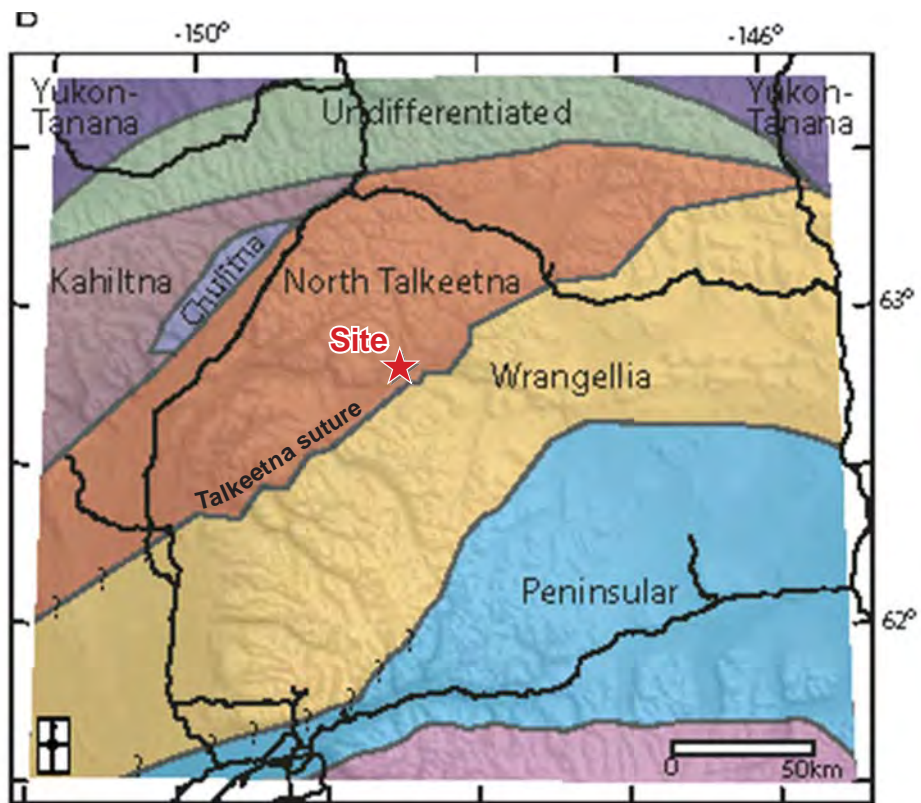
**TECTONIC OVERVIEW
OF CENTRAL INTERIOR ALASKA**

02/02/12 FIGURE 2



Fault data from Cjesty (1978), Plafker et al. (1994), and Williams and Galloway (1986).





Map based on the geophysical character of the terranes (Glen et al., 2007b).

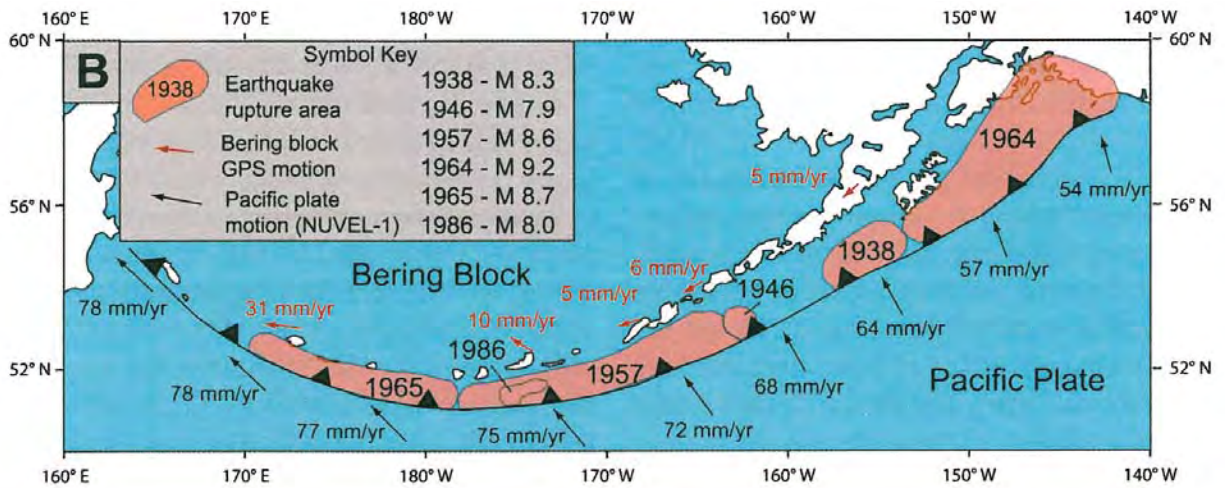


SUSITNA-WATANA HYDROELECTRIC PROJECT

TECTONOSTRATIGRAPHIC
TERRANE MAP
OF THE TALKEETNA BLOCK

02/02/12

FIGURE 4



Motion of the Pacific Plate relative to North America is indicated by black arrows. Red arrows show motion of the Bering Block relative to North America.

From Carver and Plafker (2008)

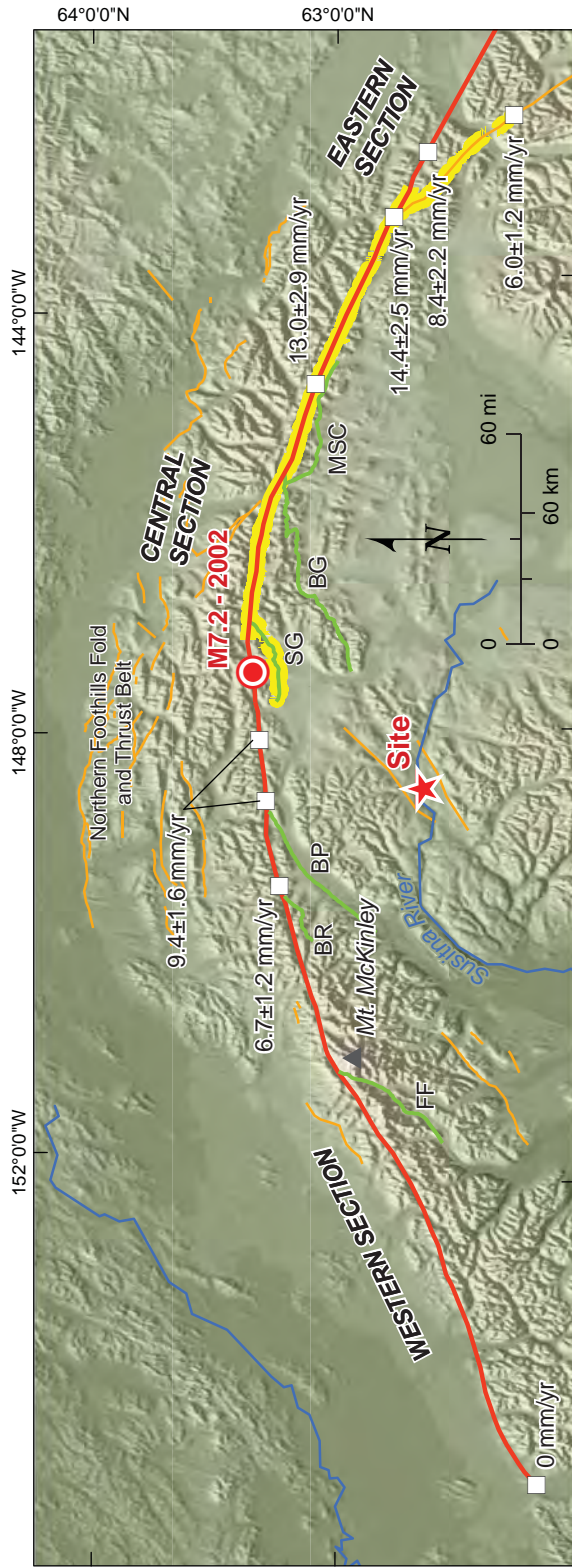


STATE OF ALASKA
 ALASKA ENERGY AUTHORITY

SUSITNA-WATANA HYDROELECTRIC PROJECT

**RUPTURE AREAS
 FOR HISTORICAL ALASKAN
 SUBDUCTION ZONE
 EARTHQUAKES**

02/02/12 FIGURE 5



Explanation

- Symbols**
- Earthquake epicenter
 - Slip rate (sources discussed in text)

- Faults**
- Denali fault
 - 2002 Denali fault rupture, Haeussler (2008)
 - Southern Denali faults
 - Other fault

Abbreviations

- BR - Bull River fault
- BP - Broad Pass fault
- BG - Broxon Gulch fault
- FF - Foraker fault
- MSC - McCallum-Slate Creek fault
- SG - Susitna Glacier fault



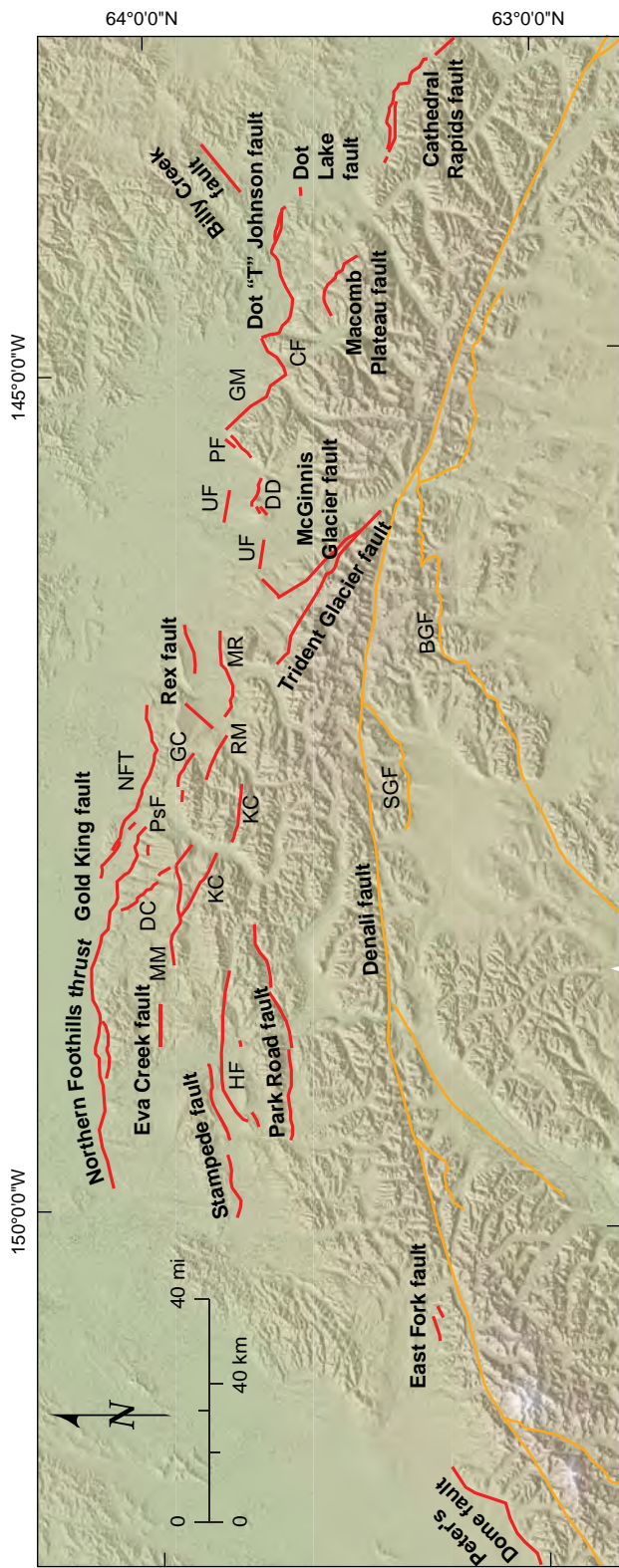
STATE OF ALASKA
ALASKA ENERGY AUTHORITY
SUSITNA-WATANA HYDROELECTRIC PROJECT

**DENALI FAULT
CHARACTERIZATION**

02/02/12

FIGURE 6





Key to Abbreviations

- BGF – Broxson Gulch fault
- CF – Canteen fault
- DC – Ditch Creek fault
- DD – Donnelly Dome fault
- GC – Glacier Creek fault
- GM – Granite Mountain fault
- HF – Healy Creek fault
- KC – Kansas Creek fault
- MM – Mystic Mountain fault
- MR – Molybdenum Ridge fault
- NFT – Northern Foothills Thrust
- PF – Panoramic fault
- PsF – Potts fault
- RM – Red Mountain fault
- SGF – Susitna Glacier fault
- UF – Unnamed fault

STATE OF ALASKA
ALASKA ENERGY AUTHORITY

ALASKA
ENERGY AUTHORITY

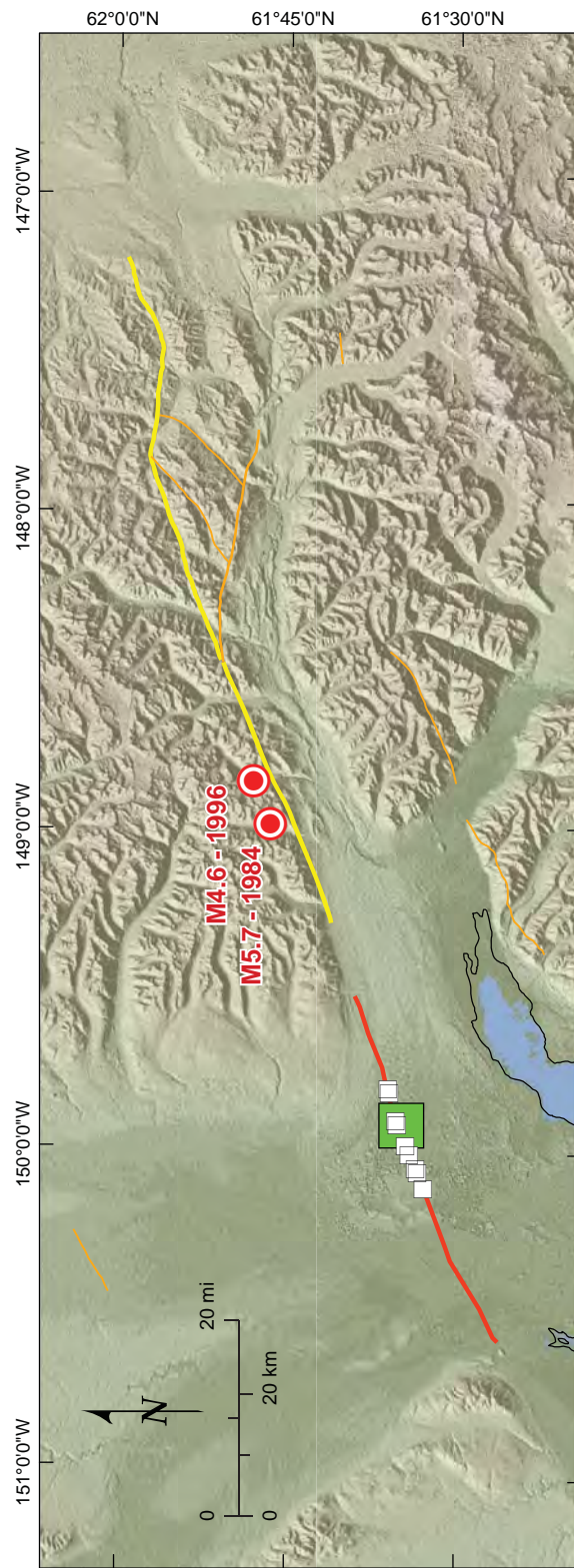
SUSITNA-WATANA HYDROELECTRIC PROJECT

**NORTHERN FOOTHILLS
FOLD AND THRUST BELT**

02/02/12

FIGURE 7





Explanation

- Earthquake epicenter
 - Paleoseismic Investigations
 - Hausler et al., 2002
 - Willis et al., 2007
- Faults**
- Castle Mtn. fault, western segment
 - Castle Mtn. fault, eastern segment and Caribou fault
 - Other fault

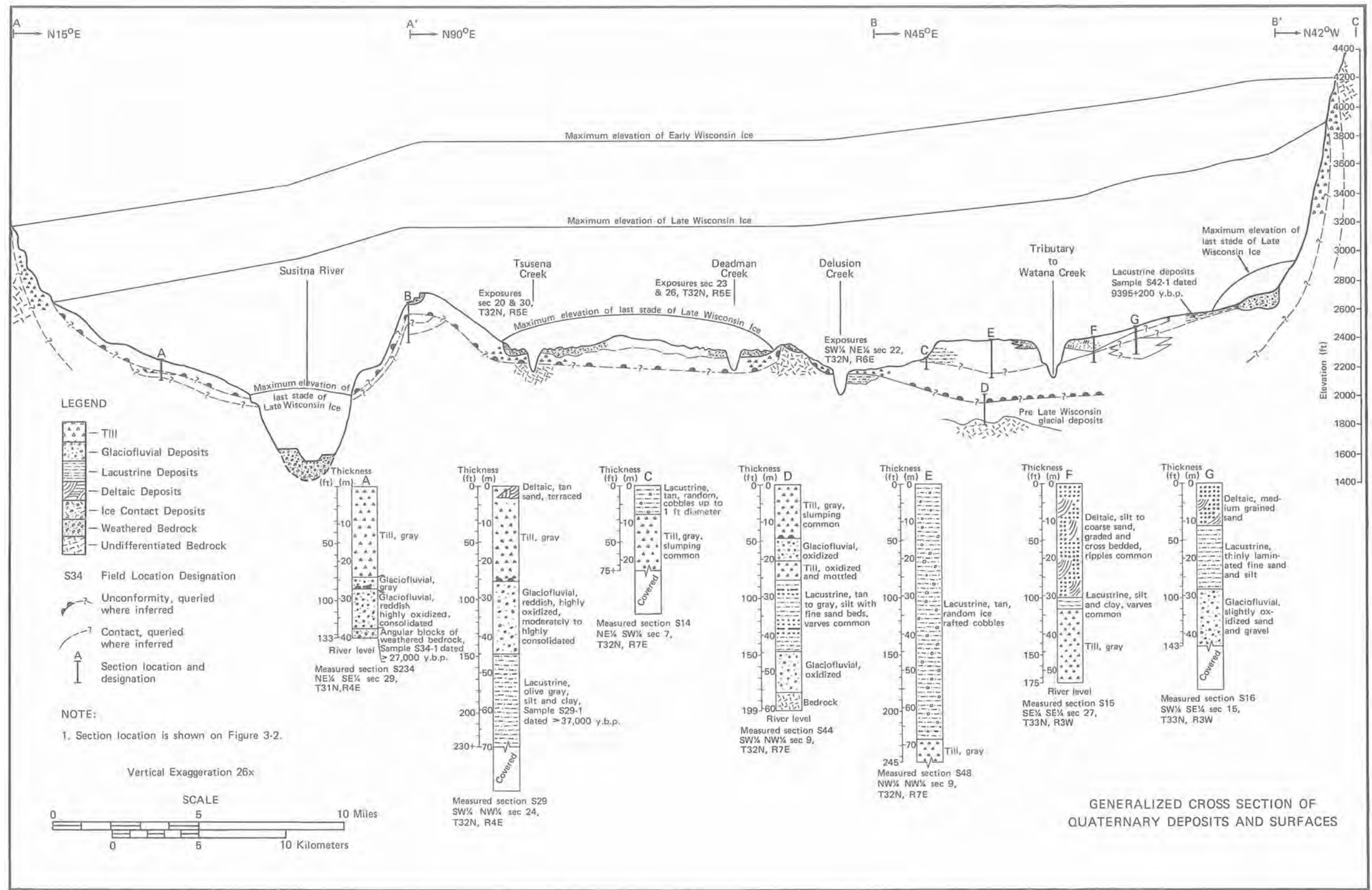
Note: Site is ~100 km to the north



SUSITNA-WATANA HYDROELECTRIC PROJECT

CASTLE MOUNTAIN FAULT





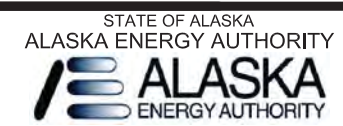
From WCC (1982)

| REV | DESCRIPTION | BY | DATE |
|-----|-------------|----|------|
| | | | |

| |
|-------|
| SCALE |
|-------|

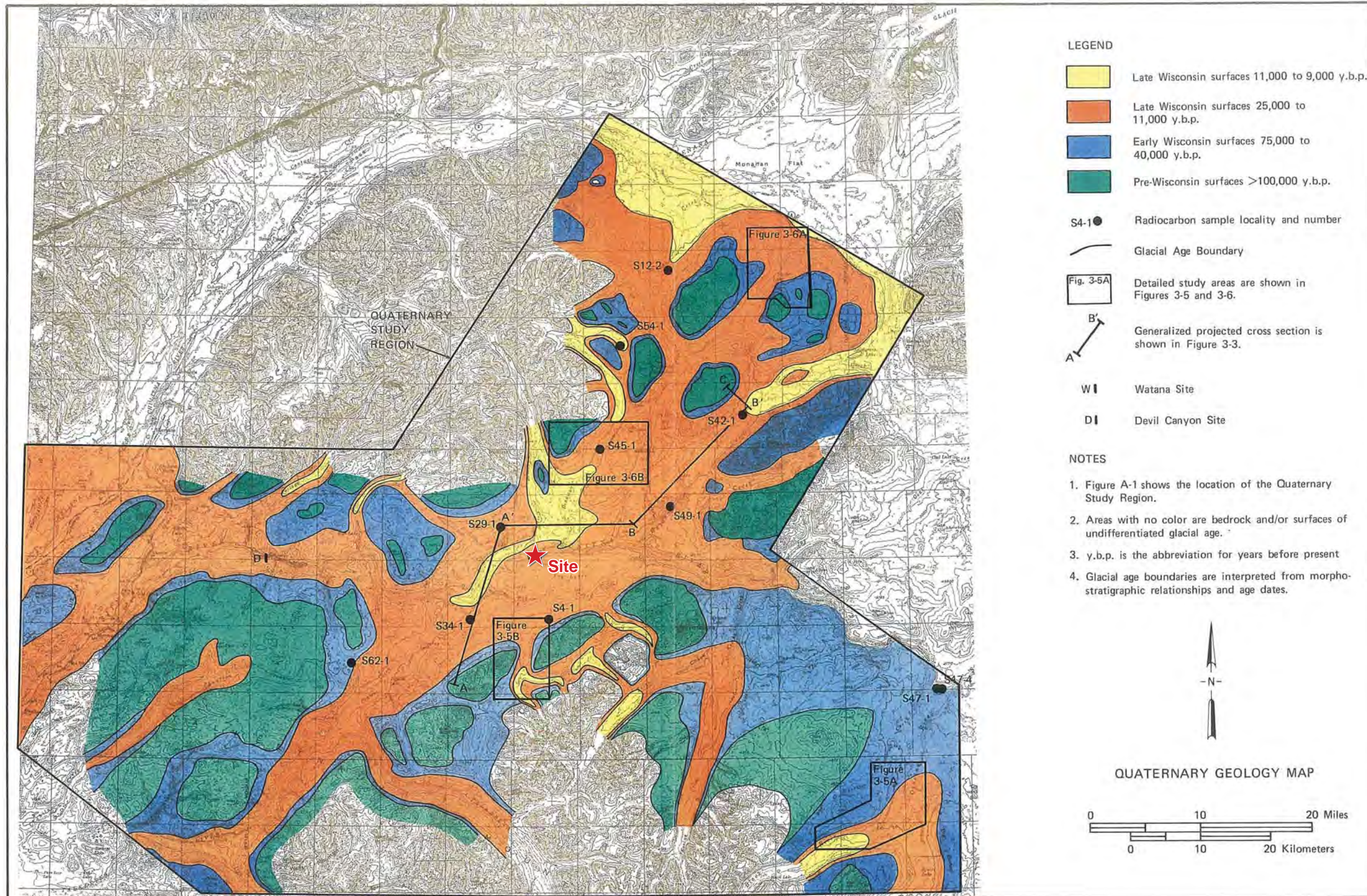
WARNING
 IF THIS BAR DOES NOT MEASURE 1" THEN DRAWING IS NOT TO SCALE

| | |
|-------------|----------|
| Project No. | |
| Date | 02/02/12 |
| Designed | |
| Drawn | |
| Approved | |



SUSITNA-WATANA HYDROELECTRIC PROJECT
GENERALIZED CROSS SECTION OF QUATERNARY DEPOSITS AND SURFACES

FIGURE
FIGURE 9



From WCC (1982)

LEGEND

- Late Wisconsin surfaces 11,000 to 9,000 y.b.p.
- Late Wisconsin surfaces 25,000 to 11,000 y.b.p.
- Early Wisconsin surfaces 75,000 to 40,000 y.b.p.
- Pre-Wisconsin surfaces >100,000 y.b.p.

S4-1 ● Radiocarbon sample locality and number

— Glacial Age Boundary

Fig. 3-5A Detailed study areas are shown in Figures 3-5 and 3-6.

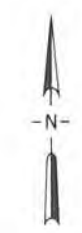
A-A' Generalized projected cross section is shown in Figure 3-3.

W I Watana Site

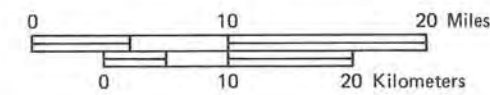
D I Devil Canyon Site

NOTES

1. Figure A-1 shows the location of the Quaternary Study Region.
2. Areas with no color are bedrock and/or surfaces of undifferentiated glacial age.
3. y.b.p. is the abbreviation for years before present
4. Glacial age boundaries are interpreted from morphostratigraphic relationships and age dates.



QUATERNARY GEOLOGY MAP



| REV | DESCRIPTION | BY | DATE |
|-----|-------------|----|------|
| | | | |

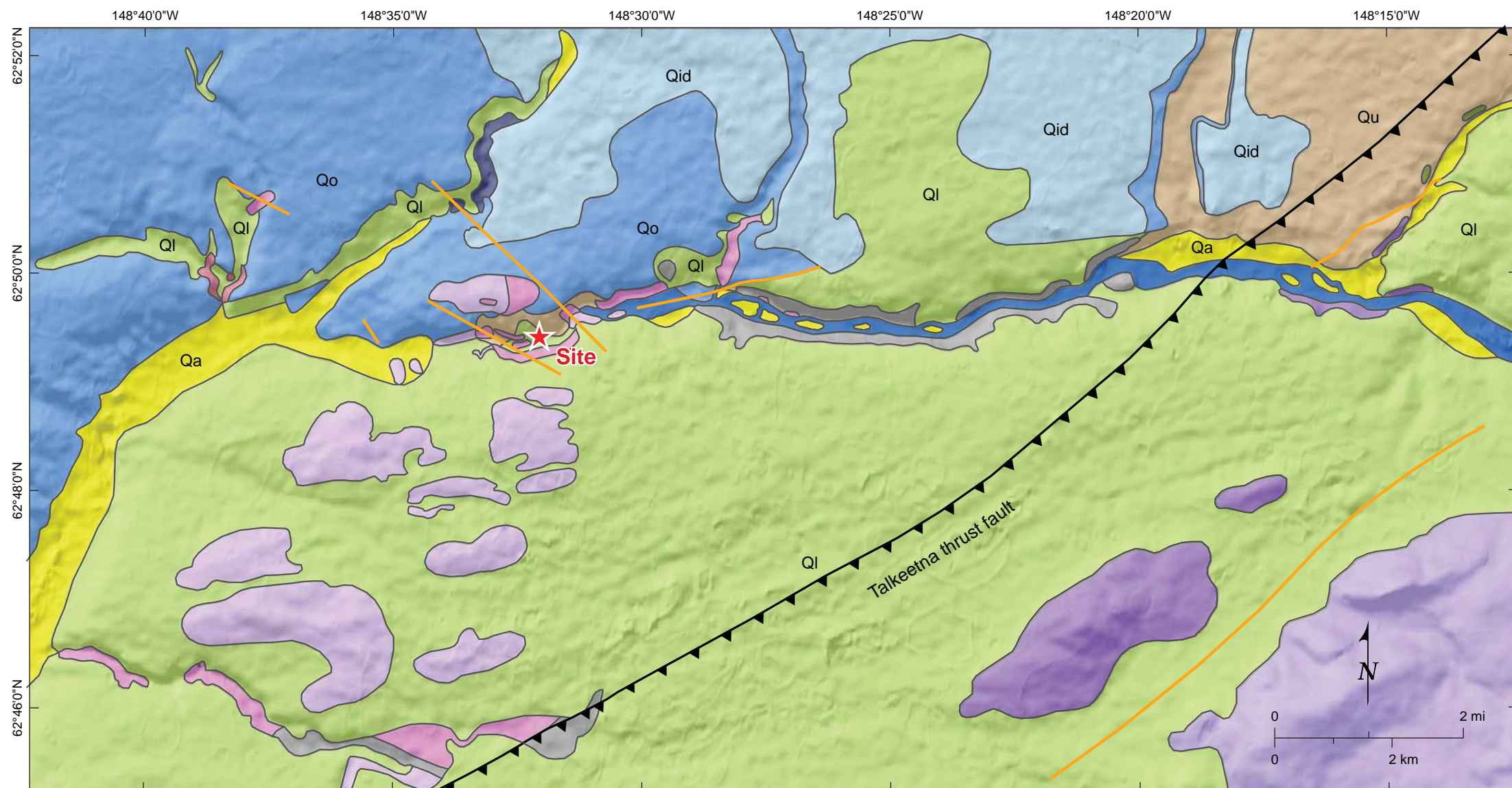
SCALE
 0 1/2 1
 WARNING
 IF THIS BAR DOES NOT MEASURE 1" THEN DRAWING IS NOT TO SCALE

Project No. _____
 Date 02/02/12
 Designed _____
 Drawn _____
 Approved _____



SUSITNA-WATANA HYDROELECTRIC PROJECT
 SITE VICINITY
 QUATERNARY GEOLOGY

FIGURE
 FIGURE 10



- Explanation**
- Contact
 - ▲▲▲ Thrust fault
 - Shear
- QUATERNARY**
- Qa** Alluvium, alluvial terraces and fans
 - Qid** Ice disintegration deposits
 - Ql** Till
 - Qo** Outwash
 - Qu** Surficial deposits, undifferentiated, generally thin
- TERTIARY**
- Conglomerate, sandstone and claystone
 - Volcaniclastic sandstone, siltstone and shale
 - Andesite porphyry, minor basalt
 - Diorite to quartz diorite, minor granodiorite
 - Biotite granodiorite
- MESOZOIC**
- CRETACEOUS** – Argillite and graywacke
 - TRIASSIC** – Basaltic metavolcanic rocks, metabasalt and slate
 - PALEOZOIC** – Basaltic to andesitic metavolcanic rocks

Geology from Acres (1982)

| REV | DESCRIPTION | BY | DATE |
|-----|-------------|----|------|
| | | | |

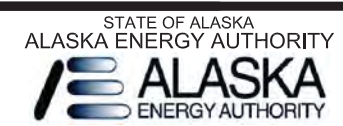
SCALE

WARNING

0 1/2 1

IF THIS BAR DOES NOT MEASURE 1" THEN DRAWING IS NOT TO SCALE

Project No. _____
 Date 02/02/12
 Designed _____
 Drawn _____
 Approved _____

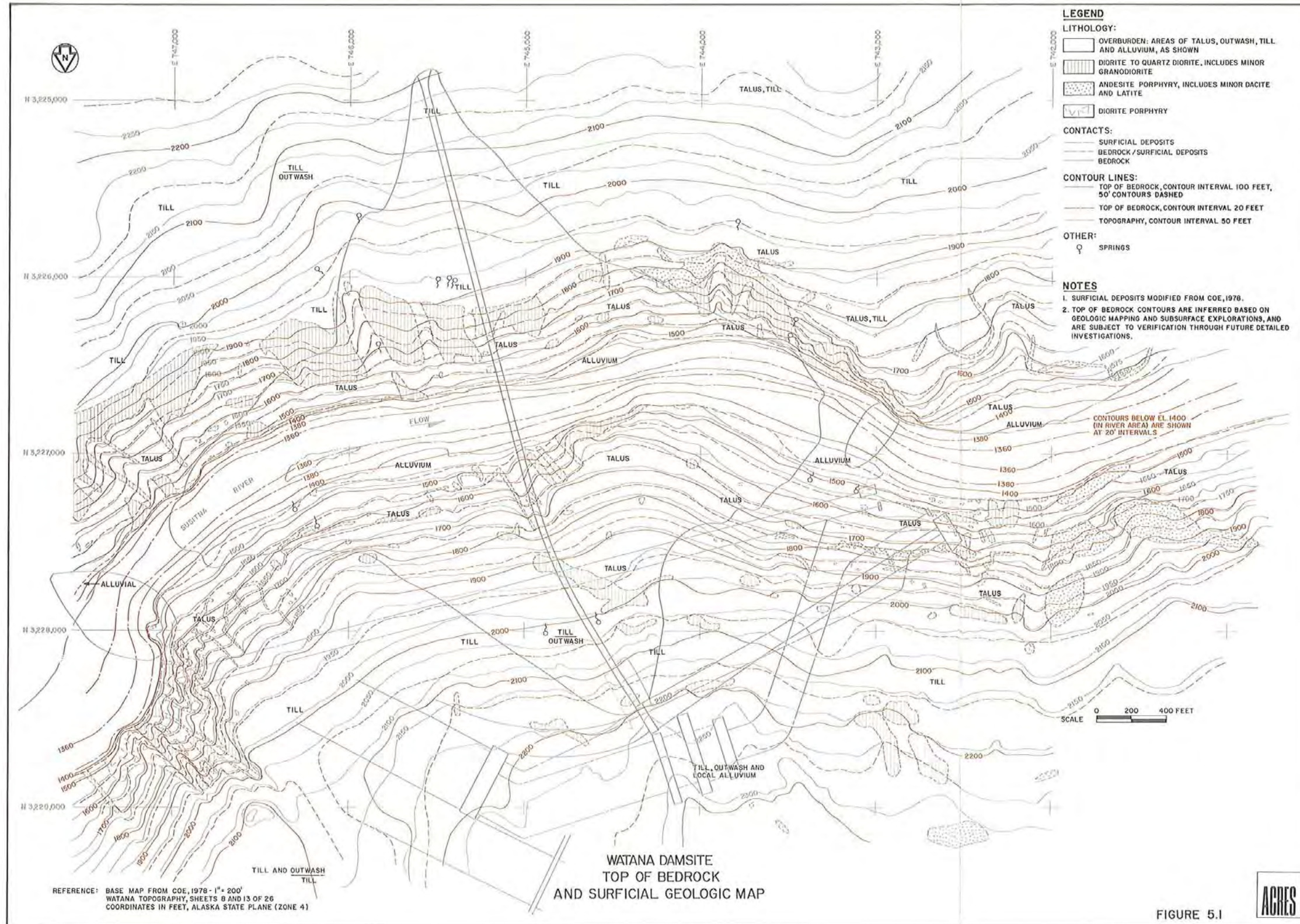


SUSITNA-WATANA HYDROELECTRIC PROJECT

SITE GEOLOGY

FIGURE

FIGURE 11



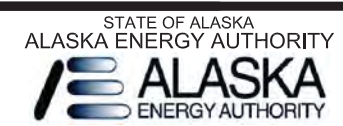
From Acres (1981)

| REV | DESCRIPTION | BY | DATE |
|-----|-------------|----|------|
| | | | |

SCALE

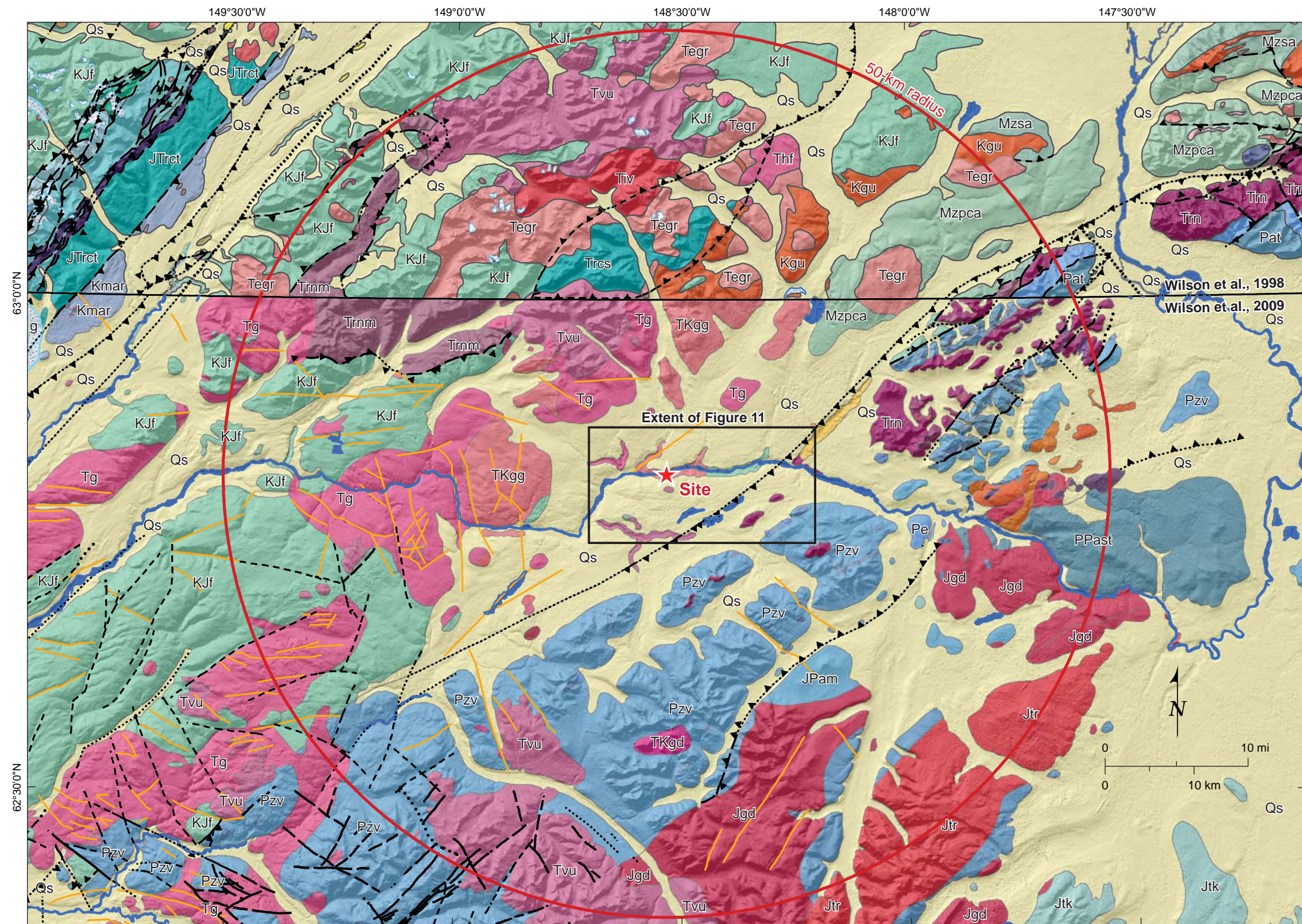
WARNING
0 1/2 1
IF THIS BAR DOES NOT MEASURE 1" THEN DRAWING IS NOT TO SCALE

Project No.
Date 02/02/12
Designed
Drawn
Approved



SUSITNA-WATANA HYDROELECTRIC PROJECT
WATANA DAM SITE
TOP OF BEDROCK AND
SURFICIAL GEOLOGIC MAP

FIGURE
FIGURE 12



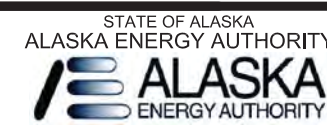
Geology from Wilson et al., 1998 (USGS Open-File Report 98-133) and Wilson et al., 2009 (USGS Open-file Report 2009-1108)

See Figure 13B for map legend

| REV | DESCRIPTION | BY | DATE |
|-----|-------------|----|------|
| | | | |
| | | | |
| | | | |

| | |
|---------|--------------------------------------------------------------|
| SCALE | WARNING |
| 0 1/2 1 | IF THIS BAR DOES NOT MEASURE 1" THEN DRAWING IS NOT TO SCALE |

| | |
|-------------|----------|
| Project No. | 02/02/12 |
| Date | |
| Designed | |
| Drawn | |
| Approved | |



SUSITNA-WATANA HYDROELECTRIC PROJECT
SITE REGION GEOLOGY

FIGURE
FIGURE 13A

 Ice fields or glaciers


QUATERNARY DESPOSITS

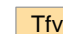
 Surficial deposits, undifferentiated

**TERTIARY ROCKS
Sedimentary Rocks**

 Sedimentary rocks, undivided


 Nenana Gravel

 Coal-bearing rocks

 Fluvial sedimentary rocks and subordinate volcanic rocks

**Igneous Rocks
Volcanic and Hypabyssal Rocks**

 Tertiary volcanic rocks, undivided


 Hypabyssal felsic and intermediate intrusions

 Hypabyssal mafic intrusions

Intrusive Rocks

 Granite and volcanic rocks, undivided

EOCENE

 Granite and granodiorite


PALEOCENE

 Granitic rocks


TERTIARY AND/OR CRETACEOUS

**Igneous Rocks
Intrusive Rocks**

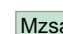
 Granitic rocks


 Granodiorite, tonalite and monzonite dikes, and stocks

Metamorphic Rocks

 Gneissose granitic rocks

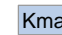
**UNDIVIDED MESOZOIC ROCKS
METAMORPHIC ROCKS**

 Schist and amphibolite

 Phyllite, pelitic schist, calc-schist, and amphibolite of the McClaren metamorphic belt

CRETACEOUS


Melange

 Melanges of the Alaska Range

 Limestone blocks

Igneous Rocks

Volcanic and hypabyssal rocks

 Andesite subvolcanic rocks

Intrusive Rocks


 Granitic rocks

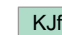
 Granitic rocks younger than 85 Ma


 Ultramafic rocks

CRETACEOUS AND/OR JURASSIC

Sedimentary Rocks

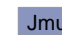
 Argillite, chert, sandstone, and limestone


 Kahiltna flysch sequence

 Conglomerate, sandstone, siltstone, shale, and volcanic rocks


JURASSIC

Igneous Rocks

 Mafic and ultramafic rocks

 Alaska-Aleutian Range and Chitina Valley batholiths, undifferentiated

Metamorphic Rocks

 Uranatina metaplutonic complex


Sedimentary Rocks

 Limestone and marble

 Talkeetna Formation

TRIASSIC

Sedimentary Rocks


 Calcareous sedimentary rocks

 Kamishak limestone


Plutonic Rocks

 Gabbro, diabase, and metagabbro


Volcanic Rocks


 Nikolai Greenstone and related similar rocks

Metamorphic Rocks


 Metavolcanics and associated metasedimentary rocks


**MESOZOIC AND PALEOZOIC
Assemblages and Sequences**

 Red and brown sedimentary rocks and basalt

 Crystal tuff, argillite, chert, graywacke, and limestone


 Red beds


 Volcanic and sedimentary rocks


 Serpentinite, basalt, chert and gabbro

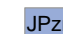
**PALEOZOIC
Assemblages and Sequences
(Skolai Group)**





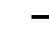

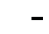


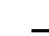


 Eagle Creek Formation

 Station Creek and Slana Spur Fm., and equivalent rocks

 Teteina Volcanics

 Streina metamorphic complex


 Marble

-  Stratigraphic contact
-  Shoreline or riverbank
-  Ice contact (glacier limit)
-  Lineament
-  Fault - Certain
-  Fault - Approximate
-  Fault - Inferred
-  Fault - Concealed
-  Thrust fault - Certain
-  Thrust fault - Approximate
-  Thrust fault - Inferred
-  Thrust fault - Concealed

Geology from Wilson et al., 1998 (USGS Open-file Report 98-133) and Wilson et al., 2009 (USGS Open-file Report 2009-1108)

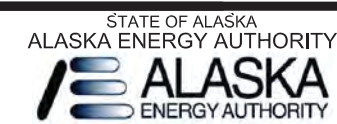
| REV | DESCRIPTION | BY | DATE |
|-----|-------------|----|------|
| | | | |

SCALE



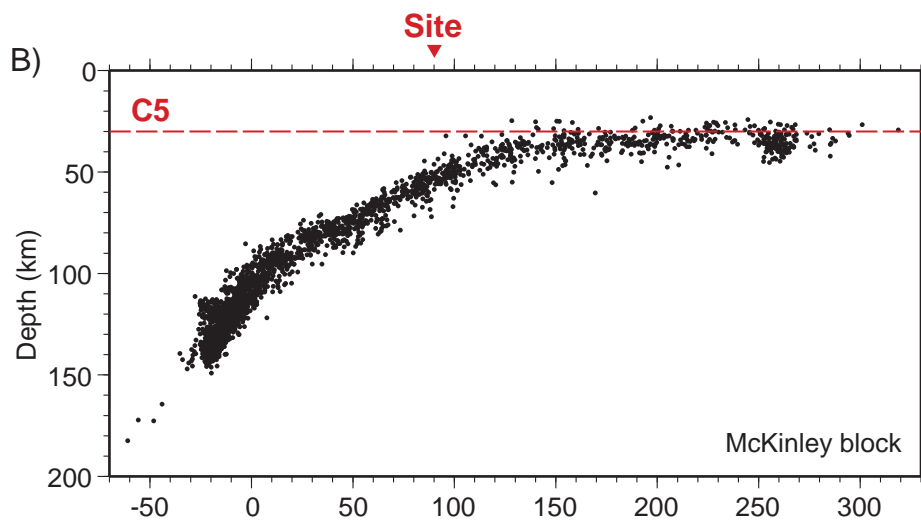
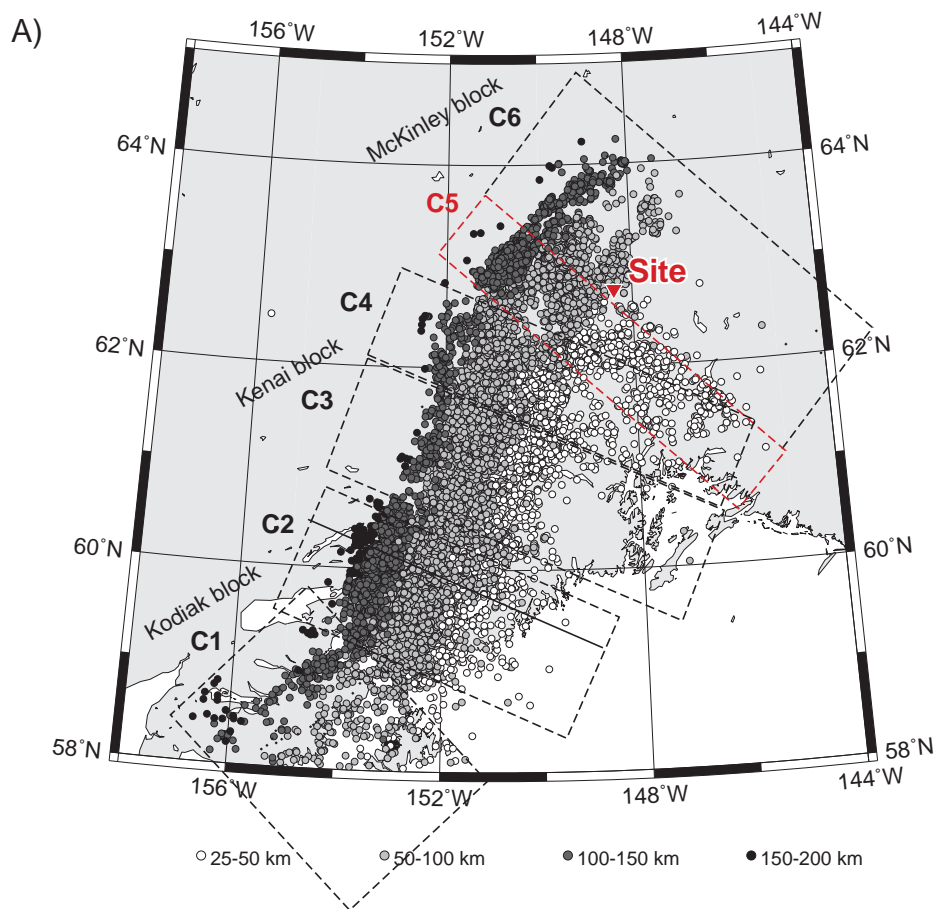
WARNING
IF THIS BAR DOES NOT MEASURE 1" THEN DRAWING IS NOT TO SCALE

Project No. _____
Date 02/02/12
Designed _____
Drawn _____
Approved _____



SUSITNA-WATANA HYDROELECTRIC PROJECT
SITE REGION
GEOLOGY LEGEND

FIGURE
FIGURE 13B



(A) Map of earthquakes showing location of cross section (dashed rectangle labeled C5) shown in (B), modified from Figure 5 of Ratchkovski and Hansen (2002). (B) Cross section (C5) of earthquakes, modified from Figure 6 of Ratchkovski and Hansen (2002). Triangle indicates approximate site location.

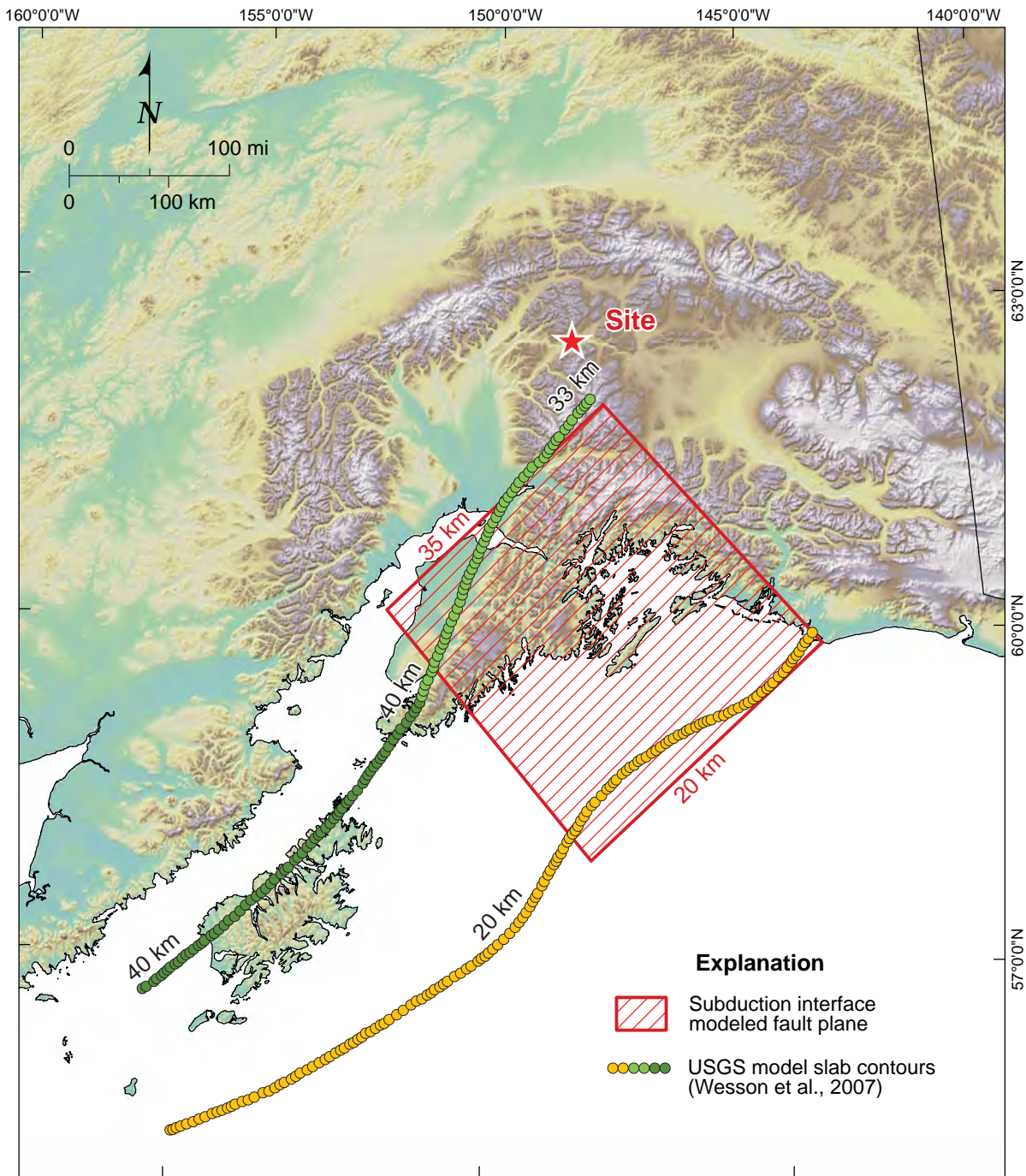


SUSITNA-WATANA HYDROELECTRIC PROJECT

MAP AND CROSS SECTION
OF SUBDUCTION-ZONE
EARTHQUAKES

02/02/12

FIGURE 14



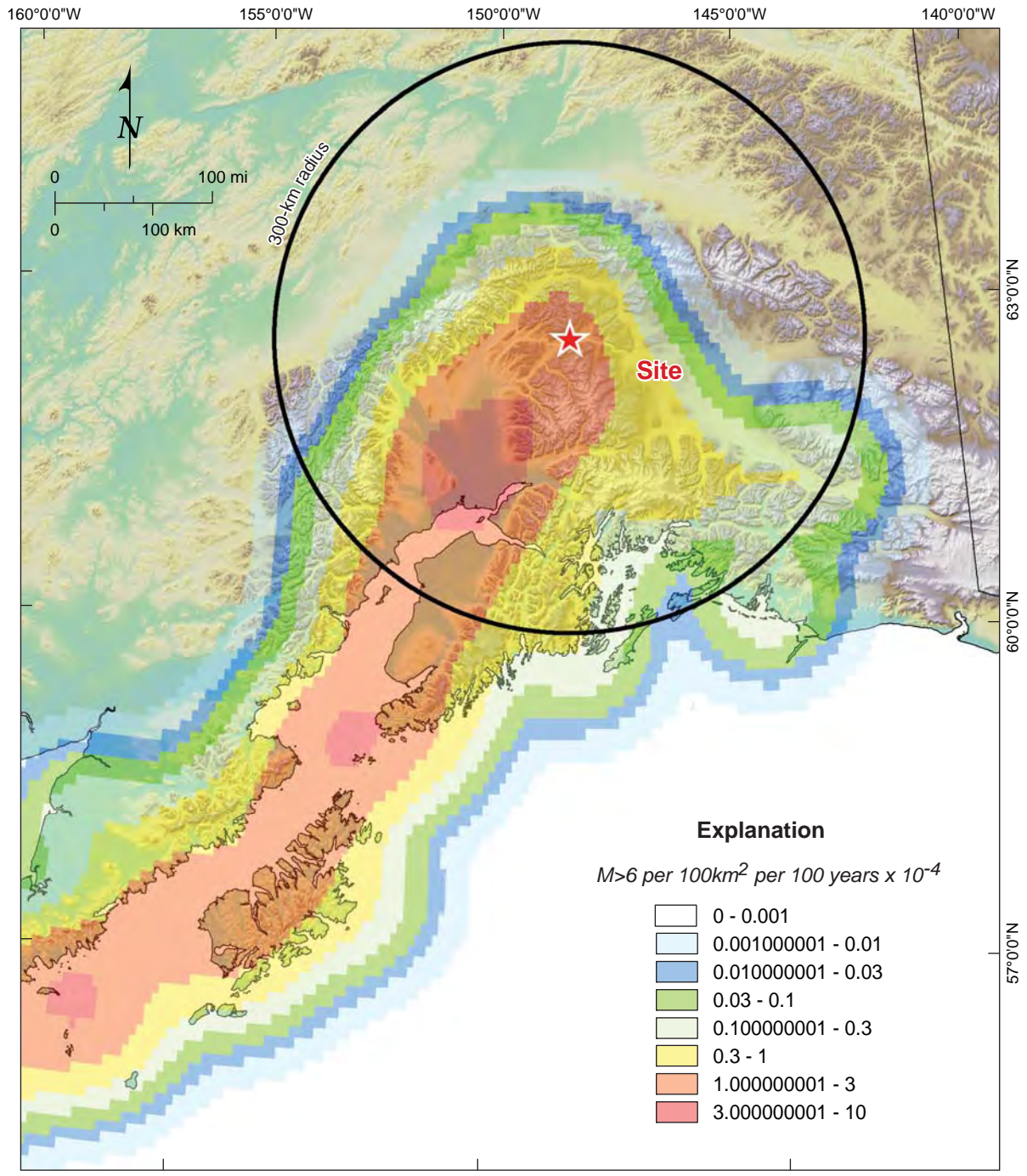
STATE OF ALASKA
ALASKA ENERGY AUTHORITY

SUSITNA-WATANA HYDROELECTRIC PROJECT

SUBDUCTION INTERFACE
MODEL

02/02/12

FIGURE 15



From Wesson et al. (2007)

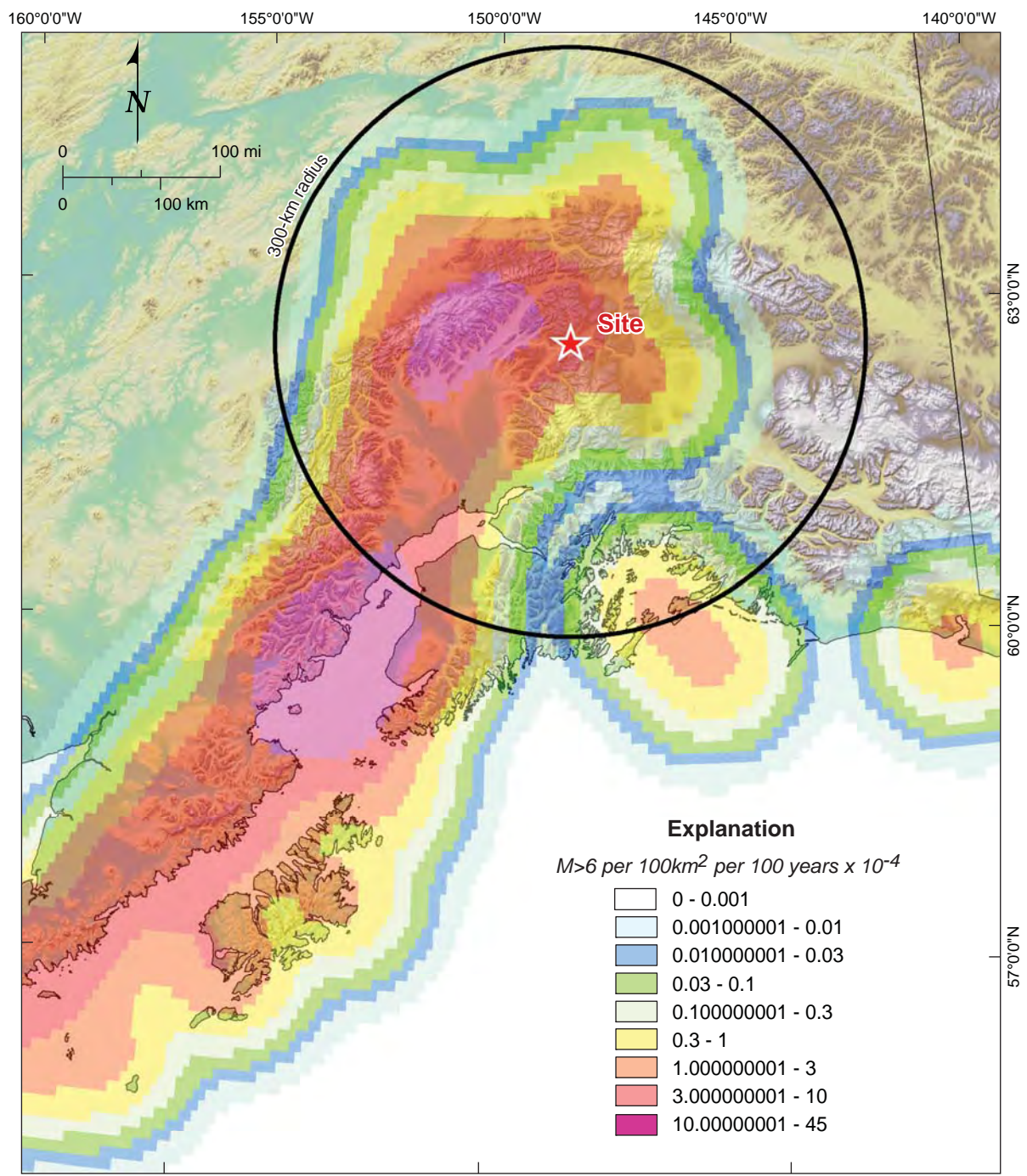


STATE OF ALASKA
ALASKA ENERGY AUTHORITY

SUSITNA-WATANA HYDROELECTRIC PROJECT

USGS INTRASLAB MODEL,
31-50 MI (50-80 KM)

02/02/12 FIGURE 16



From Wesson et al. (2007)

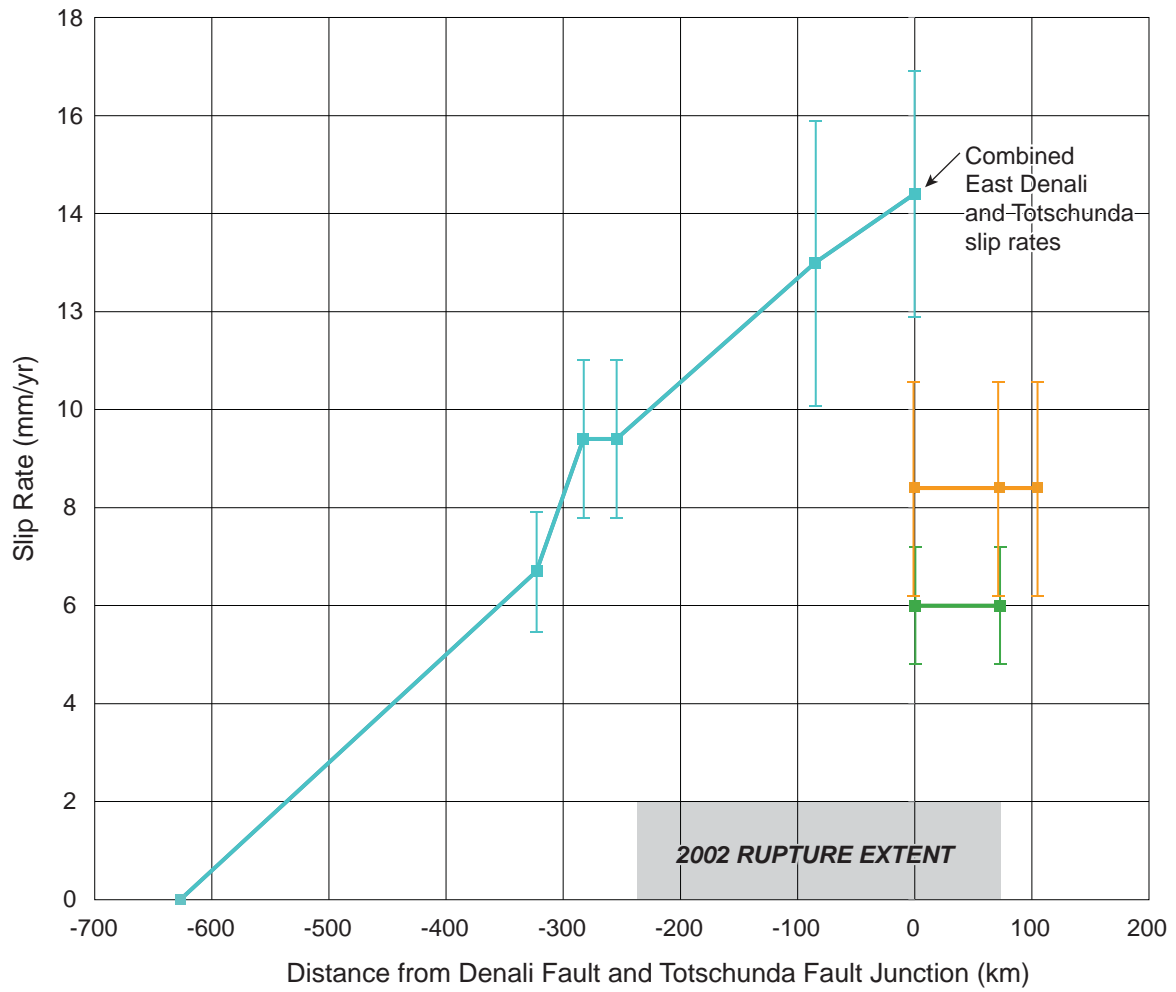


STATE OF ALASKA
ALASKA ENERGY AUTHORITY

SUSITNA-WATANA HYDROELECTRIC PROJECT

USGS INTRASLAB MODEL,
50-75 MI (80-120 KM)

02/02/12 FIGURE 17



Explanation

- Central and western Denali fault slip rate
- Eastern Denali fault slip rate
- Totschunda fault slip rate
- | Error bar



SUSITNA-WATANA HYDROELECTRIC PROJECT

DENALI FAULT SLIP RATES

02/02/12

FIGURE 18



Active (?) fault, lower Sonona Creek, offsetting unconsolidated deposits.

As shown above, Sonona Creek fault is ~4.5 km long, and the site is ~70 km to the west-northwest. From Williams and Galloway (1986).



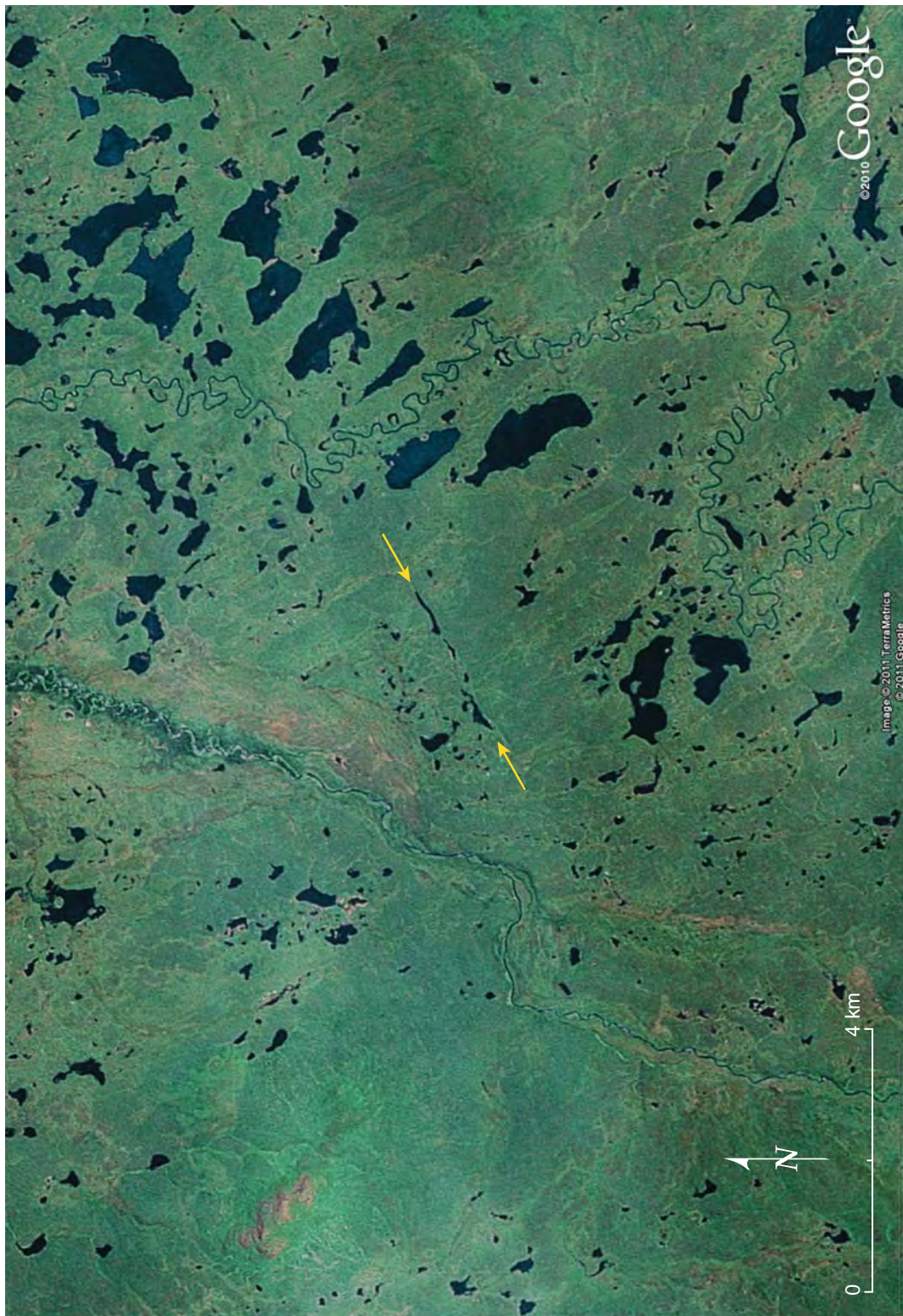
STATE OF ALASKA
ALASKA ENERGY AUTHORITY

ALASKA
ENERGY AUTHORITY

SUSITNA-WATANA HYDROELECTRIC PROJECT

SONONA CREEK FAULT TRACE

02/02/12 FIGURE 19



From Google Earth imagery



STATE OF ALASKA
ALASKA ENERGY AUTHORITY



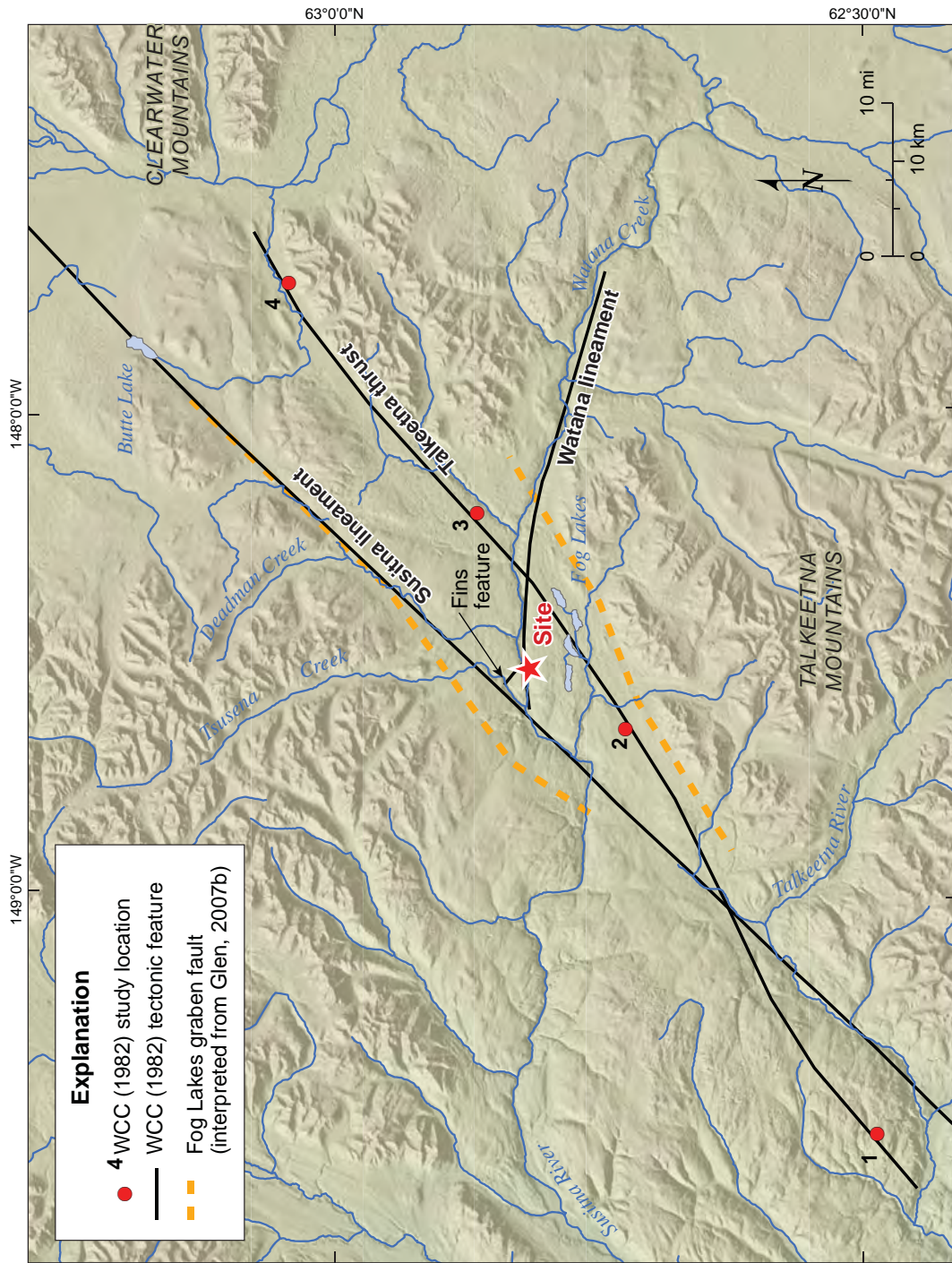
ALASKA ENERGY AUTHORITY

SUSITNA-WATANA HYDROELECTRIC PROJECT

SONONA CREEK FAULT SCARP

02/02/12

FIGURE 20



Explanation

- 4 WCC (1982) study location
- WCC (1982) tectonic feature
- Fog Lakes graben fault (interpreted from Glen, 2007b)

STATE OF ALASKA
ALASKA ENERGY AUTHORITY

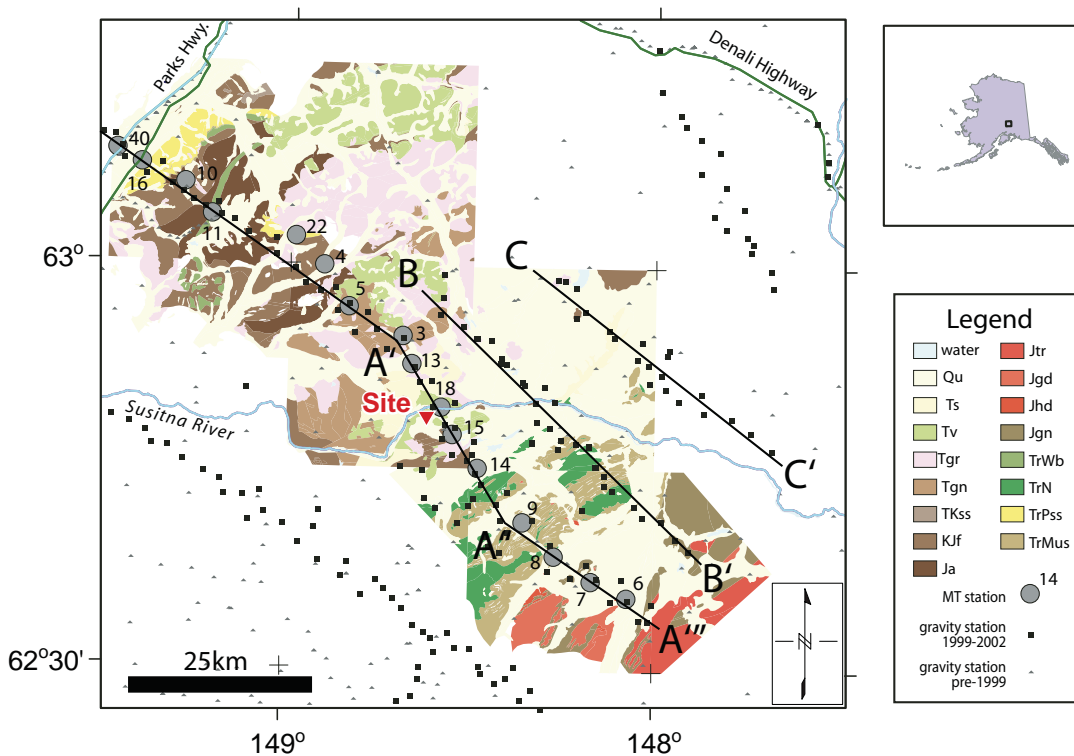


SUSTINA-WATANA HYDROELECTRIC PROJECT

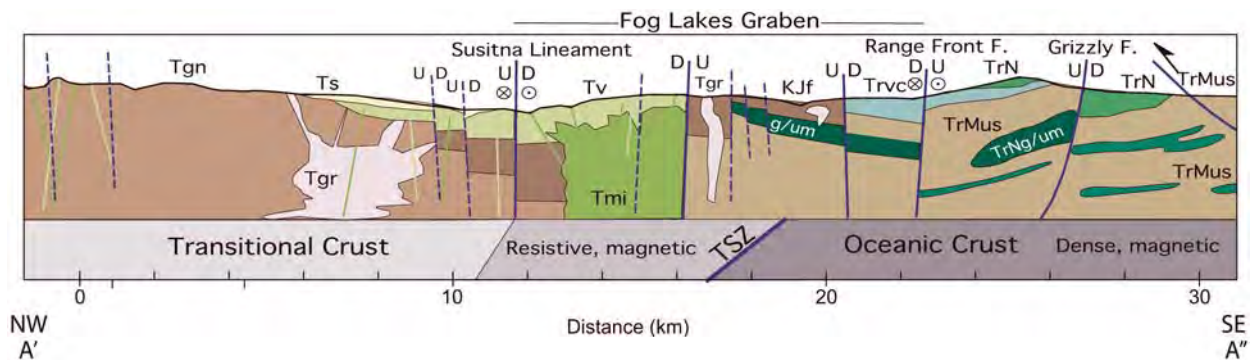
**SITE VICINITY
TECTONIC FEATURES**

02/02/12 **FIGURE 21**





Gravity = squares (1999–2000) and triangles; MT stations and potential field profiles = black lines A–A', B–B', and C–C'; Qu = Quaternary sediments, undifferentiated; Ts = Tertiary nonmarine clastic sedimentary rocks; Tv = Tertiary volcanic rocks; Tgr = Tertiary granitoid intrusive rocks; Tgn = Tertiary gneiss and granitoid intrusive rocks, undifferentiated; TKss = Tertiary or Cretaceous sandstone; KJf = Jurassic to Cretaceous flysch, shale, sandstone, and conglomerate; Ja = Jurassic(?) argillite; Jtr = Jurassic trondjemite; Jgd = Jurassic granodiorite; Jhd = Jurassic hornblende diorite; Jgn = Jurassic gneiss; Trwb = Triassic basalts of Whale Ridge; TrN = Triassic Nikolai Greenstone and gabbros; TrPss = Permian(?) to Triassic quartzosedimentary rocks; TrMus = Mississippian to early Triassic siliceous and calcareous sedimentary rocks. Geology modified from Wilson et al., 1998, and unpublished U.S. Geological Survey mapping.



Simplified geologic map and cross section A'–A'' along a transect through the northern Talkeetna Mountains,

Modified from Figures 3 and 7 in Glen et al. (2007)

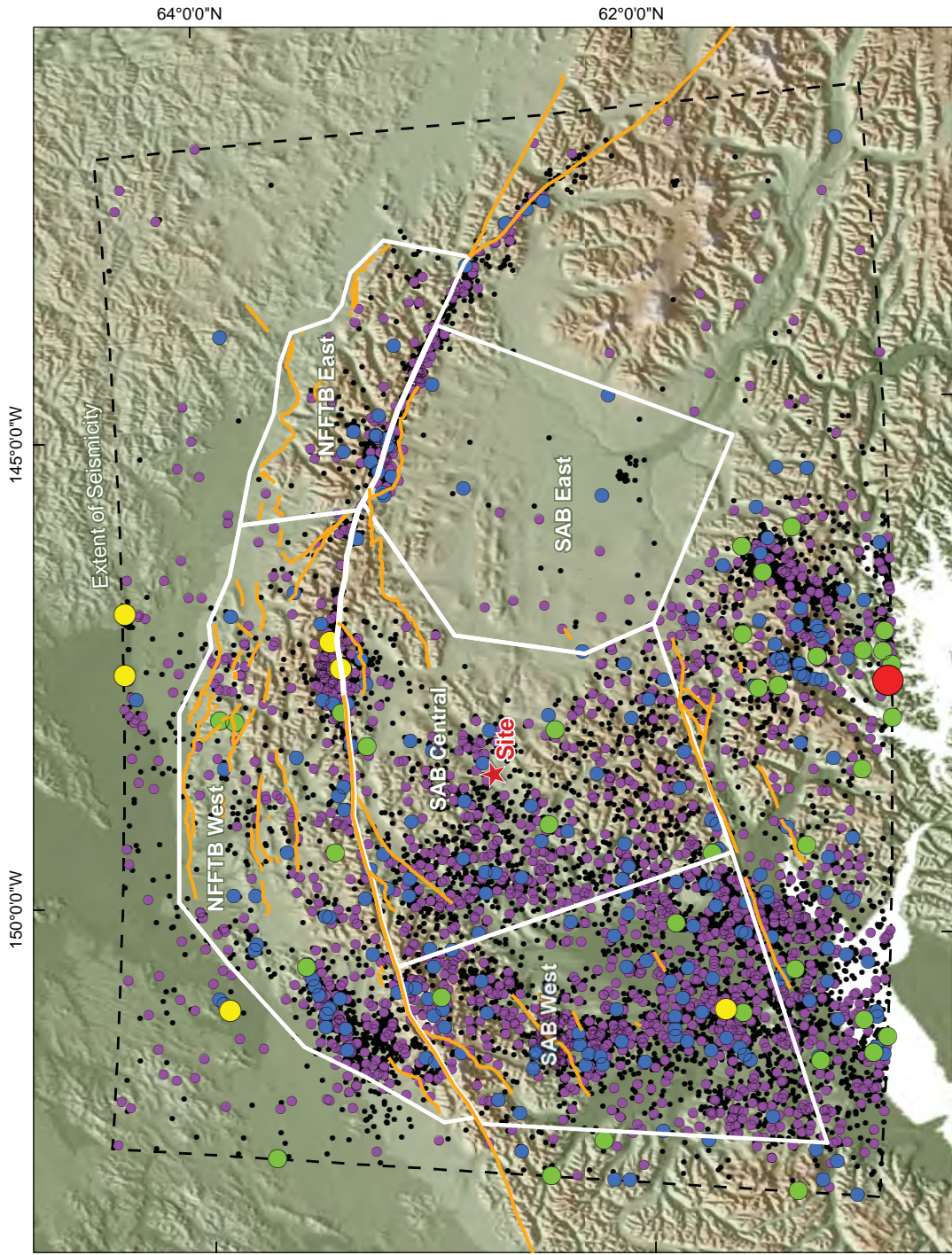


STATE OF ALASKA
ALASKA ENERGY AUTHORITY

SUSITNA-WATANA HYDROELECTRIC PROJECT

SIMPLIFIED GEOLOGIC MAP AND CROSS SECTION

02/02/12 FIGURE 22



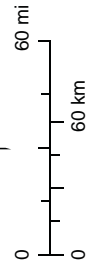
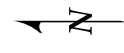
Explanation

— Fault

Seismicity (Mw)

- 3.0 - 3.9
- 4.0 - 4.9
- 5.0 - 5.9
- 6.0 - 6.9
- 7.0 - 7.9
- 8.0 - 8.9
- 9.0 - 9.2

Note: Merged AEIC and USGS catalogs, with earthquake relocations, as noted in text. Earthquake depths range from 0 to 126 km.



145°00'W

150°00'W

64°00'N

62°00'N

Extent of Seismicity

NFFTIB West

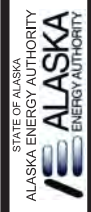
NFFTIB East

SAB West

SAB Central

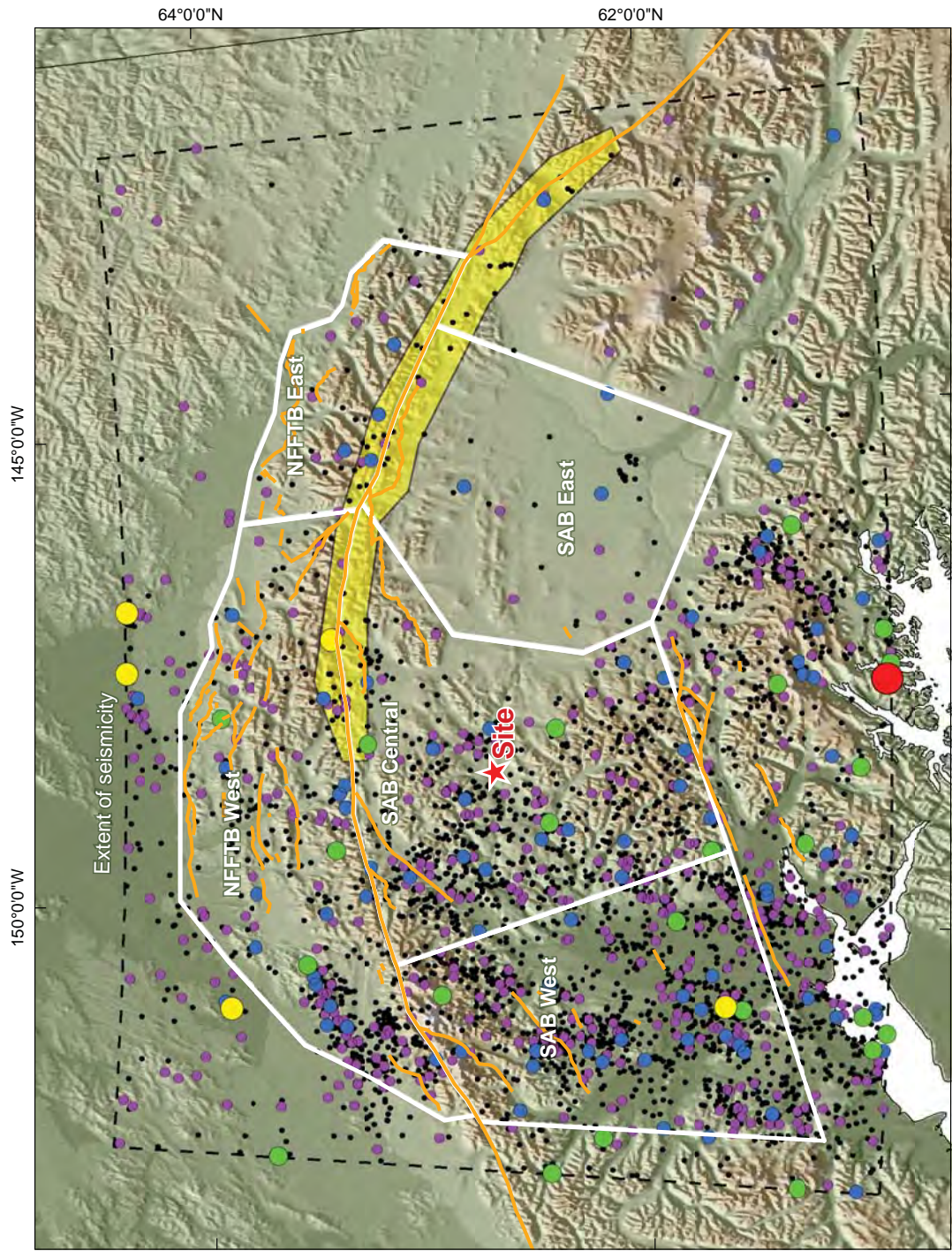
SAB East

Site



SUSTINA-WATANA HYDROELECTRIC PROJECT

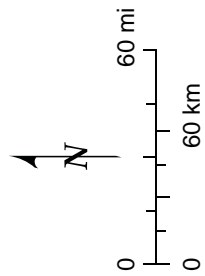
UNFILTERED EARTHQUAKE CATALOG

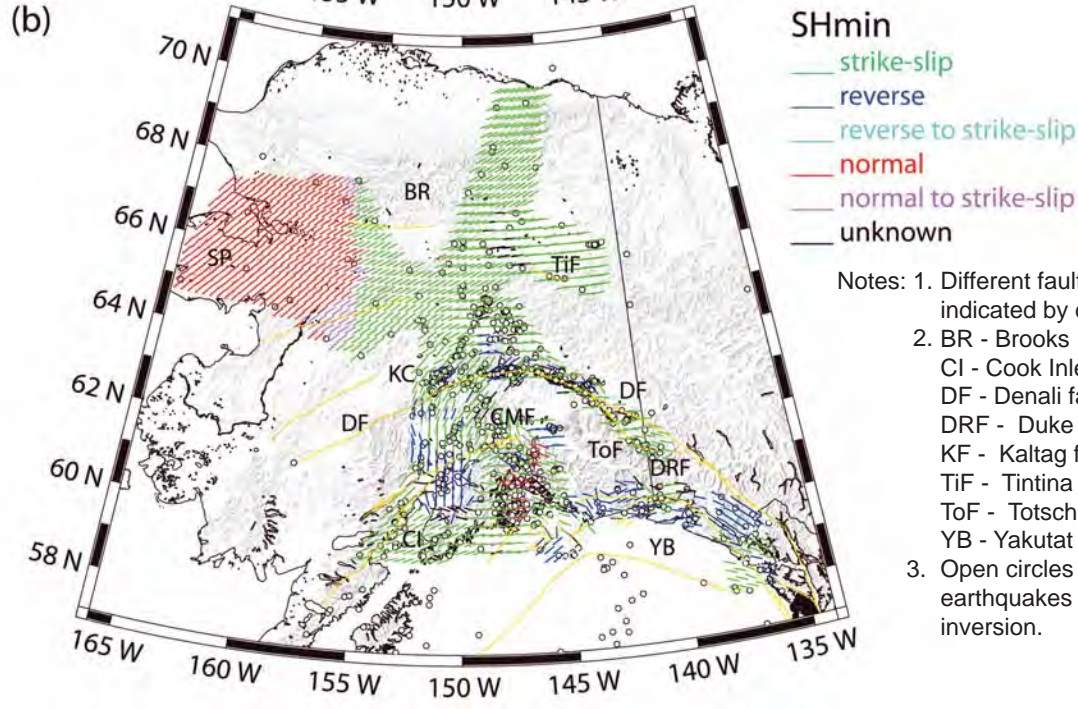
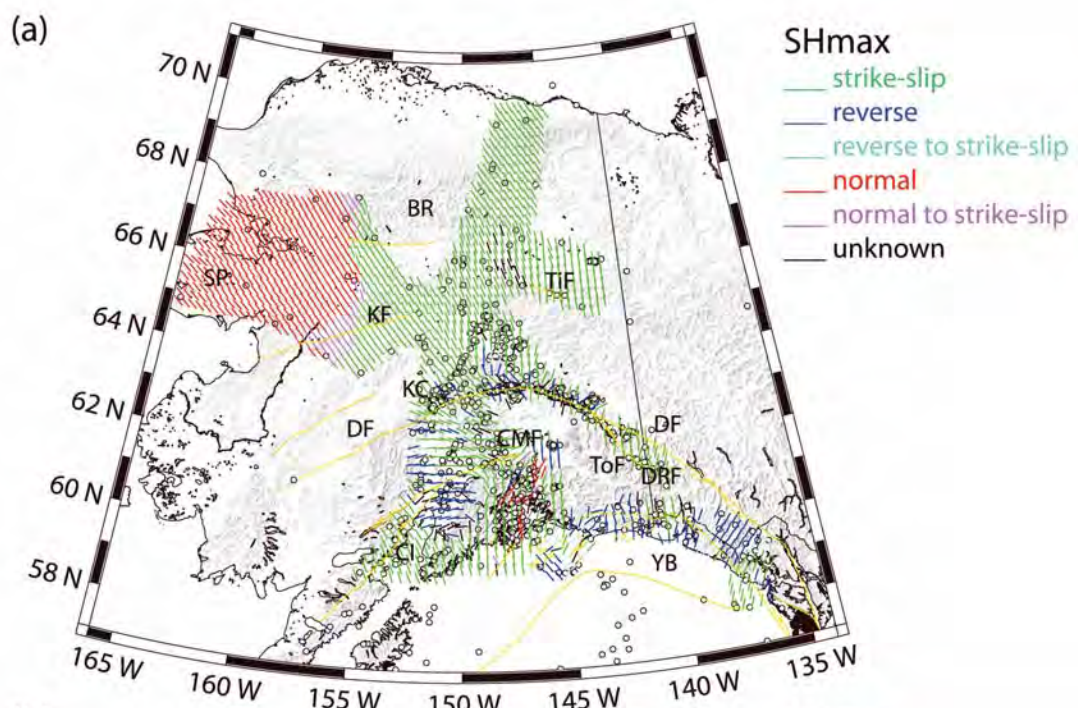


Explanation

- Fault
 - Denali fault aftershock exclusion zone
- Seismicity (Mw)**
- 3.0 - 3.9
 - 4.0 - 4.9
 - 5.0 - 5.9
 - 6.0 - 6.9
 - 7.0 - 7.9
 - 8.0 - 8.9
 - 9.0 - 9.2

Note: Aftershocks of the 2002 Denali earthquake removed (aftershock exclusion zone), as noted in text. Earthquake depths range from 0 to 126 km.





- Notes: 1. Different faulting regimes are indicated by different colors.
 2. BR - Brooks Range
 CI - Cook Inlet
 DF - Denali fault
 DRF - Duke River fault
 KF - Kaltag fault
 TiF - Tintina fault
 ToF - Totschunda fault
 YB - Yakutat block
 3. Open circles are locations of earthquakes used in the inversion.

(a) Maximum horizontal stress SHmax
 (b) Minimum horizontal stress SHmin

From Rupert (2008)

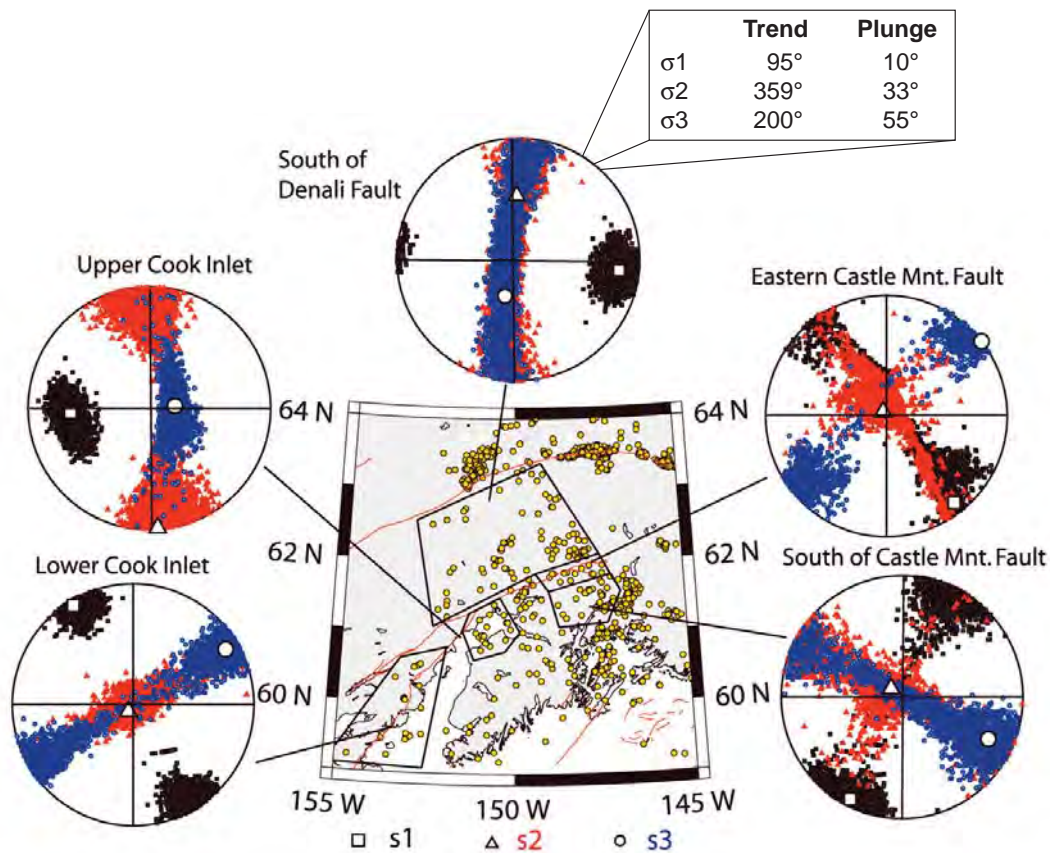


STATE OF ALASKA
ALASKA ENERGY AUTHORITY

SUSITNA-WATANA HYDROELECTRIC PROJECT

**STRESS TENSOR
INVERSION RESULTS
FROM CRUSTAL EARTHQUAKE
FOCAL MECHANISMS**

02/02/12FIGURE 25



Larger symbols (square, triangle, and circle) show locations of the best-fitting maximum, intermediate, and least stress axis, respectively. Black, maximum stress s_1 ; red, intermediate stress s_2 ; blue, least stress s_3 . Yellow circles shown on map are locations of crustal earthquakes.

From Rupert (2008)



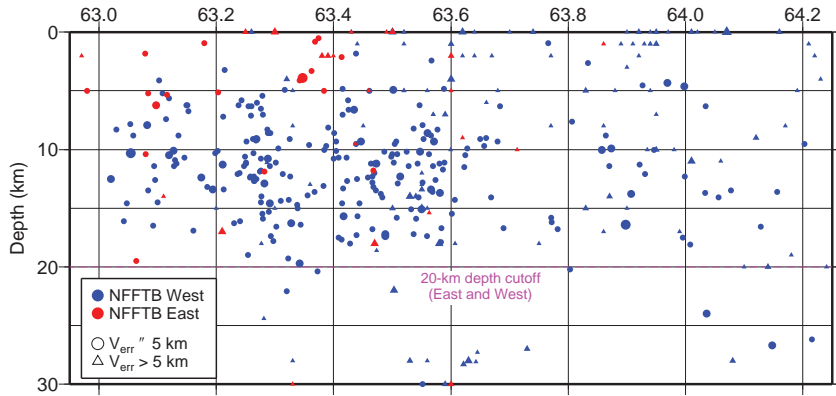
STATE OF ALASKA
ALASKA ENERGY AUTHORITY

SUSITNA-WATANA HYDROELECTRIC PROJECT

**STRESS TENSORS INVERSION
RESULTS FOR INDIVIDUAL
CRUSTAL DATA VOLUMES IN
SOUTH CENTRAL ALASKA**

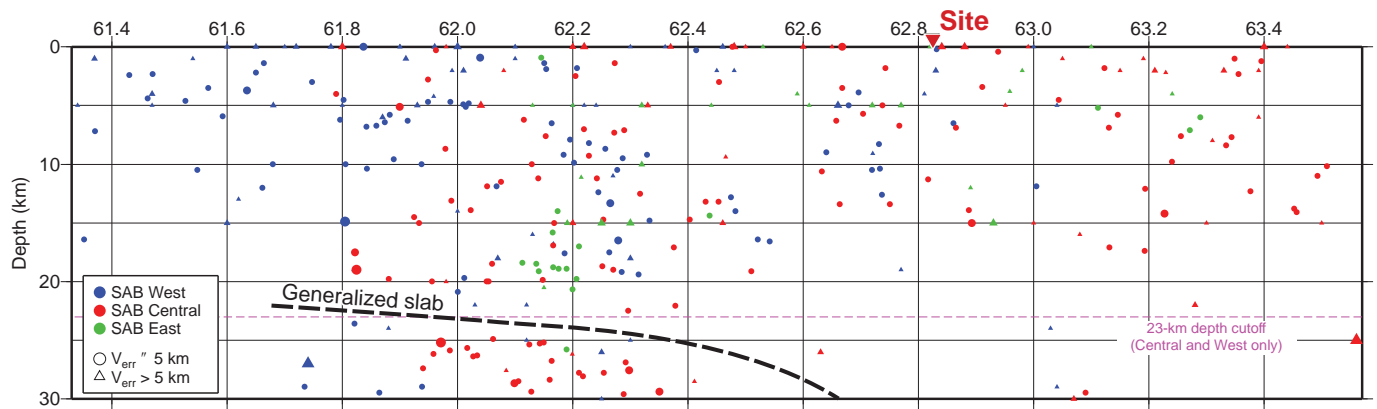
02/02/12 FIGURE 26

Northern Foothills Fold and Thrust Belt Areal Zones



NFFTB areal zones, showing the 20-km depth cutoff used for both the East and West zone recurrence catalogs

Southern Areal Background Zones



SAB areal zones, showing a schematic slab and the 23-km depth cutoff used for the Central and West zone recurrence catalogs.

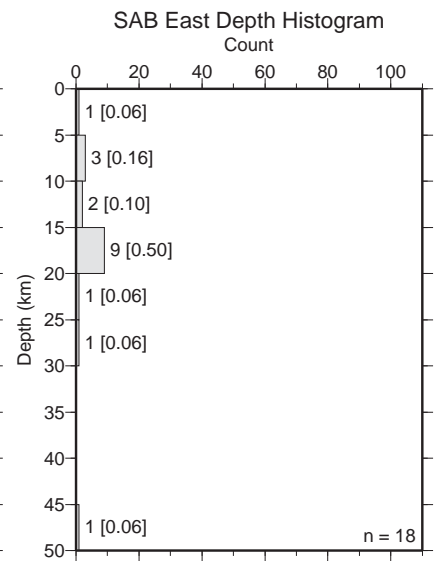
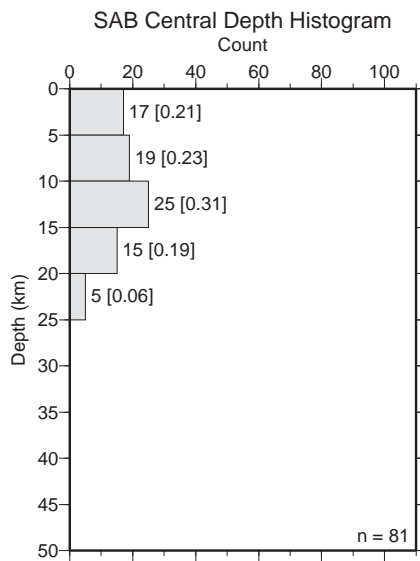
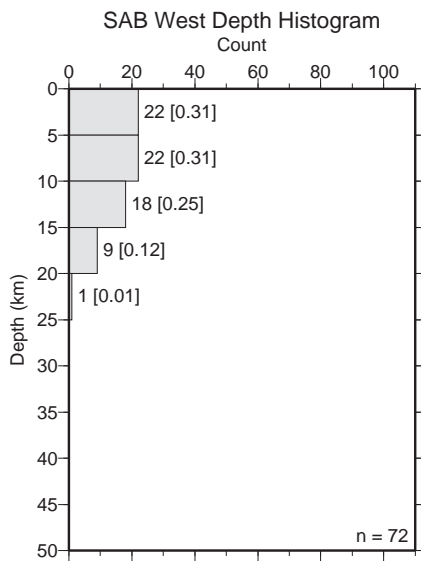
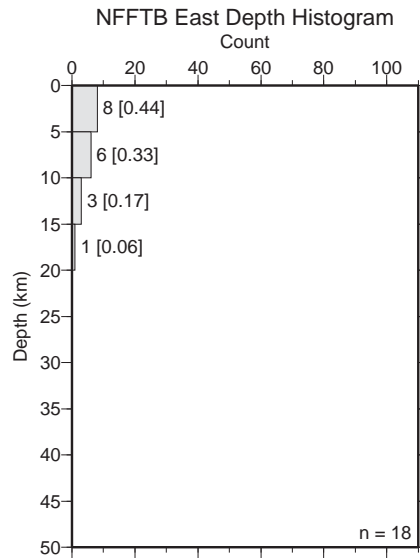
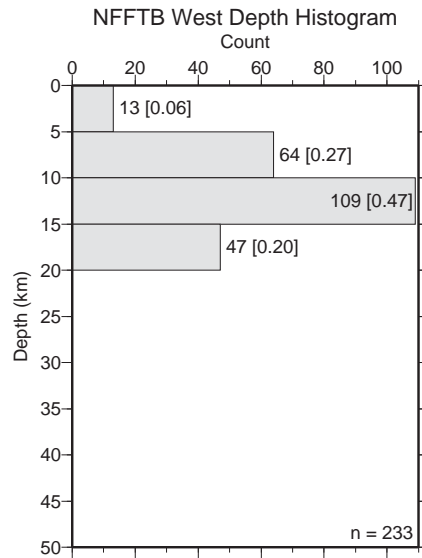


SUSITNA-WATANA HYDROELECTRIC PROJECT

AREAL ZONE LATITUDE VS. DEPTH EARTHQUAKE PLOTS

02/02/12

FIGURE 27



Depth histograms of events in each areal zone that have vertical errors ≤ 5 km. These discrete distributions are used to model areal zone seismicity.

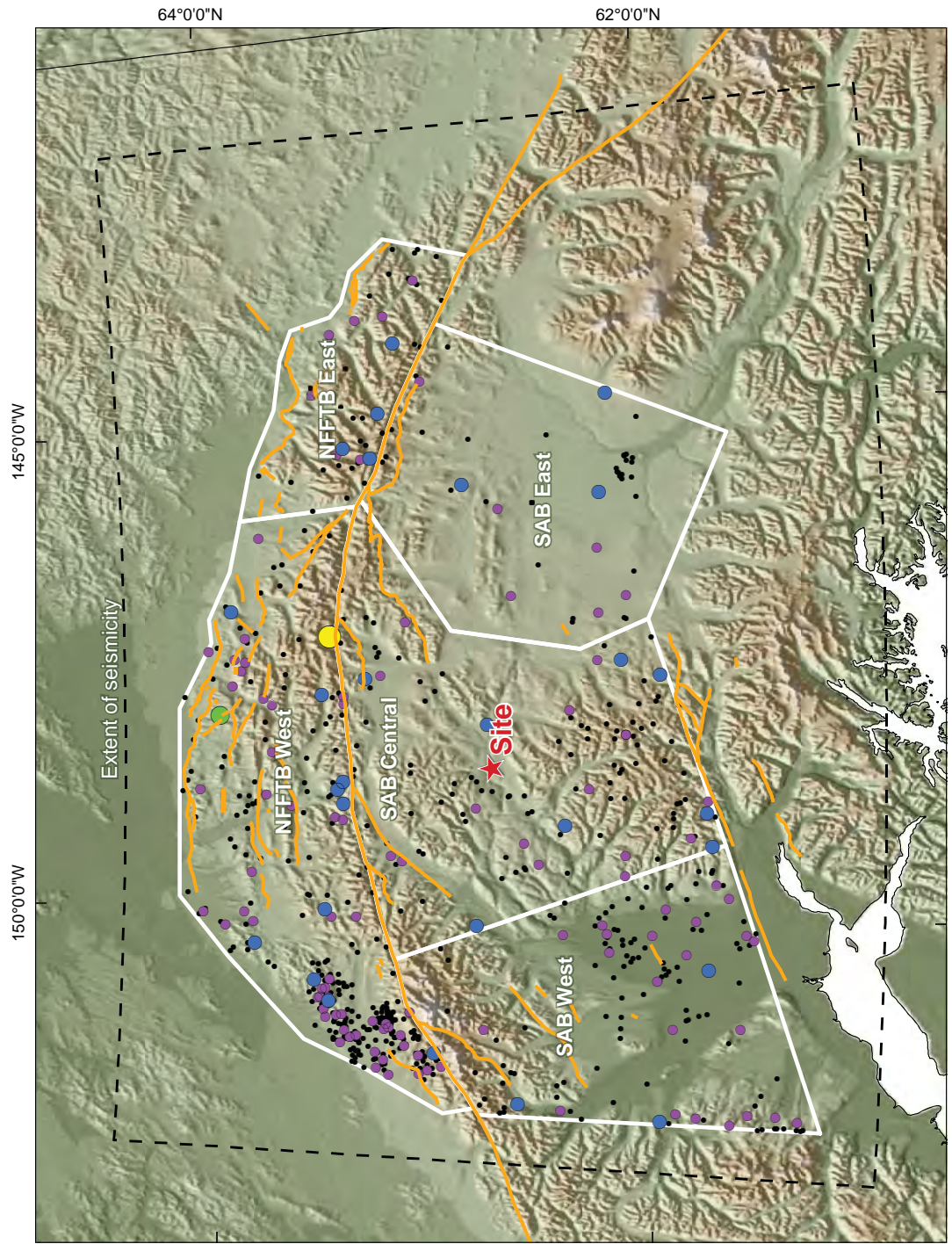


SUSITNA-WATANA HYDROELECTRIC PROJECT

AREAL ZONE SEISMICITY DEPTH HISTOGRAMS

02/02/12

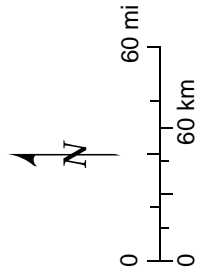
FIGURE 28



Explanation

- Fault
- Seismicity (Mw)**
- 3.0 - 3.9
 - 4.0 - 4.9
 - 5.0 - 5.9
 - 6.0 - 6.9
 - 7.0 - 7.9

Note: The 1912 event (yellow circle NE of site) is located in the NFFT West zone but is conservatively included in the SAB Central zone for the recurrence calculation, as discussed in text. Maximum earthquake depths in each zone are discussed in text.



150°00"W 145°00"W

64°00"N 62°00"N

Extent of seismicity

NFFT West

NFFT East

SAB West

SAB Central

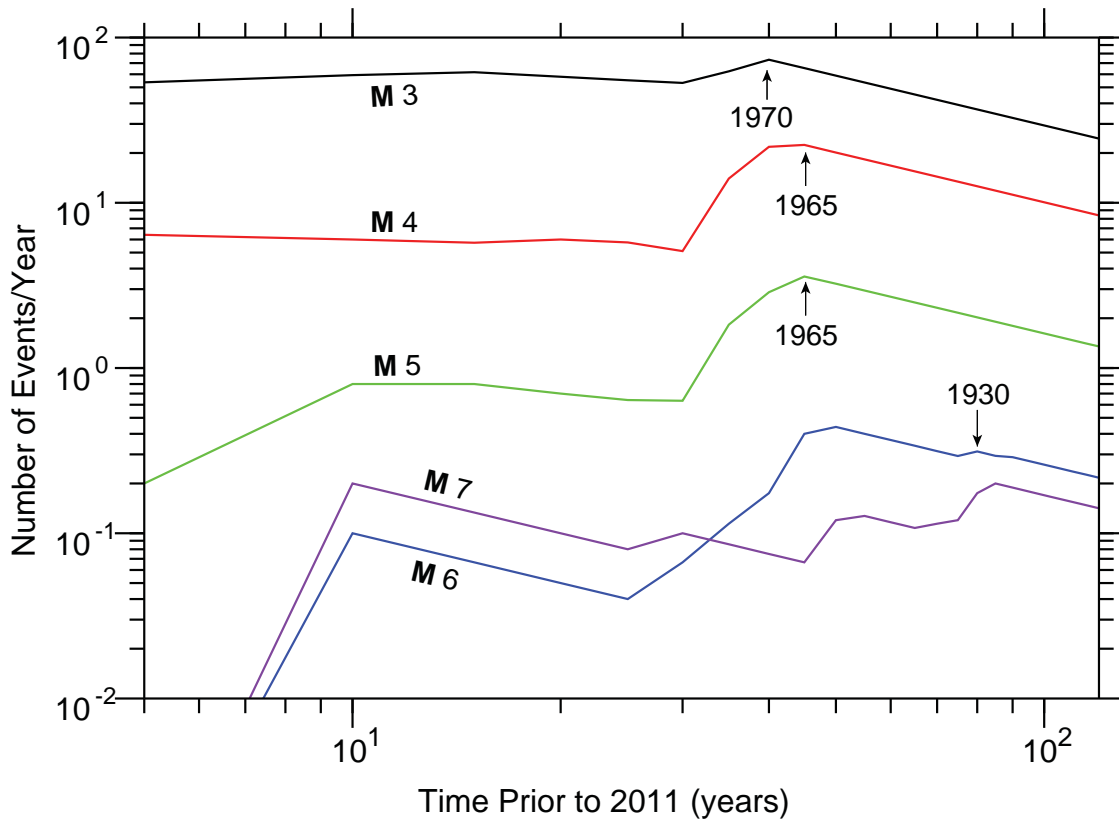
SAB East

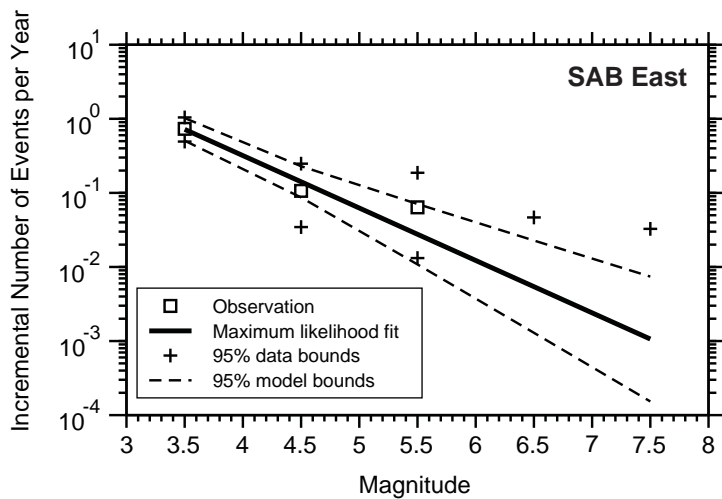
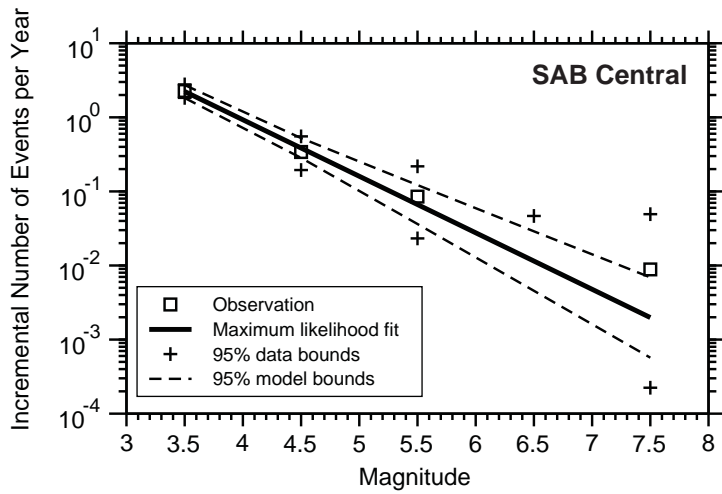
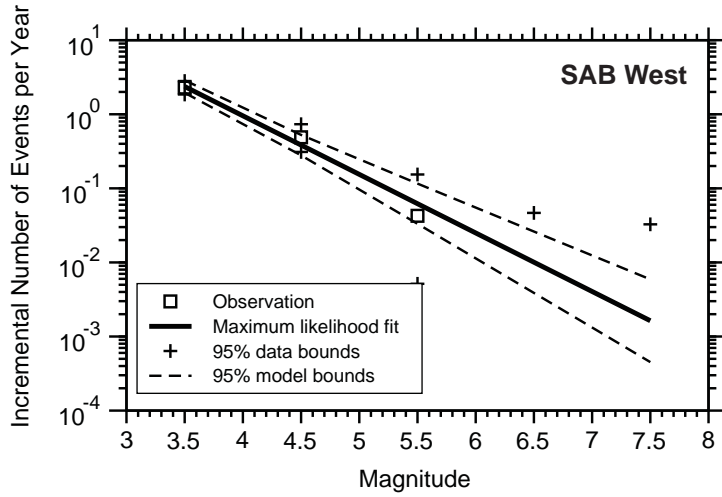
Site



SUSTINA-WATANA HYDROELECTRIC PROJECT

FINAL RECURRENCE CATALOGS



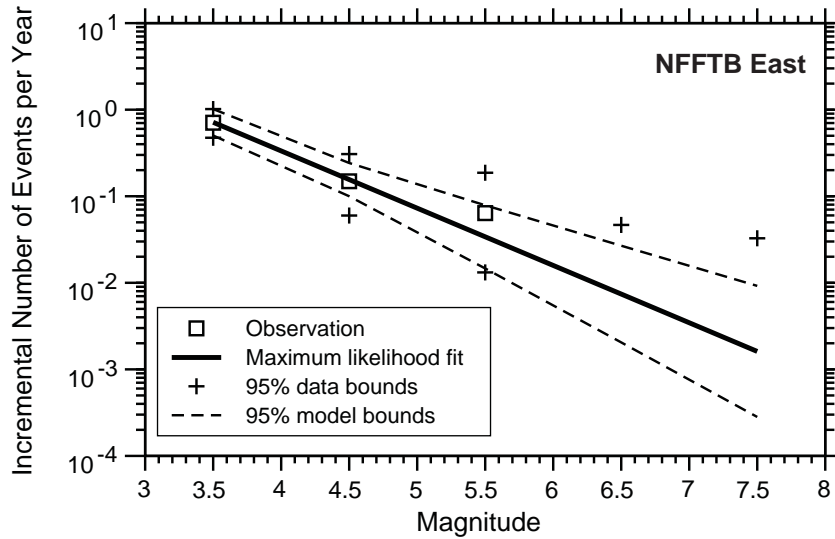
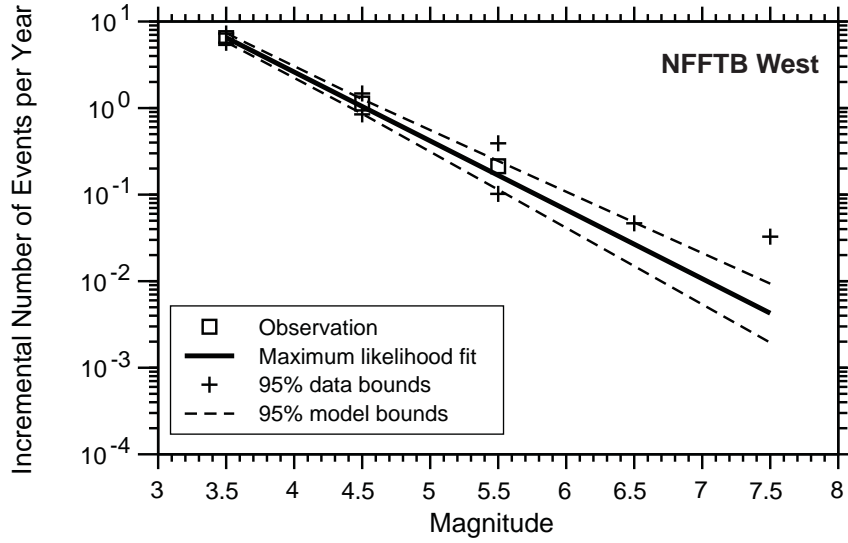


SUSITNA-WATANA HYDROELECTRIC PROJECT

**MAXIMUM LIKELIHOOD
RECURRENCE CURVES
FOR SAB AREAL ZONES**

02/02/12

FIGURE 31

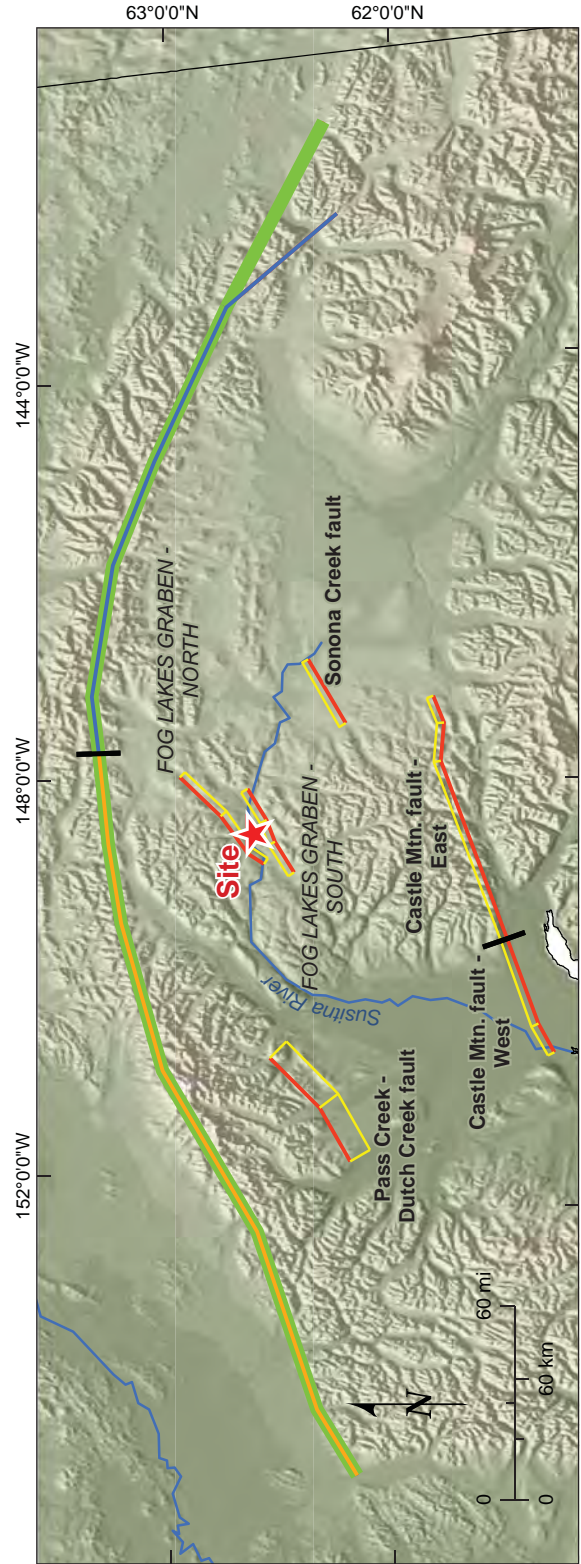


SUSITNA-WATANA HYDROELECTRIC PROJECT

**MAXIMUM LIKELIHOOD
RECURRENCE CURVES
FOR NFFTB AREAL ZONES**

02/02/12

FIGURE 32



Explanation

- Denali Fault Crustal Sources
 - 2002 rupture
 - West of 2002 rupture
 - Entire modeled Denali fault
- Other crustal fault source
(red = surface trace;
yellow = down-dip projection)

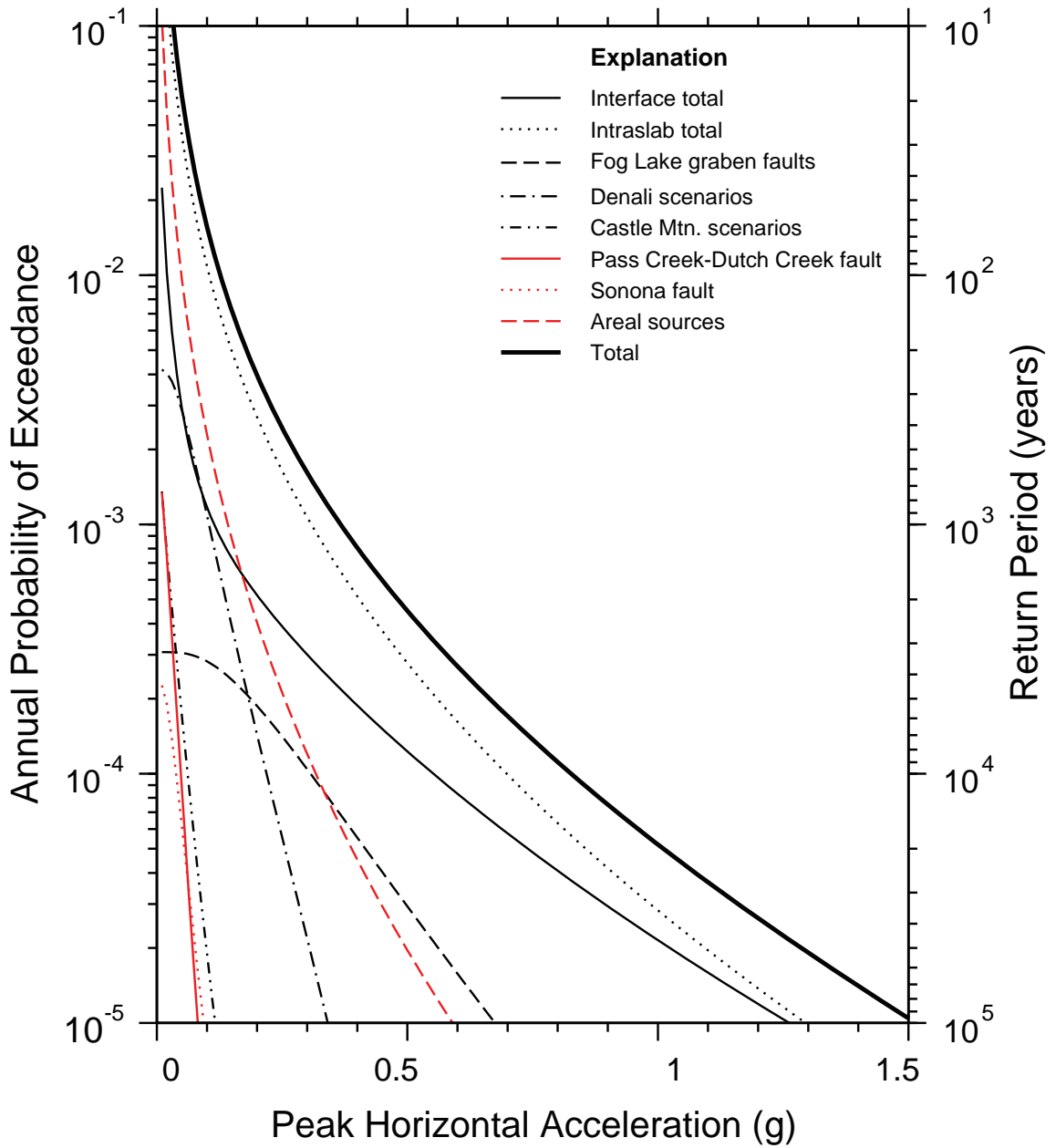
STATE OF ALASKA
ALASKA ENERGY AUTHORITY

SUSITNA-WATANA HYDROELECTRIC PROJECT

CRUSTAL FAULT MODEL

02/02/12

FIGURE 33

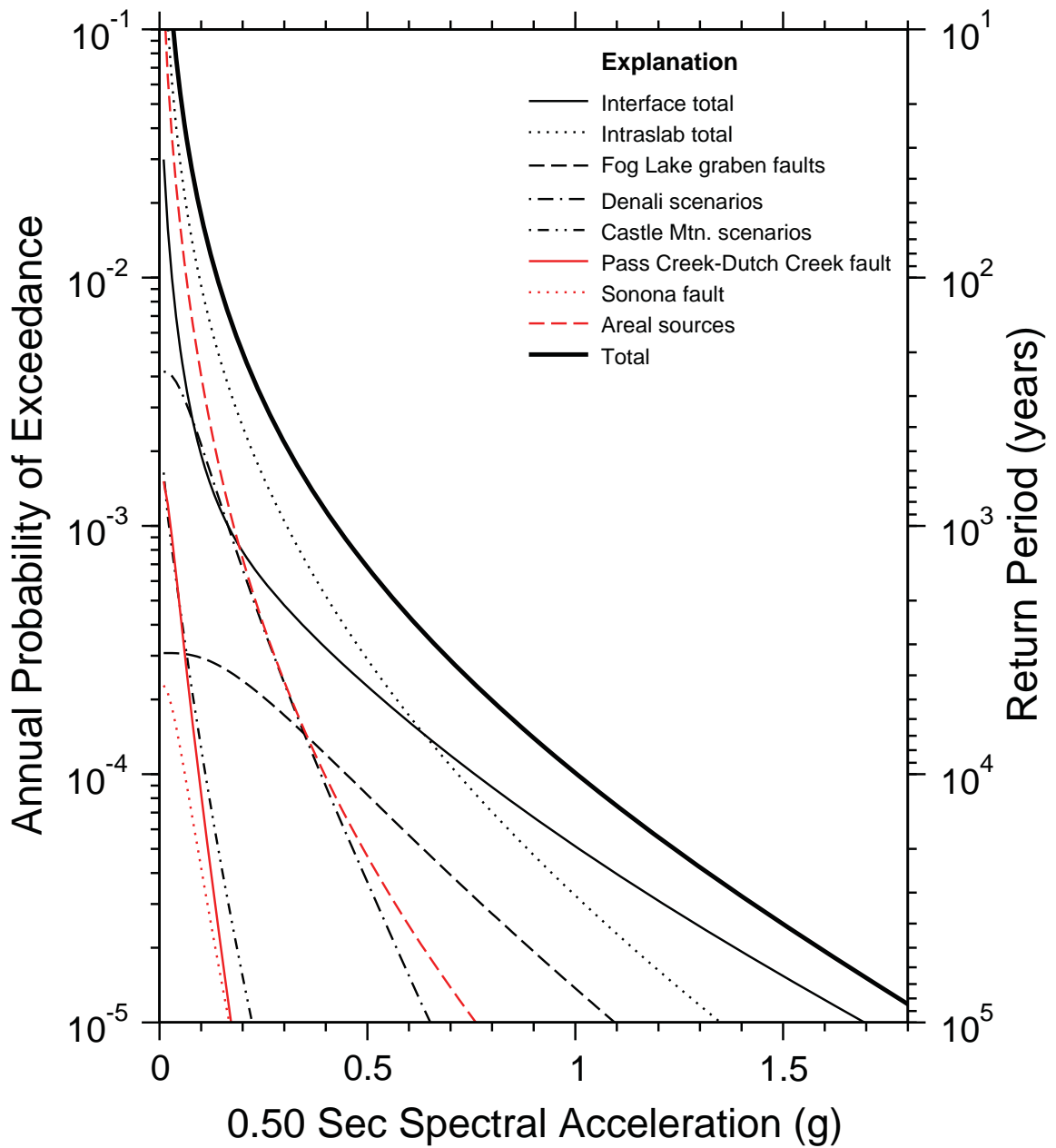


STATE OF ALASKA
ALASKA ENERGY AUTHORITY

SUSITNA-WATANA HYDROELECTRIC PROJECT

HAZARD CURVES FOR PEAK HORIZONTAL ACCELERATION

02/02/12 FIGURE 34

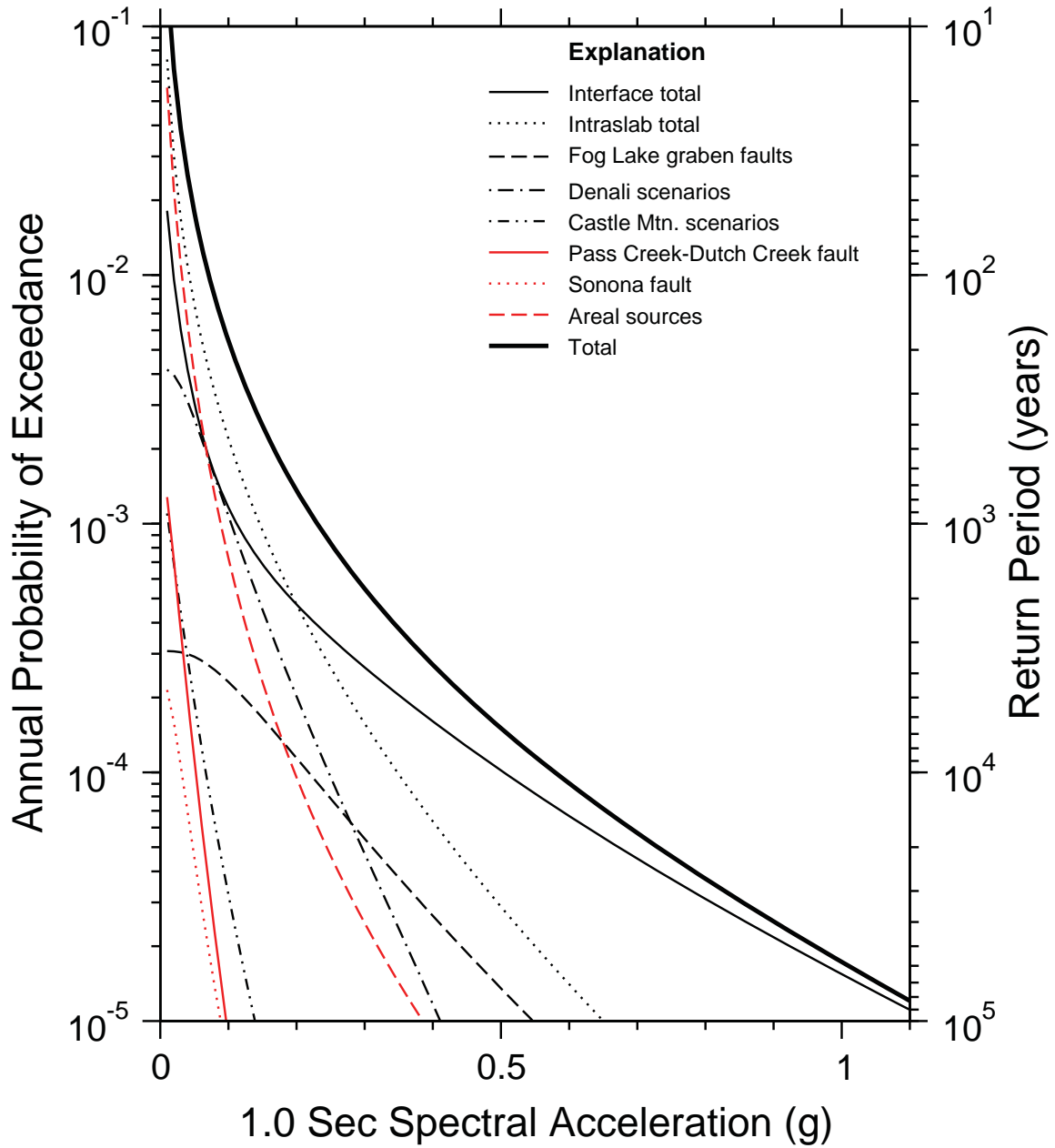


STATE OF ALASKA
ALASKA ENERGY AUTHORITY

SUSITNA-WATANA HYDROELECTRIC PROJECT

**HAZARD CURVES
FOR 0.5 SECOND SPECTRAL
ACCELERATION**

02/02/12 FIGURE 35

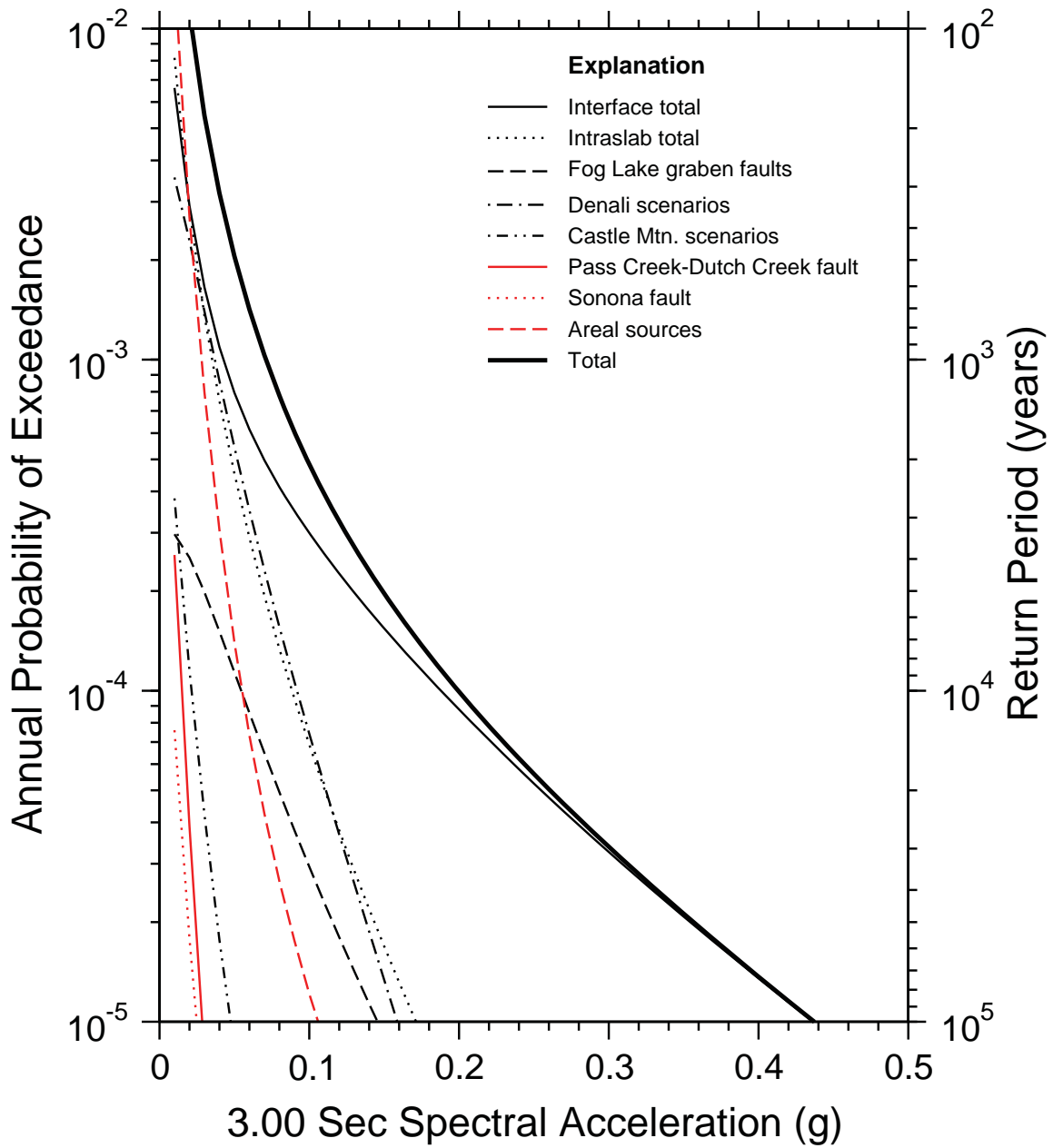


STATE OF ALASKA
ALASKA ENERGY AUTHORITY

SUSITNA-WATANA HYDROELECTRIC PROJECT

**HAZARD CURVES
FOR 1.0-SECOND SPECTRAL
ACCELERATION**

02/02/12 FIGURE 36

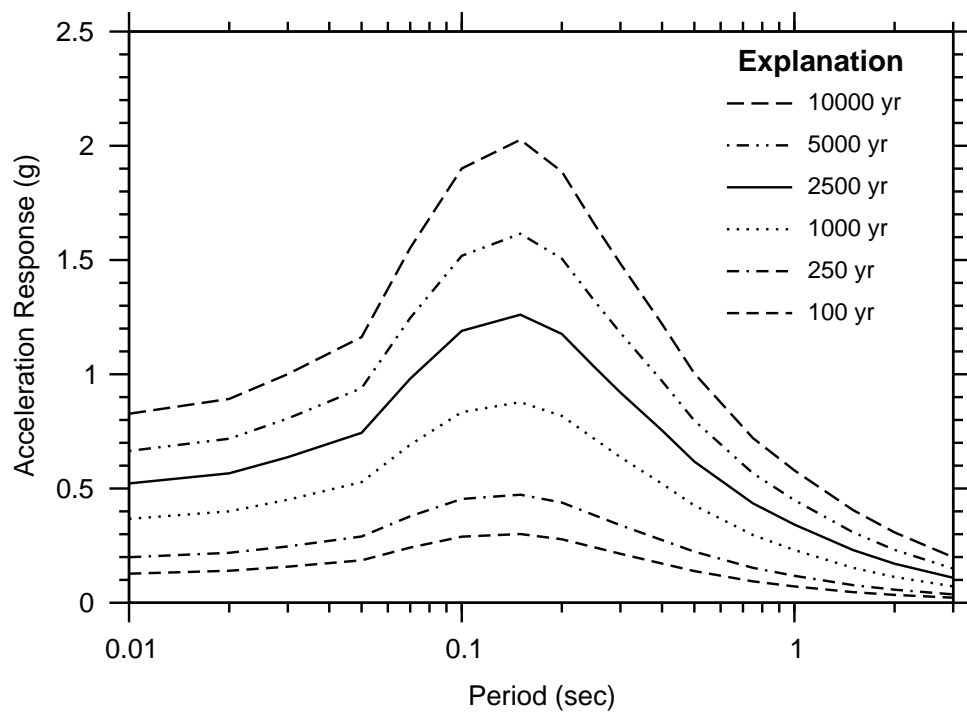


STATE OF ALASKA
ALASKA ENERGY AUTHORITY

SUSITNA-WATANA HYDROELECTRIC PROJECT

**HAZARD CURVES
FOR 3.0-SECOND
SPECTRAL ACCELERATION**

02/02/12 FIGURE 37

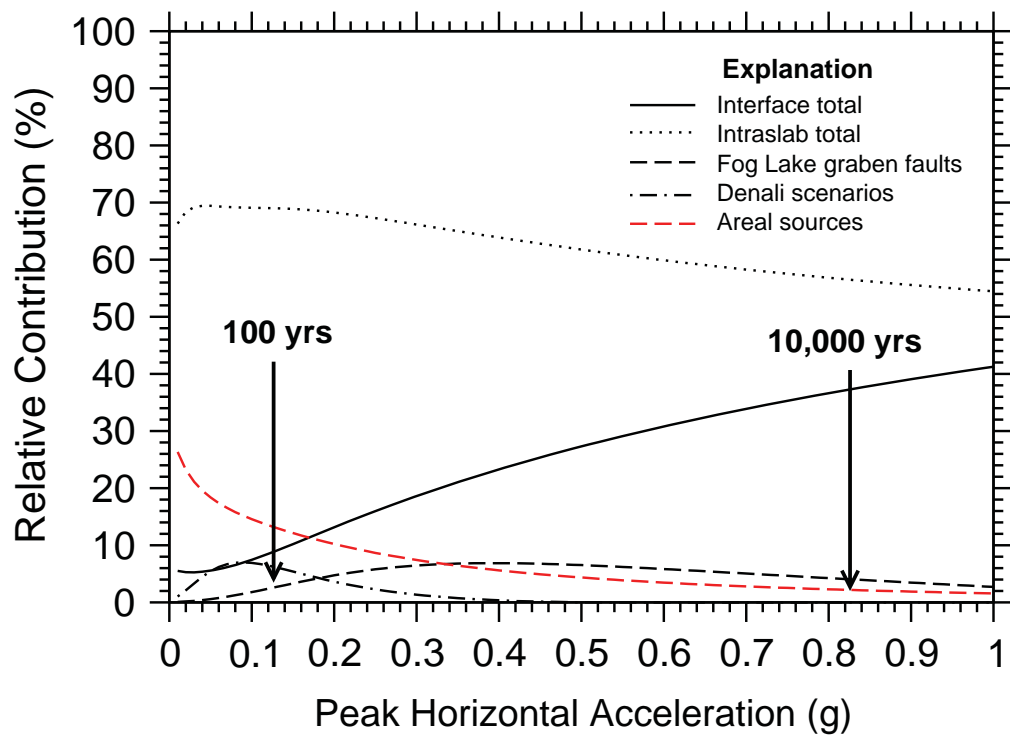


SUSITNA-WATANA HYDROELECTRIC PROJECT

MEAN UNIFORM
HAZARD SPECTRA,
TOTAL HAZARD

02/02/12

FIGURE 38

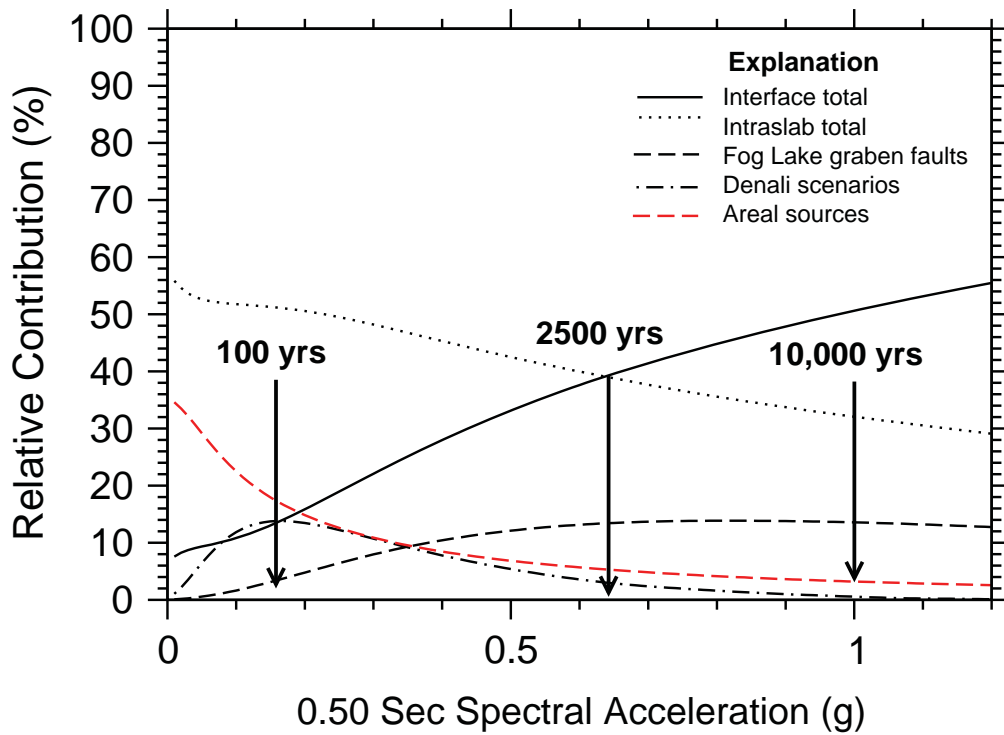


SUSITNA-WATANA HYDROELECTRIC PROJECT

RELATIVE CONTRIBUTIONS,
PEAK HORIZONTAL
ACCELERATION

02/02/12

FIGURE 39

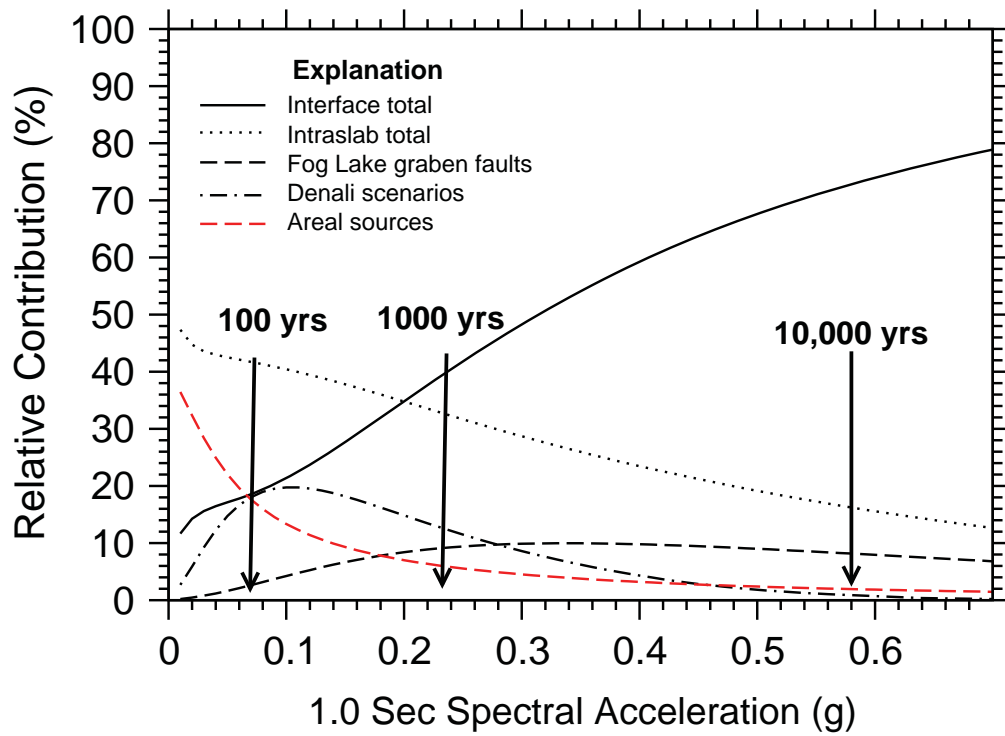


SUSITNA-WATANA HYDROELECTRIC PROJECT

RELATIVE CONTRIBUTIONS,
0.5-SECOND SPECTRAL
ACCELERATION

02/02/12

FIGURE 40

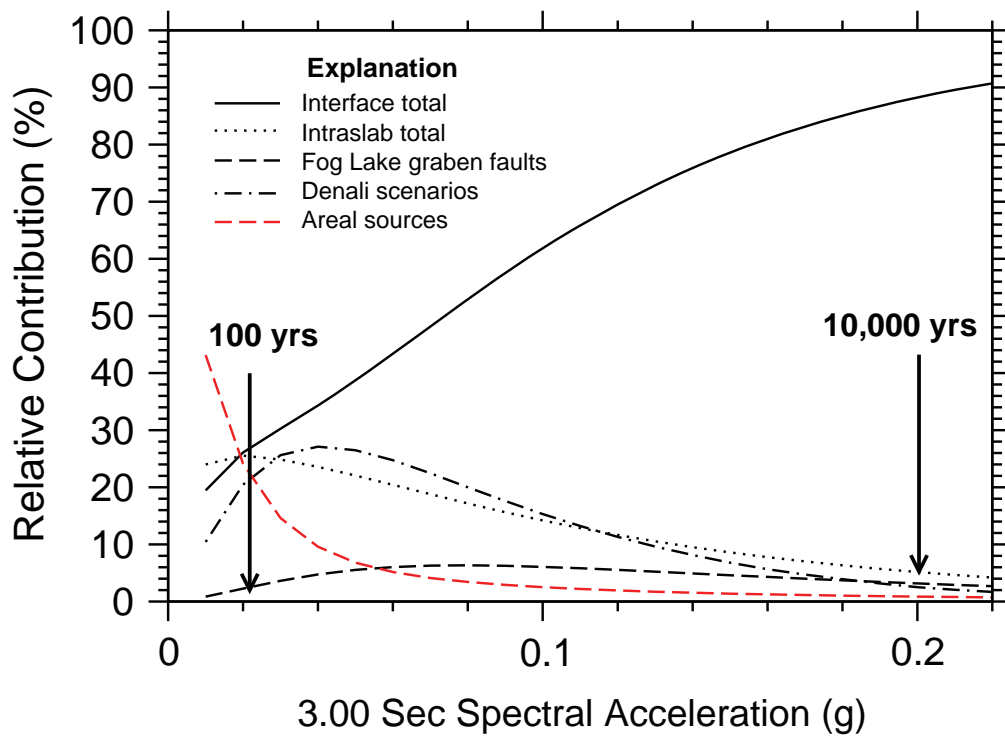


SUSITNA-WATANA HYDROELECTRIC PROJECT

RELATIVE CONTRIBUTIONS,
1.0-SECOND SPECTRAL
ACCELERATION

02/02/12

FIGURE 41



SUSITNA-WATANA HYDROELECTRIC PROJECT

RELATIVE CONTRIBUTIONS,
3.0-SECOND SPECTRAL
ACCELERATION

02/02/12

FIGURE 42

Watana Dam, AK
Seismic Hazard Deaggregation

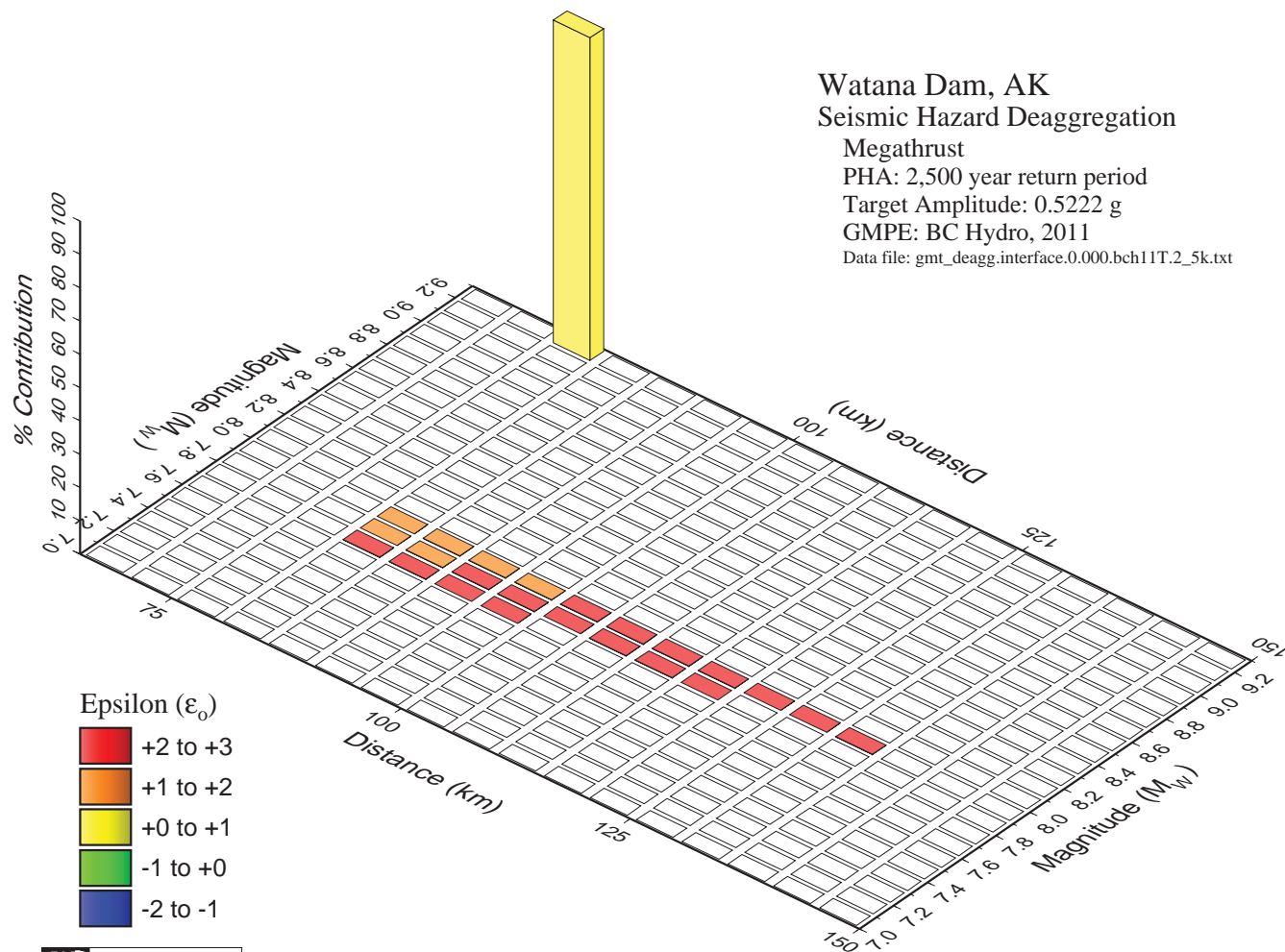
Megathrust

PHA: 2,500 year return period

Target Amplitude: 0.5222 g

GMPE: BC Hydro, 2011

Data file: gmt_deagg.interface.0.000.bch11T.2_5k.txt



STATE OF ALASKA
ALASKA ENERGY AUTHORITY

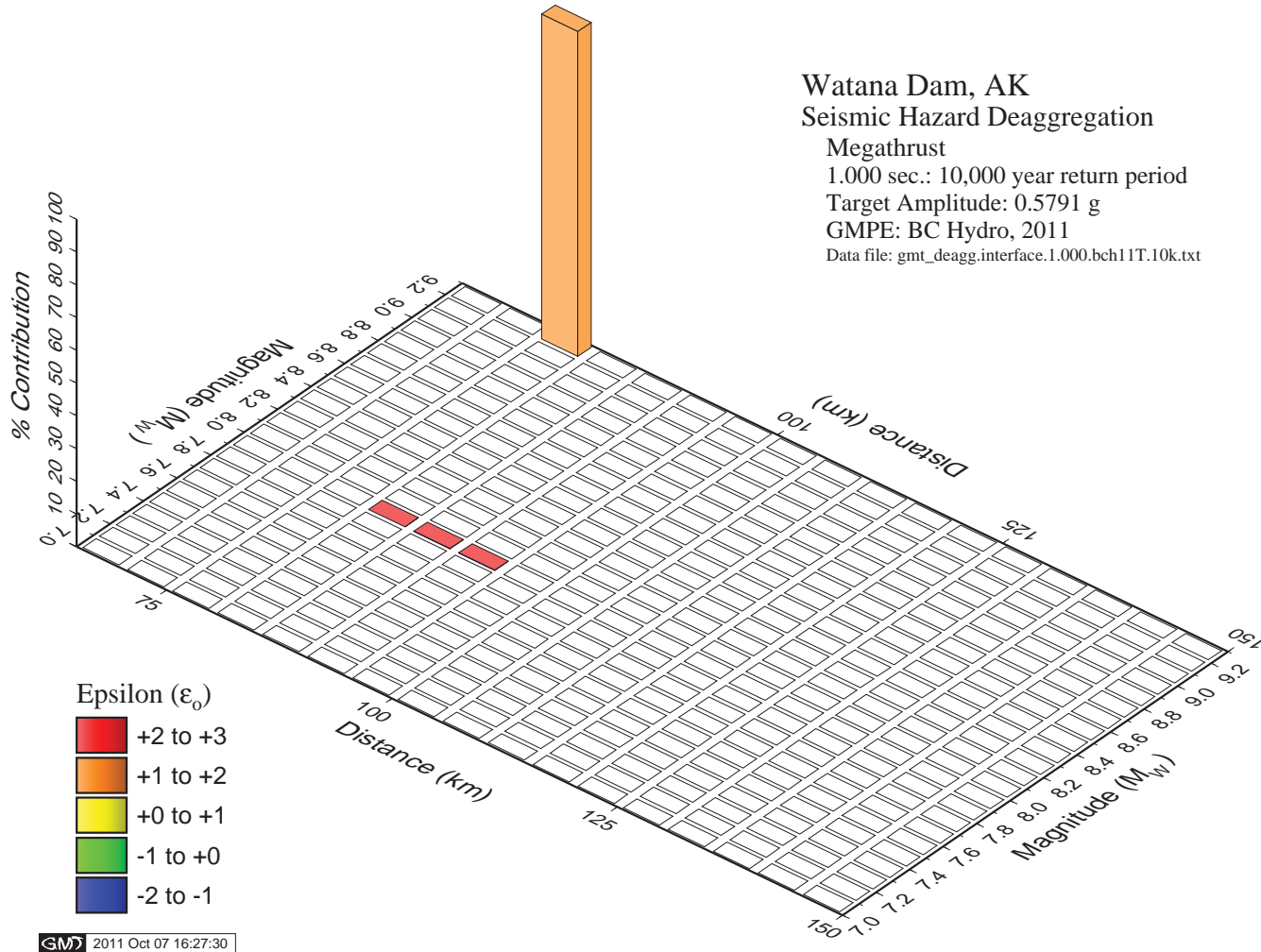
SUSITNA-WATANA HYDROELECTRIC PROJECT
DEAGGREGATION
FOR THE MEGATHRUST,
PEAK HORIZONTAL ACCELERATION,
2500-YEAR RETURN PERIOD

02/02/12
FIGURE 43



Watana Dam, AK
Seismic Hazard Deaggregation

Megathrust
 1.000 sec.: 10,000 year return period
 Target Amplitude: 0.5791 g
 GMPE: BC Hydro, 2011
 Data file: gmt_deagg.interface.1.000.bch11T.10k.txt



STATE OF ALASKA
 ALASKA ENERGY AUTHORITY

ALASKA
 ENERGY AUTHORITY

SUSITNA-WATANA HYDROELECTRIC PROJECT

**DEAGGREGATION
 FOR THE MEGATHRUST,
 1.0-SECOND
 SPECTRAL ACCELERATION,
 10,000-YEAR RETURN PERIOD**

02/02/12 FIGURE 44



Watana Dam, AK
Seismic Hazard Deaggregation

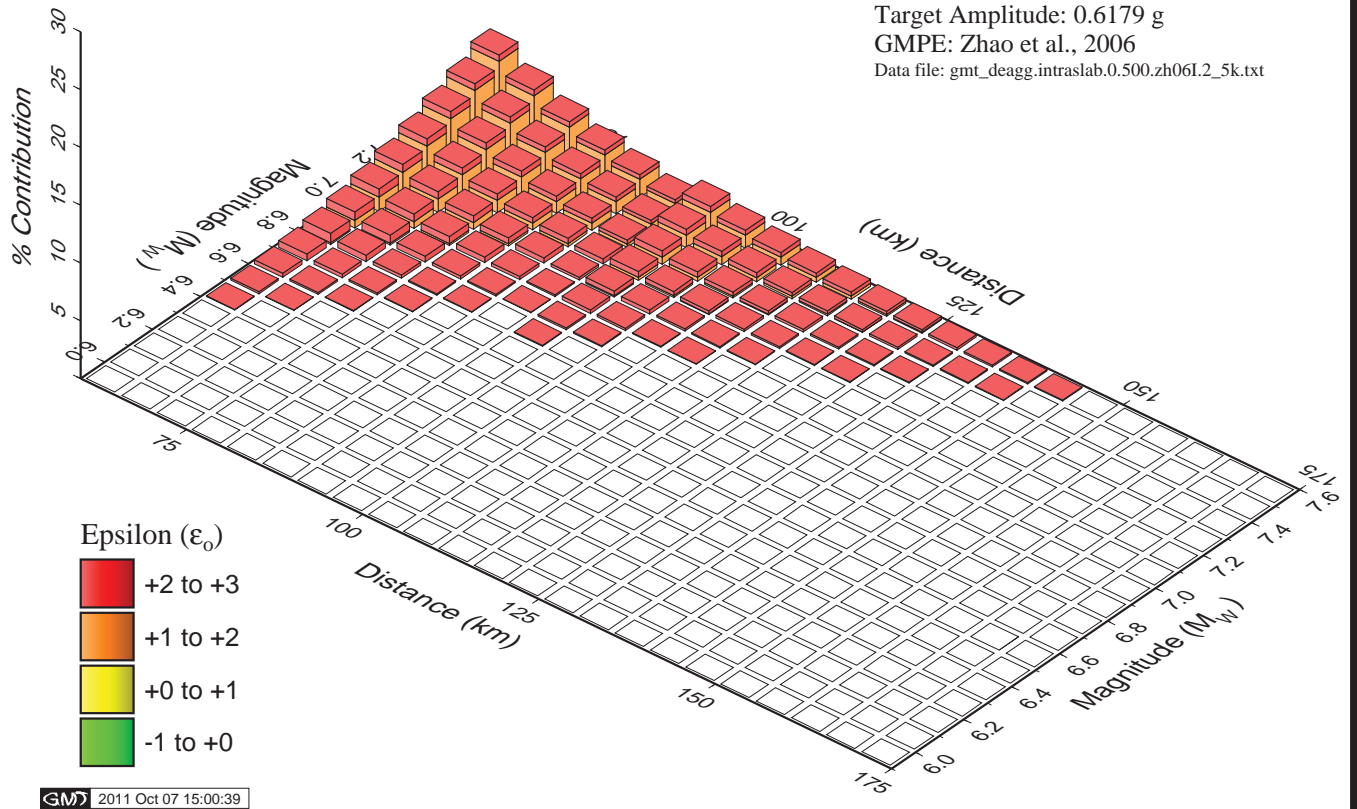
Intraslab

0.500 sec.: 2,500 year return period

Target Amplitude: 0.6179 g

GMPE: Zhao et al., 2006

Data file: gmt_deagg.intraslab.0.500.zh06l.2_5k.txt



STATE OF ALASKA
ALASKA ENERGY AUTHORITY

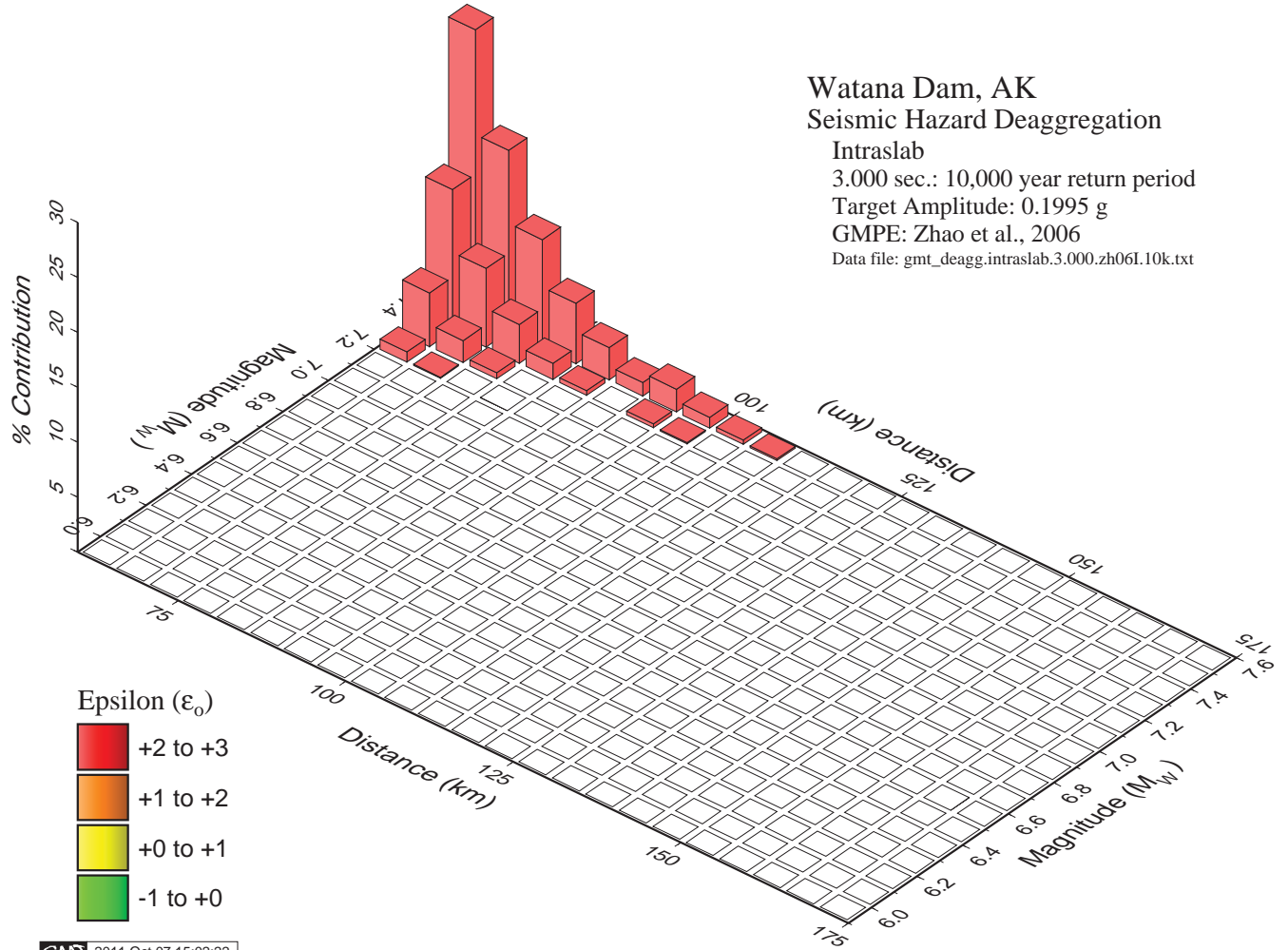
ALASKA
ENERGY AUTHORITY

SUSITNA-WATANA HYDROELECTRIC PROJECT
**DEAGGREGATION
FOR THE INTRASLAB,
0.5-SECOND
SPECTRAL ACCELERATION,
2500-YEAR RETURN PERIOD**

02/02/12 FIGURE 45

Watana Dam, AK
Seismic Hazard Deaggregation

Intraslab
 3.000 sec.: 10,000 year return period
 Target Amplitude: 0.1995 g
 GMPE: Zhao et al., 2006
 Data file: gmt_deagg.intraslab.3.000.zh06I.10k.txt



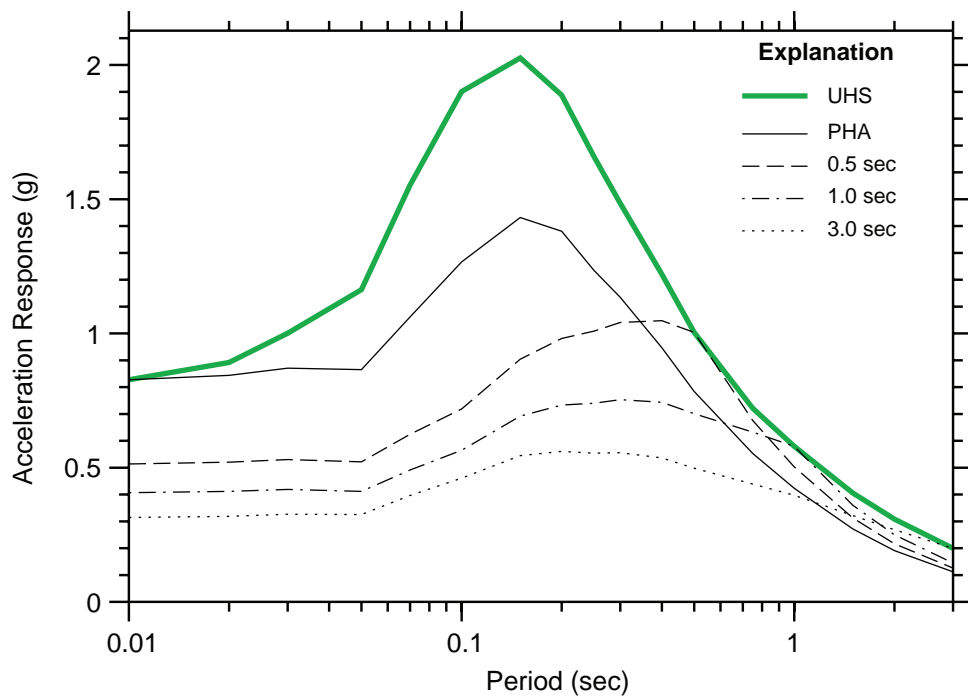
STATE OF ALASKA
 ALASKA ENERGY AUTHORITY

ALASKA
 ENERGY AUTHORITY

SUSITNA-WATANA HYDROELECTRIC PROJECT
DEAGGREGATION
FOR THE INTRASLAB,
3.0-SECOND
SPECTRAL ACCELERATION,
10,000-YEAR RETURN PERIOD

02/01/12 FIGURE 46



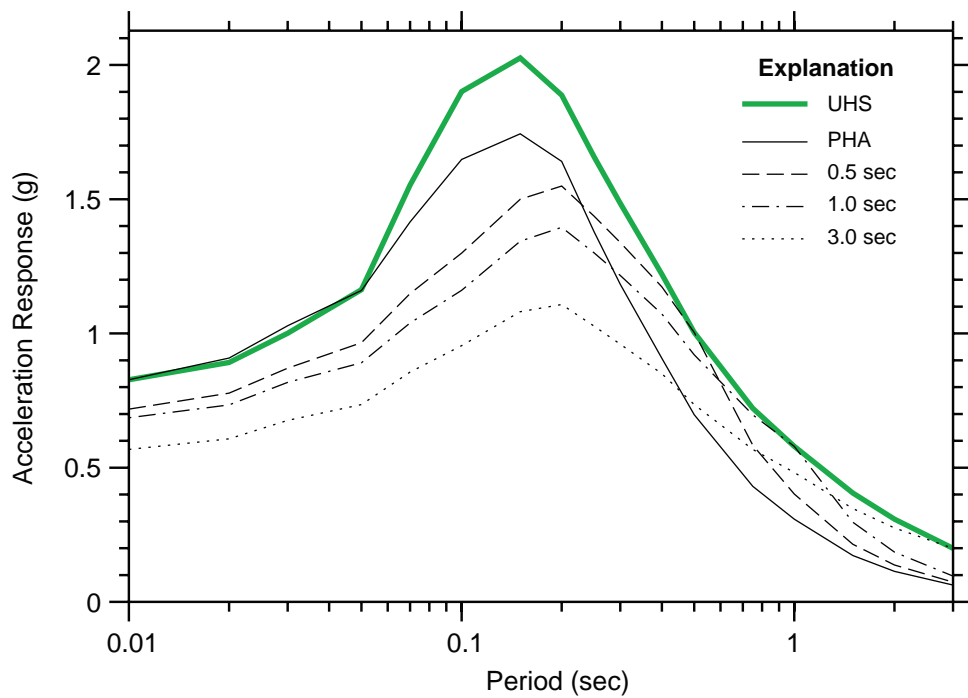


SUSITNA-WATANA HYDROELECTRIC PROJECT

UHS AND CMS, MEGATHRUST,
10,000-YEAR RETURN PERIOD

02/02/12

FIGURE 47

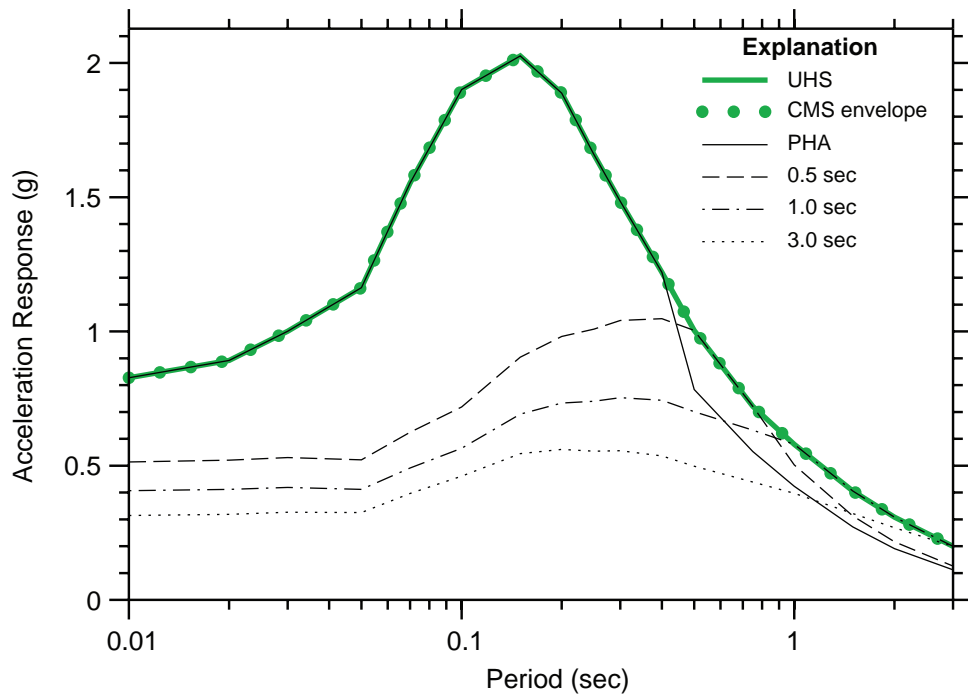


SUSITNA-WATANA HYDROELECTRIC PROJECT

UHS AND CMS, INTRASLAB,
10,000-YEAR RETURN PERIOD

02/02/12

FIGURE 48

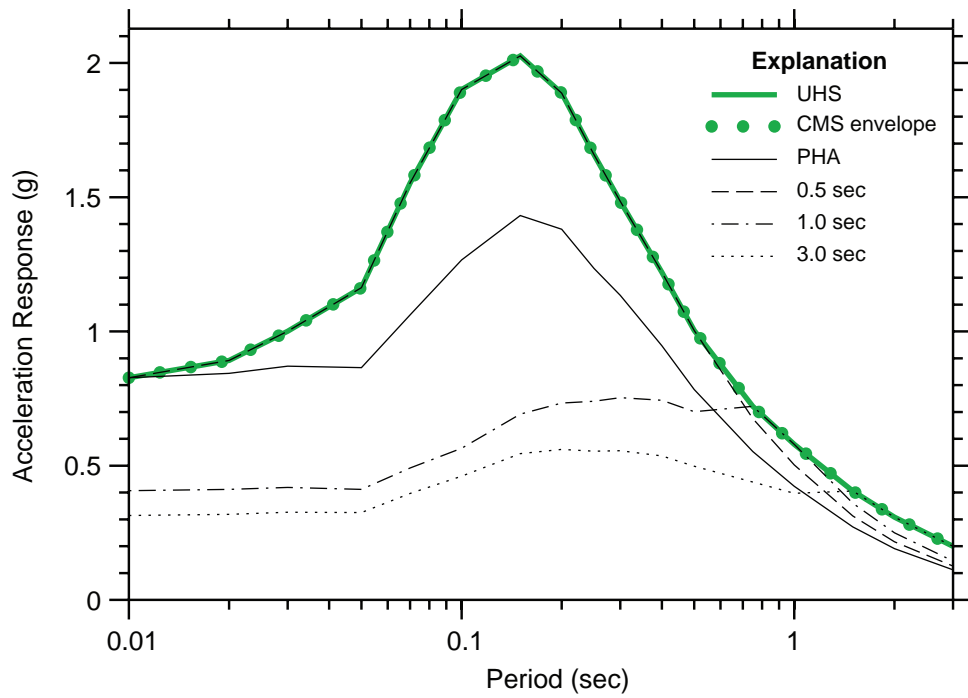


SUSITNA-WATANA HYDROELECTRIC PROJECT

UHS AND EXTENDED CMS,
MEGATHRUST,
10,000-YEAR RETURN PERIOD,
ALTERNATIVE 1

02/02/12

FIGURE 49

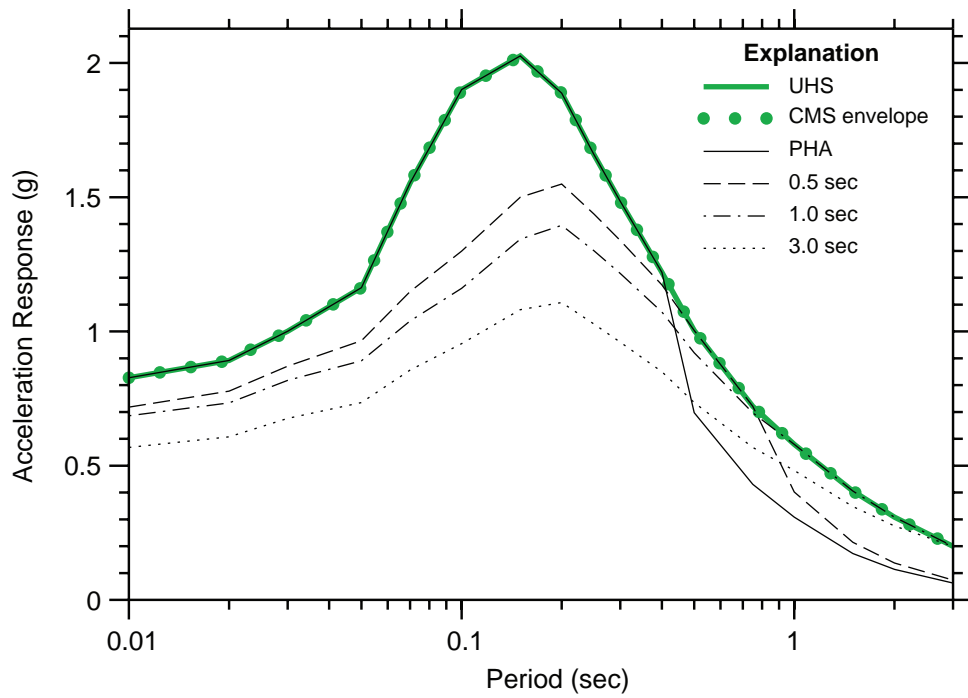


STATE OF ALASKA
ALASKA ENERGY AUTHORITY

SUSITNA-WATANA HYDROELECTRIC PROJECT

**UHS AND EXTENDED CMS,
MEGATHRUST,
10,000-YEAR RETURN PERIOD,
ALTERNATIVE 2**

02/02/12
FIGURE 50

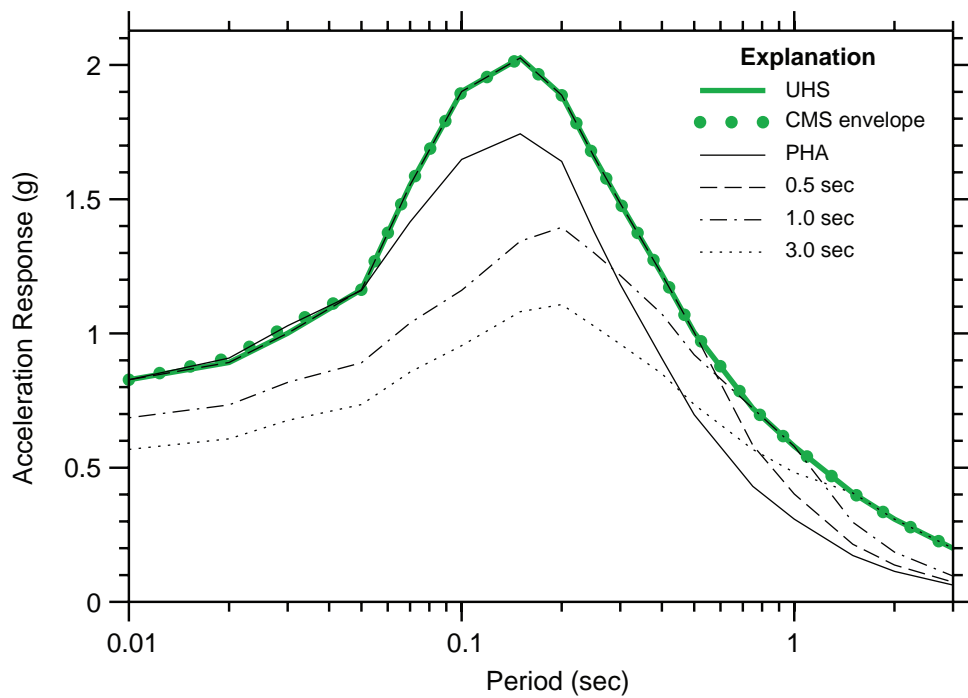


STATE OF ALASKA
ALASKA ENERGY AUTHORITY

SUSITNA-WATANA HYDROELECTRIC PROJECT

**UHS AND EXTENDED CMS,
INTRASLAB,
10,000-YEAR RETURN PERIOD,
ALTERNATIVE 1**

02/02/12
FIGURE 51

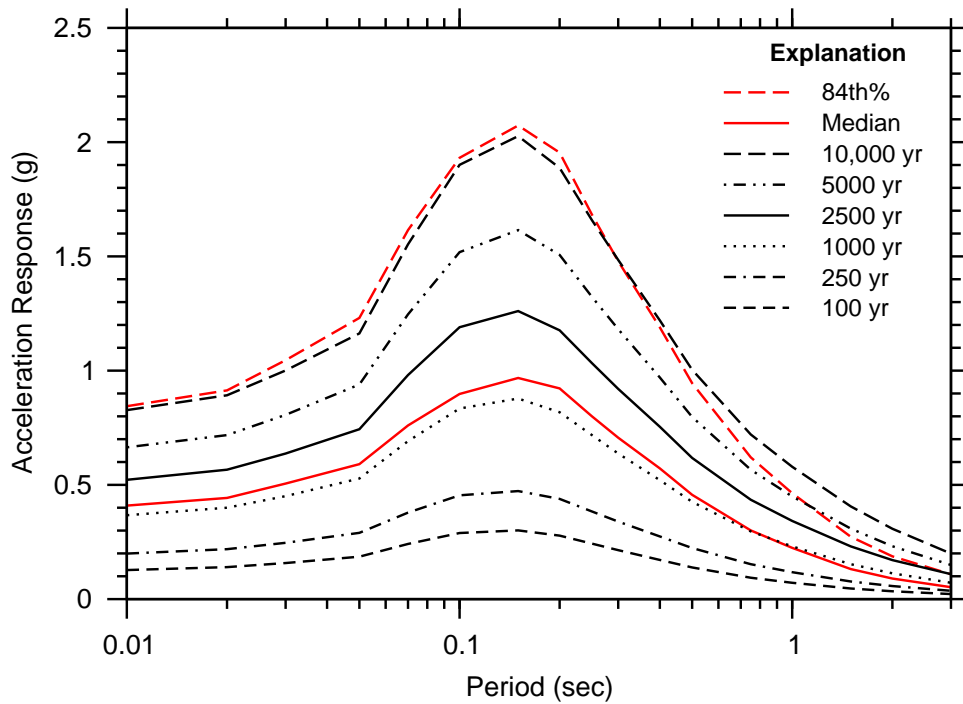


STATE OF ALASKA
ALASKA ENERGY AUTHORITY

SUSITNA-WATANA HYDROELECTRIC PROJECT

**UHS AND EXTENDED CMS,
INTRASLAB,
10,000-YEAR RETURN PERIOD,
ALTERNATIVE 2**

02/02/12
FIGURE 52



Red curves are intraslab deterministic hazard (M 7.5, 50 km).
 Black curves are total hazard UHS.

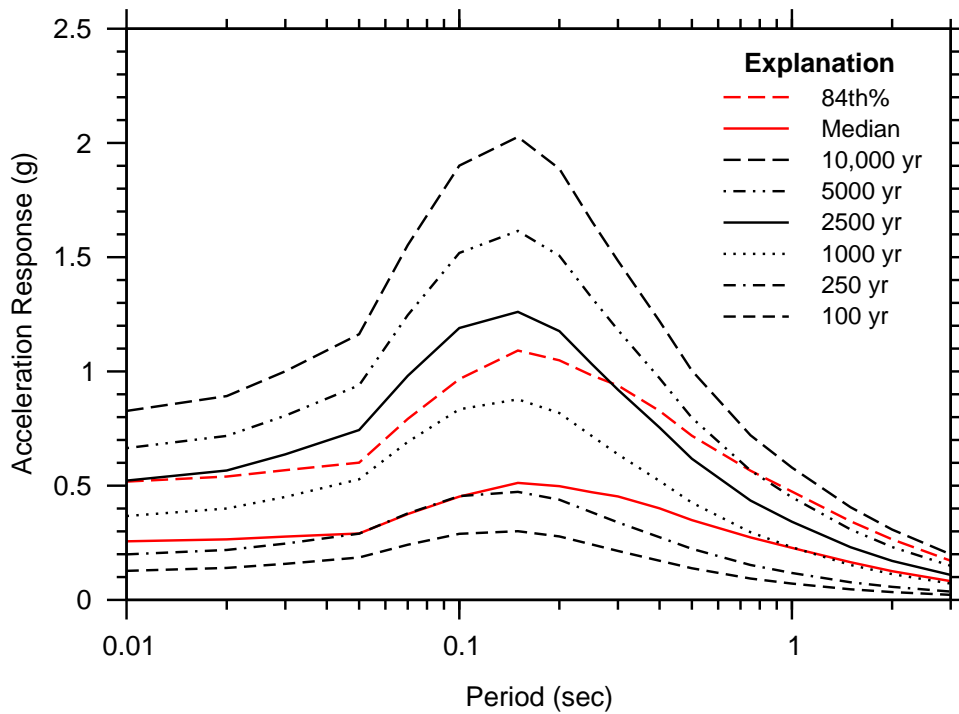


SUSITNA-WATANA HYDROELECTRIC PROJECT

**INTRASLAB
 DETERMINISTIC HAZARD
 COMPARED TO THE TOTAL
 HAZARD UHS**

02/02/12

FIGURE 53



Red curves are megathrust deterministic hazard (M9.2, 78 km).
 Black curves are total hazard UHS.

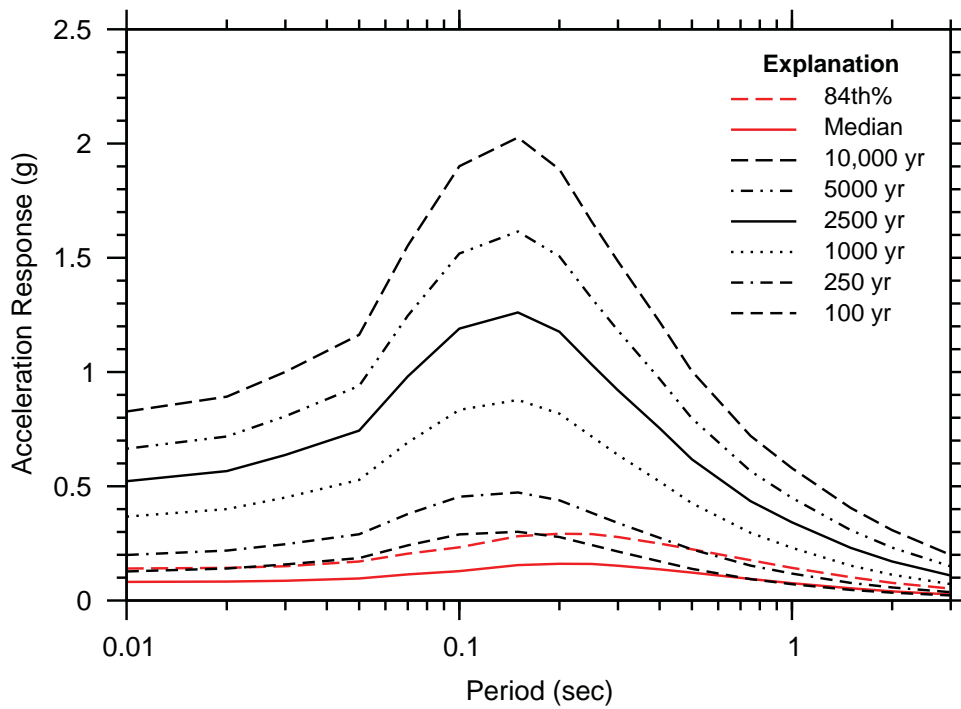


STATE OF ALASKA
 ALASKA ENERGY AUTHORITY

SUSITNA-WATANA HYDROELECTRIC PROJECT

**MEGATHRUST
 DETERMINISTIC HAZARD
 COMPARED TO THE TOTAL
 HAZARD UHS**

02/02/12 FIGURE 54



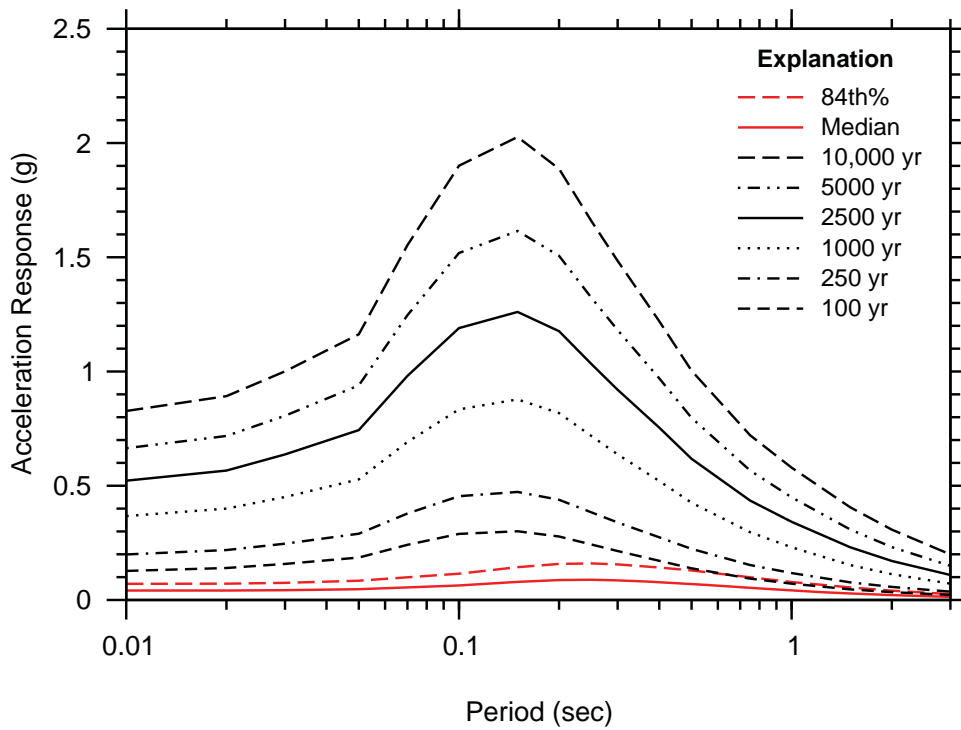
Red curves are Denali fault deterministic hazard (M7.9, 72 km).
 Black curves are total hazard UHS.



STATE OF ALASKA
 ALASKA ENERGY AUTHORITY

SUSITNA-WATANA HYDROELECTRIC PROJECT
**DENALI FAULT
 DETERMINISTIC HAZARD
 COMPARED TO THE TOTAL
 HAZARD UHS**

02/02/12FIGURE 55



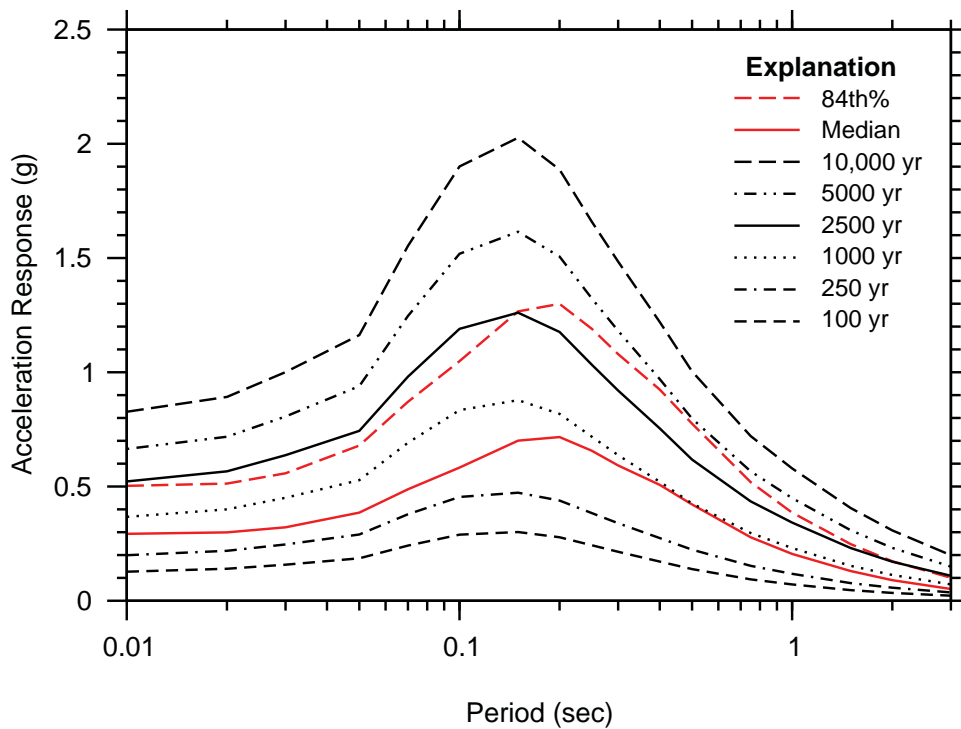
Red curves are Castle Mountain fault deterministic hazard (M7.6, 98 km).
 Black curves are total hazard UHS.



STATE OF ALASKA
 ALASKA ENERGY AUTHORITY

SUSITNA-WATANA HYDROELECTRIC PROJECT
**CASTLE MOUNTAIN FAULT
 DETERMINISTIC HAZARD
 COMPARED TO THE TOTAL
 HAZARD UHS**

02/02/12 FIGURE 56



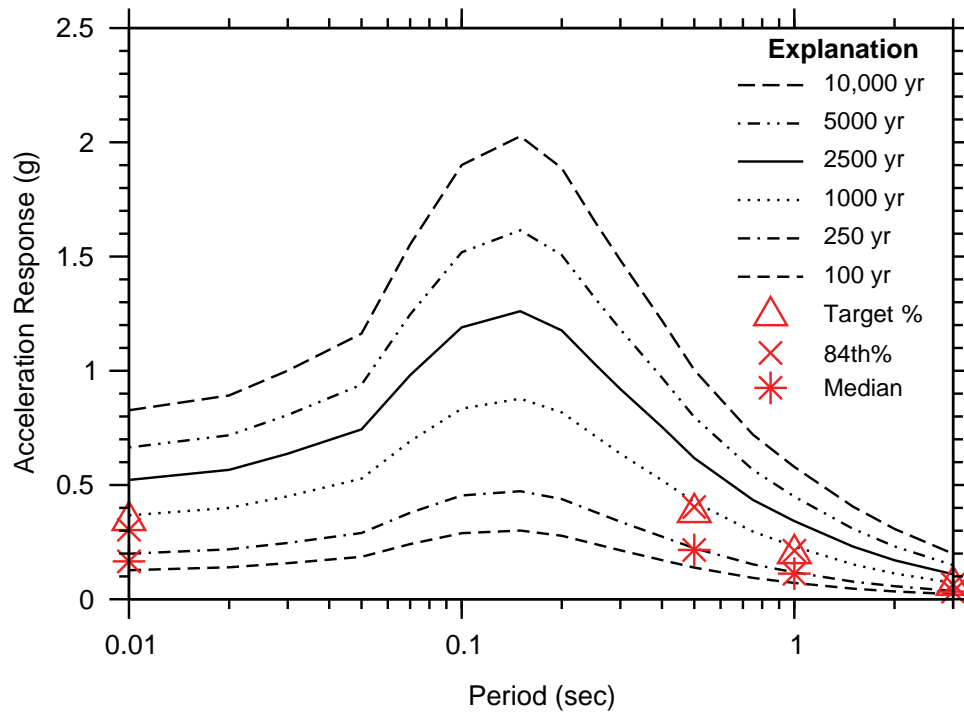
Red curves are Fog Lake graben deterministic hazard (M7.0, 7 km).
 Black curves are total hazard UHS.



STATE OF ALASKA
 ALASKA ENERGY AUTHORITY

SUSITNA-WATANA HYDROELECTRIC PROJECT
**FOG LAKE GRABEN
 DETERMINISTIC HAZARD
 COMPARED TO THE TOTAL
 HAZARD UHS**

02/02/12 FIGURE 57



Red symbols are Southern Alaska Block Central areal source deterministic hazard (see Table 16 for magnitudes, distances, and epsilon values). Black lines are total hazard UHS.

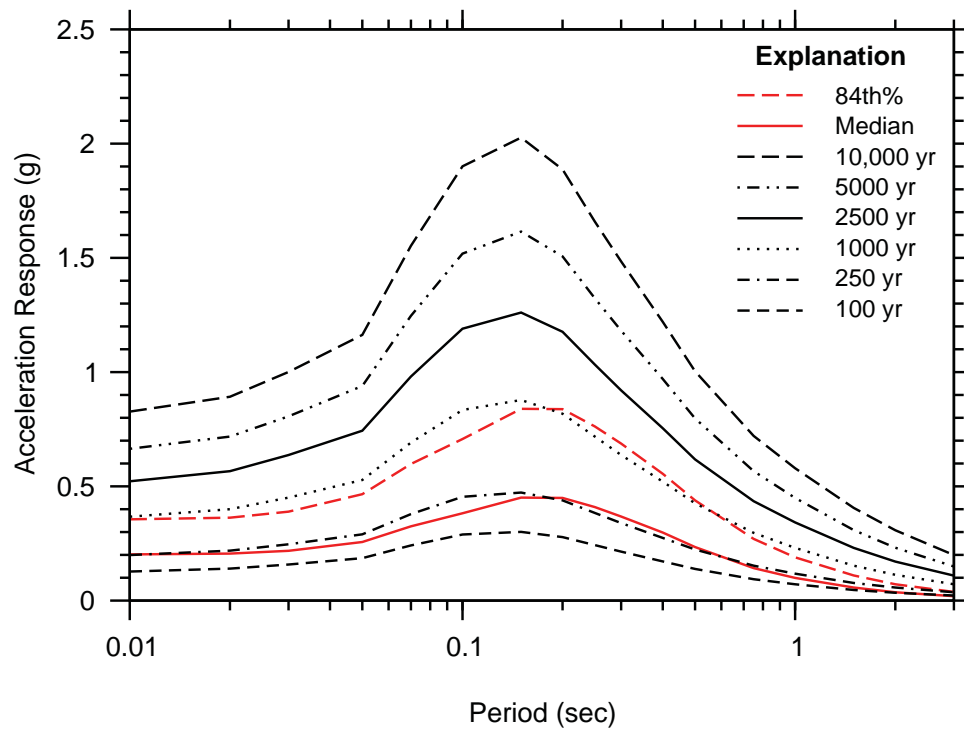


STATE OF ALASKA
ALASKA ENERGY AUTHORITY

SUSITNA-WATANA HYDROELECTRIC PROJECT

**SOUTHERN ALASKA BLOCK
CENTRAL PERIOD-
DEPENDENT DETERMINISTIC
HAZARD COMPARED TO
THE TOTAL HAZARD UHS**

02/02/12 FIGURE 58



Red lines are Southern Alaska Block Central single-earthquake deterministic hazard (M6.6, Rrup = 15 km, Rjb = 10 km). Black lines are total hazard UHS.



STATE OF ALASKA
ALASKA ENERGY AUTHORITY

SUSITNA-WATANA HYDROELECTRIC PROJECT
**SOUTHERN ALASKA BLOCK
CENTRAL SINGLE
EARTHQUAKE DETERMINISTIC
HAZARD COMPARED TO
THE TOTAL HAZARD UHS**

02/02/12 FIGURE 59

Appendix A – TIME-DEPENDANT CALCULATIONS

Cover Page

Appendix A – TIME-DEPENDENT CALCULATIONS

1.0 TIME-DEPENDENT CALCULATIONS

A time-dependent occurrence rate for a seismic source supports the concept that if the last earthquake occurred recently, the longer it will be until the next one, and vice versa. These rates thus should be lower and higher, respectively, than the average (Poissonian) rate. For this study we have employed time-dependent rates for three sources: the megathrust, source of the 1964 M 9.2 earthquake, and two sections of the Denali fault. The eastern part of the Denali ruptured in 2002, but the western part, from paleoseismic evidence, has not ruptured for about 600 years. The Poissonian rate is simply the reciprocal of the average interevent time, and is constant from year to year.

Two time-dependent models are utilized here, the lognormal model, and the Brownian Passage Time (BPT) model (Matthews et al., 2002). The lognormal model assumes that interevent times are lognormally distributed about a mean value, with a standard deviation. The BPT model is more complex, and claims to be more realistic in modeling interevent times. Each requires a parameter quantifying the uncertainty in interevent times. For the lognormal it is sigma (σ), the standard deviation, and for the BPT it is alpha, the “aperiodicity parameter”. In California (Cramer et al., 2000) and Cascadia (Petersen et al., 2002) σ was found to be about 0.5. The BPT alpha parameter is more difficult to quantify, but here we also use 0.5, as suggested in Petersen et al. (2002). The other two parameters both models require are the exposure period, in this case the life of the structure, and the number of years since the last earthquake exposure to the hazard begins.

Results from the two time-dependent calculations were weighted equally. The time-dependent and Poissonian rates were weighted 0.67 to 0.33. In other words, it was felt that the time-dependent scenarios were twice as likely as the non-time-dependent scenarios.

Table A-1 shows the input parameters and calculation results for the three sources. An exposure period of 150 years was assumed as the life of the structure, and a time-to-construct of 10 years from 2011.

Figure TD1 shows probability of occurrence in the 150-year window on the y-axis, and probability of occurrence during that window as a function of fractional time into the average repeat time on the x-axis, for the megathrust source. The assumed “start date”, i.e., initiation of dam operation, is shown as the red triangle. The 150-year occurrence probabilities from the start date are the intersections of the vertical projection of the start date with the three model results. It can be seen that since we are only 10% into the cycle, the probability of occurrence

is very low. Those values are shown in Table A-1 rows 6 and 11. . The Poissonian rate for a 150-year window is shown in row 5. The annual rates for the two time-dependent models are shown in rows 7 and 10. The ratios of the time-dependent rates to the Poissonian rate are in rows 8 and 11. These ratios are quite low. Row 12 contains the final weighted annual rate for the source, and row 13 contains the ratio of the final rate to the Poissonian rate. For the megathrust source the final rate is 63% of the Poissonian rate, or an effective return period of 886 years (row 14).

Similar figures for the Denali-2002 Rupture and Denali-West of 2002 Segment are shown in TD2 and TD3. TD2 appears similar to TD1, but the long elapsed time since last rupture on the Denali-West of 2002 segment is evident in TD3. Table A-1 indicates an effective annual rate of 1/866 for the megathrust event, 1/633 for the Denali-2002 segment, and 1/253 for the Denali-West of 2002 segment.

Table A-1. Time-Dependent and non-Time Dependent (Poissonian) Rates

| | | Megathrust | Denali – 2002 Rupture | Denali – West of 2002 Rupture |
|----|---------------------------------------------------------------------------|------------|-----------------------|-------------------------------|
| 1 | Maximum magnitude | 9.2 | 7.9 | 7.9 |
| 2 | Return period for maximum magnitude (years) | 560 | 398 | 380 |
| 3 | Years since most recent event | 27 | 9 | 625 |
| 4 | Poissonian annual frequency | 1.79e-3 | 2.51e-3 | 2.63e-3 |
| 5 | 150-yr P(occurrence), Poissonian | 0.235 | 0.314 | 0.326 |
| 6 | 150-yr P(occurrence), lognormal | 0.024 | 0.044 | 0.518 |
| 7 | Annual rate, lognormal | 1.60e-4 | 2.93e-4 | 3.45e-3 |
| 8 | Ratio, lognormal to Poissonian | 0.090 | 0.117 | 1.31 |
| 9 | 150-yr P(occurrence), BPT | 0.030 | 0.059 | 0.590 |
| 10 | Annual rate, BPT | 2.00e-4 | 3.93e-4 | 3.93e-3 |
| 11 | Ratio, BPT to Poissonian | 0.031 | 0.156 | 1.49 |
| 12 | Weighted annual rate ¹ | 1.13e-3 | 1.61e-3 | 2.69e-3 |
| 13 | Ratio weighted annual rate to Poissonian (non-time-dependent) annual rate | 0.632 | 0.600 | 1.50 |
| 14 | Final effective return period (years) | 886 | 633 | 253 |

Note: (1) Lognormal and BPT weighted equally, time-dependent vs. Poissonian weighted 0.67 – 0.33.

2.0 REFERENCES

Cramer, C. H., M. D. Petersen, T. Cao, T. R. Topozada, and M. S. Reichle, 2000. A time-dependent probabilistic seismic-hazard model for California. Bulletin of the Seismological Society of America 90, 1–21.

Matthews, M. V., W. L. Ellsworth, and P. A. Reasenber, 2002, A Brownian Model for Recurrent Earthquakes: Bull. Seismol. Soc. Am., 92, 2233-2250.

Petersen, M. D., C. H. Cramer, and A. D. Frankel, 2002. Simulations of seismic hazard for the Pacific Northwest of the United States from earthquakes associated with the Cascadia subduction zone. Pure and Applied Geophysics 159, 2,147–2,168.

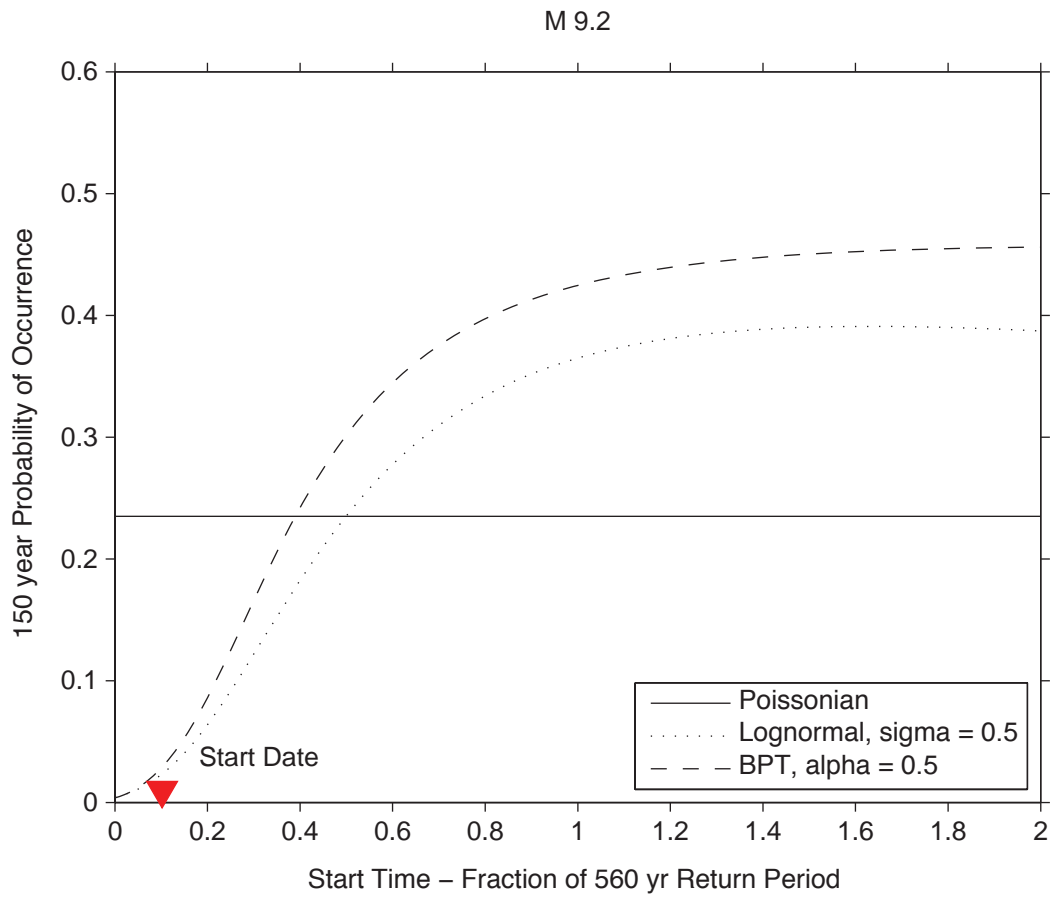


Figure A1 . 150-year probability of occurrence of M 9.2 megathrust.

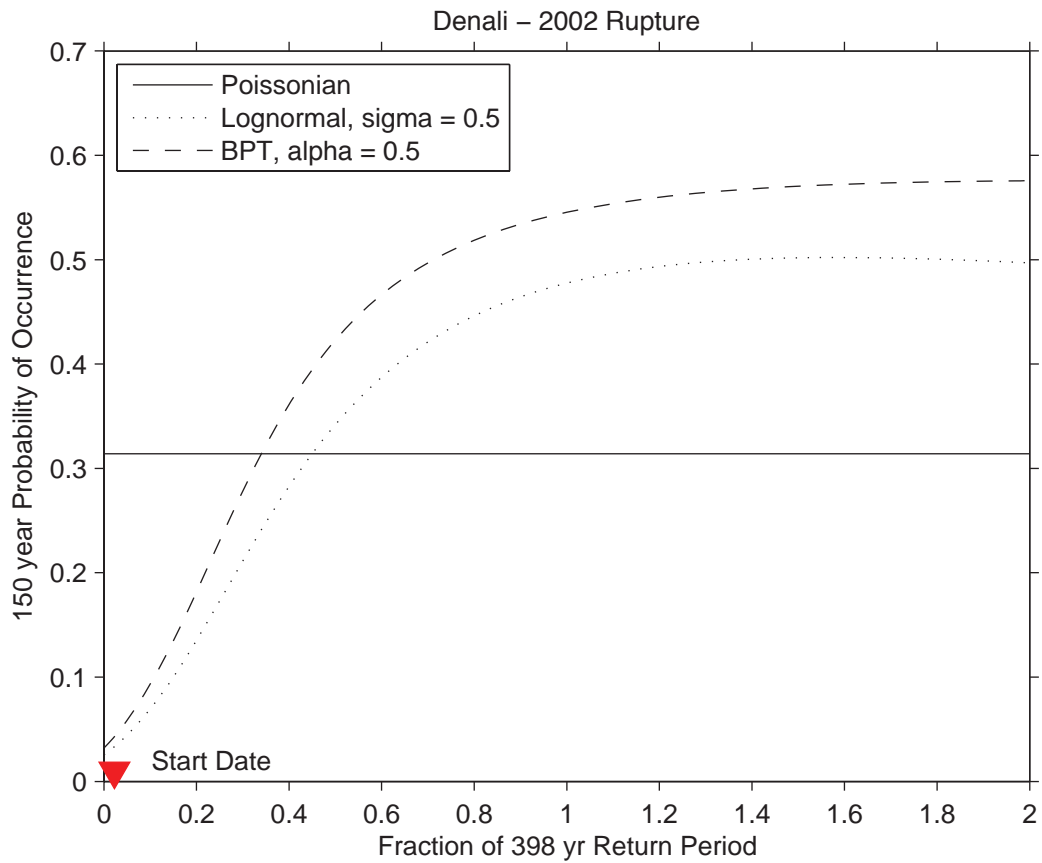


Figure A2. 150-year probability of occurrence of M 7.9 Denali-2002 rupture.

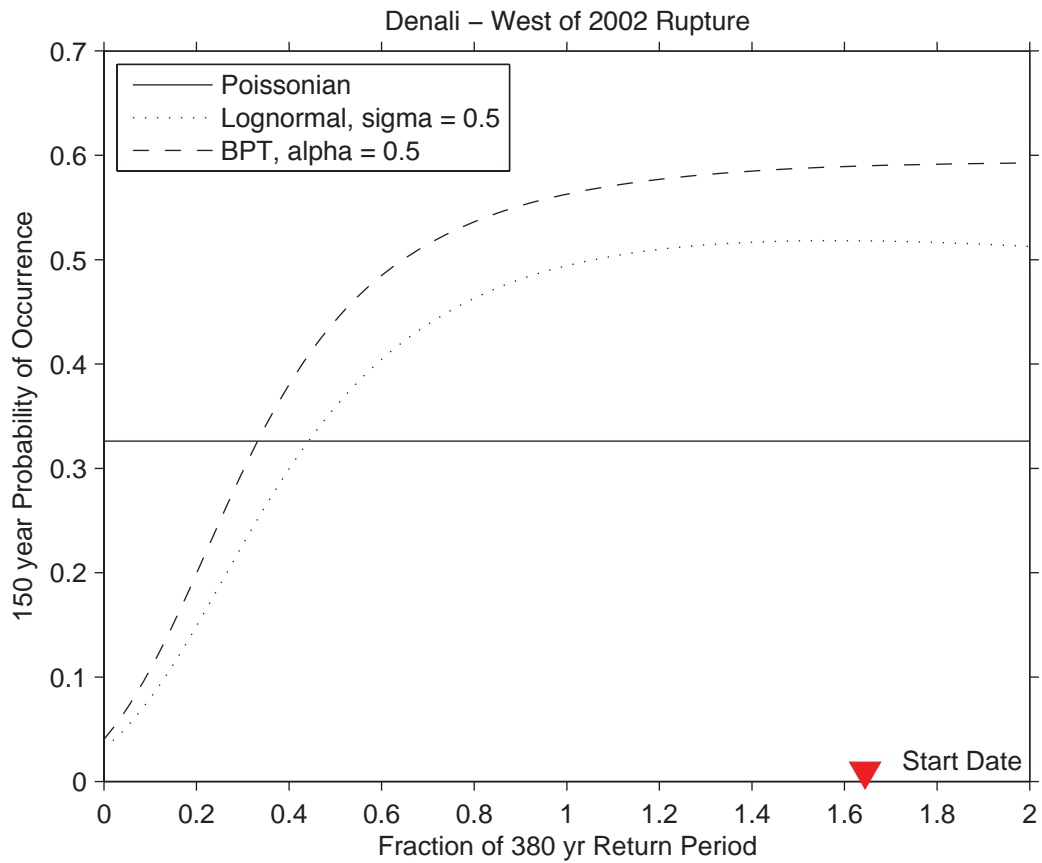
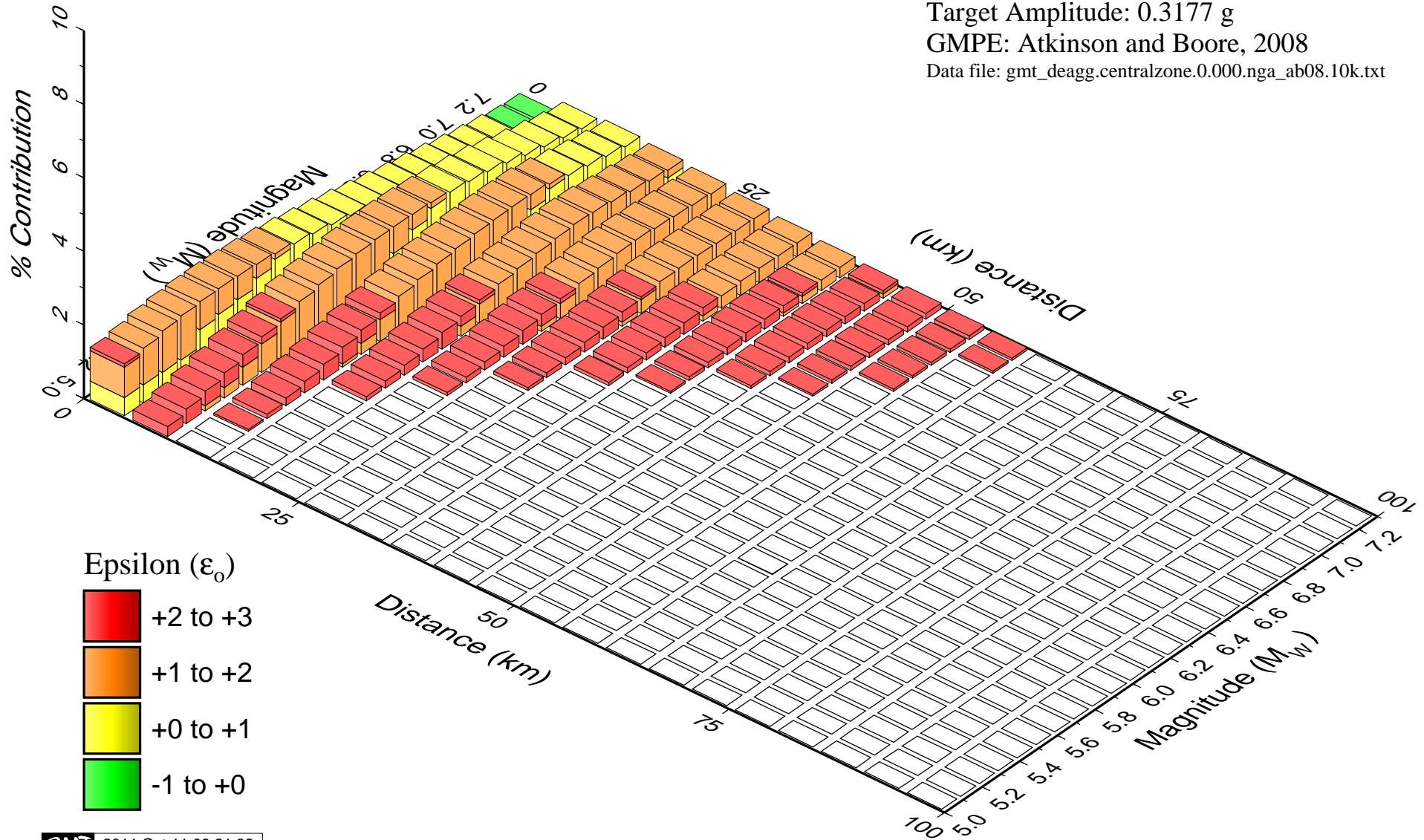


Figure A3. 150-year probability of occurrence of M 7.9 Denali-west of 2002 rupture.

Appendix B - DEAGGREGATION STACK PLOTS

Cover Page

Watana Dam, AK
 Seismic Hazard Deaggregation
 SAB Central Areal Zone
 PHA: 10,000 year return period
 Target Amplitude: 0.3177 g
 GMPE: Atkinson and Boore, 2008
 Data file: gmt_deagg.centralzone.0.000.nga_ab08.10k.txt



Watana Dam, AK

Seismic Hazard Deaggregation

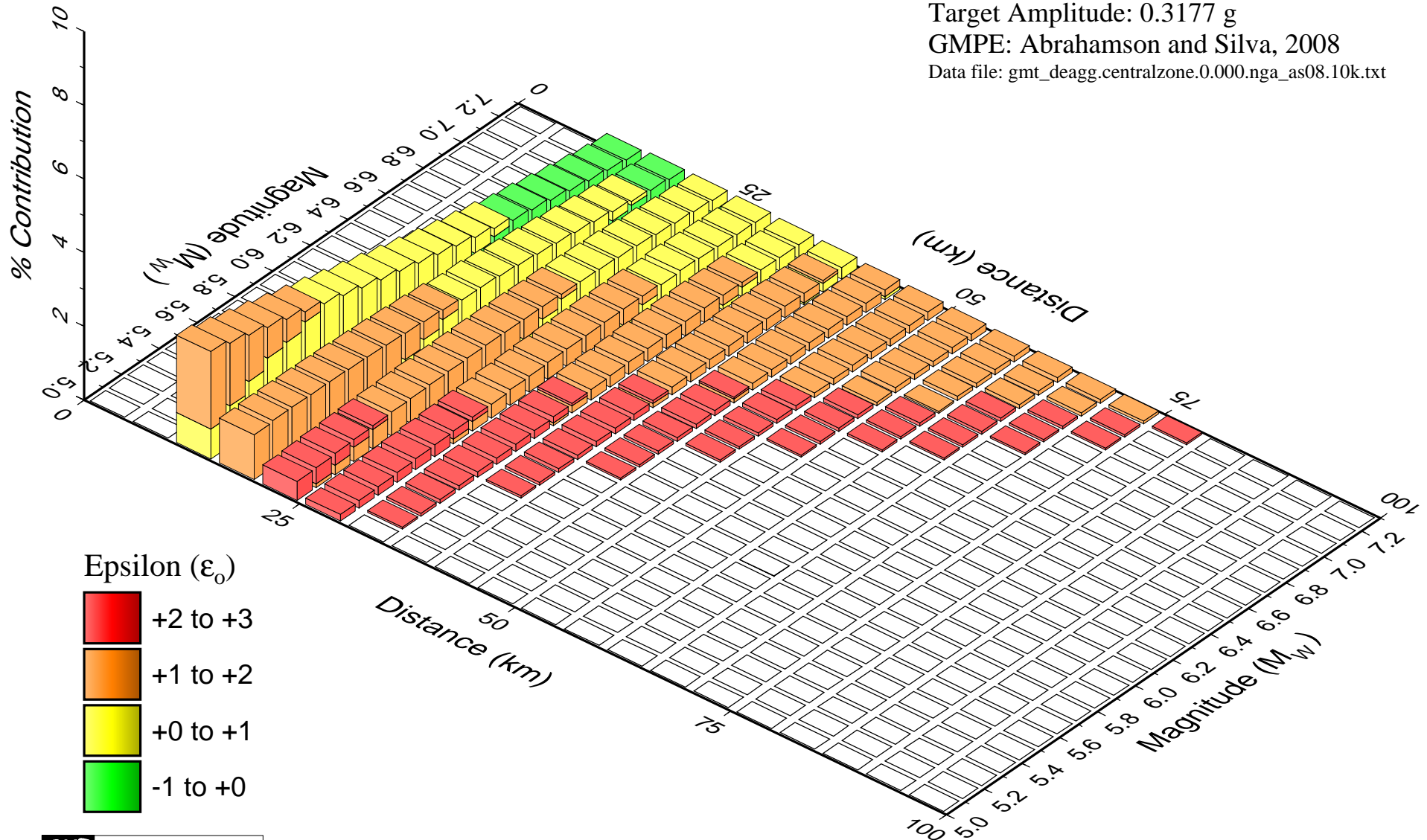
SAB Central Areal Zone

PHA: 10,000 year return period

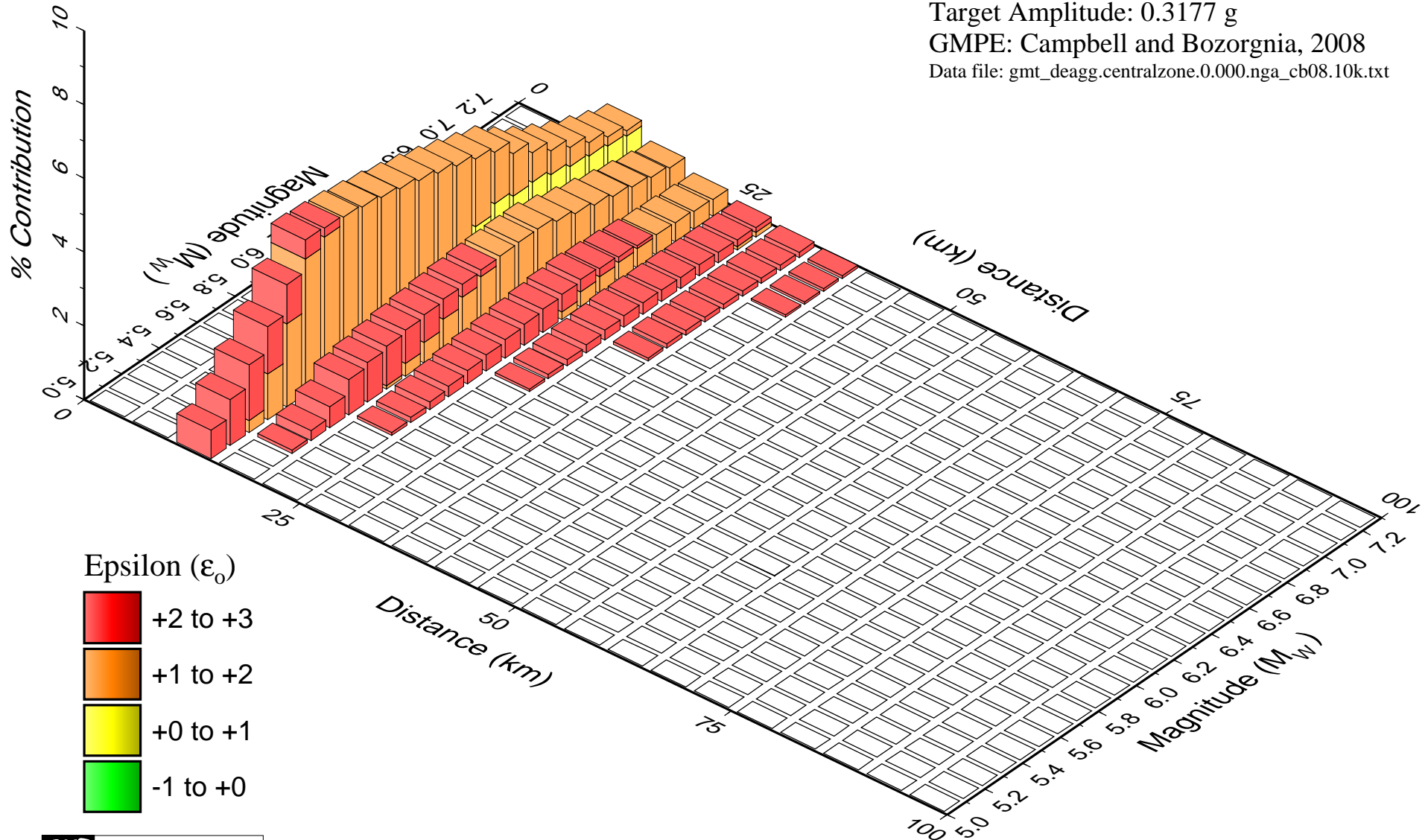
Target Amplitude: 0.3177 g

GMPE: Abrahamson and Silva, 2008

Data file: gmt_deagg.centralzone.0.000.nga_as08.10k.txt



Watana Dam, AK
 Seismic Hazard Deaggregation
 SAB Central Areal Zone
 PHA: 10,000 year return period
 Target Amplitude: 0.3177 g
 GMPE: Campbell and Bozorgnia, 2008
 Data file: gmt_deagg.centralzone.0.000.nga_cb08.10k.txt



Watana Dam, AK

Seismic Hazard Deaggregation

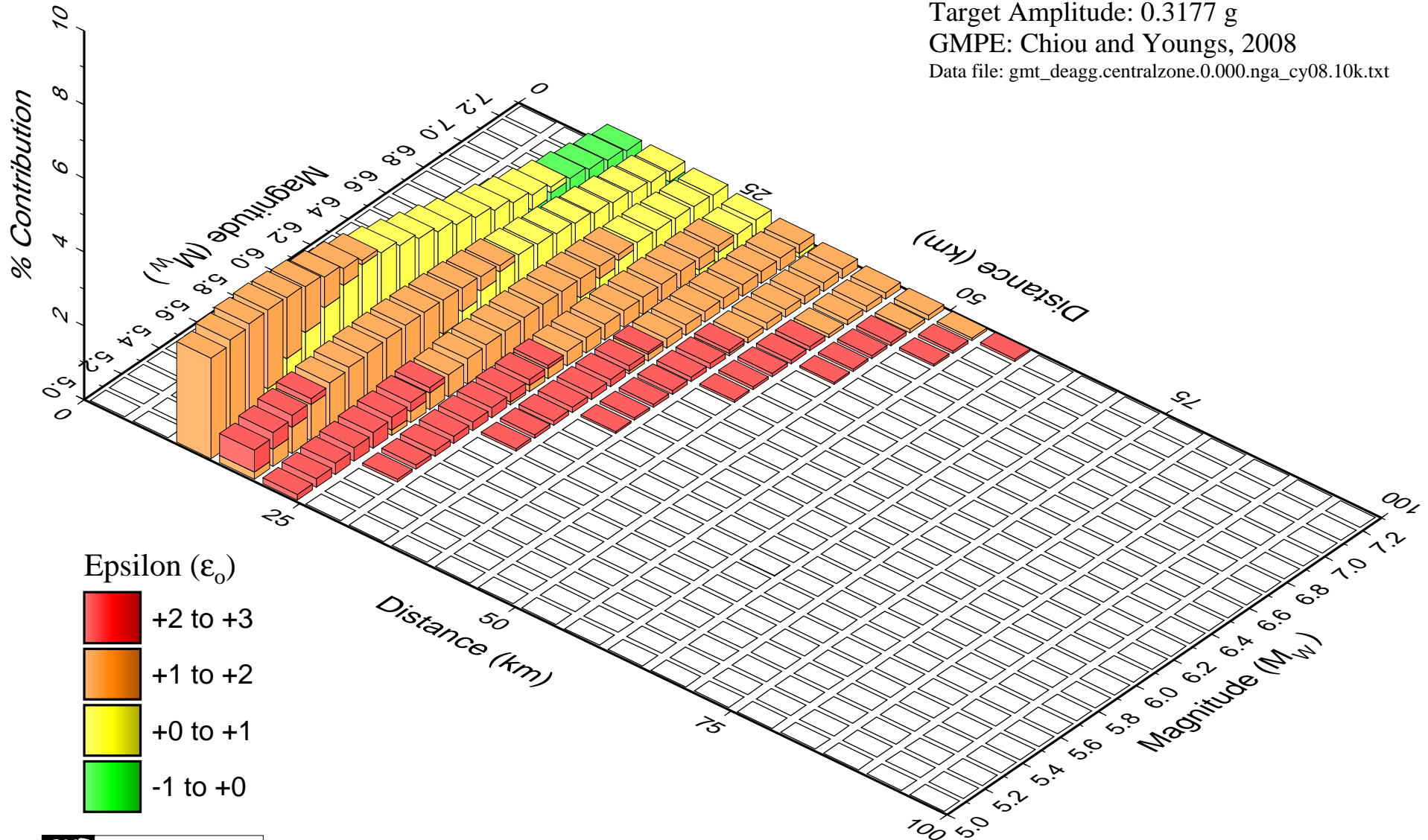
SAB Central Areal Zone

PHA: 10,000 year return period

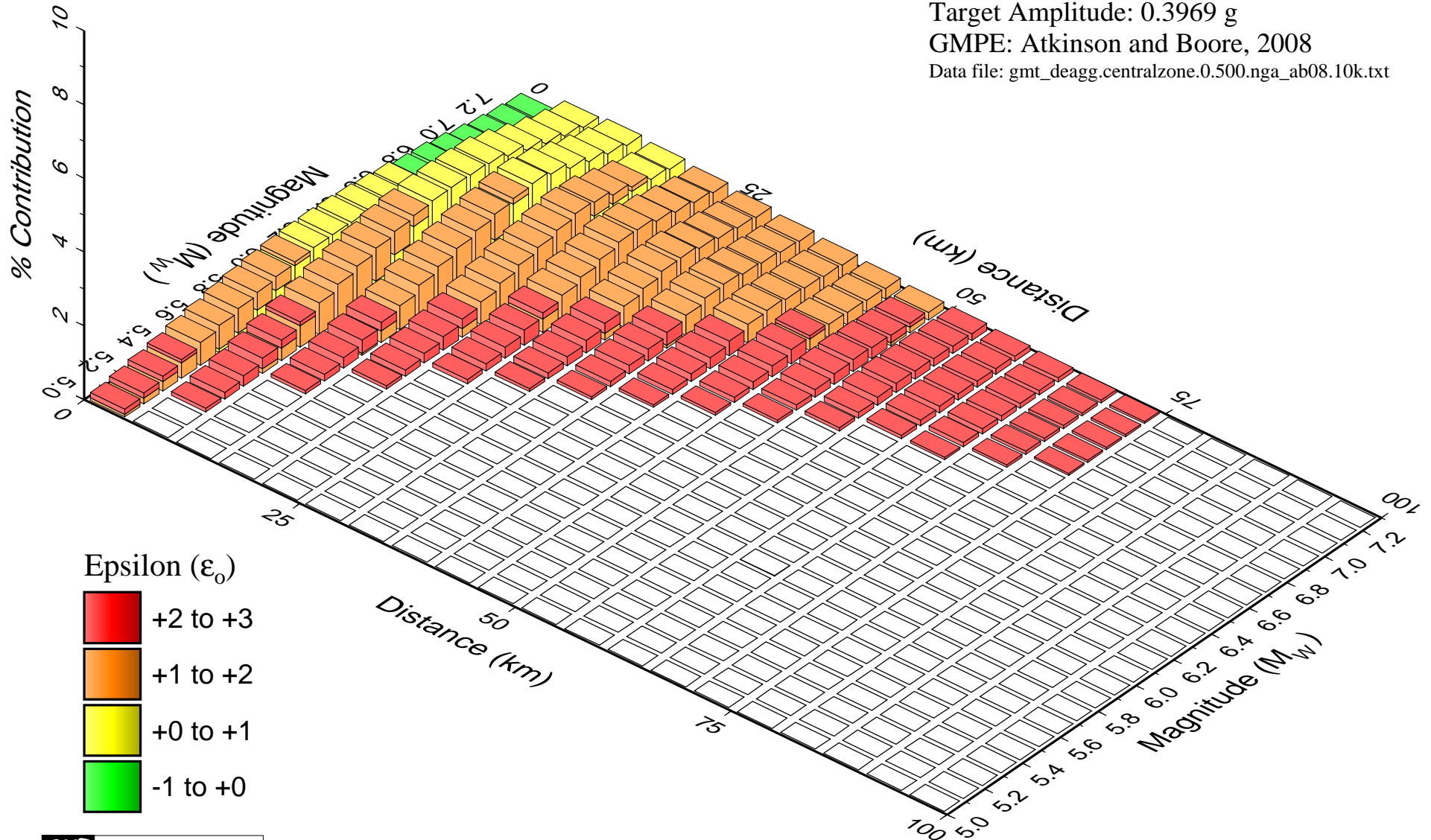
Target Amplitude: 0.3177 g

GMPE: Chiou and Youngs, 2008

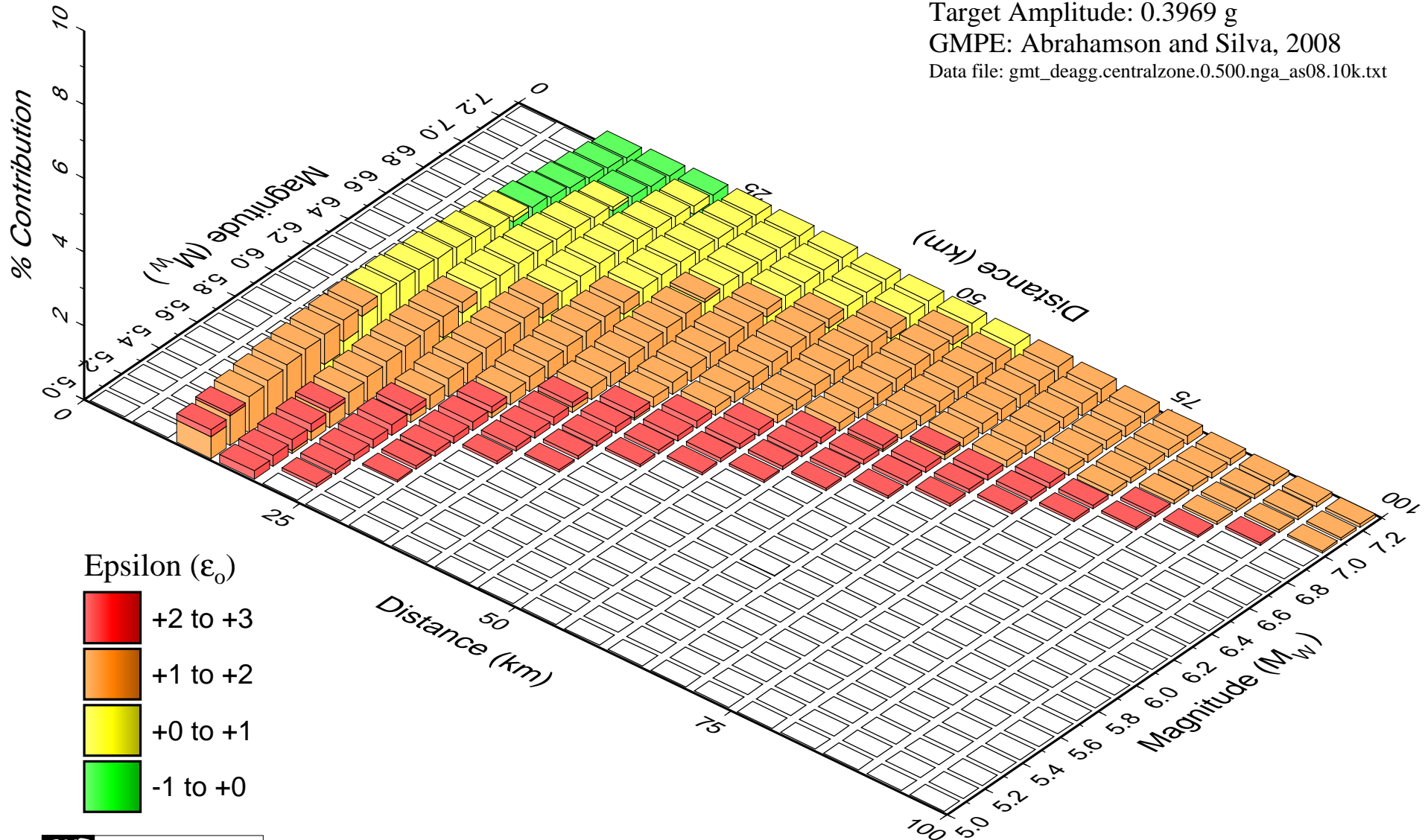
Data file: gmt_deagg.centralzone.0.000.nga_cy08.10k.txt



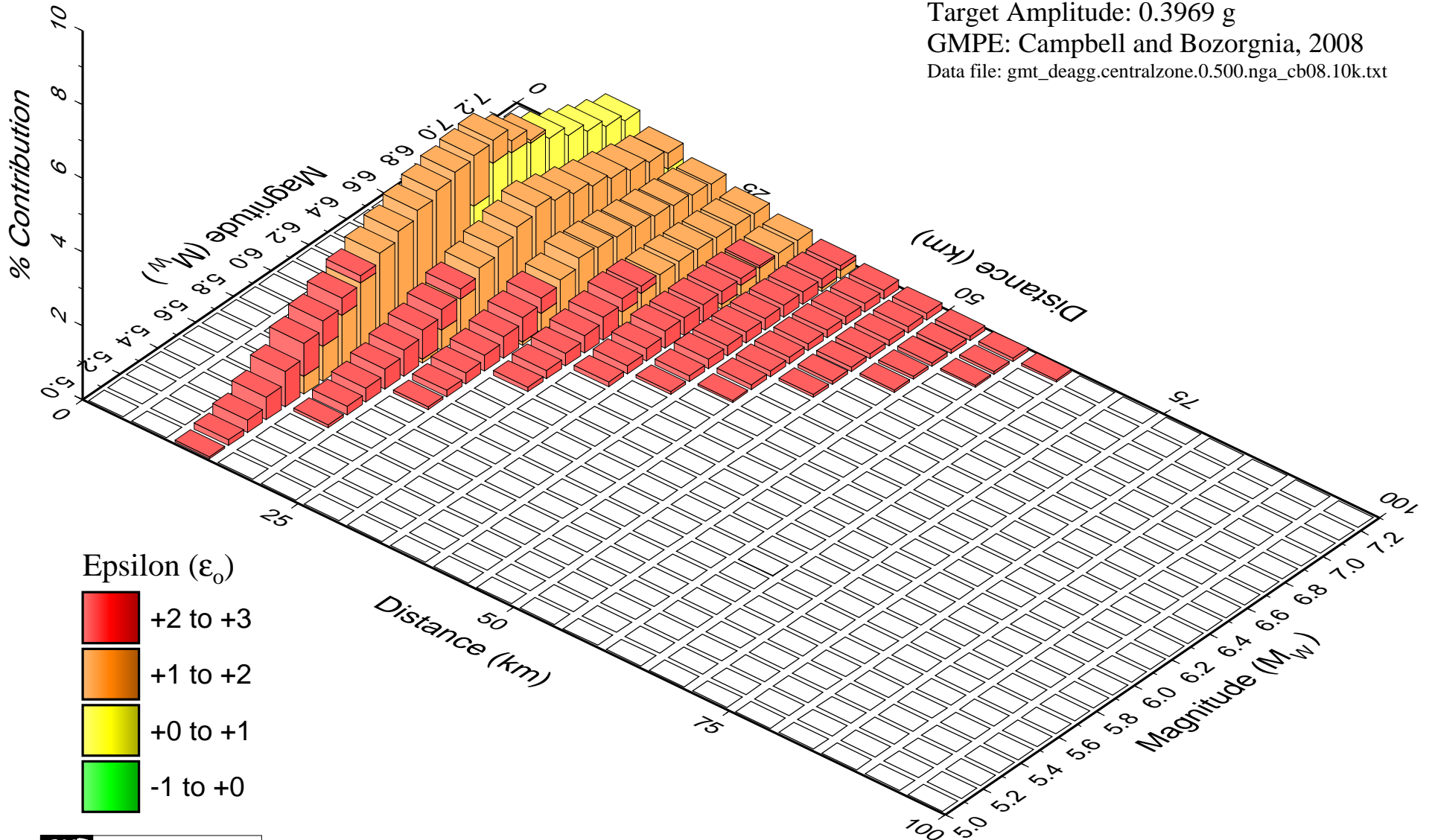
Watana Dam, AK
 Seismic Hazard Deaggregation
 SAB Central Areal Zone
 0.500 sec.: 10,000 year return period
 Target Amplitude: 0.3969 g
 GMPE: Atkinson and Boore, 2008
 Data file: gmt_deagg.centralzone.0.500.nga_ab08.10k.txt



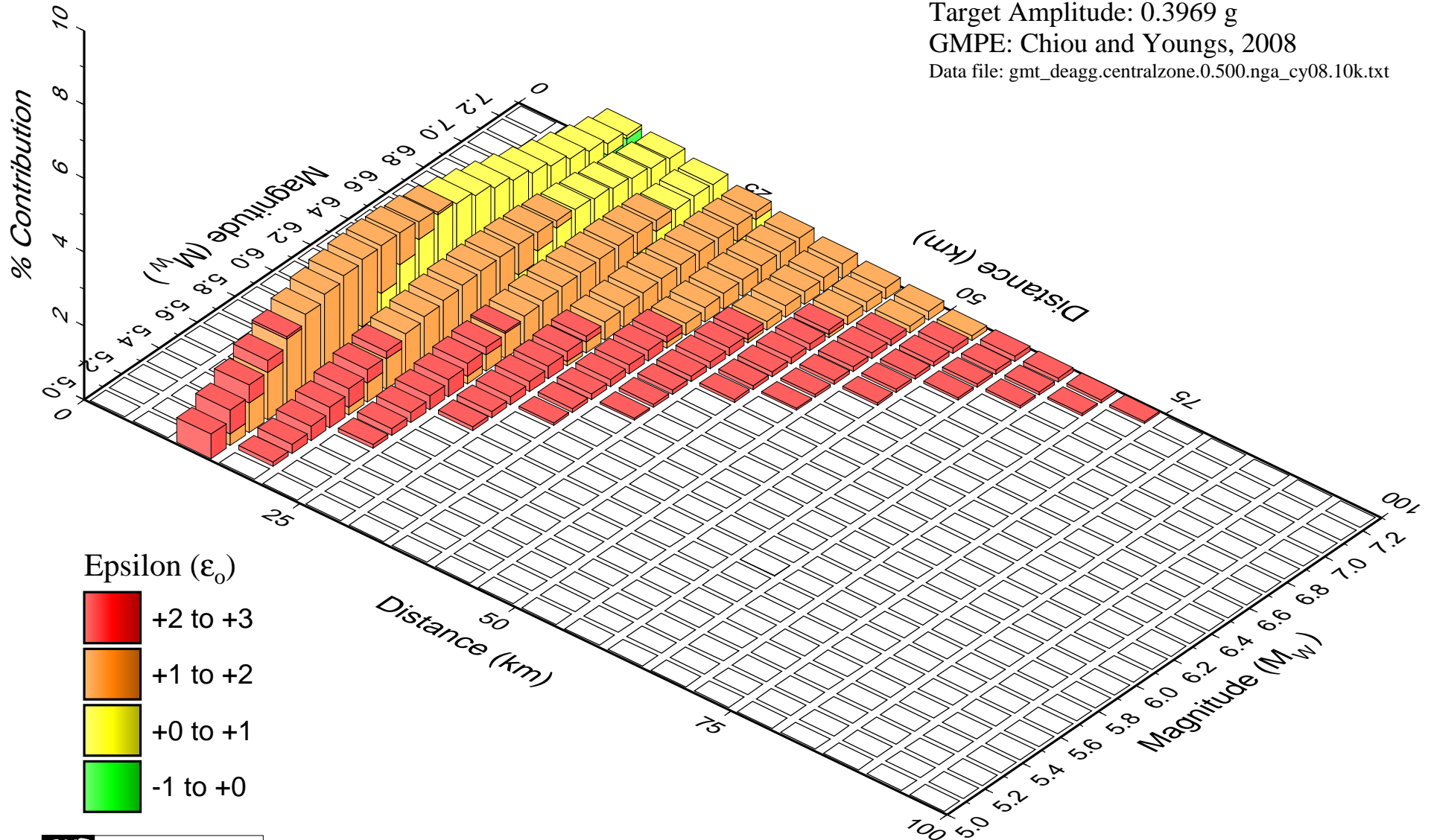
Watana Dam, AK
 Seismic Hazard Deaggregation
 SAB Central Areal Zone
 0.500 sec.: 10,000 year return period
 Target Amplitude: 0.3969 g
 GMPE: Abrahamson and Silva, 2008
 Data file: gmt_deagg.centralzone.0.500.nga_as08.10k.txt



Watana Dam, AK
 Seismic Hazard Deaggregation
 SAB Central Areal Zone
 0.500 sec.: 10,000 year return period
 Target Amplitude: 0.3969 g
 GMPE: Campbell and Bozorgnia, 2008
 Data file: gmt_deagg.centralzone.0.500.nga_cb08.10k.txt



Watana Dam, AK
 Seismic Hazard Deaggregation
 SAB Central Areal Zone
 0.500 sec.: 10,000 year return period
 Target Amplitude: 0.3969 g
 GMPE: Chiou and Youngs, 2008
 Data file: gmt_deagg.centralzone.0.500.nga_cy08.10k.txt



Watana Dam, AK

Seismic Hazard Deaggregation

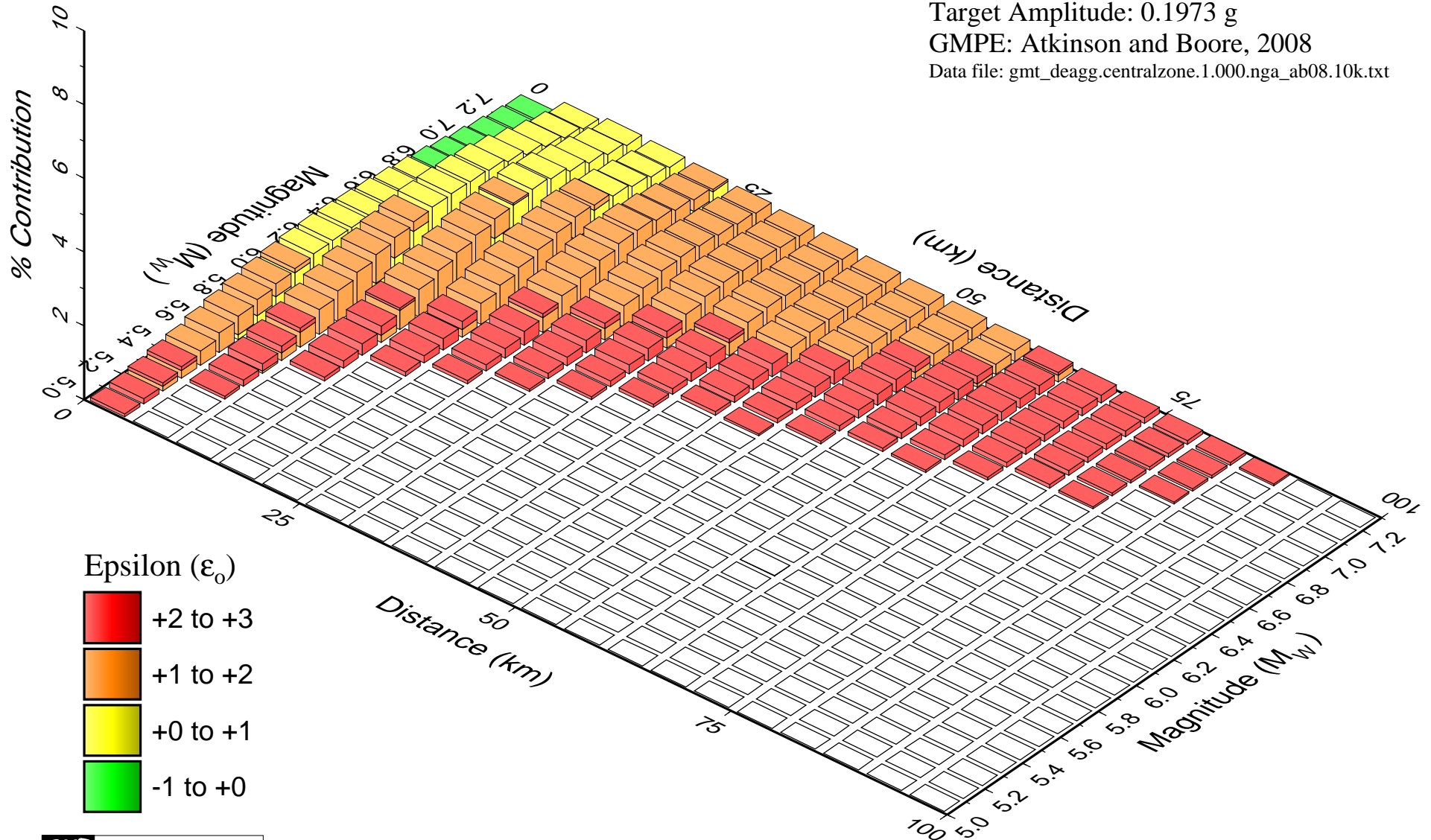
SAB Central Areal Zone

1.000 sec.: 10,000 year return period

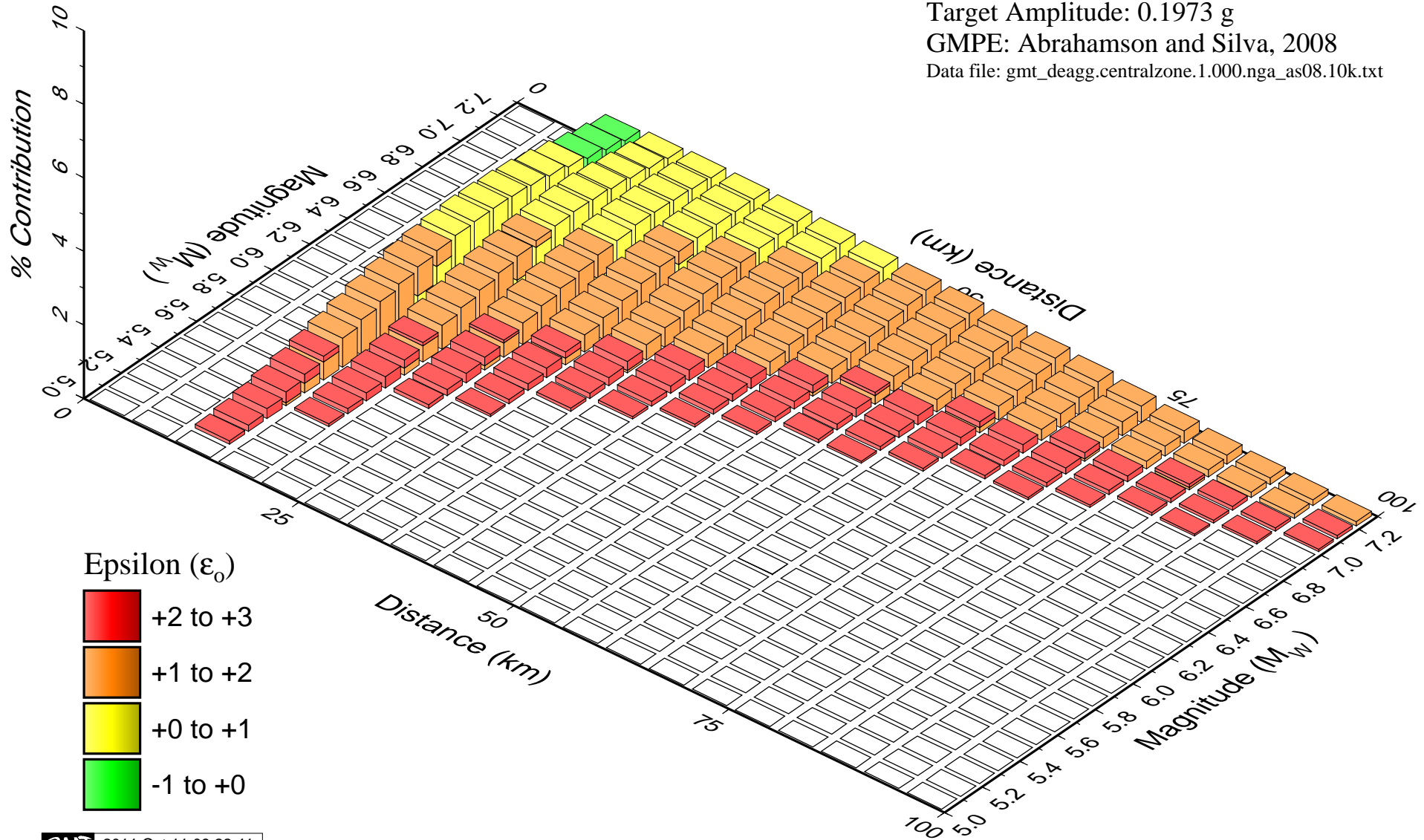
Target Amplitude: 0.1973 g

GMPE: Atkinson and Boore, 2008

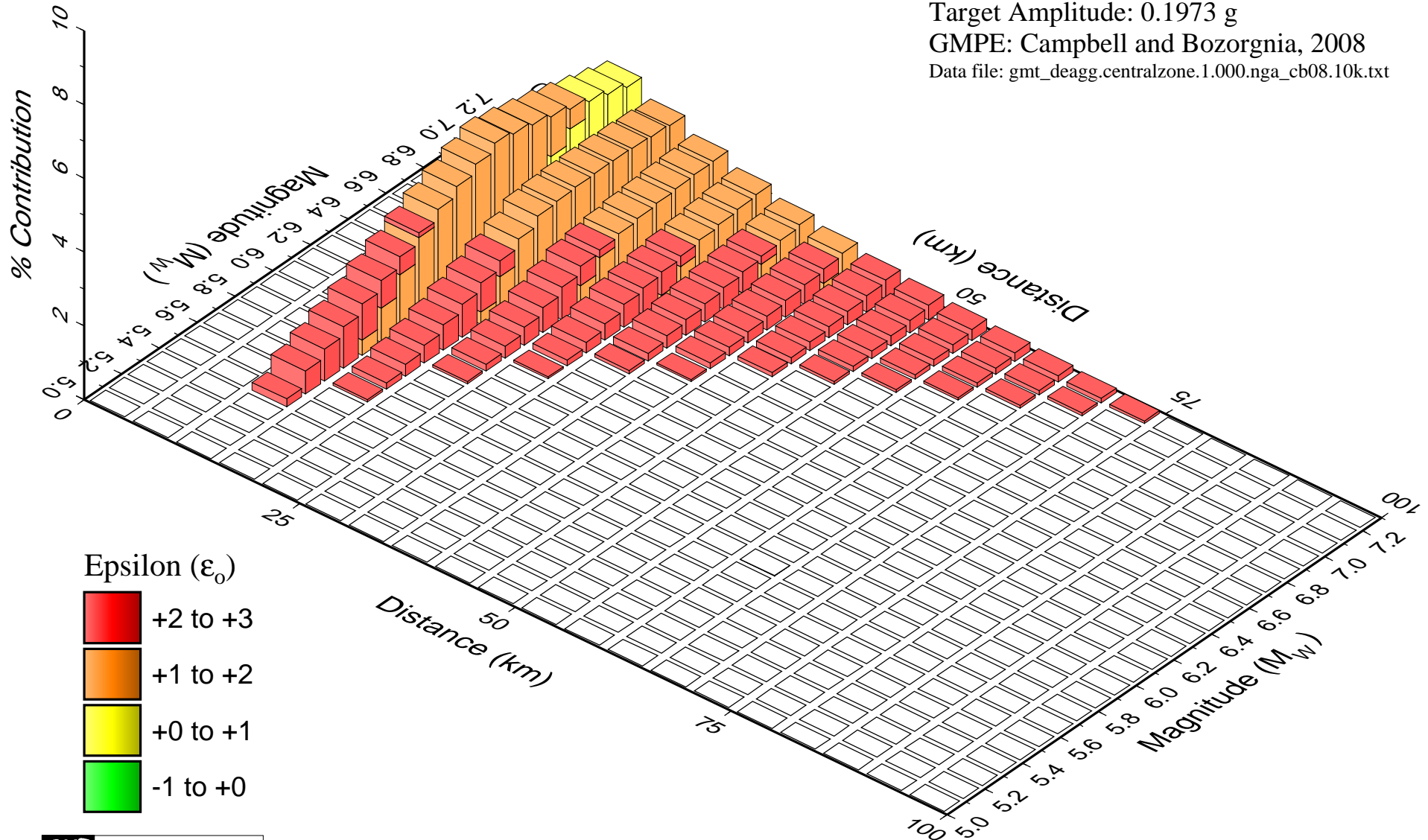
Data file: gmt_deagg.centralzone.1.000.nga_ab08.10k.txt



Watana Dam, AK
 Seismic Hazard Deaggregation
 SAB Central Areal Zone
 1.000 sec.: 10,000 year return period
 Target Amplitude: 0.1973 g
 GMPE: Abrahamson and Silva, 2008
 Data file: gmt_deagg.centralzone.1.000.nga_as08.10k.txt



Watana Dam, AK
 Seismic Hazard Deaggregation
 SAB Central Areal Zone
 1.000 sec.: 10,000 year return period
 Target Amplitude: 0.1973 g
 GMPE: Campbell and Bozorgnia, 2008
 Data file: gmt_deagg.centralzone.1.000.nga_cb08.10k.txt



Watana Dam, AK

Seismic Hazard Deaggregation

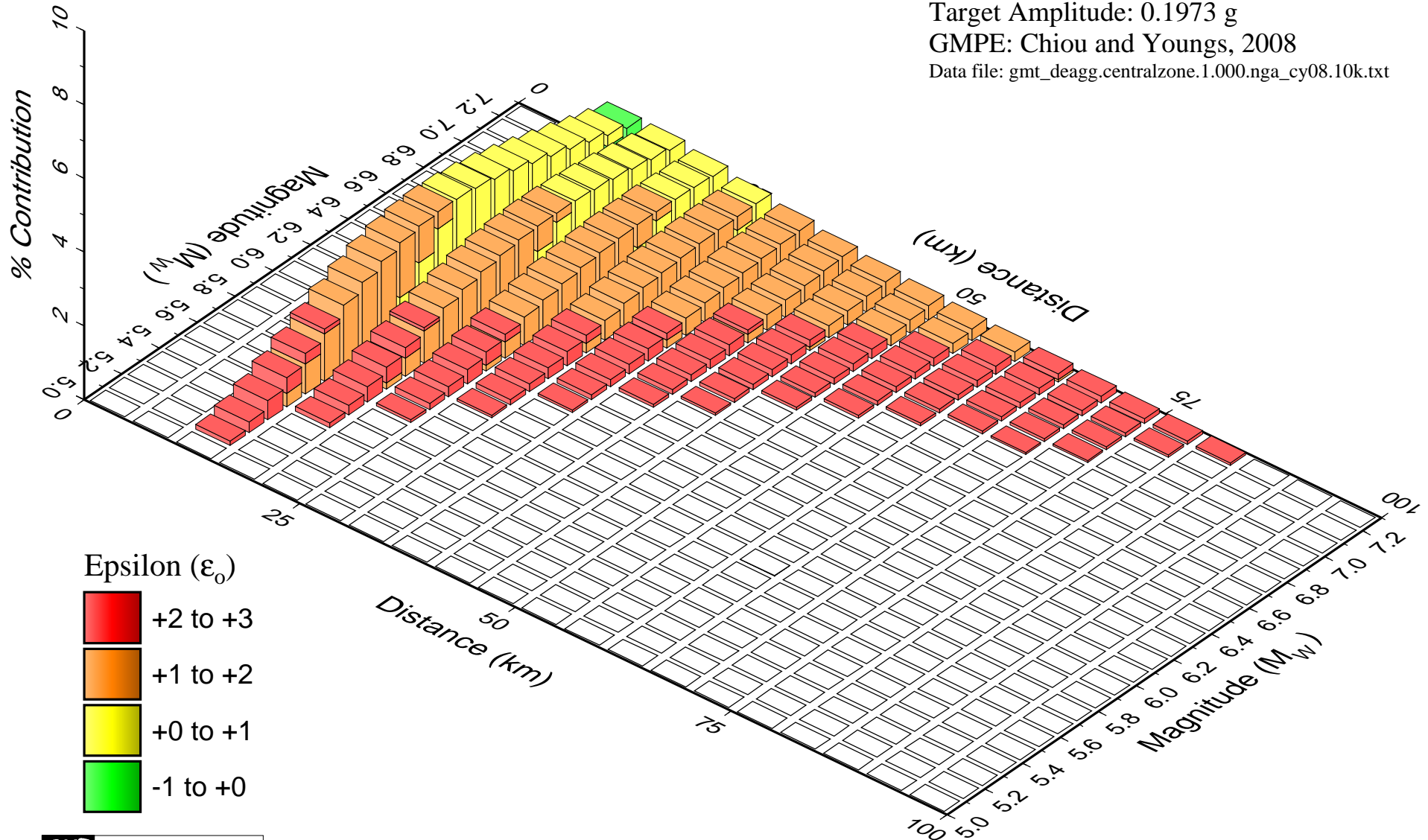
SAB Central Areal Zone

1.000 sec.: 10,000 year return period

Target Amplitude: 0.1973 g

GMPE: Chiou and Youngs, 2008

Data file: gmt_deagg.centralzone.1.000.nga_cy08.10k.txt



Watana Dam, AK

Seismic Hazard Deaggregation

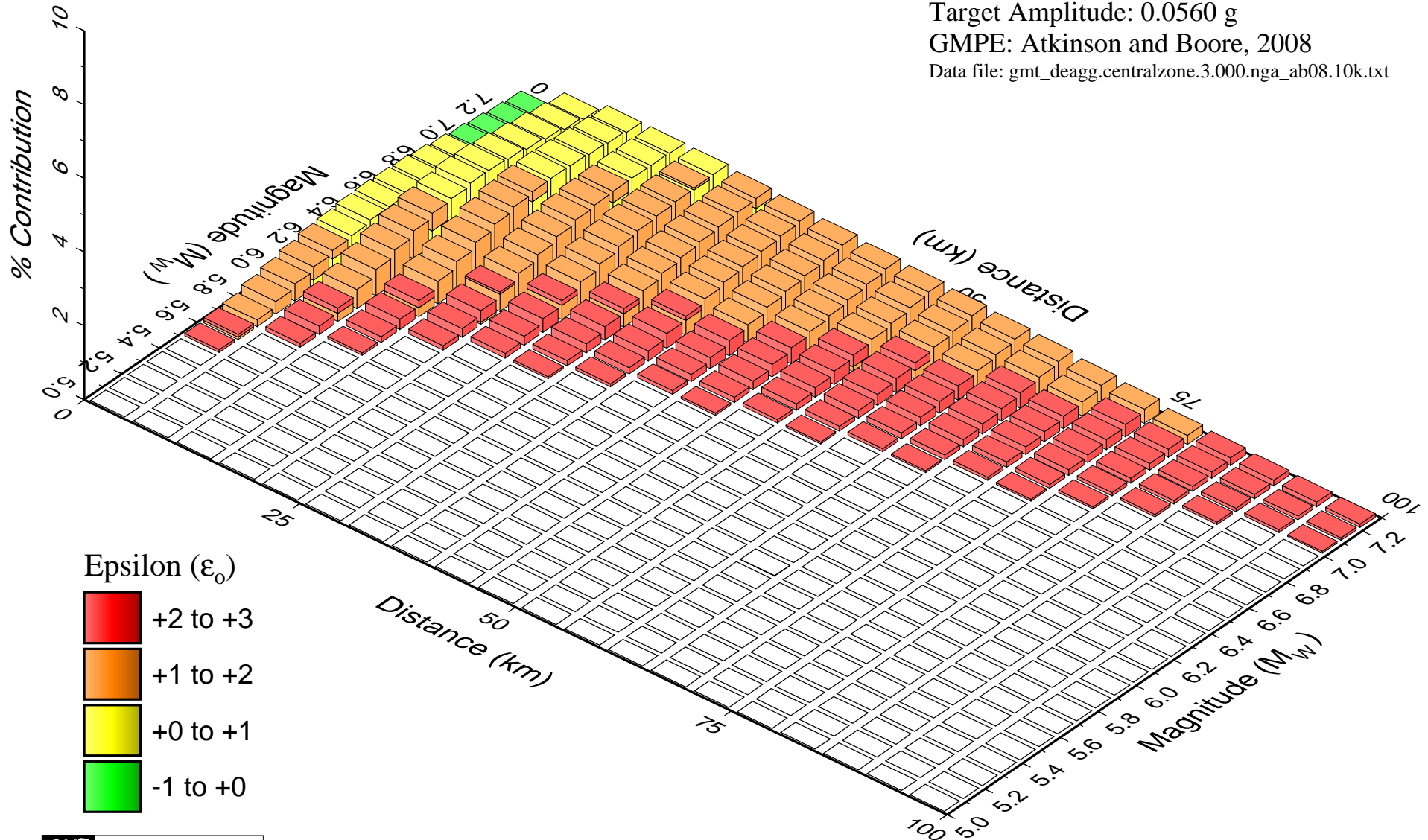
SAB Central Areal Zone

3.000 sec.: 10,000 year return period

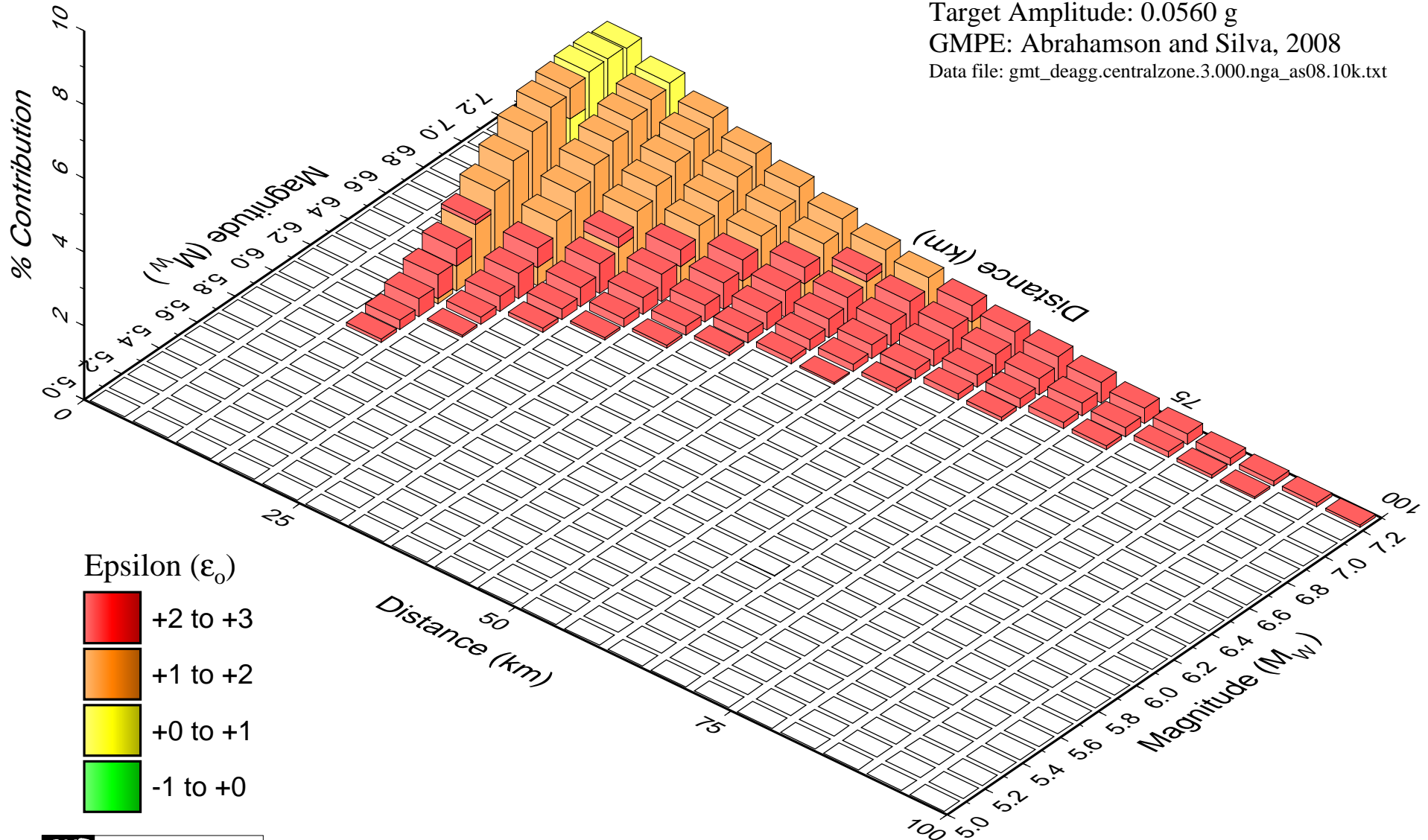
Target Amplitude: 0.0560 g

GMPE: Atkinson and Boore, 2008

Data file: gmt_deagg.centralzone.3.000.nga_ab08.10k.txt



Watana Dam, AK
 Seismic Hazard Deaggregation
 SAB Central Areal Zone
 3.000 sec.: 10,000 year return period
 Target Amplitude: 0.0560 g
 GMPE: Abrahamson and Silva, 2008
 Data file: gmt_deagg.centralzone.3.000.nga_as08.10k.txt



Watana Dam, AK Seismic Hazard Deaggregation

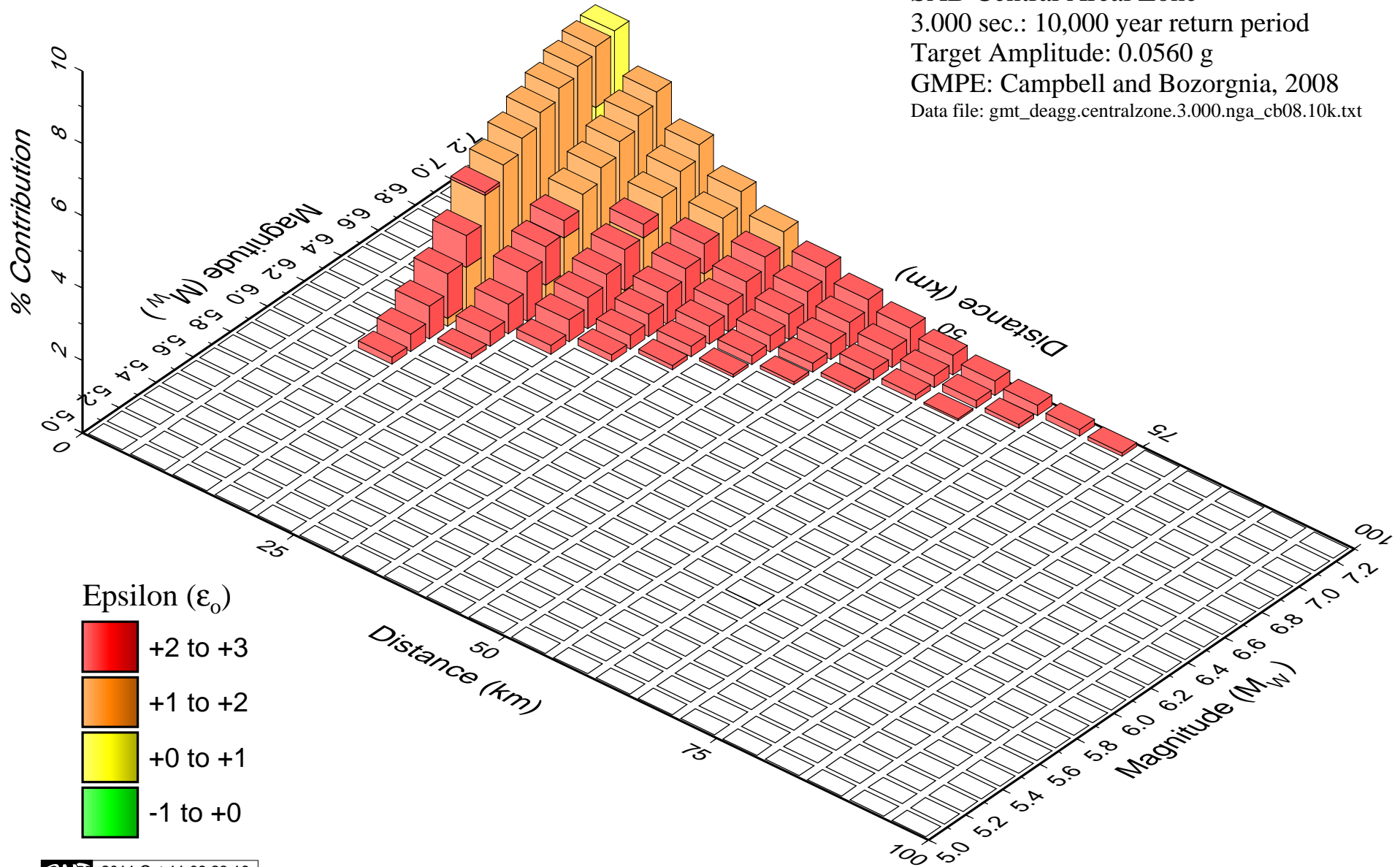
SAB Central Areal Zone

3.000 sec.: 10,000 year return period

Target Amplitude: 0.0560 g

GMPE: Campbell and Bozorgnia, 2008

Data file: gmt_deagg.centralzone.3.000.nga_cb08.10k.txt



Watana Dam, AK

Seismic Hazard Deaggregation

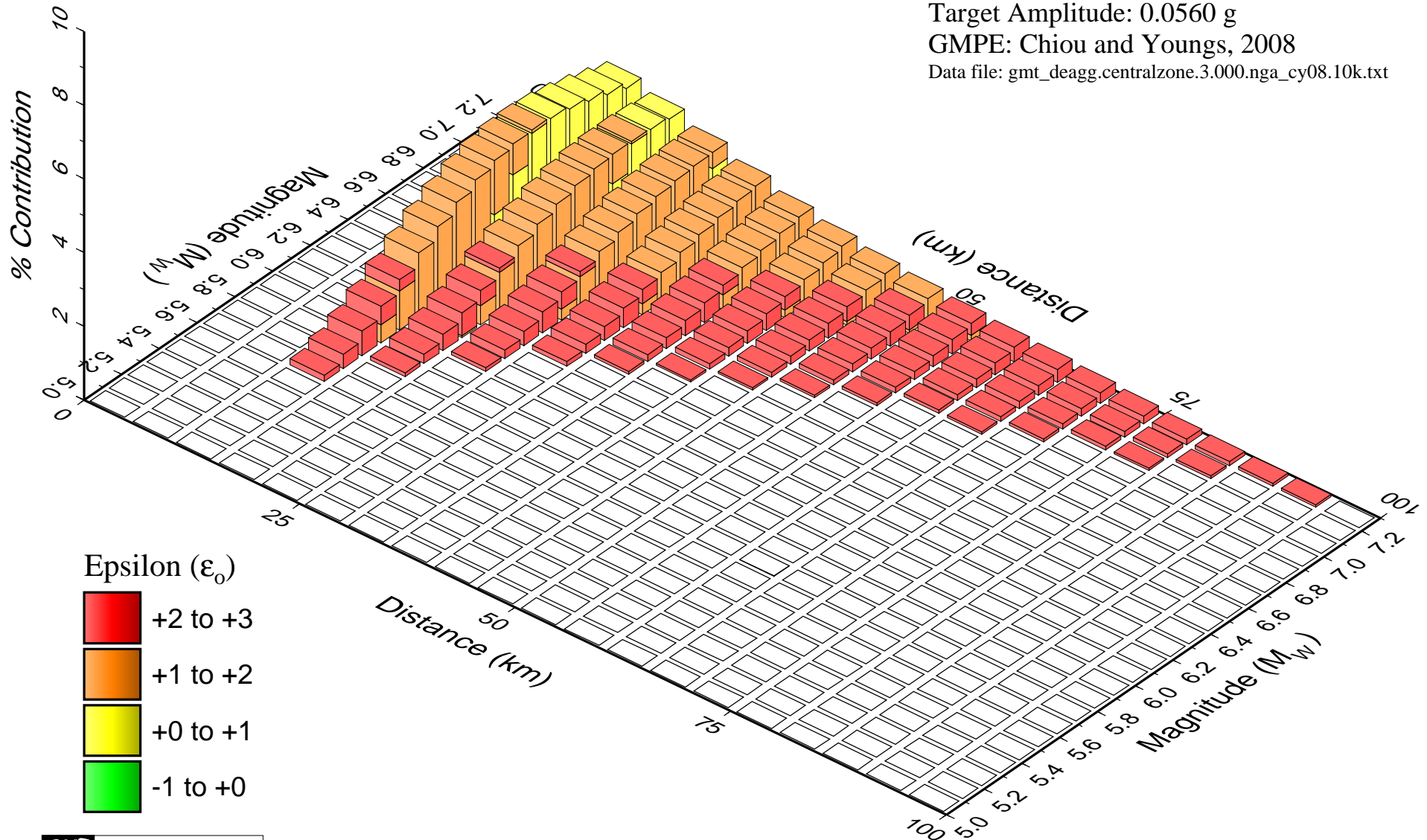
SAB Central Areal Zone

3.000 sec.: 10,000 year return period

Target Amplitude: 0.0560 g

GMPE: Chiou and Youngs, 2008

Data file: gmt_deagg.centralzone.3.000.nga_cy08.10k.txt



Watana Dam, AK Seismic Hazard Deaggregation

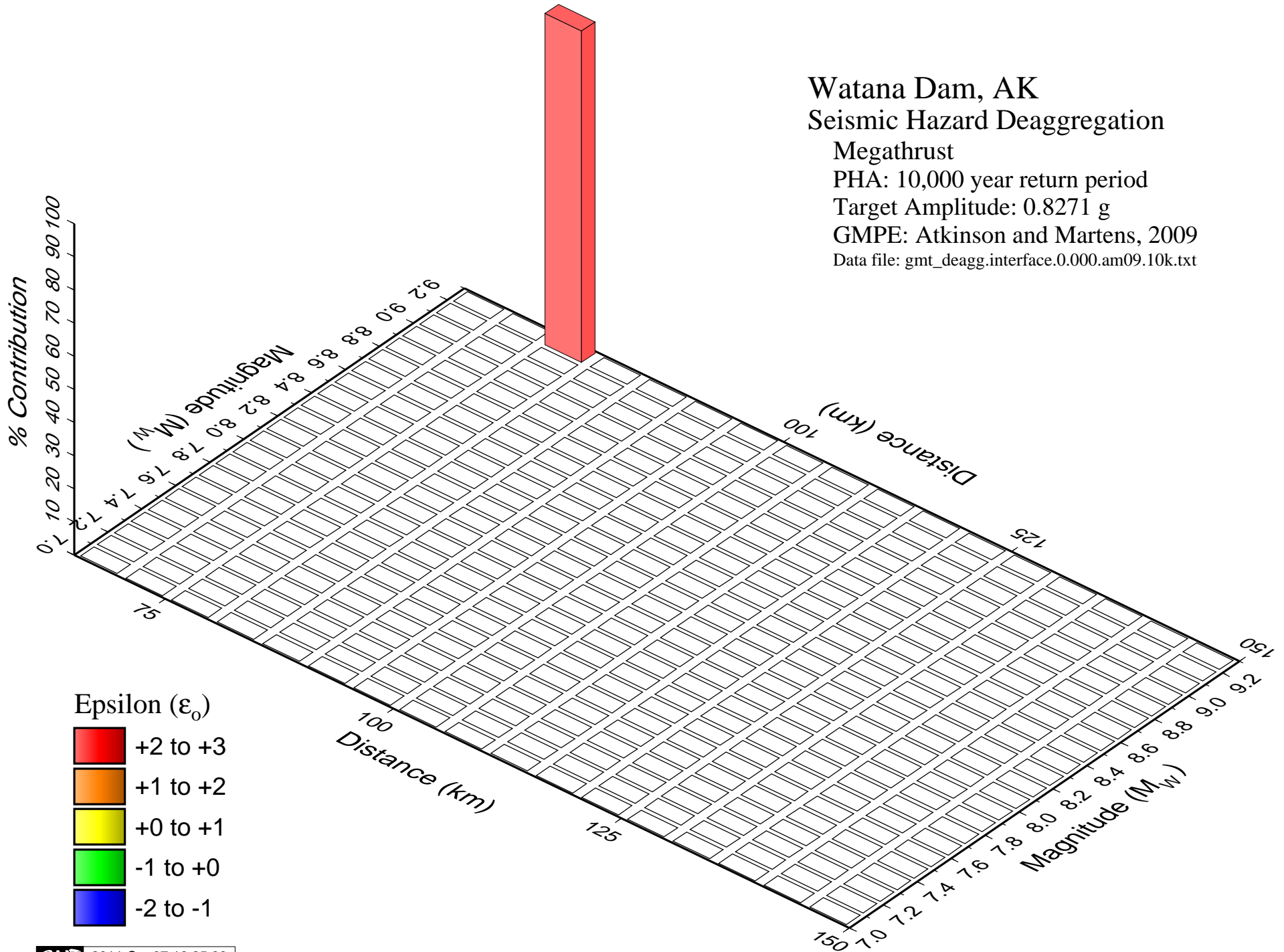
Megathrust

PHA: 10,000 year return period

Target Amplitude: 0.8271 g

GMPE: Atkinson and Martens, 2009

Data file: gmt_deagg.interface.0.000.am09.10k.txt



Watana Dam, AK Seismic Hazard Deaggregation

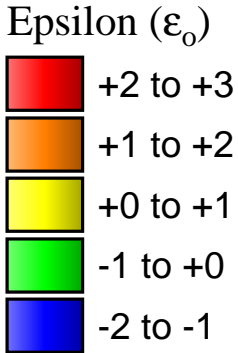
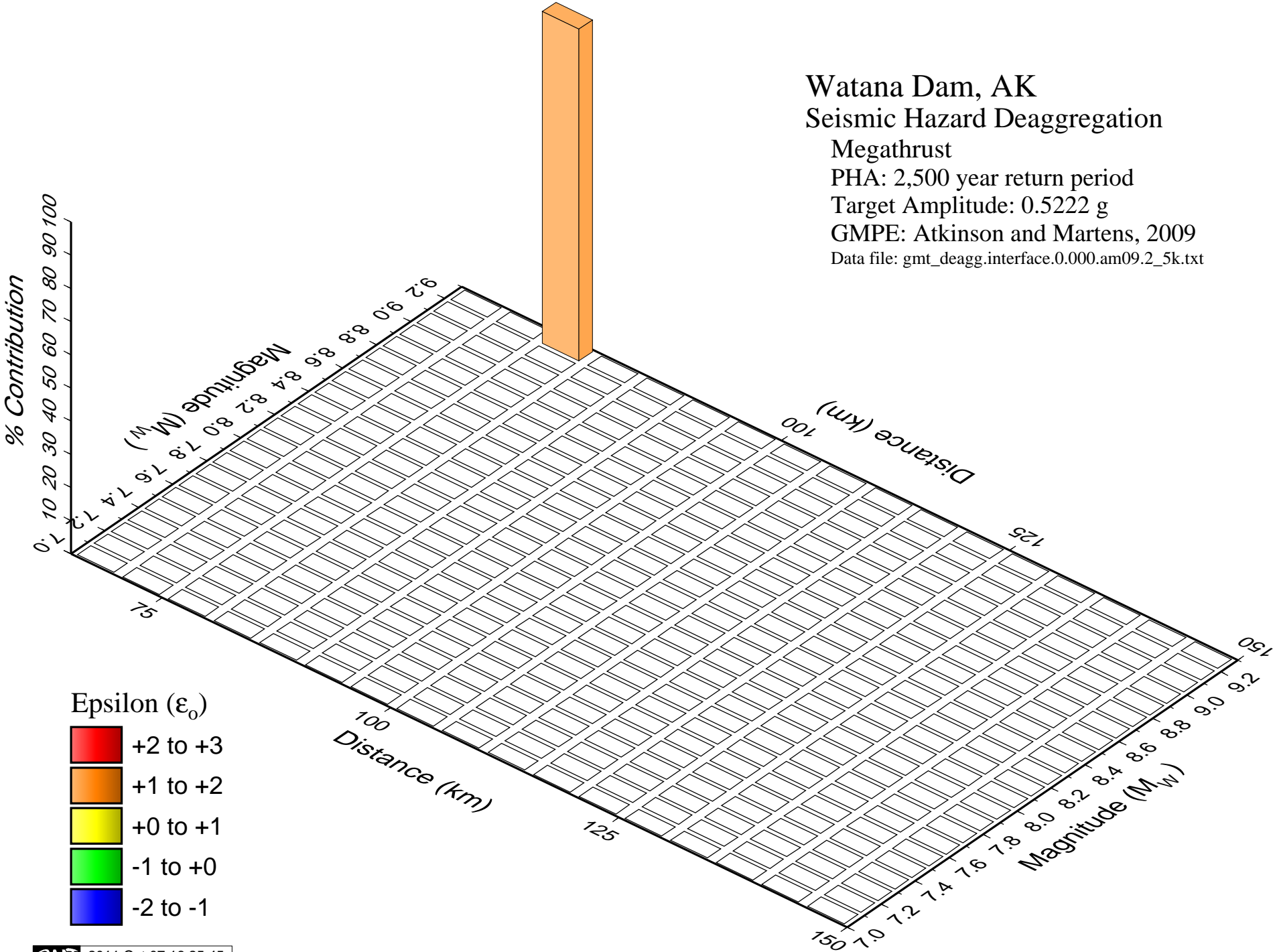
Megathrust

PHA: 2,500 year return period

Target Amplitude: 0.5222 g

GMPE: Atkinson and Martens, 2009

Data file: gmt_deagg.interface.0.000.am09.2_5k.txt



Watana Dam, AK Seismic Hazard Deaggregation

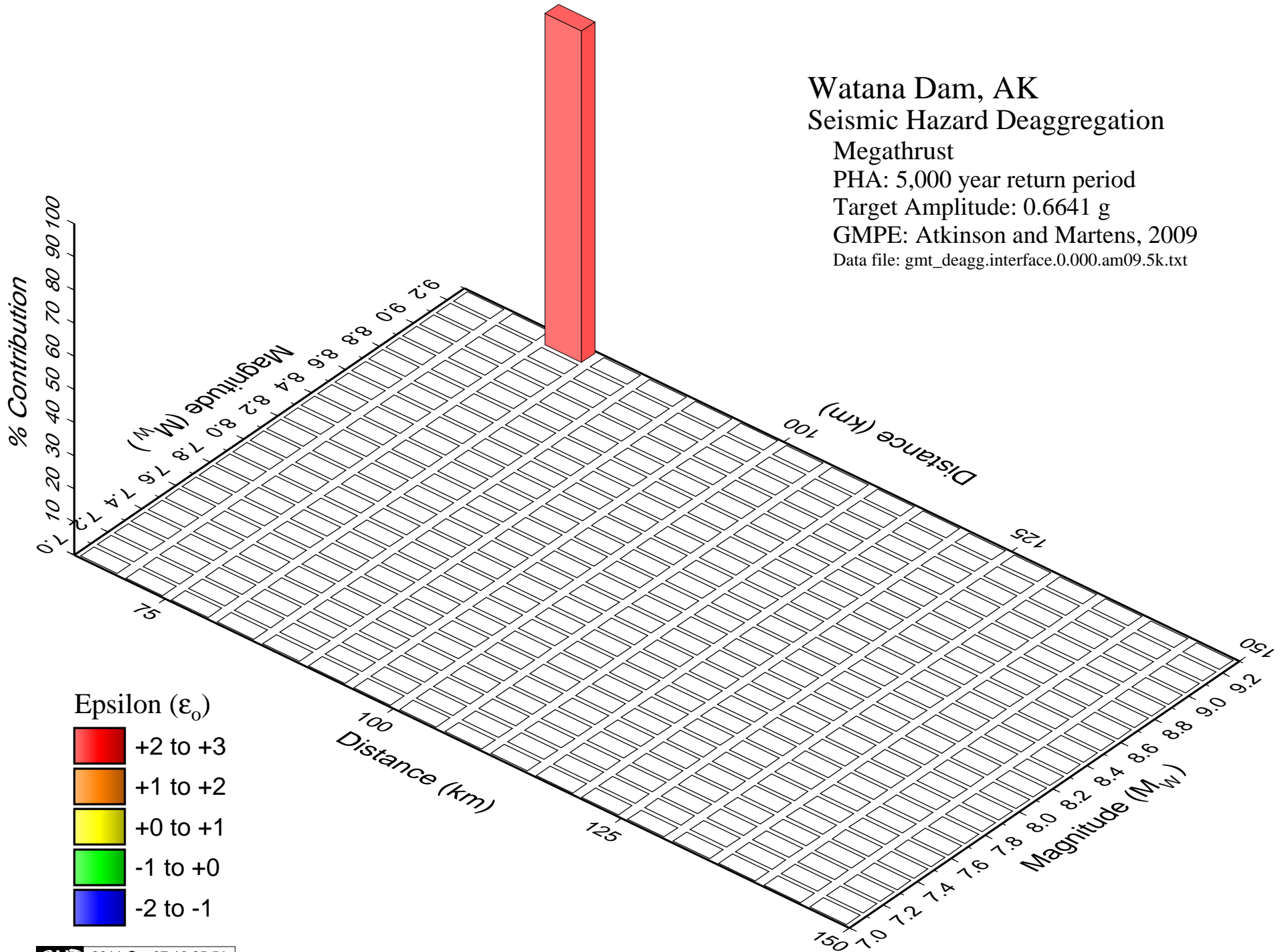
Megathrust

PHA: 5,000 year return period

Target Amplitude: 0.6641 g

GMPE: Atkinson and Martens, 2009

Data file: gmt_deagg.interface.0.000.am09.5k.txt



Epsilon (ϵ_0)

- +2 to +3
- +1 to +2
- +0 to +1
- 1 to +0
- 2 to -1

Watana Dam, AK Seismic Hazard Deaggregation

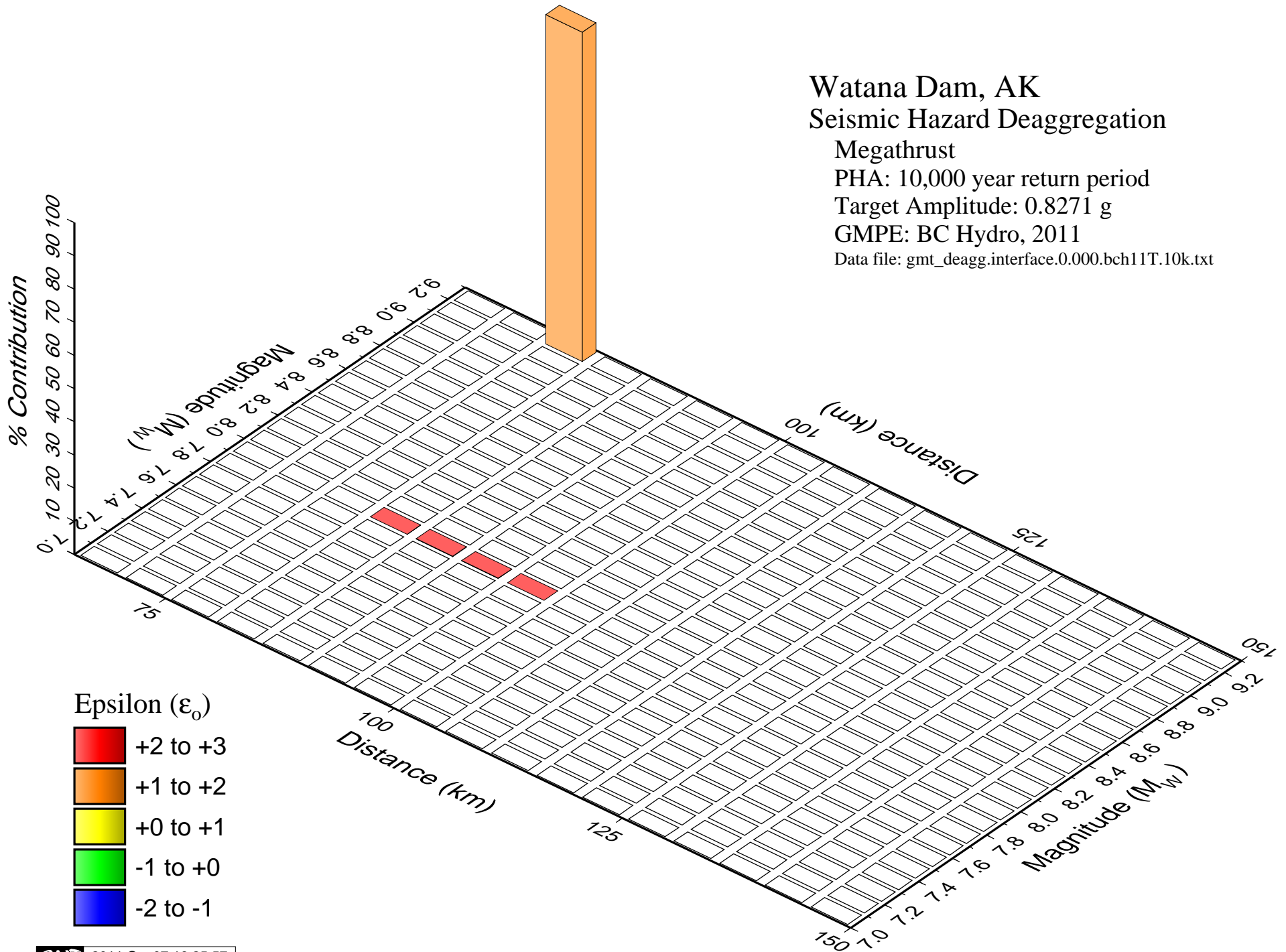
Megathrust

PHA: 10,000 year return period

Target Amplitude: 0.8271 g

GMPE: BC Hydro, 2011

Data file: gmt_deagg.interface.0.000.bch11T.10k.txt



Watana Dam, AK Seismic Hazard Deaggregation

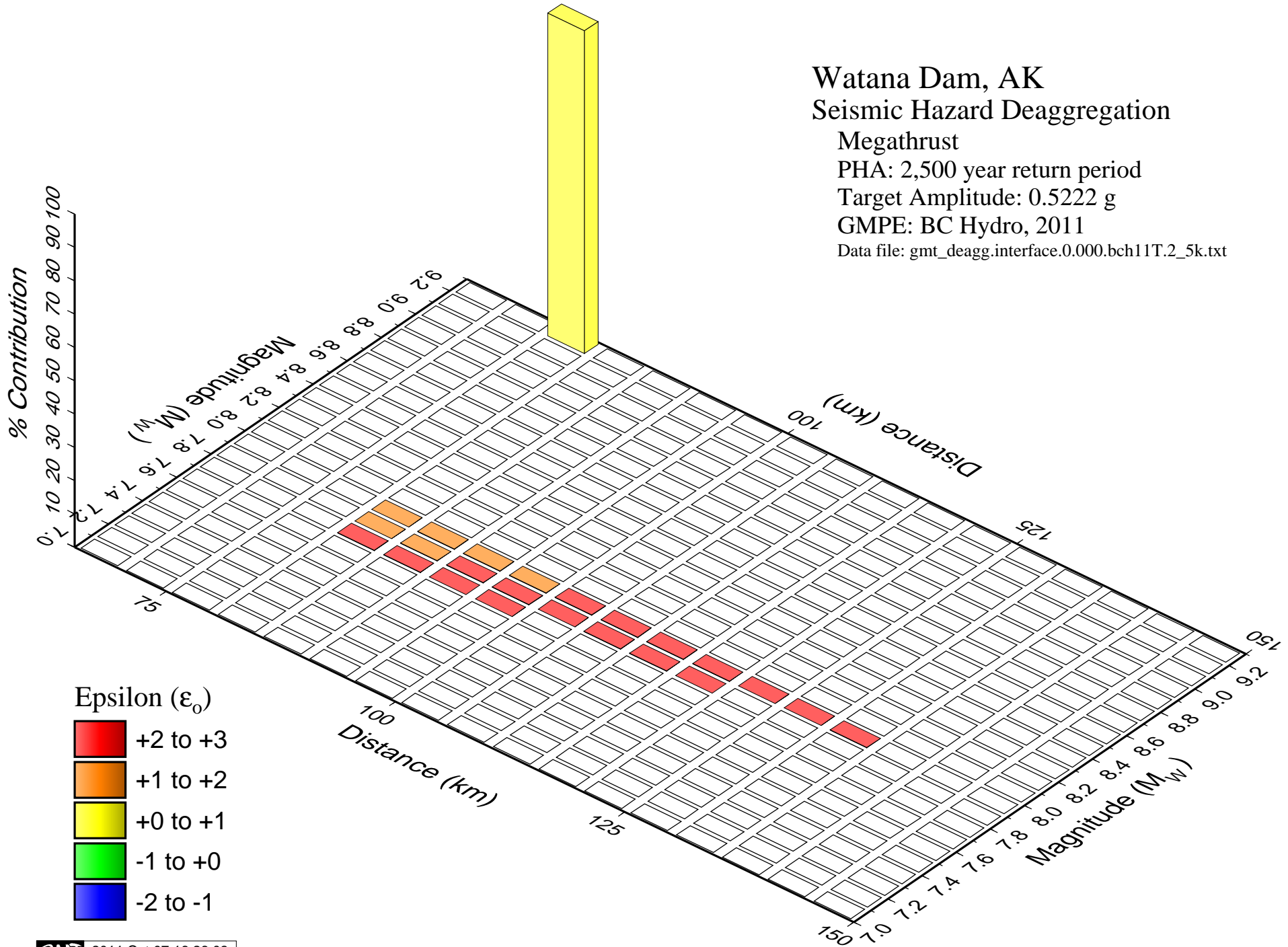
Megathrust

PHA: 2,500 year return period

Target Amplitude: 0.5222 g

GMPE: BC Hydro, 2011

Data file: gmt_deagg.interface.0.000.bch11T.2_5k.txt



Watana Dam, AK Seismic Hazard Deaggregation

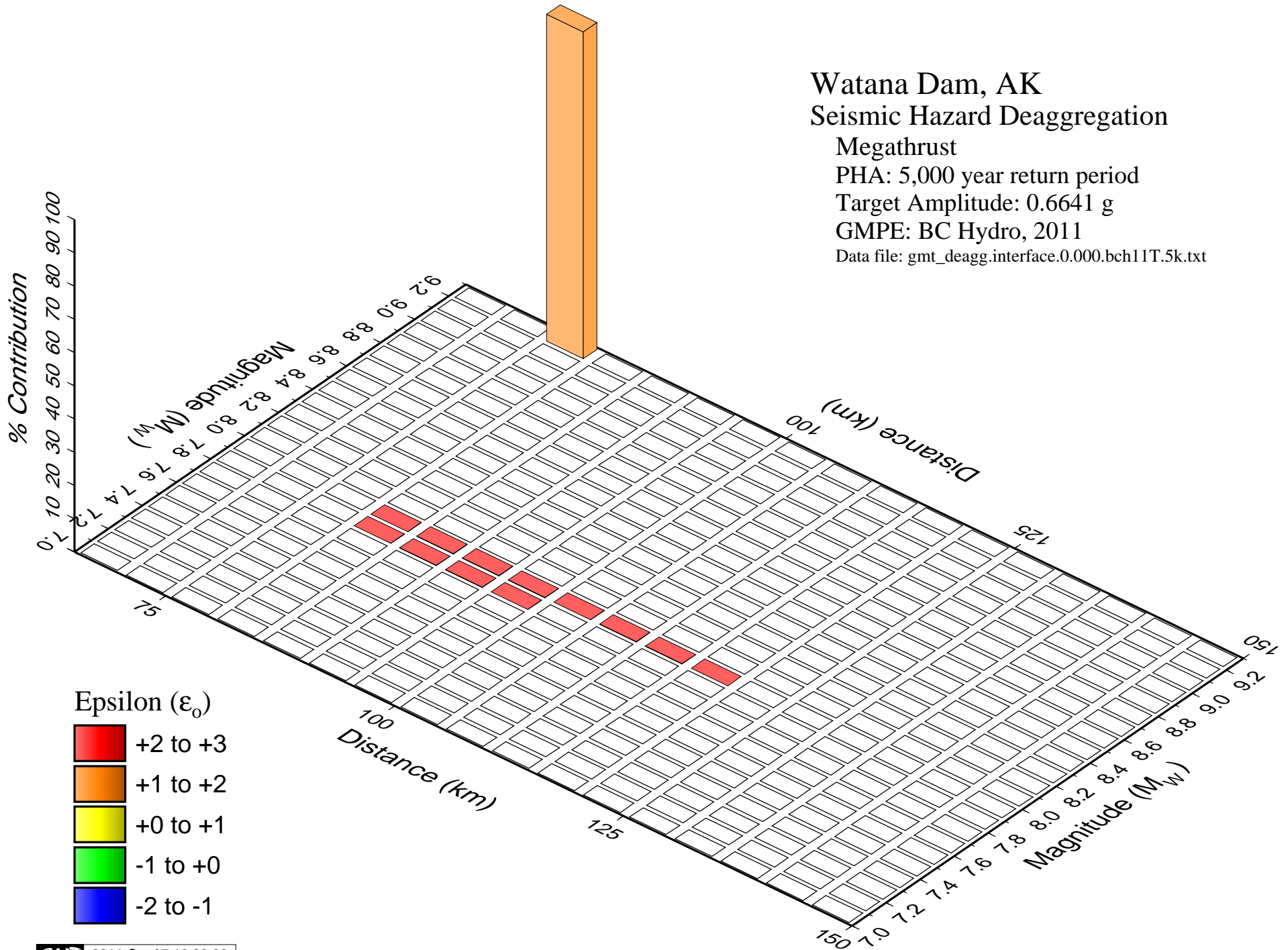
Megathrust

PHA: 5,000 year return period

Target Amplitude: 0.6641 g

GMPE: BC Hydro, 2011

Data file: gmt_deagg.interface.0.000.bch11T.5k.txt



Watana Dam, AK Seismic Hazard Deaggregation

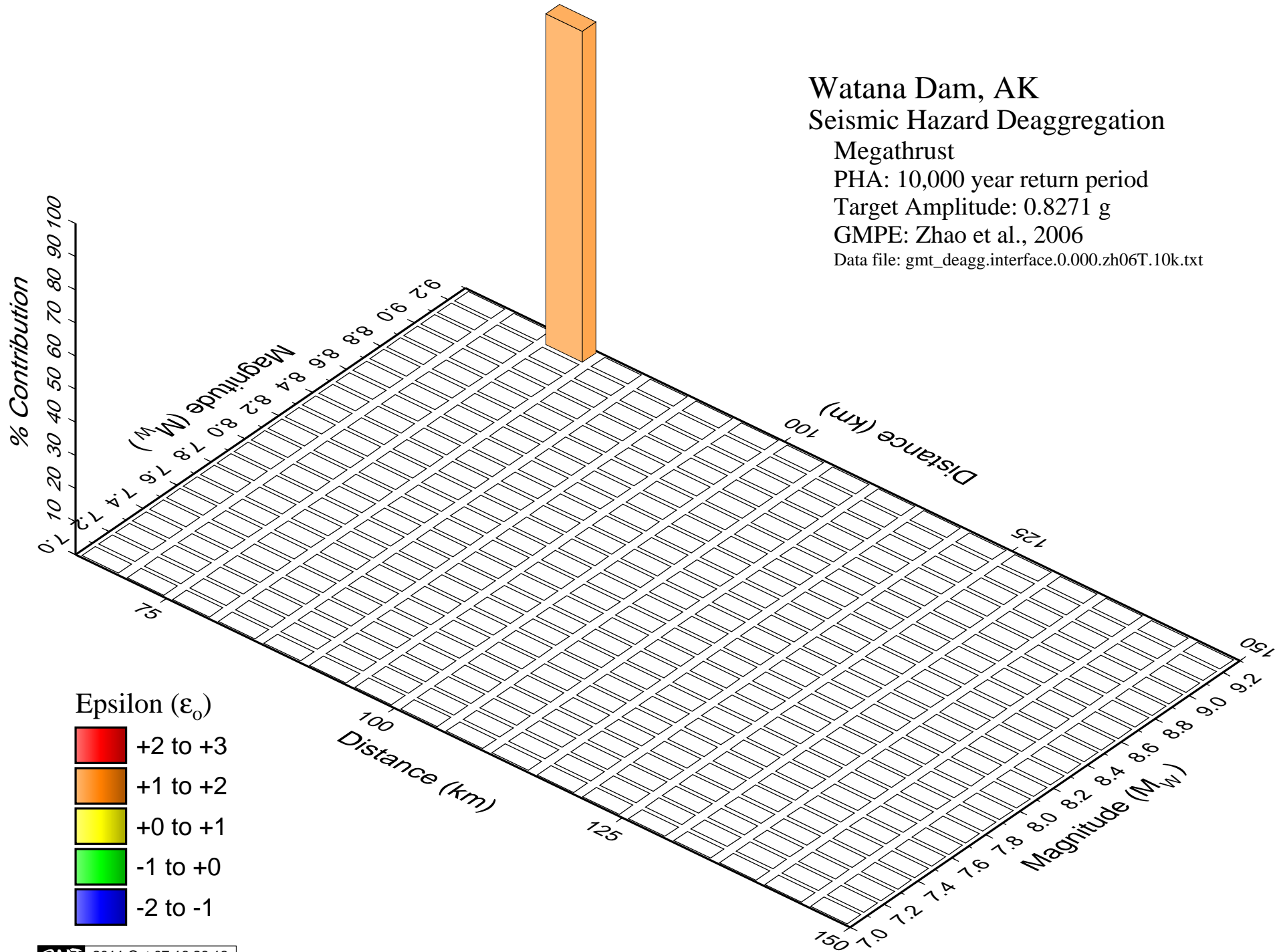
Megathrust

PHA: 10,000 year return period

Target Amplitude: 0.8271 g

GMPE: Zhao et al., 2006

Data file: gmt_deagg.interface.0.000.zh06T.10k.txt



Epsilon (ϵ_0)

- +2 to +3
- +1 to +2
- +0 to +1
- 1 to +0
- 2 to -1

Watana Dam, AK Seismic Hazard Deaggregation

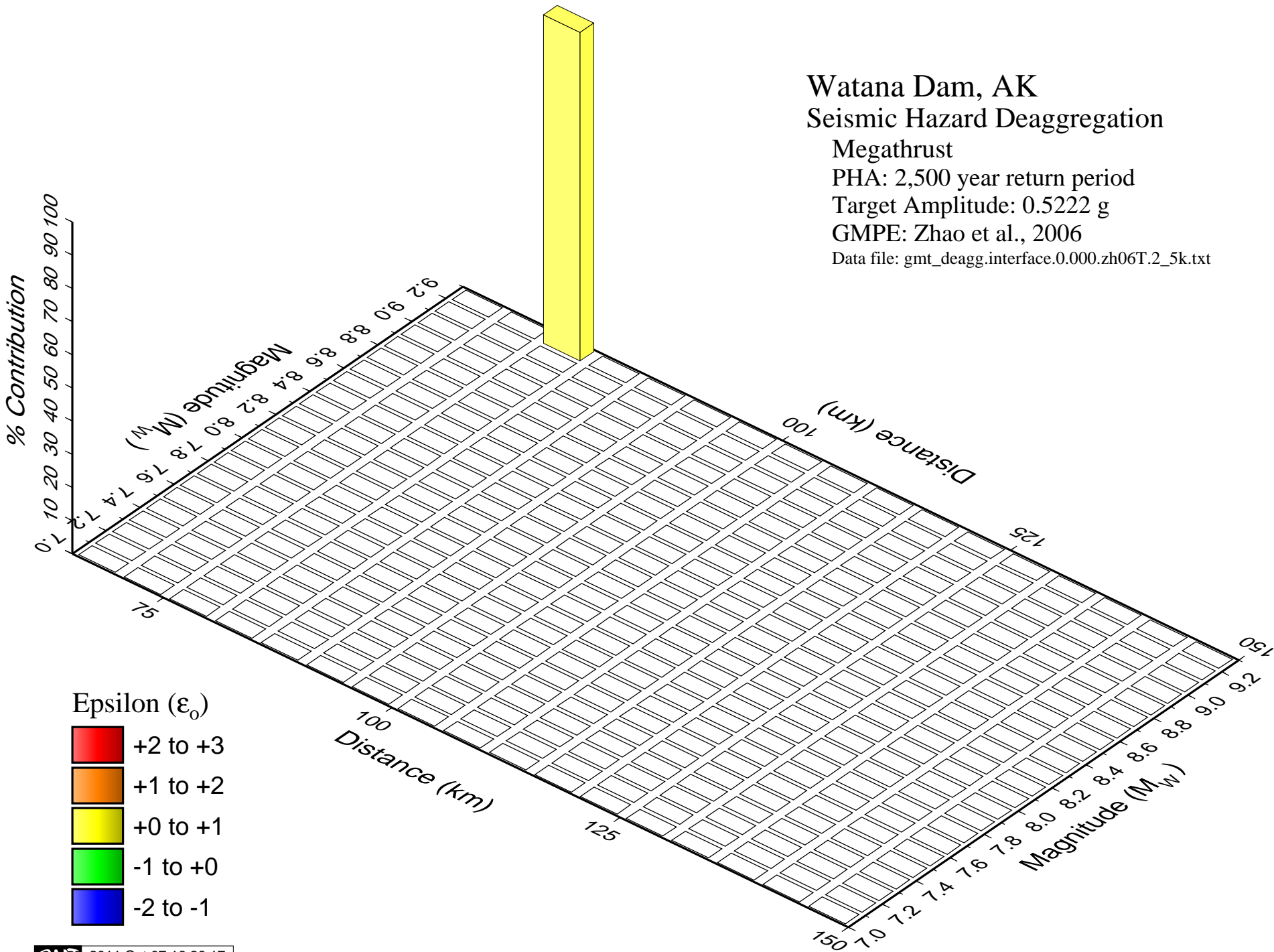
Megathrust

PHA: 2,500 year return period

Target Amplitude: 0.5222 g

GMPE: Zhao et al., 2006

Data file: gmt_deagg.interface.0.000.zh06T.2_5k.txt



Watana Dam, AK Seismic Hazard Deaggregation

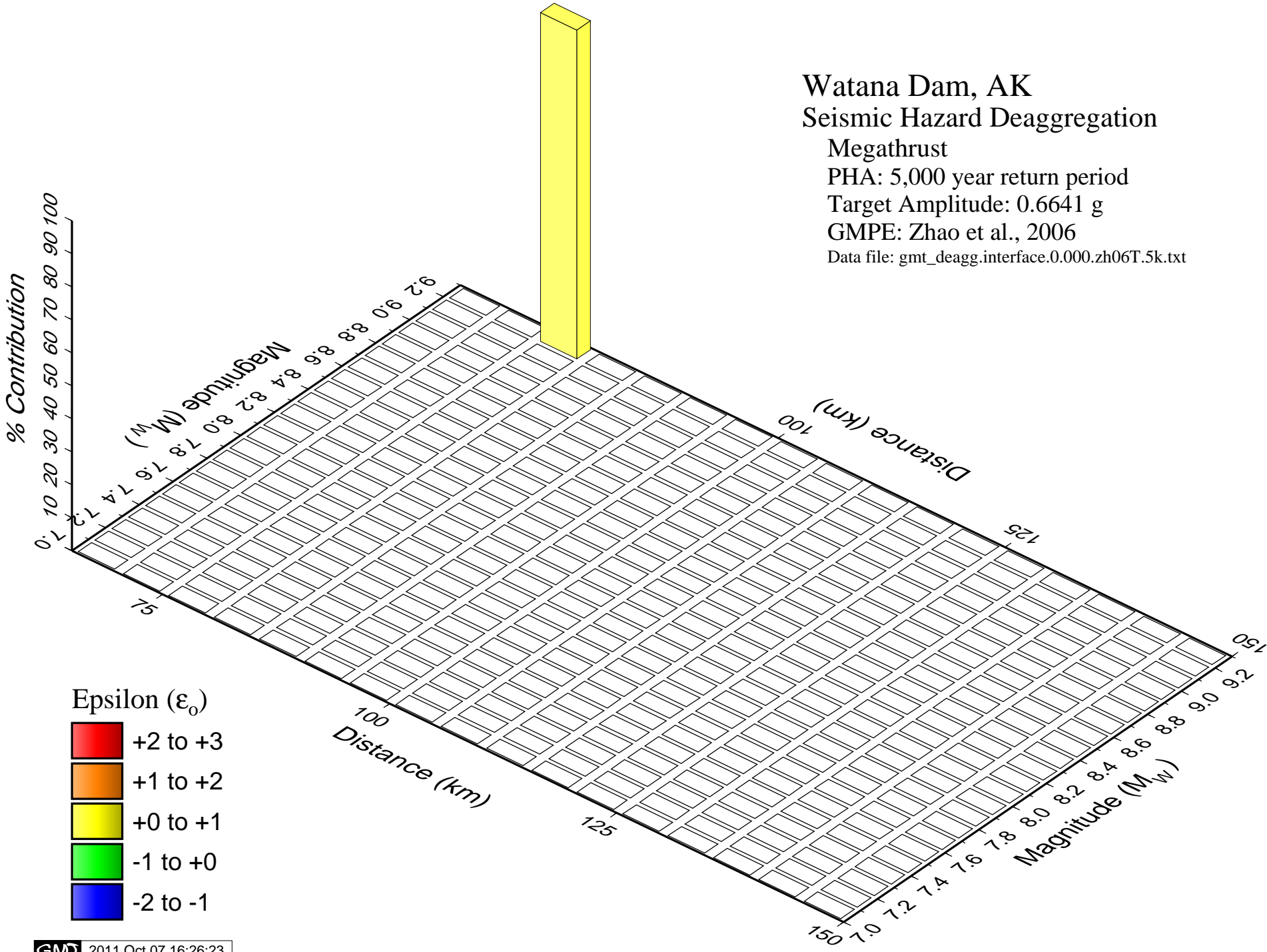
Megathrust

PHA: 5,000 year return period

Target Amplitude: 0.6641 g

GMPE: Zhao et al., 2006

Data file: gmt_deagg.interface.0.000.zh06T.5k.txt



Epsilon (ϵ_0)

- +2 to +3
- +1 to +2
- +0 to +1
- 1 to +0
- 2 to -1

Watana Dam, AK Seismic Hazard Deaggregation

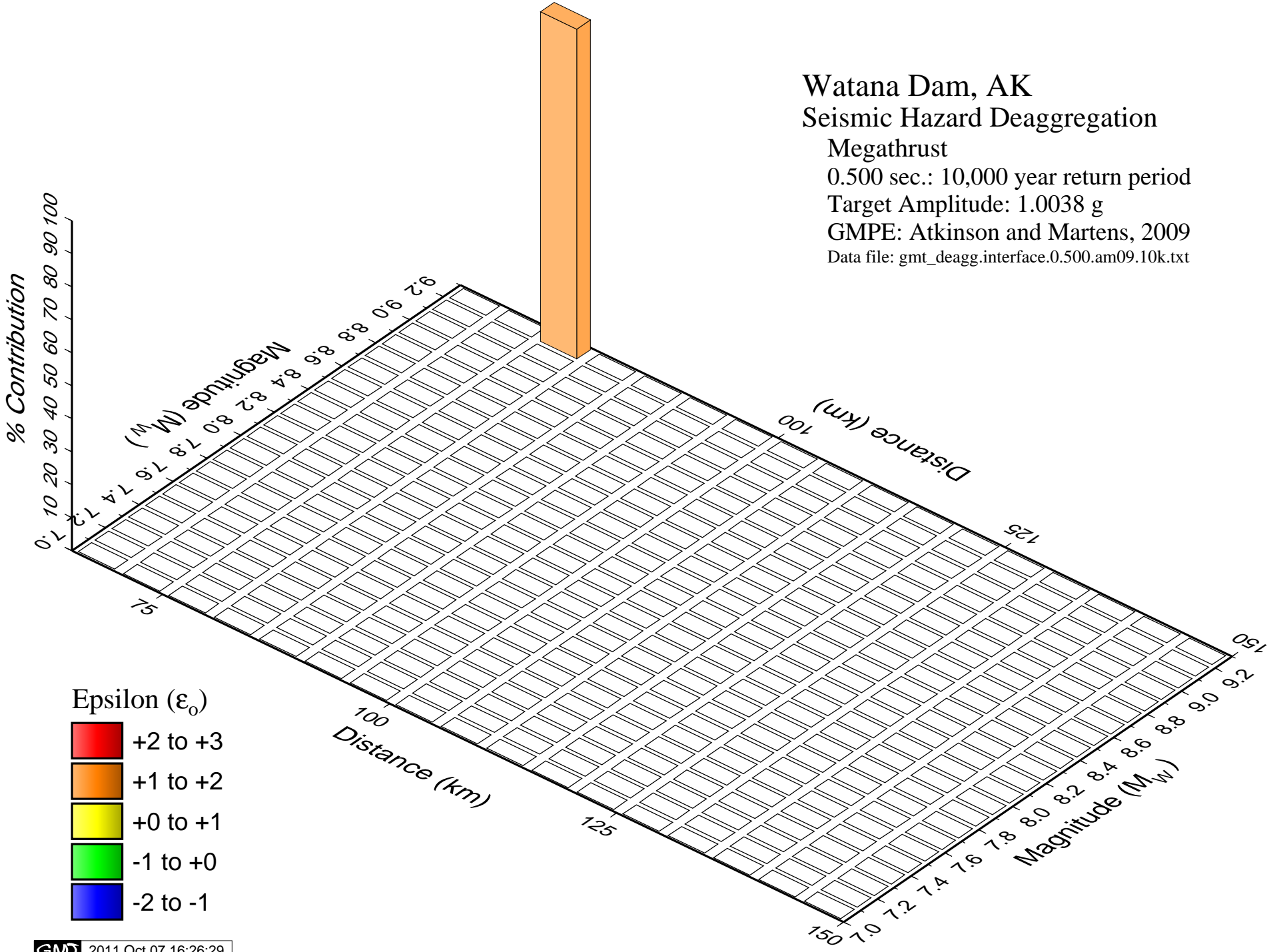
Megathrust

0.500 sec.: 10,000 year return period

Target Amplitude: 1.0038 g

GMPE: Atkinson and Martens, 2009

Data file: gmt_deagg.interface.0.500.am09.10k.txt



Epsilon (ϵ_0)

- +2 to +3
- +1 to +2
- +0 to +1
- 1 to +0
- 2 to -1

Watana Dam, AK
 Seismic Hazard Deaggregation

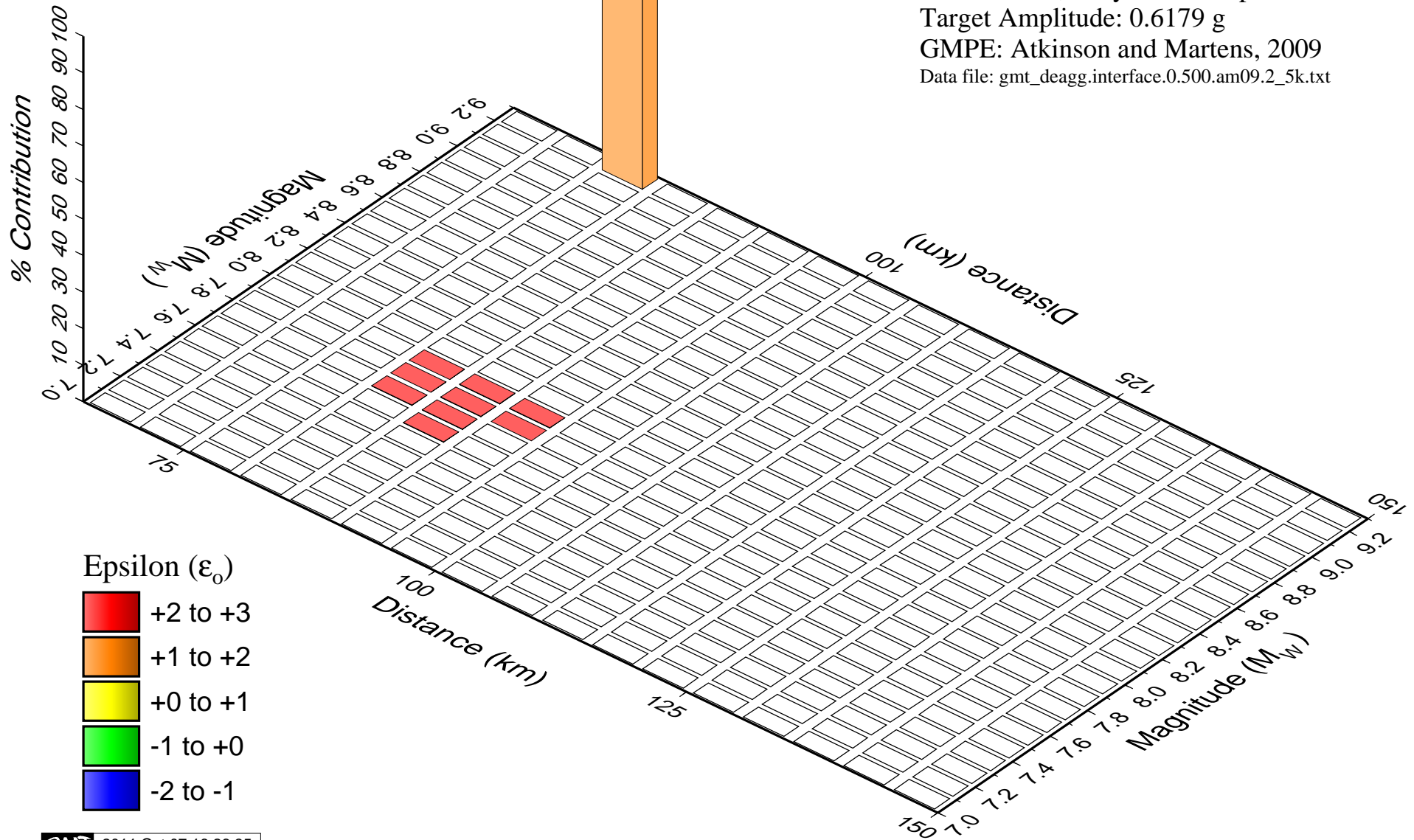
Megathrust

0.500 sec.: 2,500 year return period

Target Amplitude: 0.6179 g

GMPE: Atkinson and Martens, 2009

Data file: gmt_deagg.interface.0.500.am09.2_5k.txt



Watana Dam, AK

Seismic Hazard Deaggregation

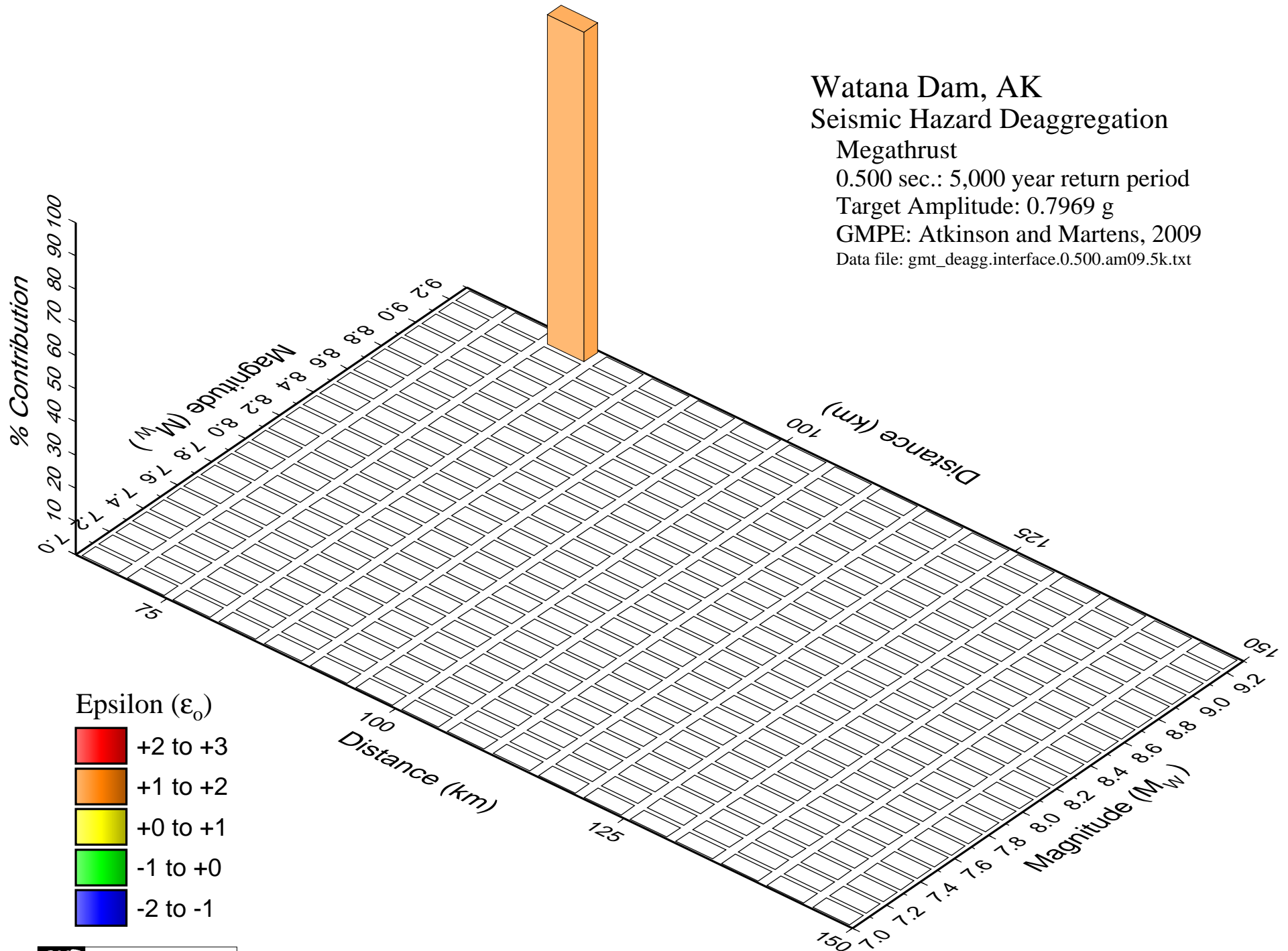
Megathrust

0.500 sec.: 5,000 year return period

Target Amplitude: 0.7969 g

GMPE: Atkinson and Martens, 2009

Data file: gmt_deagg.interface.0.500.am09.5k.txt



Epsilon (ϵ_0)

- +2 to +3
- +1 to +2
- +0 to +1
- 1 to +0
- 2 to -1

Watana Dam, AK Seismic Hazard Deaggregation

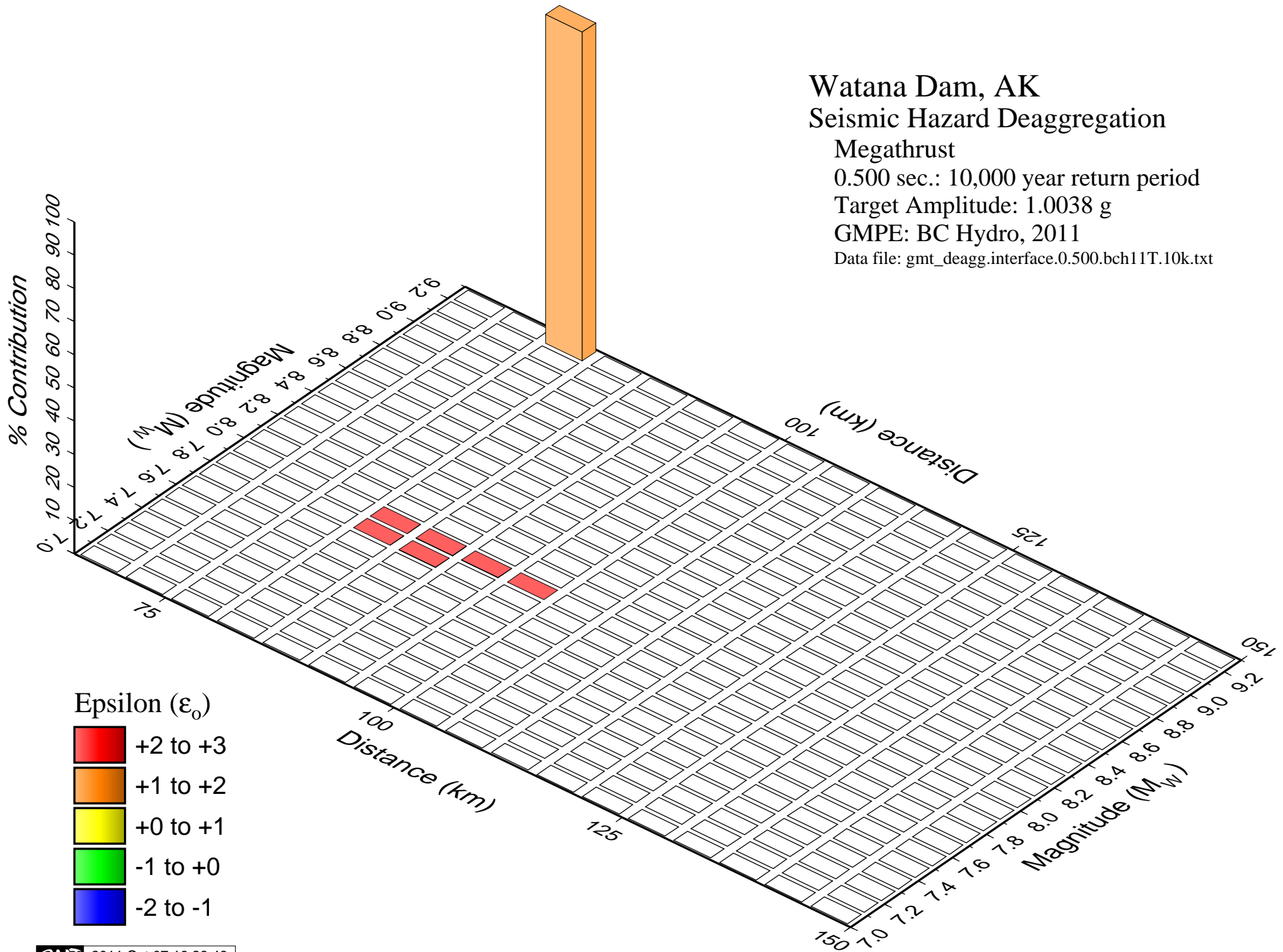
Megathrust

0.500 sec.: 10,000 year return period

Target Amplitude: 1.0038 g

GMPE: BC Hydro, 2011

Data file: gmt_deagg.interface.0.500.bch11T.10k.txt



Watana Dam, AK

Seismic Hazard Deaggregation

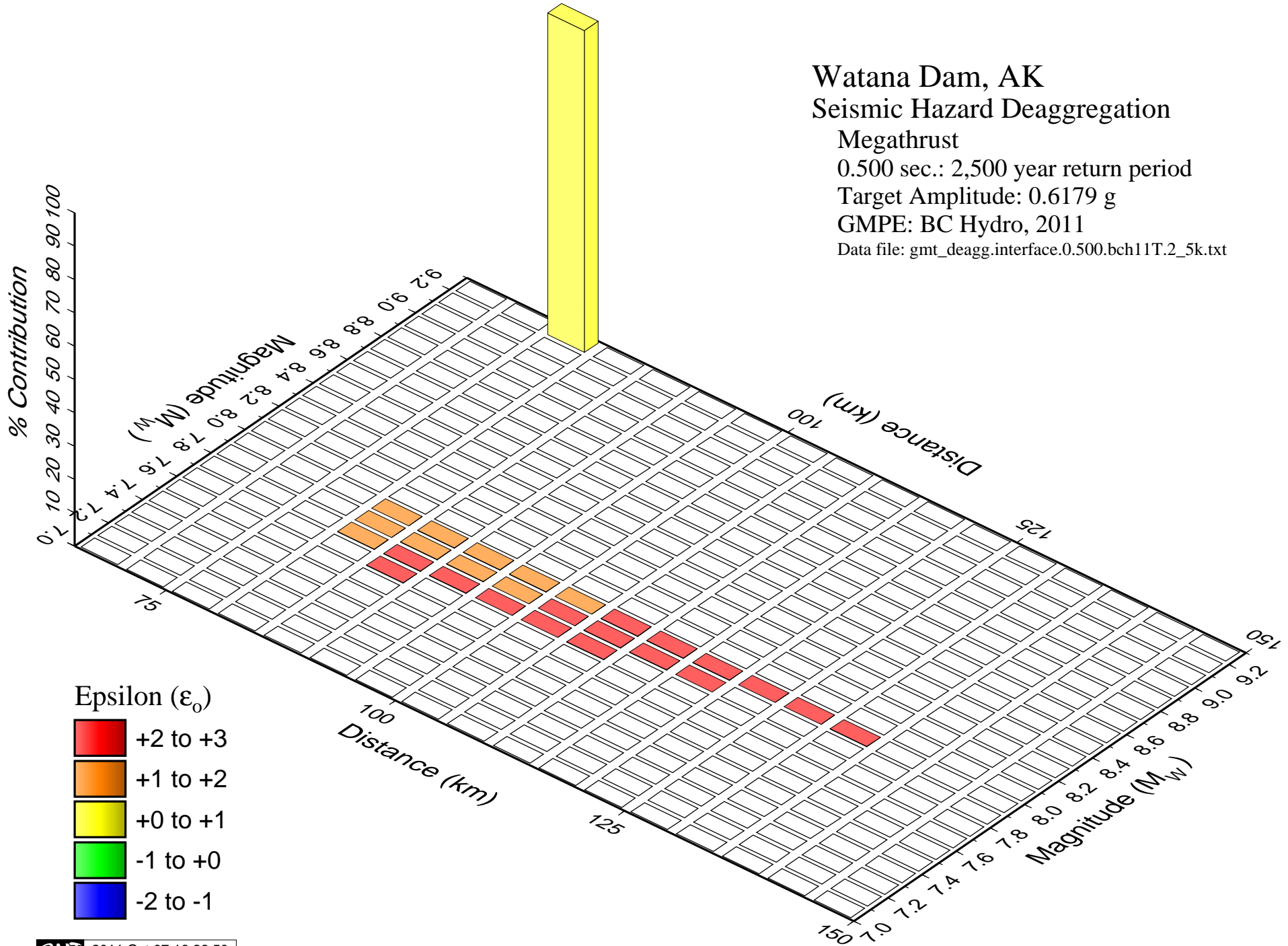
Megathrust

0.500 sec.: 2,500 year return period

Target Amplitude: 0.6179 g

GMPE: BC Hydro, 2011

Data file: gmt_deagg.interface.0.500.bch11T.2_5k.txt



Epsilon (ϵ_0)

- +2 to +3
- +1 to +2
- +0 to +1
- 1 to +0
- 2 to -1

Watana Dam, AK Seismic Hazard Deaggregation

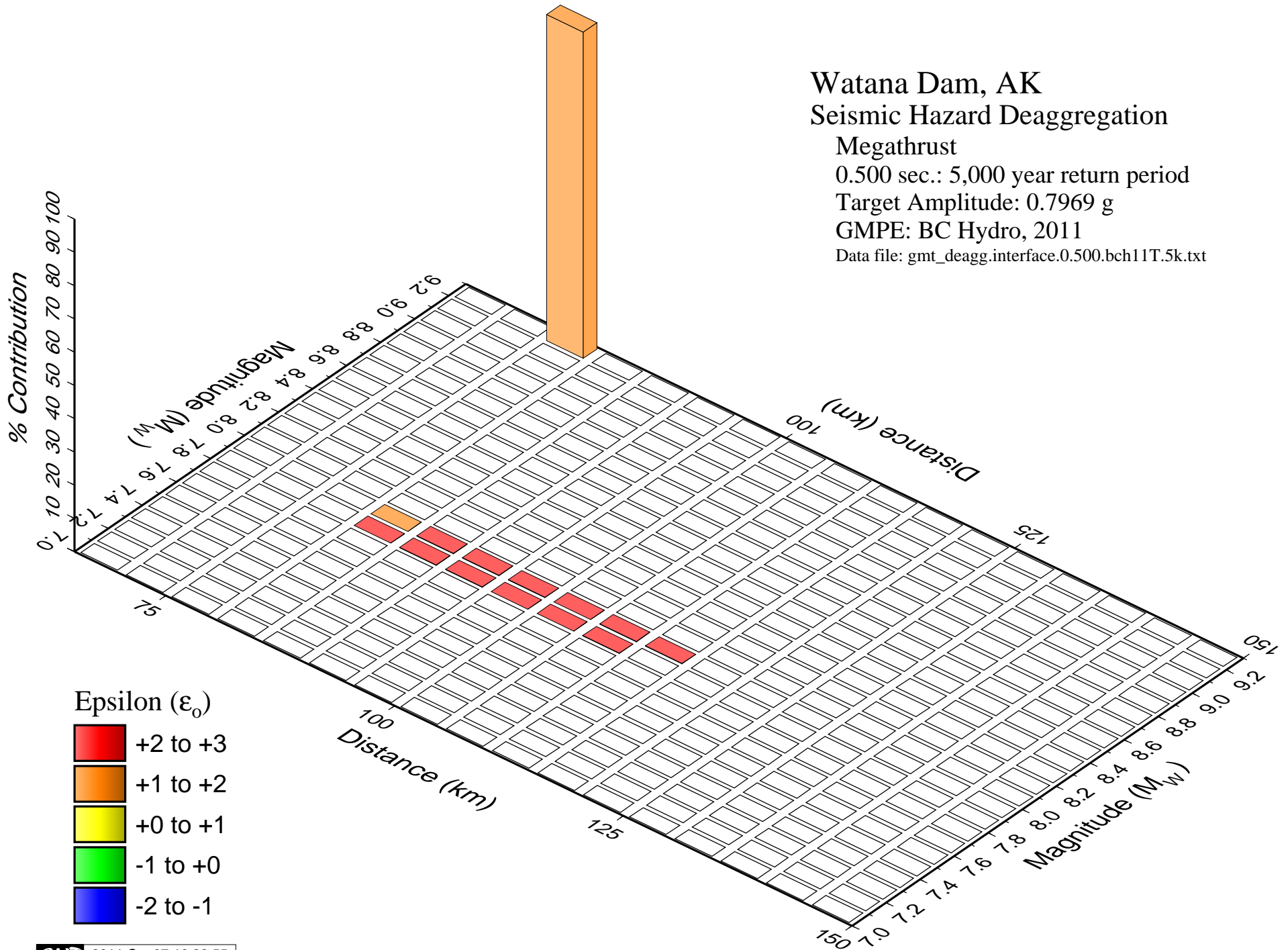
Megathrust

0.500 sec.: 5,000 year return period

Target Amplitude: 0.7969 g

GMPE: BC Hydro, 2011

Data file: gmt_deagg.interface.0.500.bch11T.5k.txt



Watana Dam, AK Seismic Hazard Deaggregation

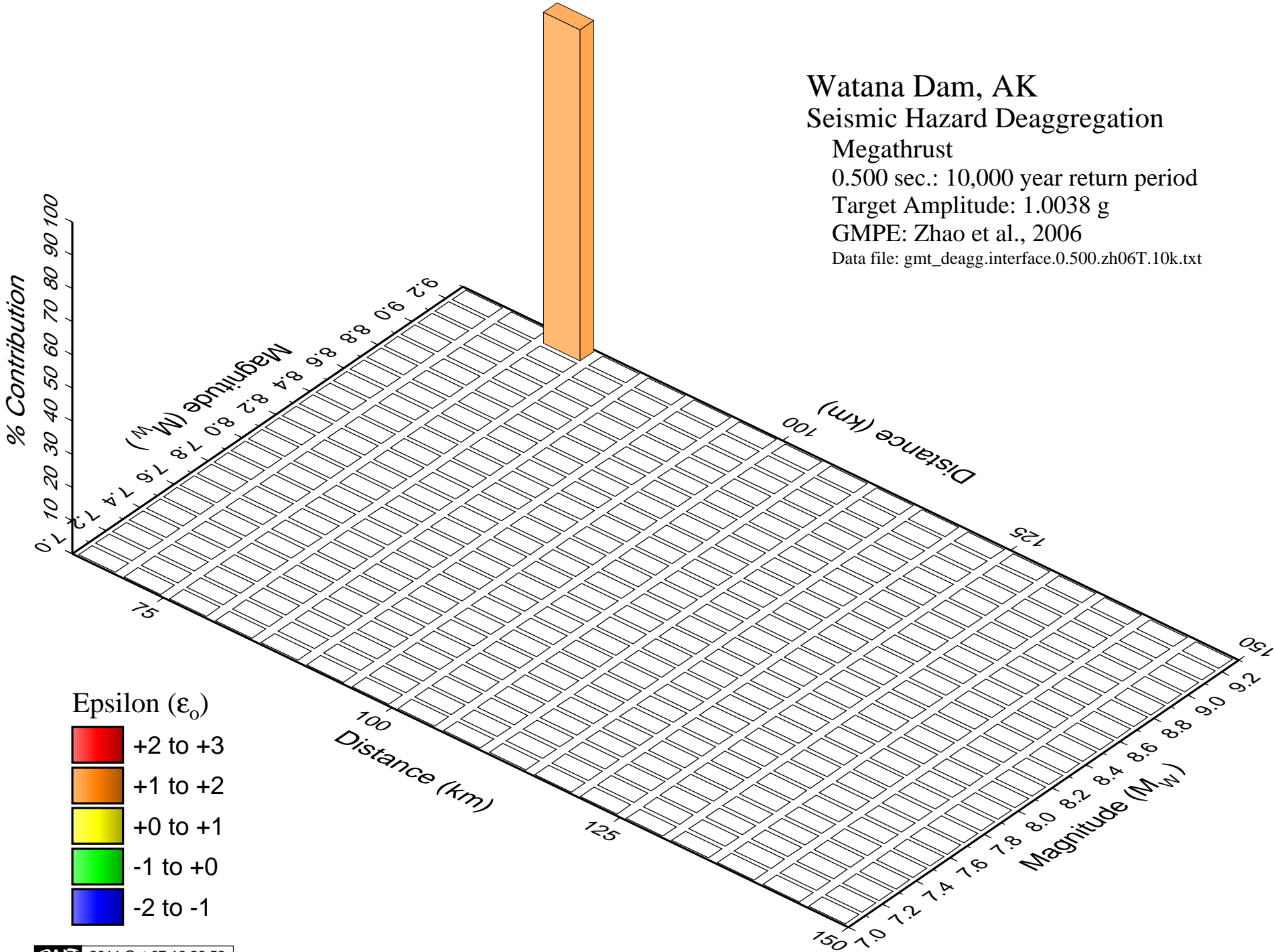
Megathrust

0.500 sec.: 10,000 year return period

Target Amplitude: 1.0038 g

GMPE: Zhao et al., 2006

Data file: gmt_deagg.interface.0.500.zh06T.10k.txt



Epsilon (ϵ_0)

- +2 to +3
- +1 to +2
- +0 to +1
- 1 to +0
- 2 to -1

Watana Dam, AK

Seismic Hazard Deaggregation

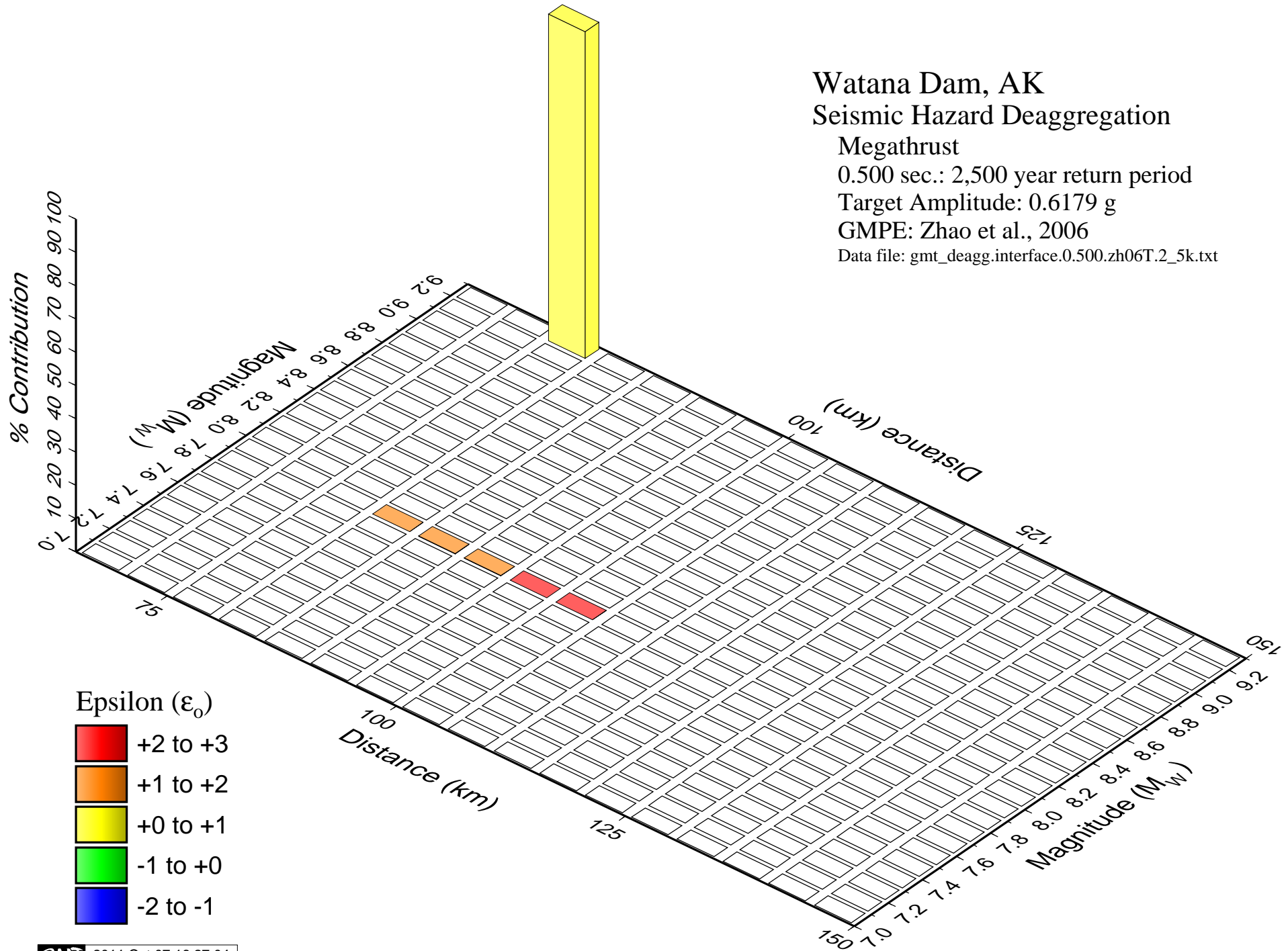
Megathrust

0.500 sec.: 2,500 year return period

Target Amplitude: 0.6179 g

GMPE: Zhao et al., 2006

Data file: gmt_deagg.interface.0.500.zh06T.2_5k.txt



Watana Dam, AK Seismic Hazard Deaggregation

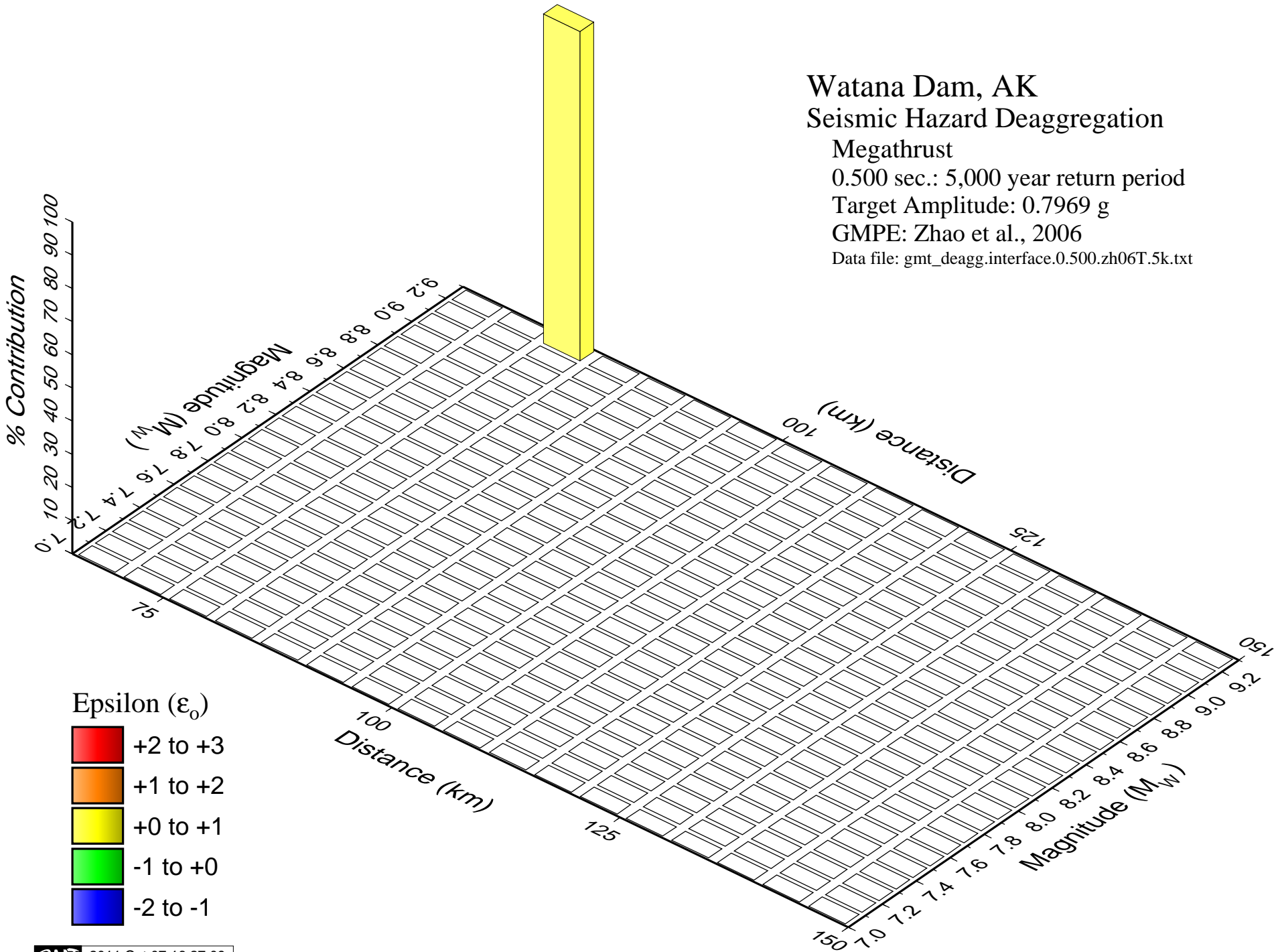
Megathrust

0.500 sec.: 5,000 year return period

Target Amplitude: 0.7969 g

GMPE: Zhao et al., 2006

Data file: gmt_deagg.interface.0.500.zh06T.5k.txt



Epsilon (ϵ_0)

- +2 to +3
- +1 to +2
- +0 to +1
- 1 to +0
- 2 to -1

Watana Dam, AK

Seismic Hazard Deaggregation

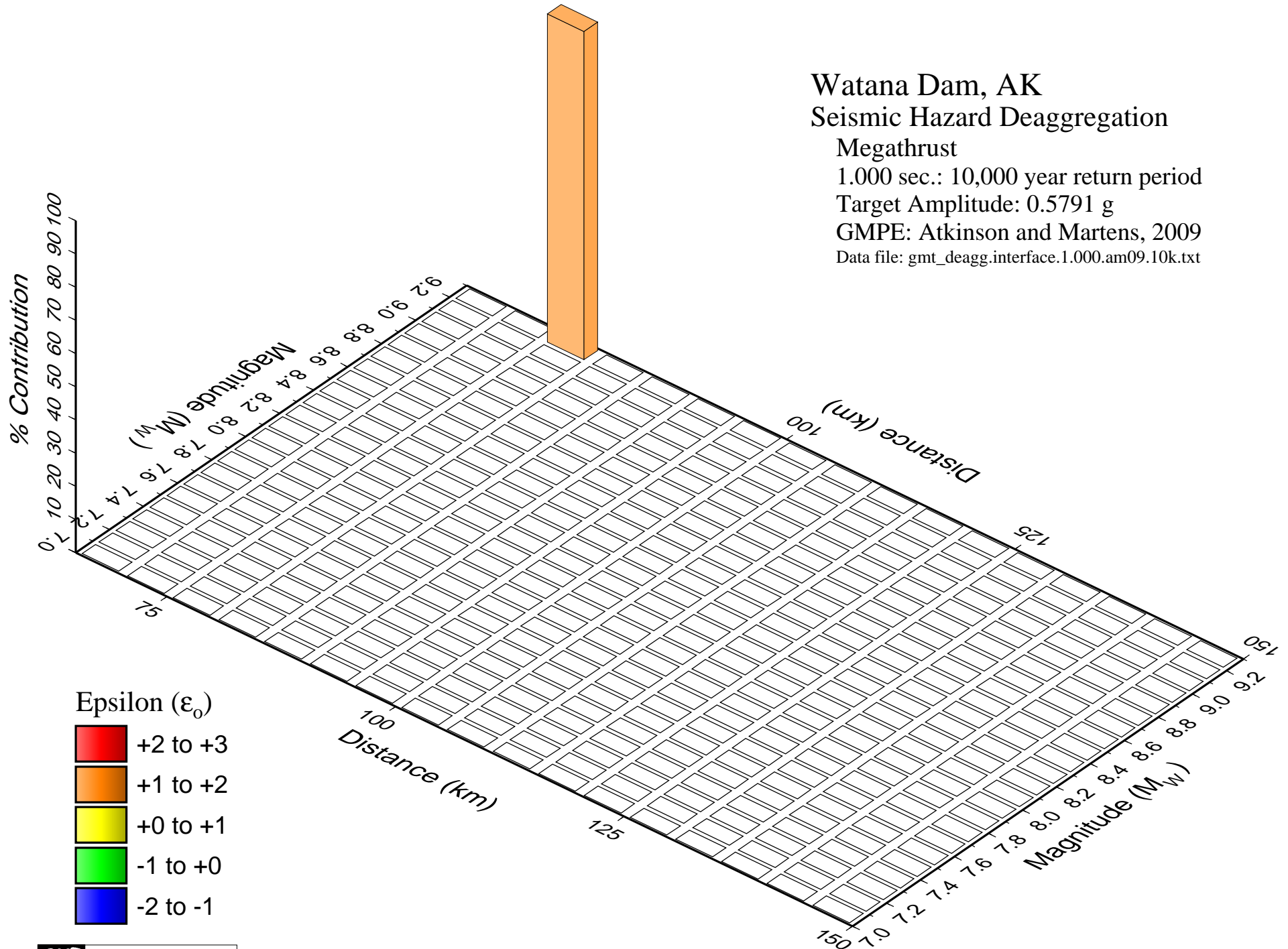
Megathrust

1.000 sec.: 10,000 year return period

Target Amplitude: 0.5791 g

GMPE: Atkinson and Martens, 2009

Data file: gmt_deagg.interface.1.000.am09.10k.txt



Epsilon (ϵ_0)

- +2 to +3
- +1 to +2
- +0 to +1
- 1 to +0
- 2 to -1

Watana Dam, AK Seismic Hazard Deaggregation

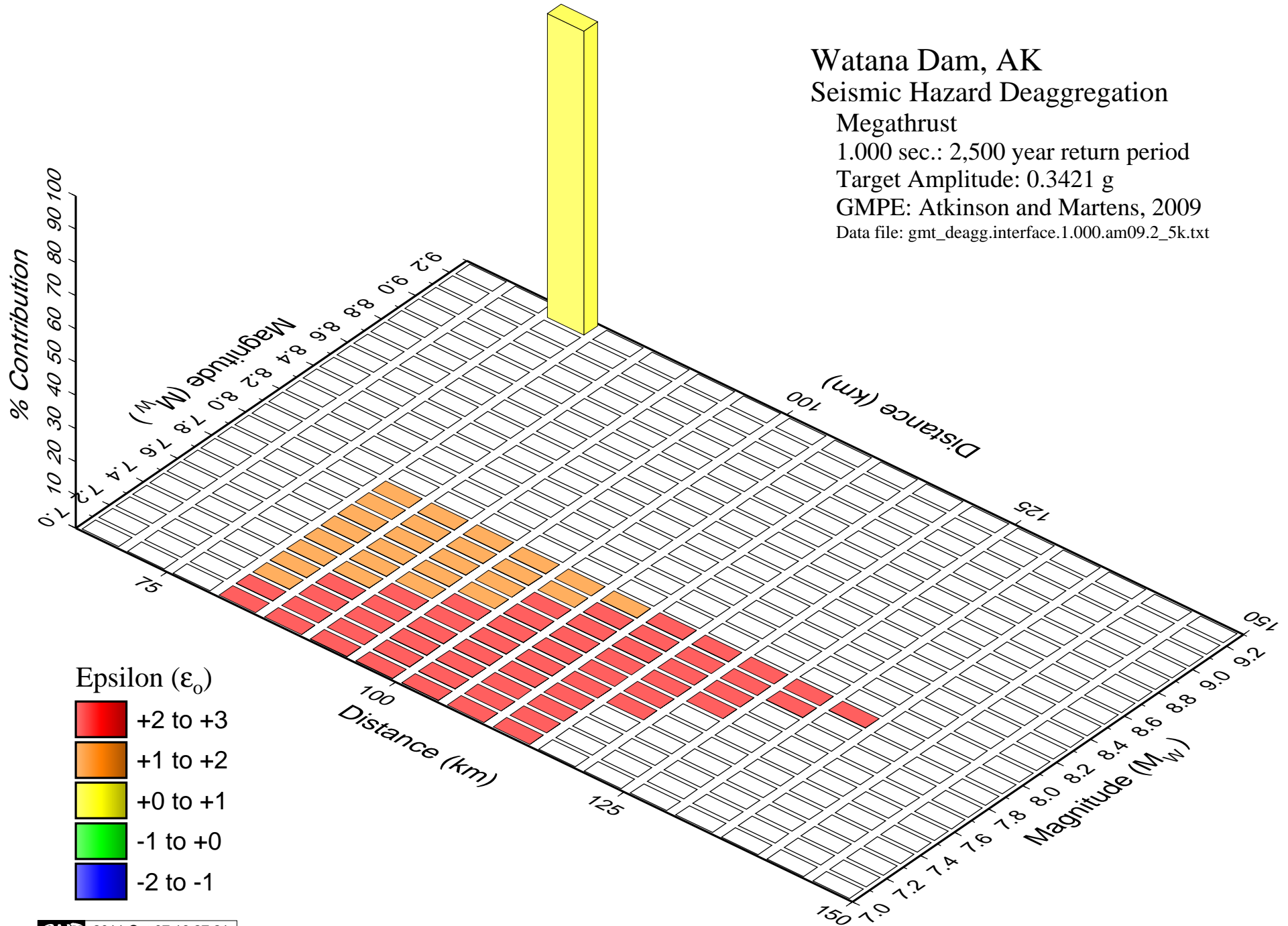
Megathrust

1.000 sec.: 2,500 year return period

Target Amplitude: 0.3421 g

GMPE: Atkinson and Martens, 2009

Data file: gmt_deagg.interface.1.000.am09.2_5k.txt



Watana Dam, AK Seismic Hazard Deaggregation

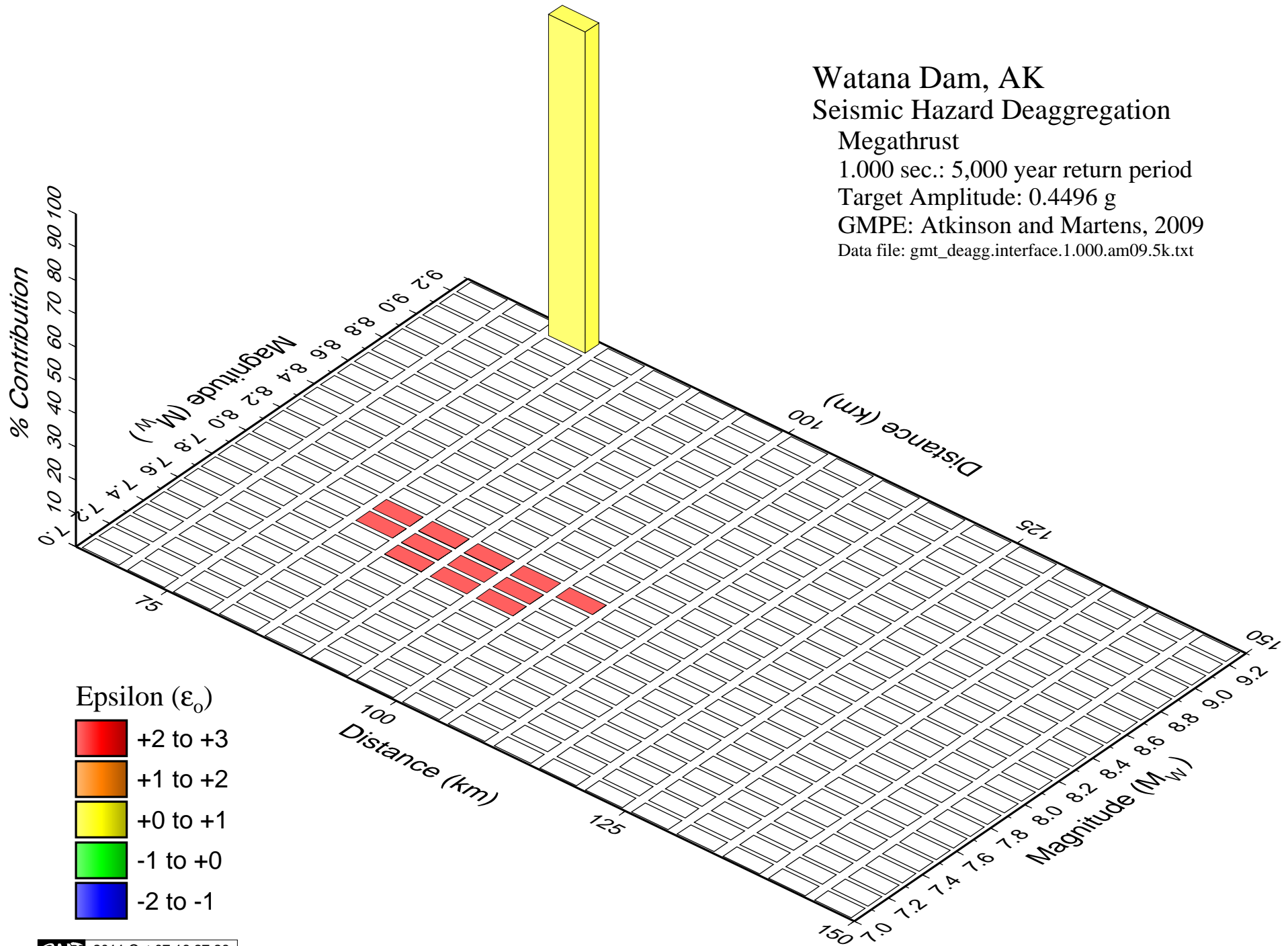
Megathrust

1.000 sec.: 5,000 year return period

Target Amplitude: 0.4496 g

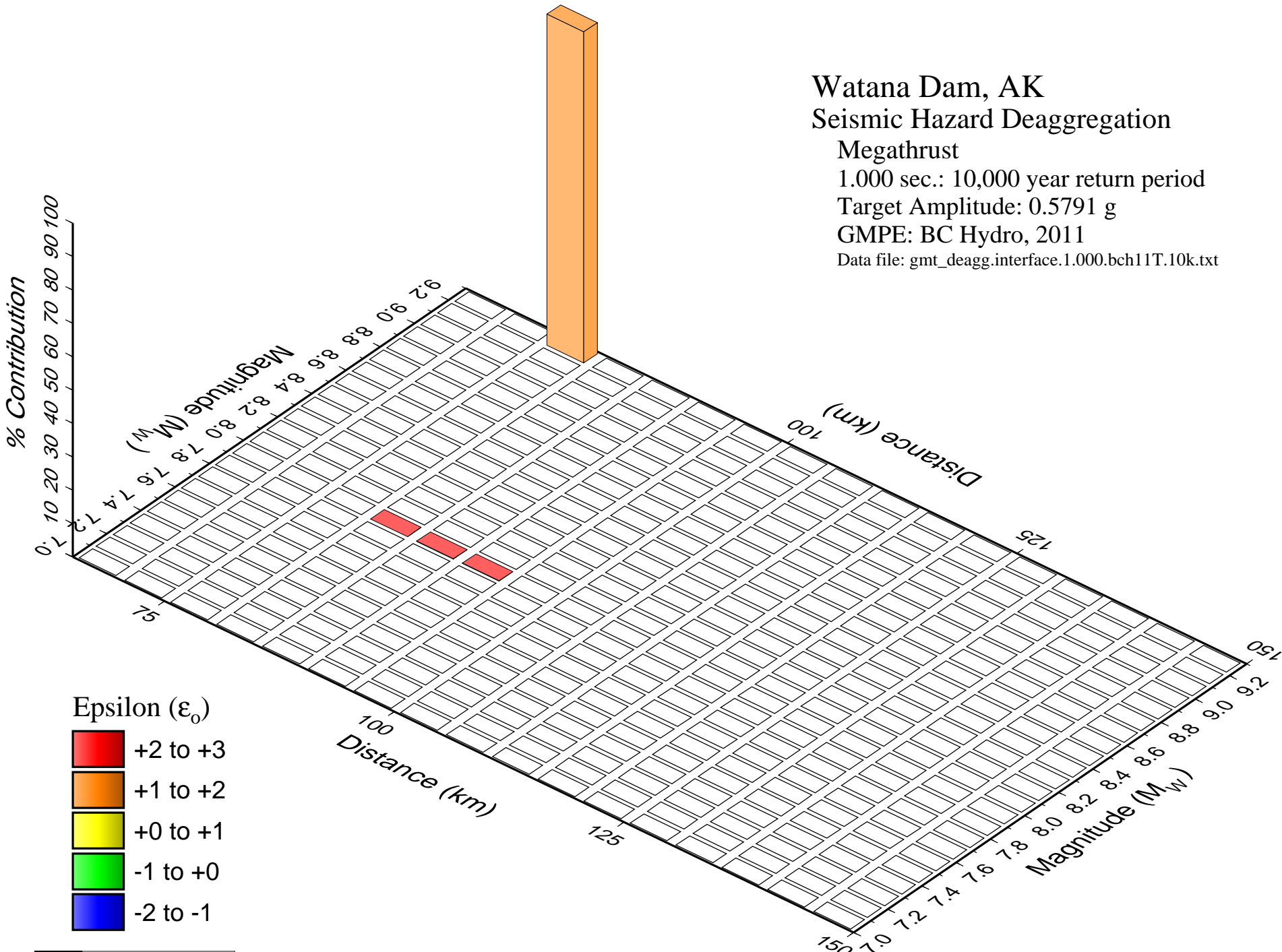
GMPE: Atkinson and Martens, 2009

Data file: gmt_deagg.interface.1.000.am09.5k.txt



Watana Dam, AK Seismic Hazard Deaggregation

Megathrust
 1.000 sec.: 10,000 year return period
 Target Amplitude: 0.5791 g
 GMPE: BC Hydro, 2011
 Data file: gmt_deagg.interface.1.000.bch11T.10k.txt



Watana Dam, AK

Seismic Hazard Deaggregation

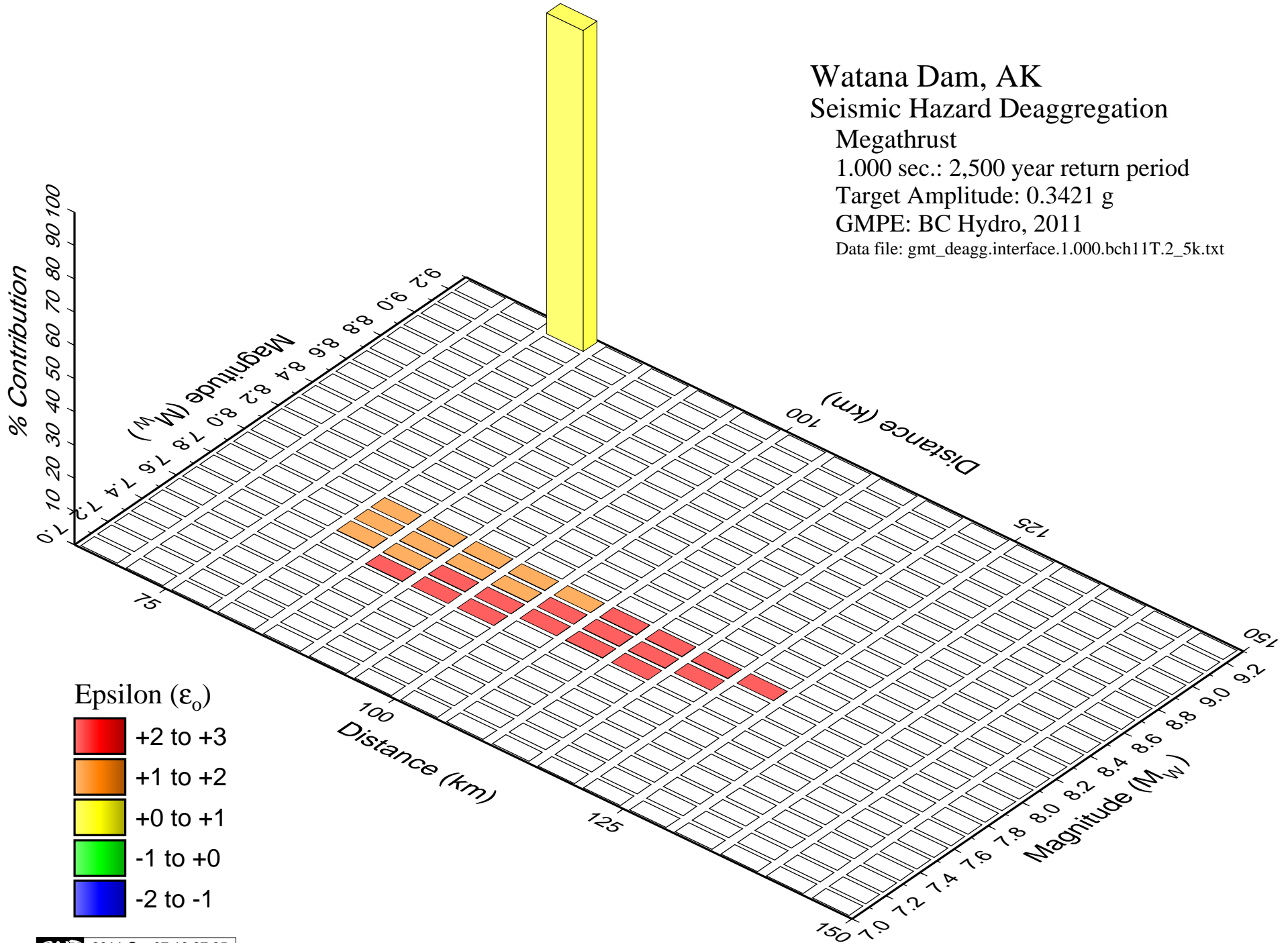
Megathrust

1.000 sec.: 2,500 year return period

Target Amplitude: 0.3421 g

GMPE: BC Hydro, 2011

Data file: gmt_deagg.interface.1.000.bch11T.2_5k.txt



Watana Dam, AK Seismic Hazard Deaggregation

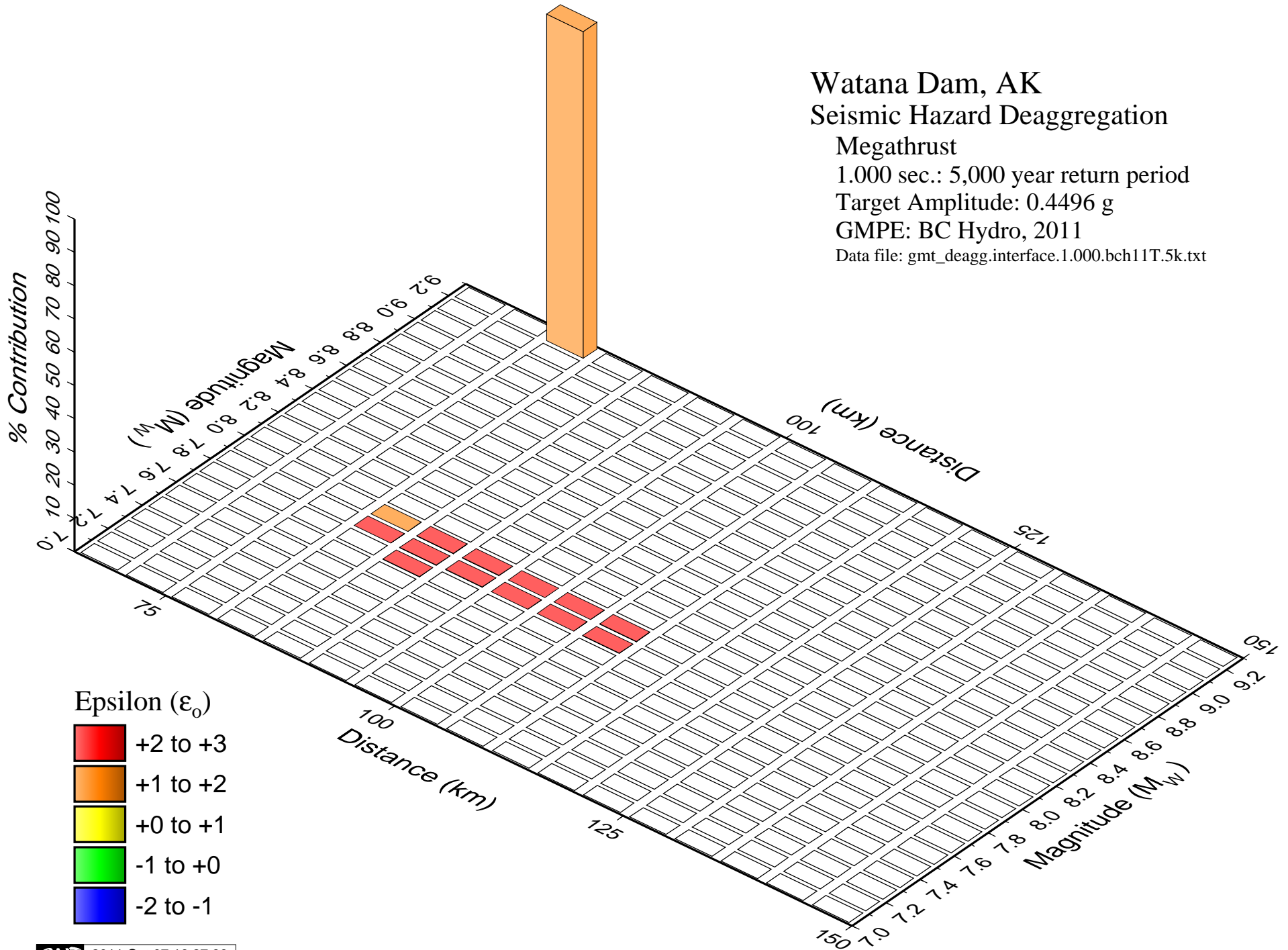
Megathrust

1.000 sec.: 5,000 year return period

Target Amplitude: 0.4496 g

GMPE: BC Hydro, 2011

Data file: gmt_deagg.interface.1.000.bch11T.5k.txt



Watana Dam, AK

Seismic Hazard Deaggregation

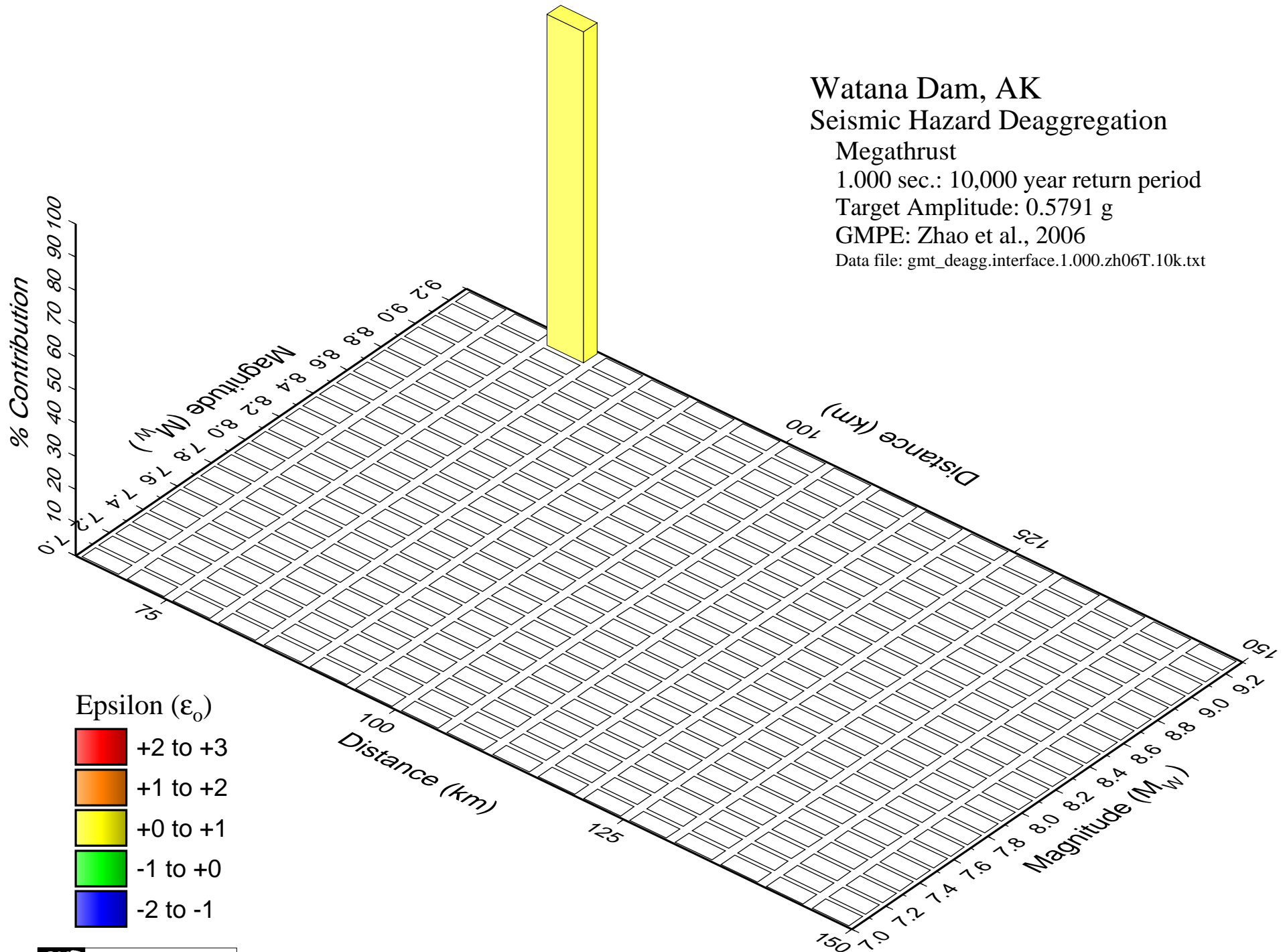
Megathrust

1.000 sec.: 10,000 year return period

Target Amplitude: 0.5791 g

GMPE: Zhao et al., 2006

Data file: gmt_deagg.interface.1.000.zh06T.10k.txt

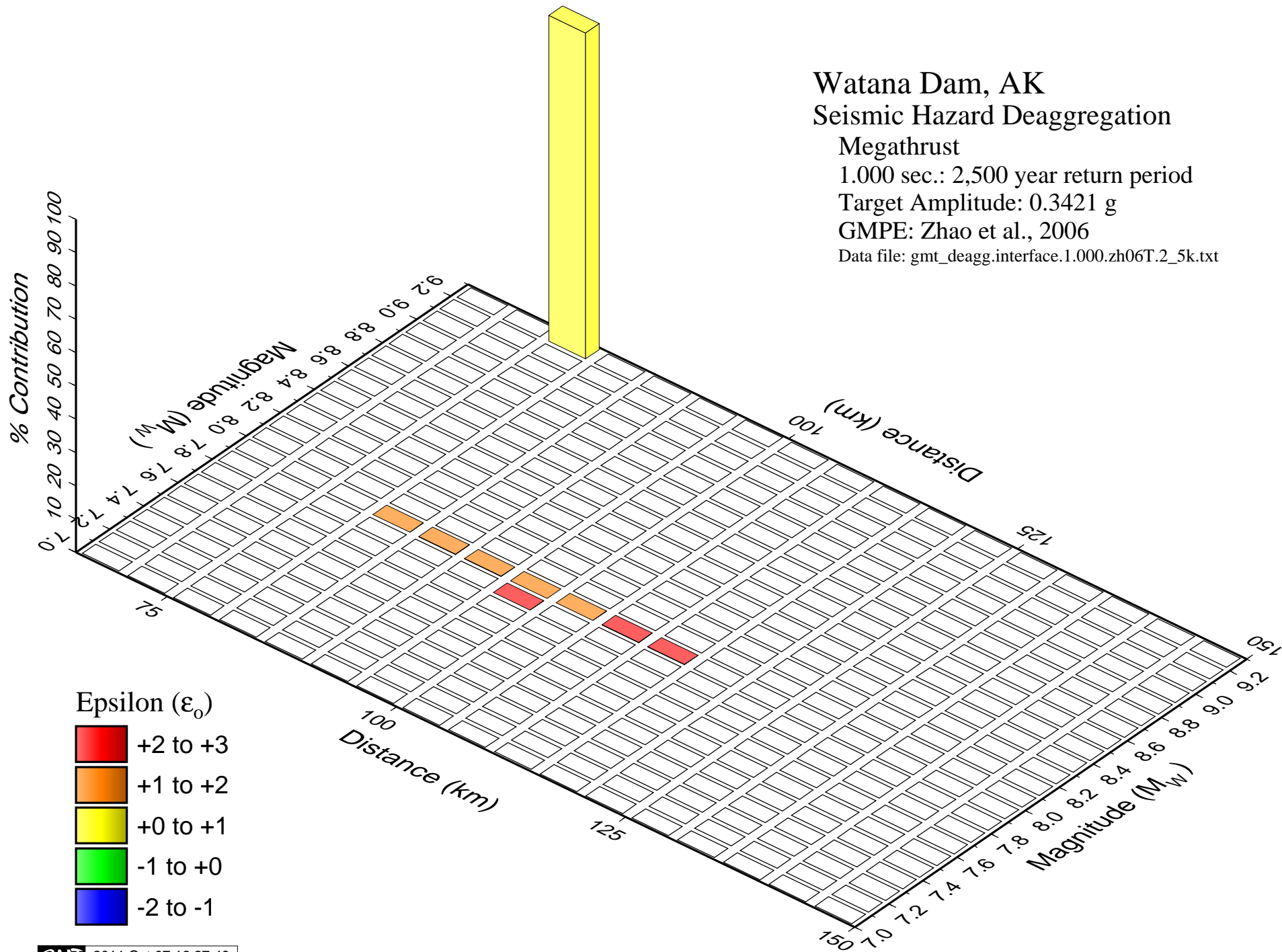


Epsilon (ϵ_0)

- +2 to +3
- +1 to +2
- +0 to +1
- 1 to +0
- 2 to -1

Watana Dam, AK
 Seismic Hazard Deaggregation

Megathrust
 1.000 sec.: 2,500 year return period
 Target Amplitude: 0.3421 g
 GMPE: Zhao et al., 2006
 Data file: gmt_deagg.interface.1.000.zh06T.2_5k.txt



Watana Dam, AK Seismic Hazard Deaggregation

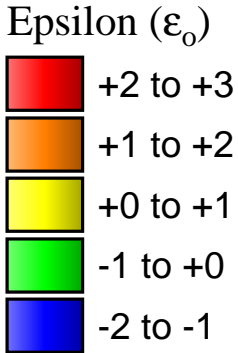
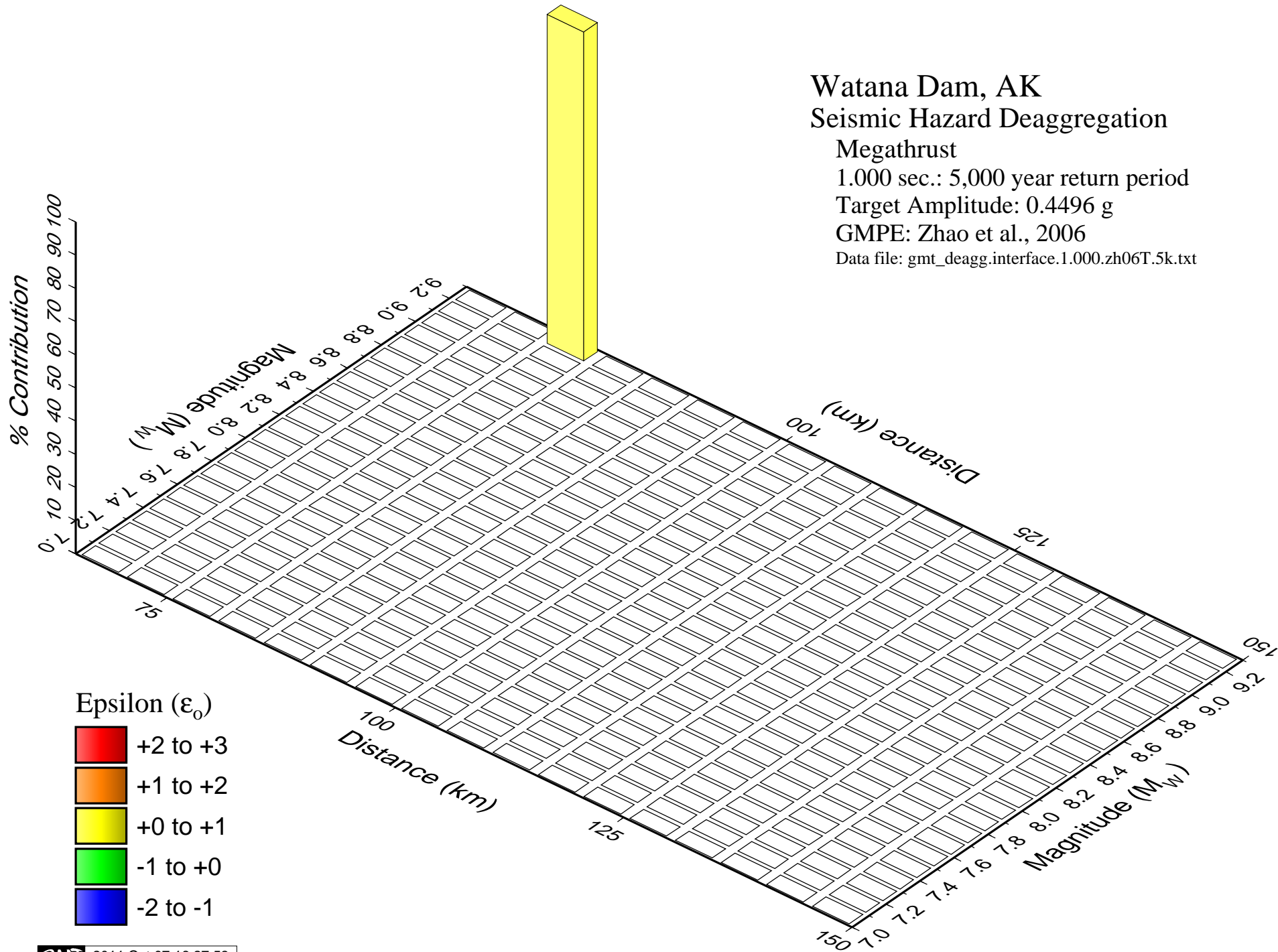
Megathrust

1.000 sec.: 5,000 year return period

Target Amplitude: 0.4496 g

GMPE: Zhao et al., 2006

Data file: gmt_deagg.interface.1.000.zh06T.5k.txt



Watana Dam, AK Seismic Hazard Deaggregation

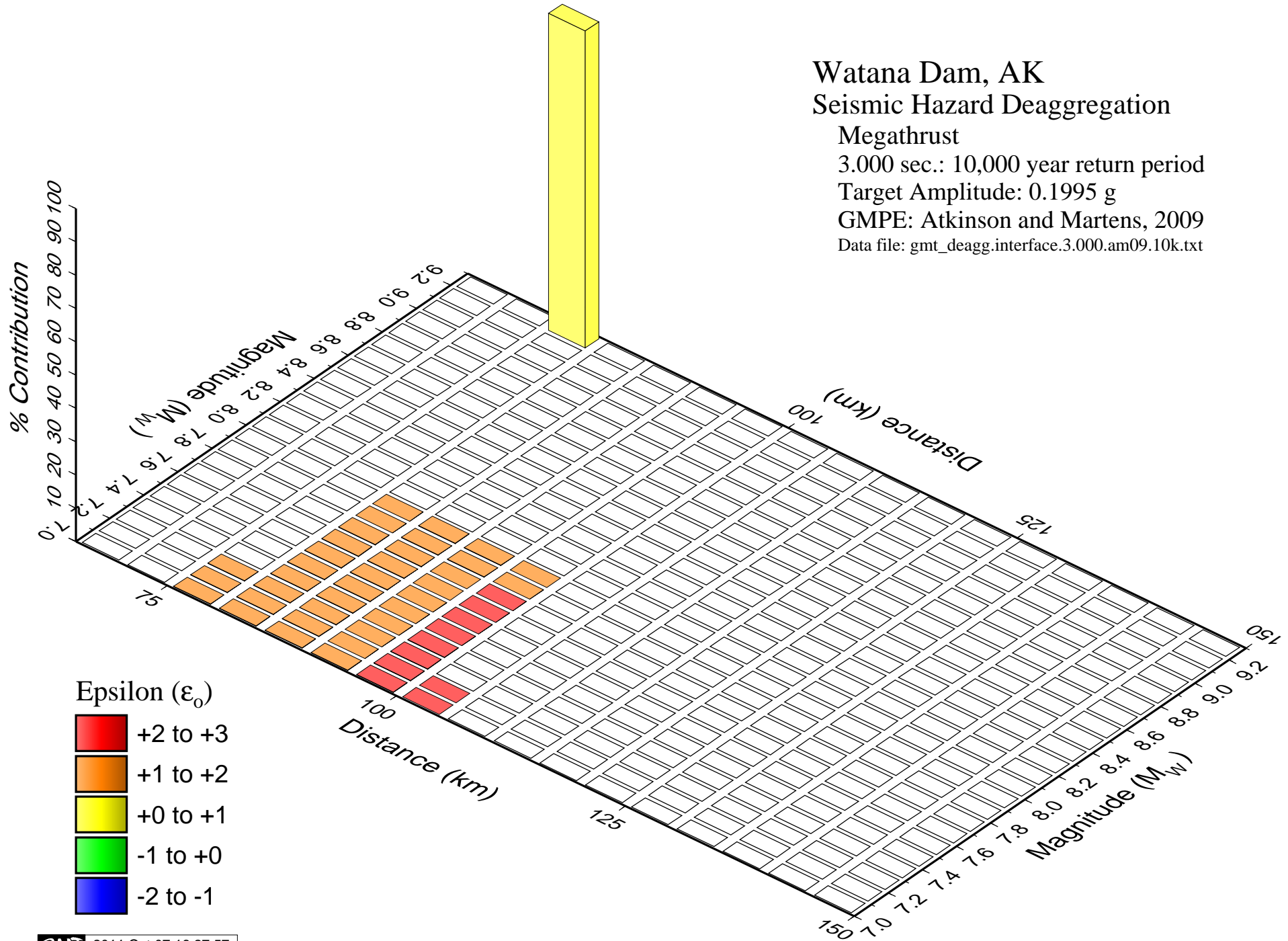
Megathrust

3.000 sec.: 10,000 year return period

Target Amplitude: 0.1995 g

GMPE: Atkinson and Martens, 2009

Data file: gmt_deagg.interface.3.000.am09.10k.txt



Watana Dam, AK Seismic Hazard Deaggregation

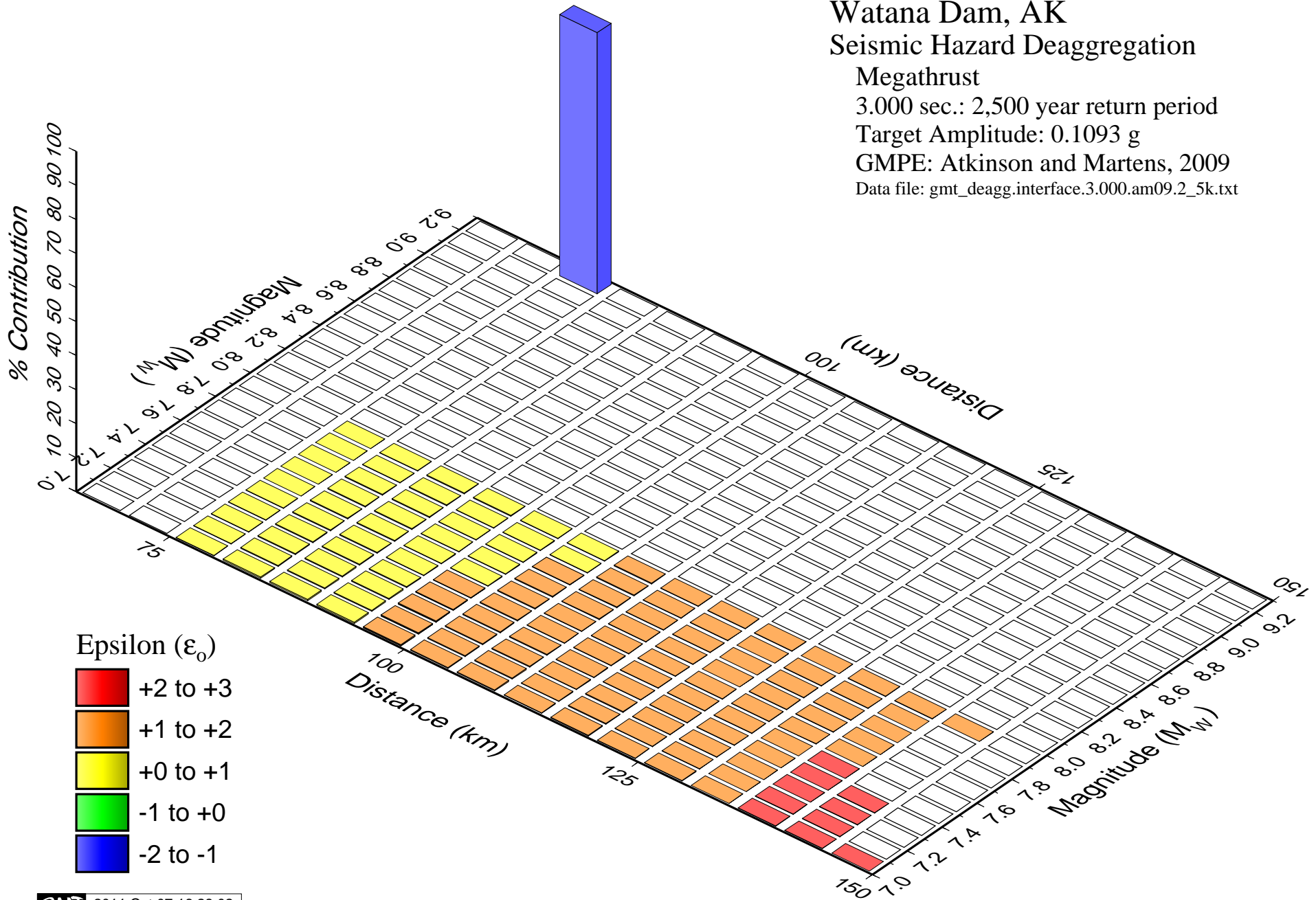
Megathrust

3.000 sec.: 2,500 year return period

Target Amplitude: 0.1093 g

GMPE: Atkinson and Martens, 2009

Data file: gmt_deagg.interface.3.000.am09.2_5k.txt



Watana Dam, AK Seismic Hazard Deaggregation

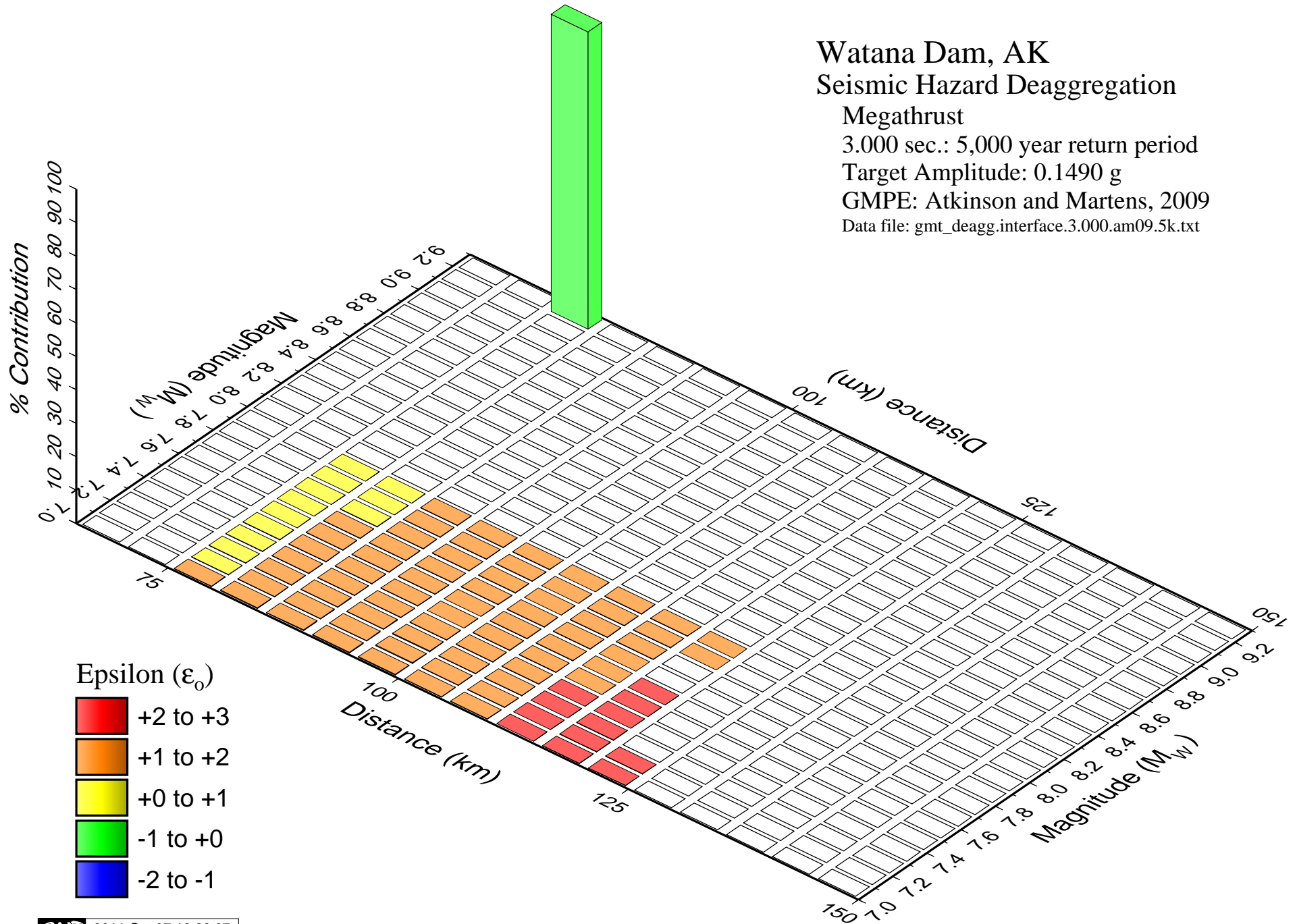
Megathrust

3.000 sec.: 5,000 year return period

Target Amplitude: 0.1490 g

GMPE: Atkinson and Martens, 2009

Data file: gmt_deagg.interface.3.000.am09.5k.txt



Watana Dam, AK Seismic Hazard Deaggregation

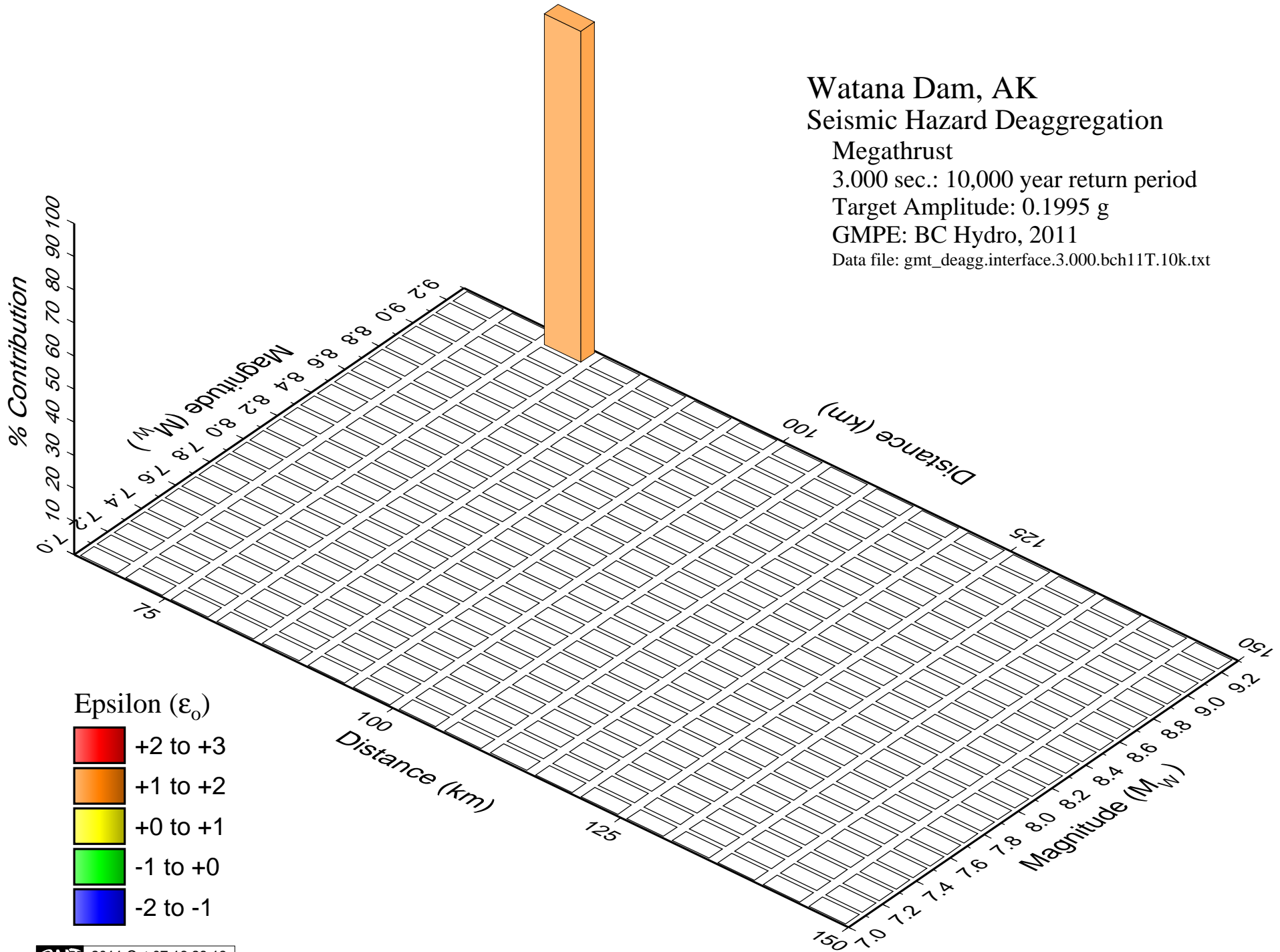
Megathrust

3.000 sec.: 10,000 year return period

Target Amplitude: 0.1995 g

GMPE: BC Hydro, 2011

Data file: gmt_deagg.interface.3.000.bch11T.10k.txt



Watana Dam, AK Seismic Hazard Deaggregation

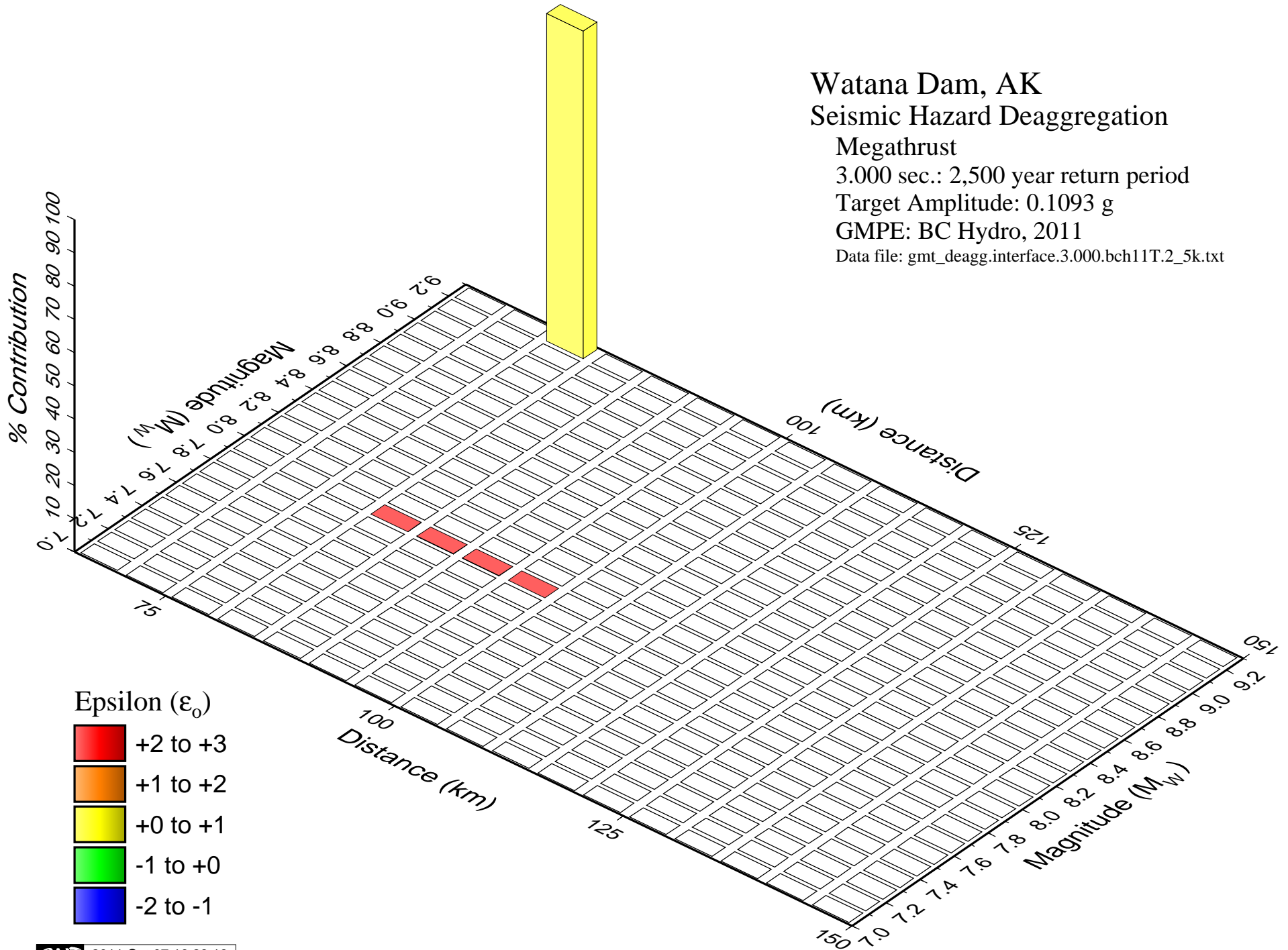
Megathrust

3.000 sec.: 2,500 year return period

Target Amplitude: 0.1093 g

GMPE: BC Hydro, 2011

Data file: gmt_deagg.interface.3.000.bch11T.2_5k.txt



Watana Dam, AK Seismic Hazard Deaggregation

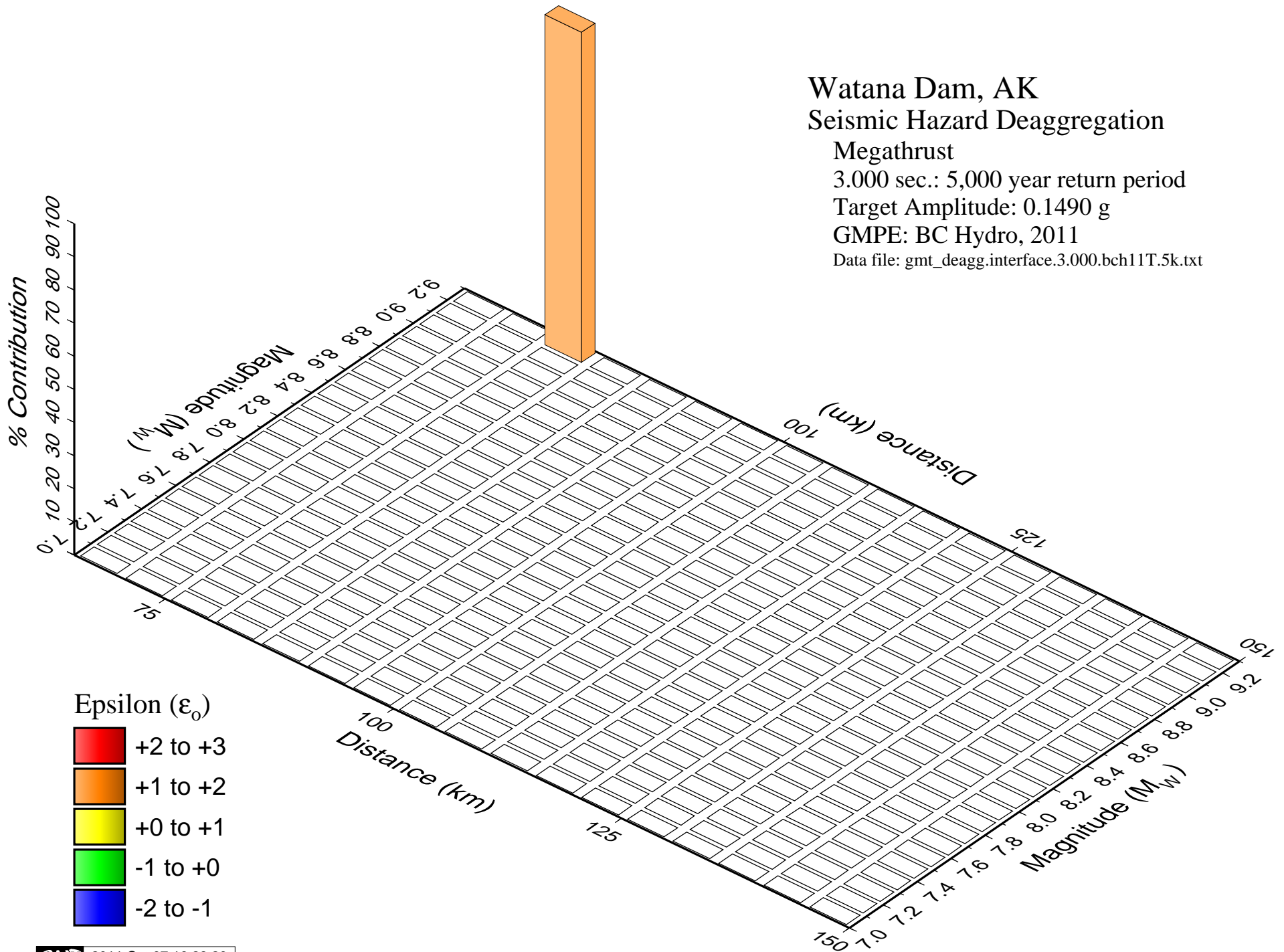
Megathrust

3.000 sec.: 5,000 year return period

Target Amplitude: 0.1490 g

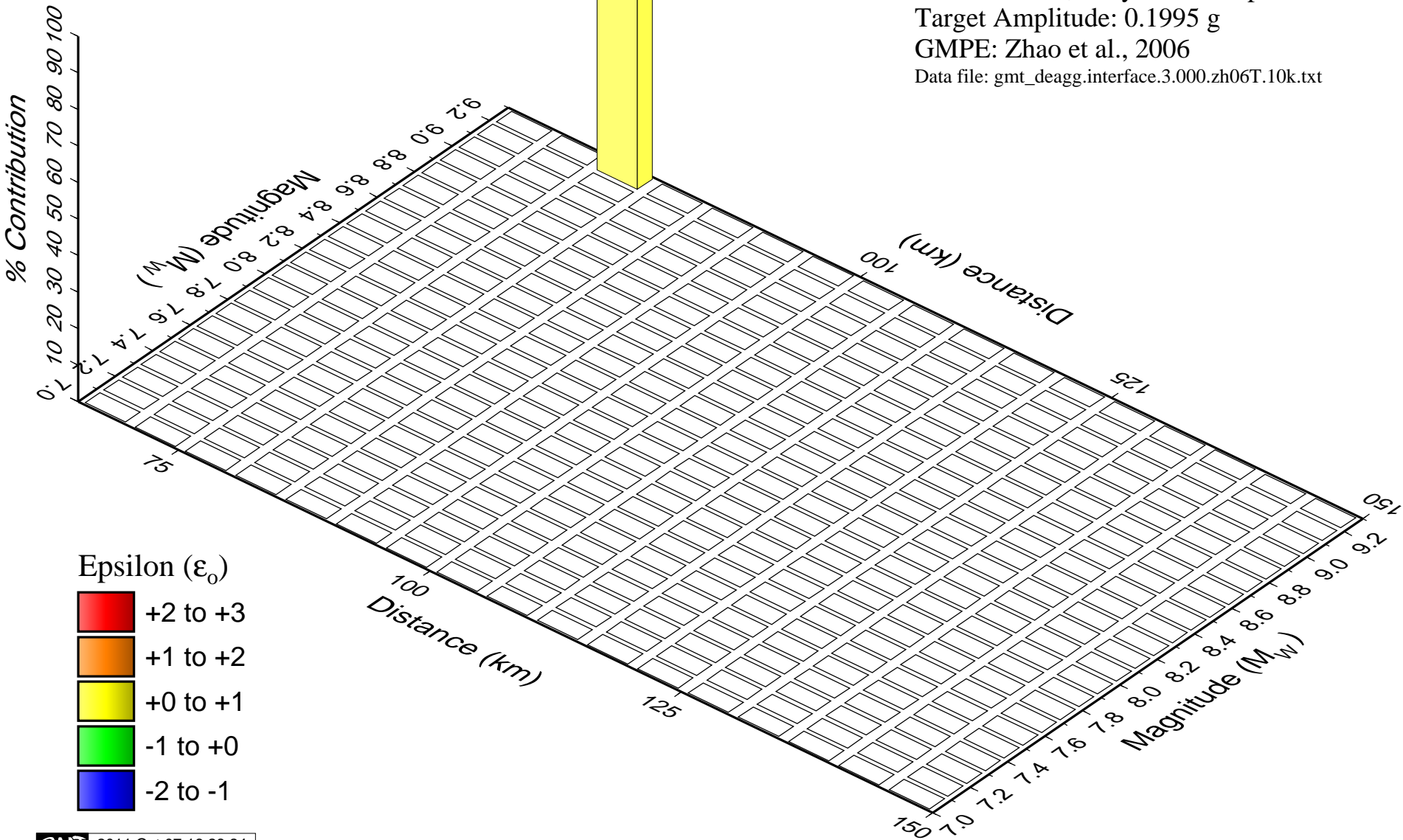
GMPE: BC Hydro, 2011

Data file: gmt_deagg.interface.3.000.bch11T.5k.txt



Watana Dam, AK Seismic Hazard Deaggregation

Megathrust
3.000 sec.: 10,000 year return period
Target Amplitude: 0.1995 g
GMPE: Zhao et al., 2006
Data file: gmt_deagg.interface.3.000.zh06T.10k.txt



Watana Dam, AK Seismic Hazard Deaggregation

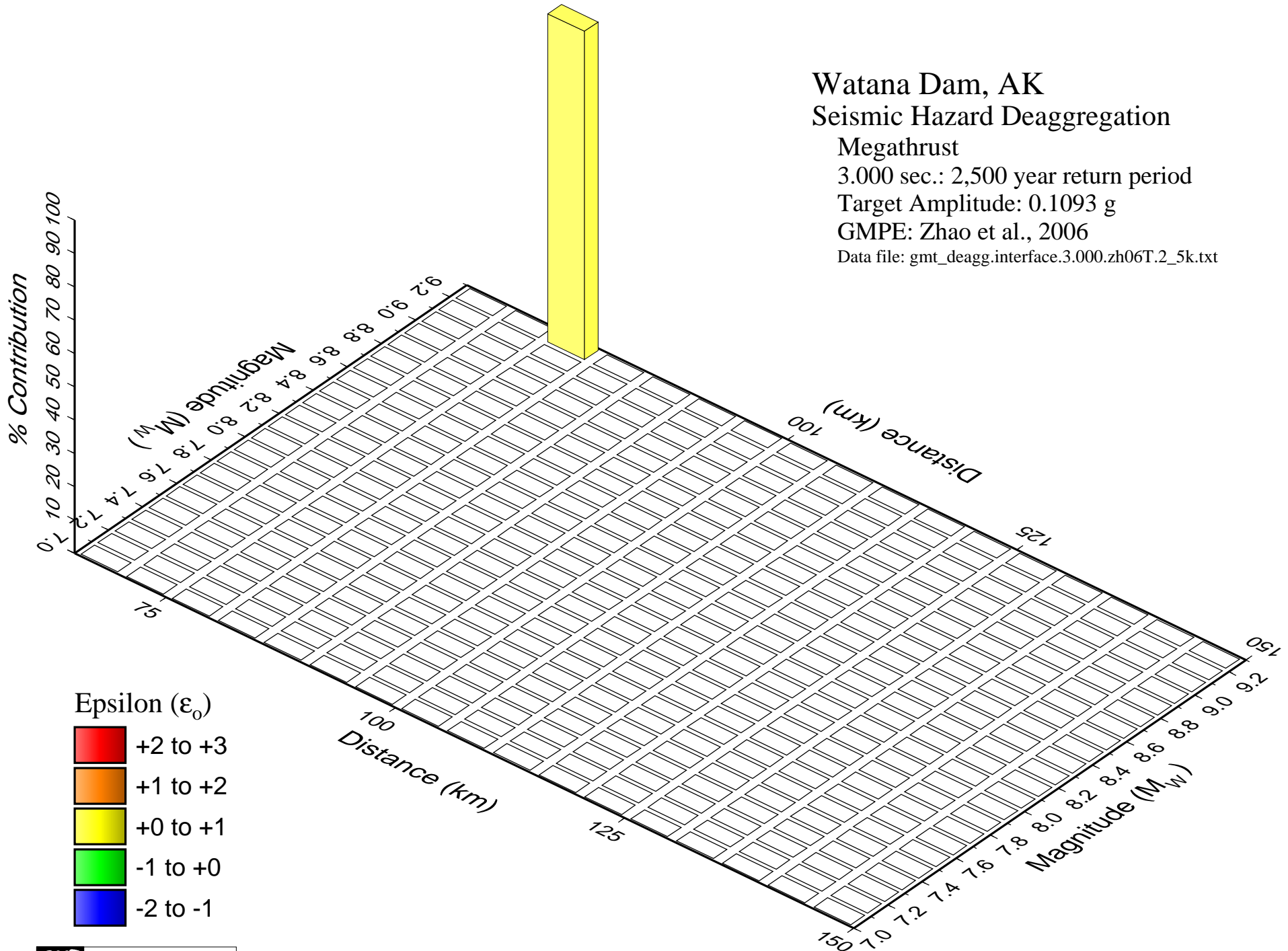
Megathrust

3.000 sec.: 2,500 year return period

Target Amplitude: 0.1093 g

GMPE: Zhao et al., 2006

Data file: gmt_deagg.interface.3.000.zh06T.2_5k.txt



Watana Dam, AK

Seismic Hazard Deaggregation

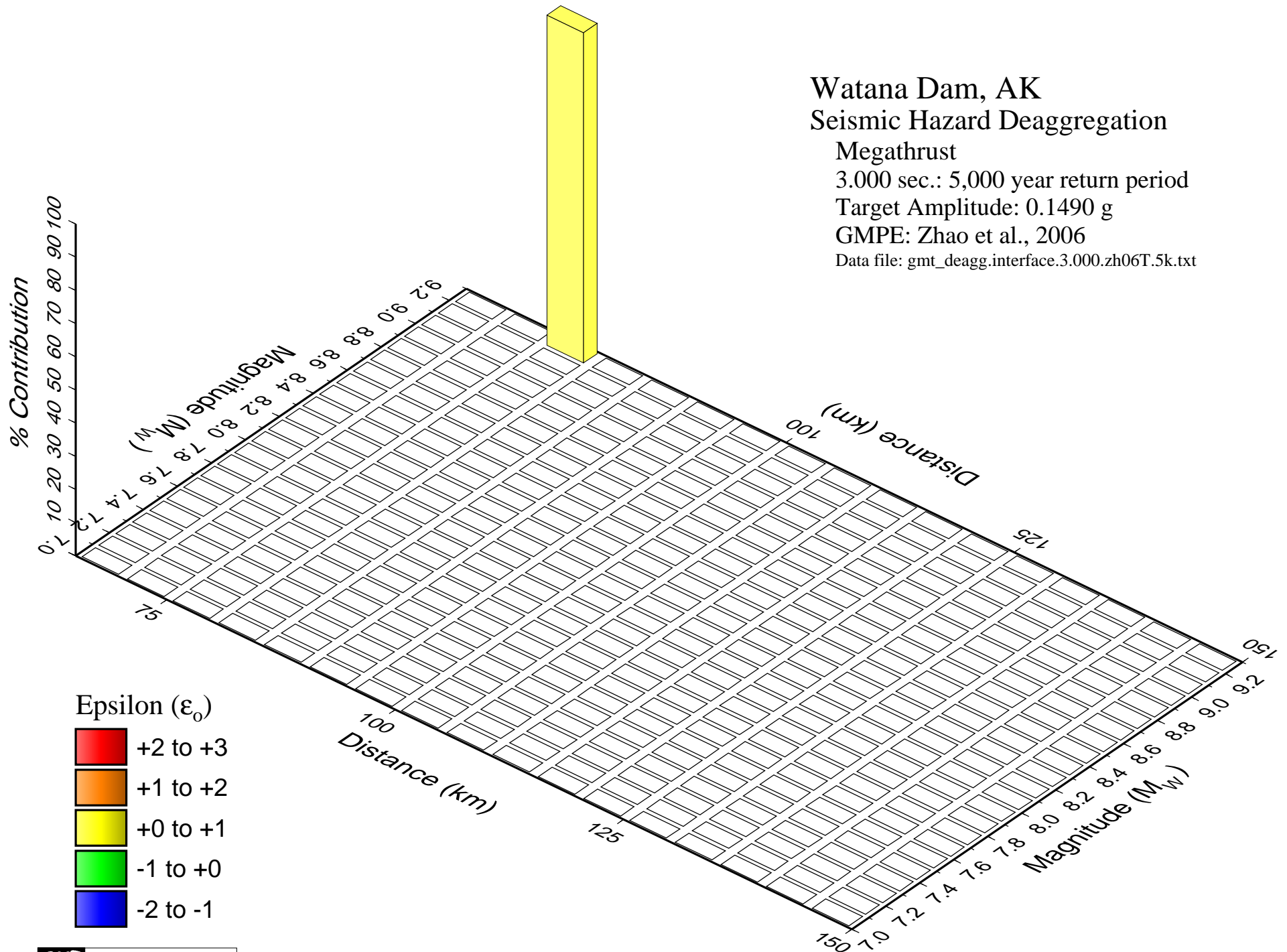
Megathrust

3.000 sec.: 5,000 year return period

Target Amplitude: 0.1490 g

GMPE: Zhao et al., 2006

Data file: gmt_deagg.interface.3.000.zh06T.5k.txt



Watana Dam, AK

Seismic Hazard Deaggregation

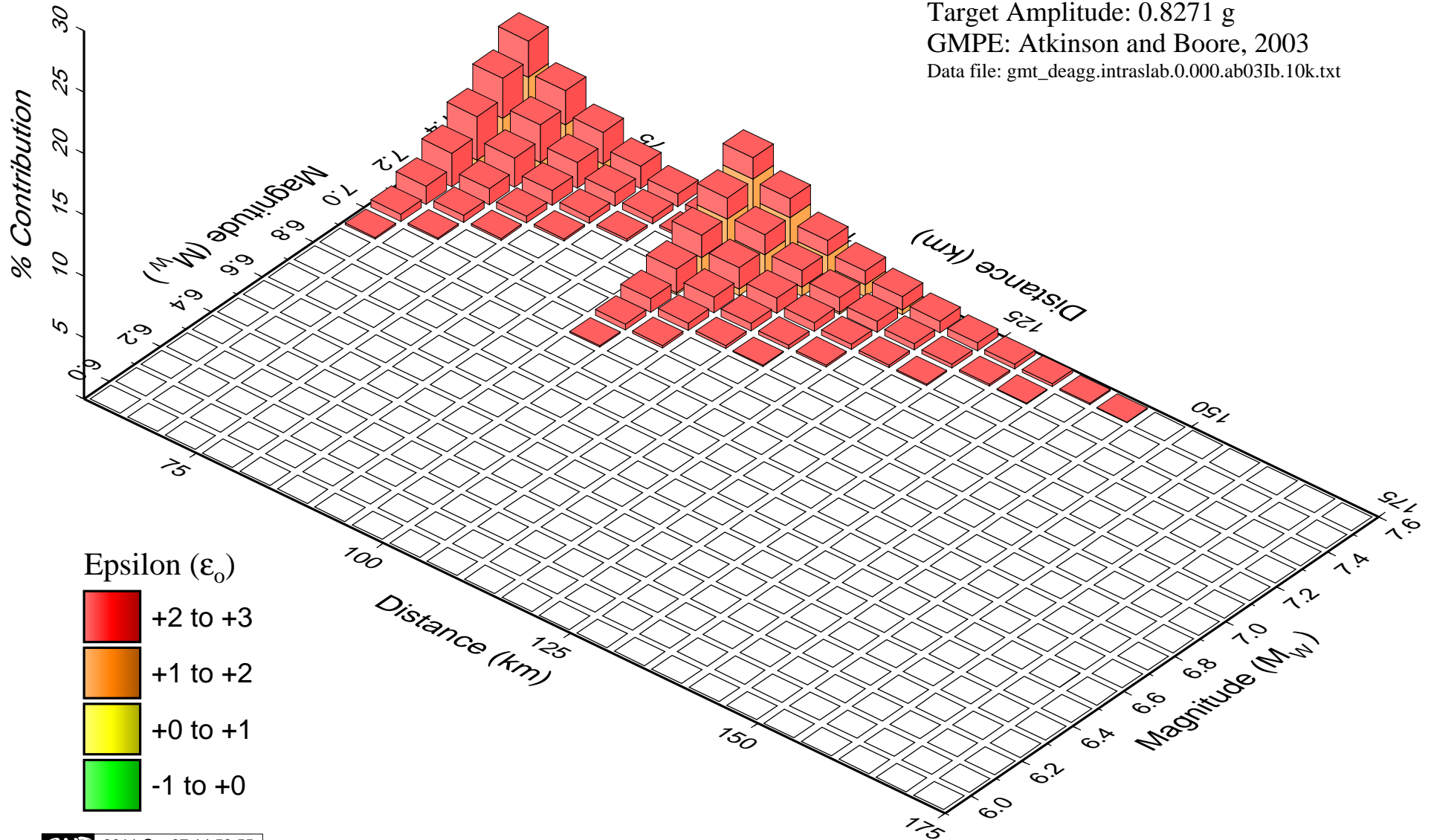
Intraslab

PHA: 10,000 year return period

Target Amplitude: 0.8271 g

GMPE: Atkinson and Boore, 2003

Data file: gmt_deagg.intraslab.0.000.ab03Ib.10k.txt



Watana Dam, AK Seismic Hazard Deaggregation

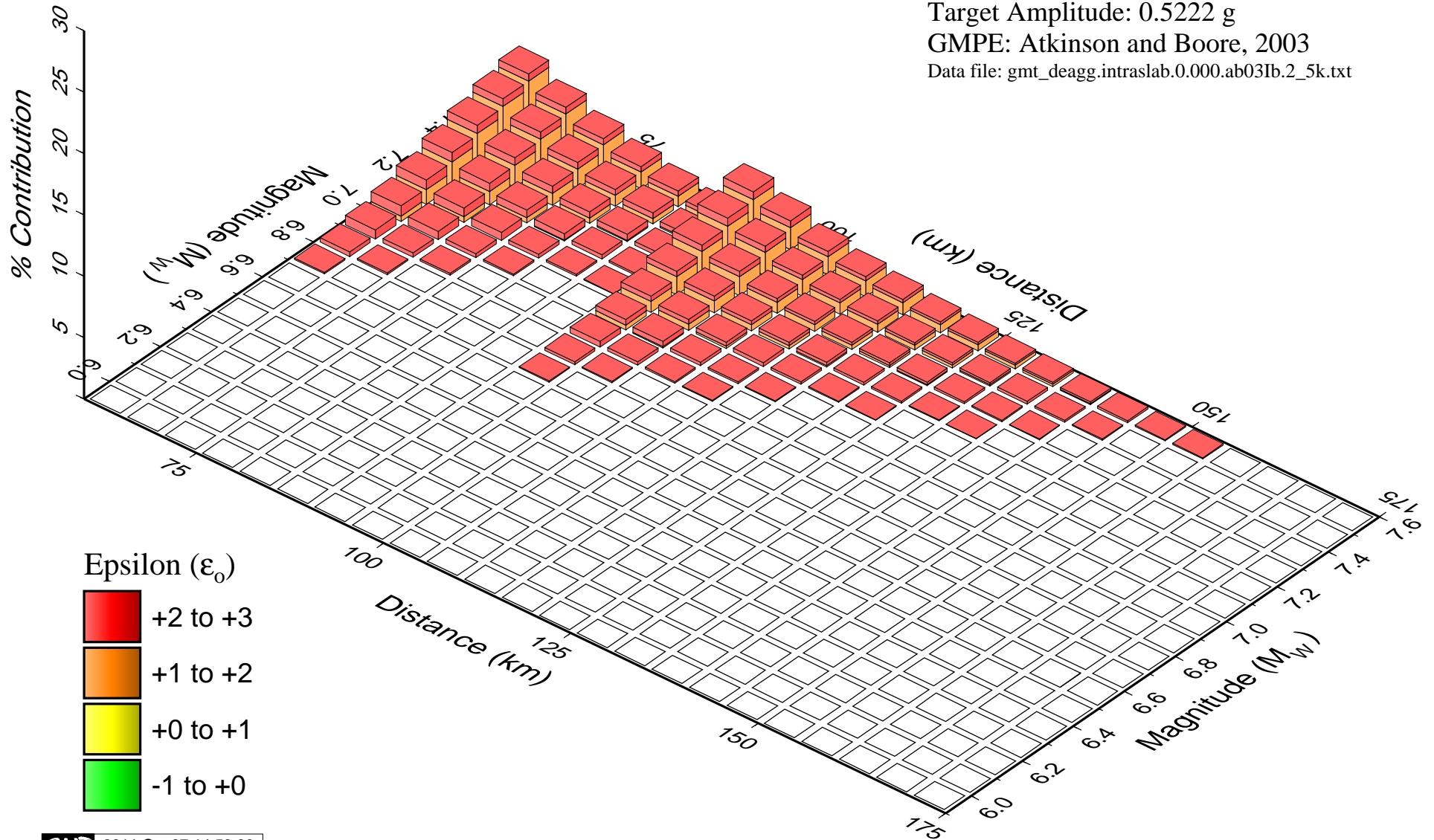
Intraslab

PHA: 2,500 year return period

Target Amplitude: 0.5222 g

GMPE: Atkinson and Boore, 2003

Data file: gmt_deagg.intraslab.0.000.ab03Ib.2_5k.txt



Watana Dam, AK

Seismic Hazard Deaggregation

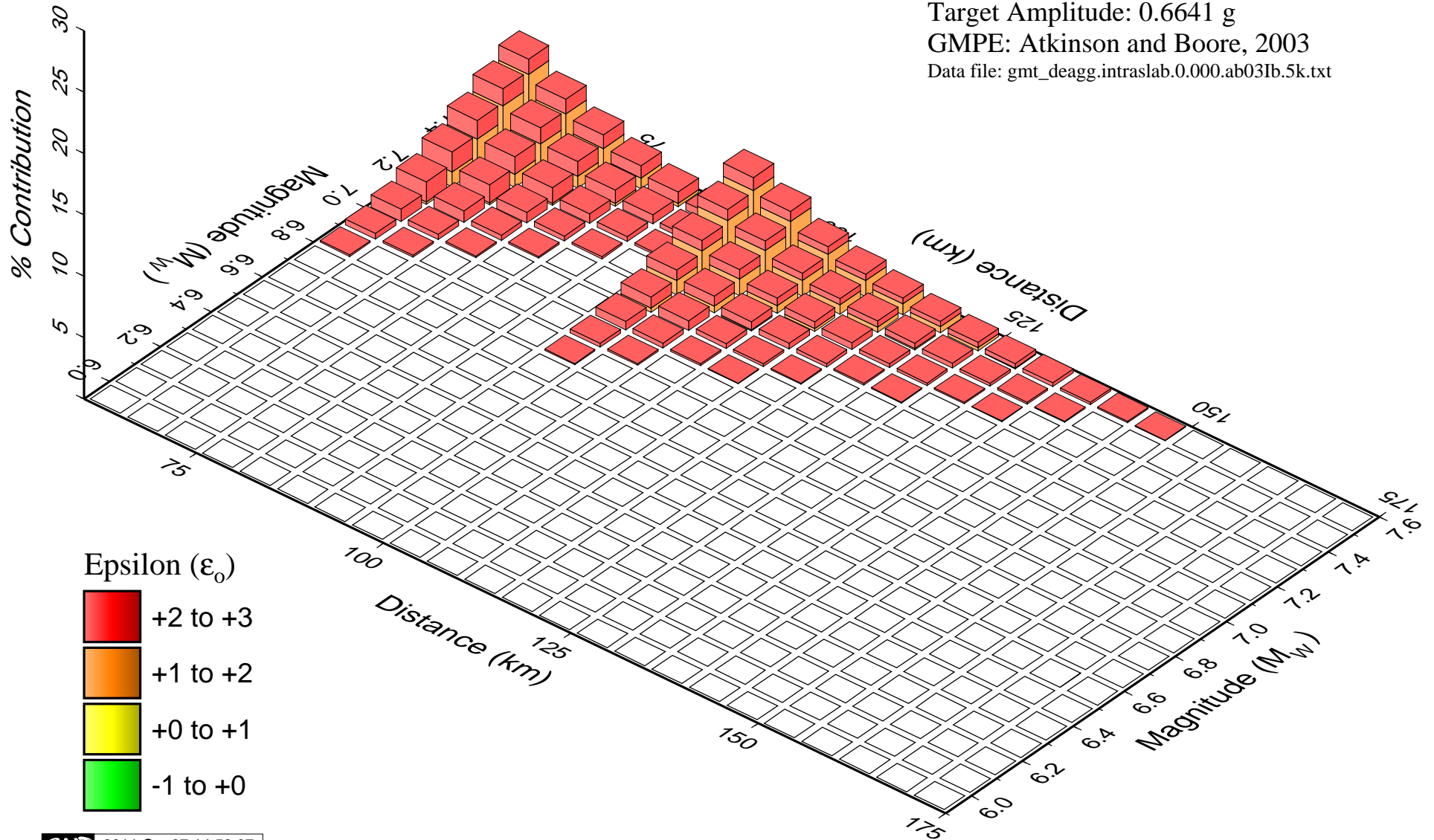
Intraslab

PHA: 5,000 year return period

Target Amplitude: 0.6641 g

GMPE: Atkinson and Boore, 2003

Data file: gmt_deagg.intraslab.0.000.ab03Ib.5k.txt



Watana Dam, AK Seismic Hazard Deaggregation

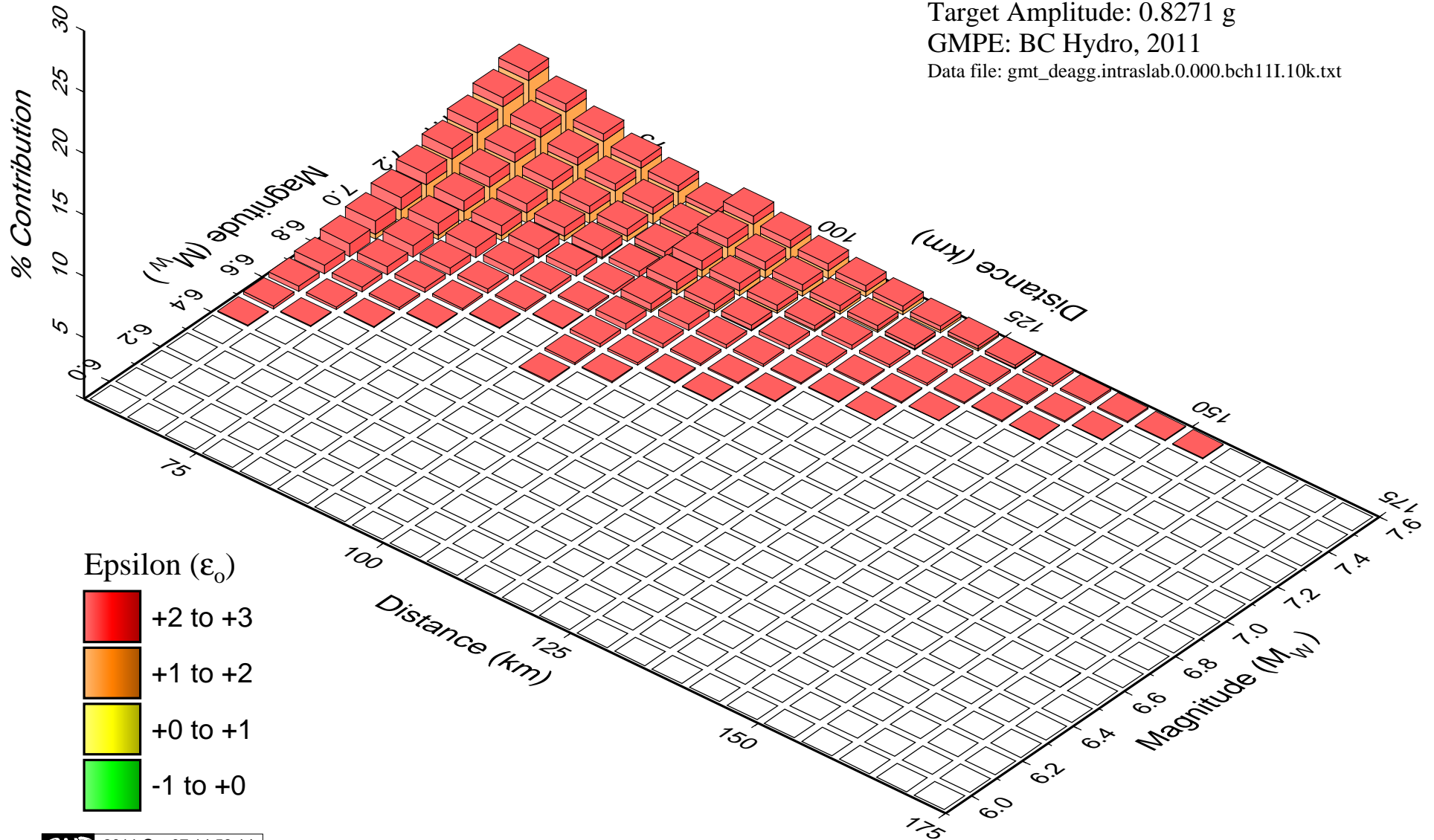
Intraslab

PHA: 10,000 year return period

Target Amplitude: 0.8271 g

GMPE: BC Hydro, 2011

Data file: gmt_deagg.intraslab.0.000.bch11I.10k.txt



Watana Dam, AK Seismic Hazard Deaggregation

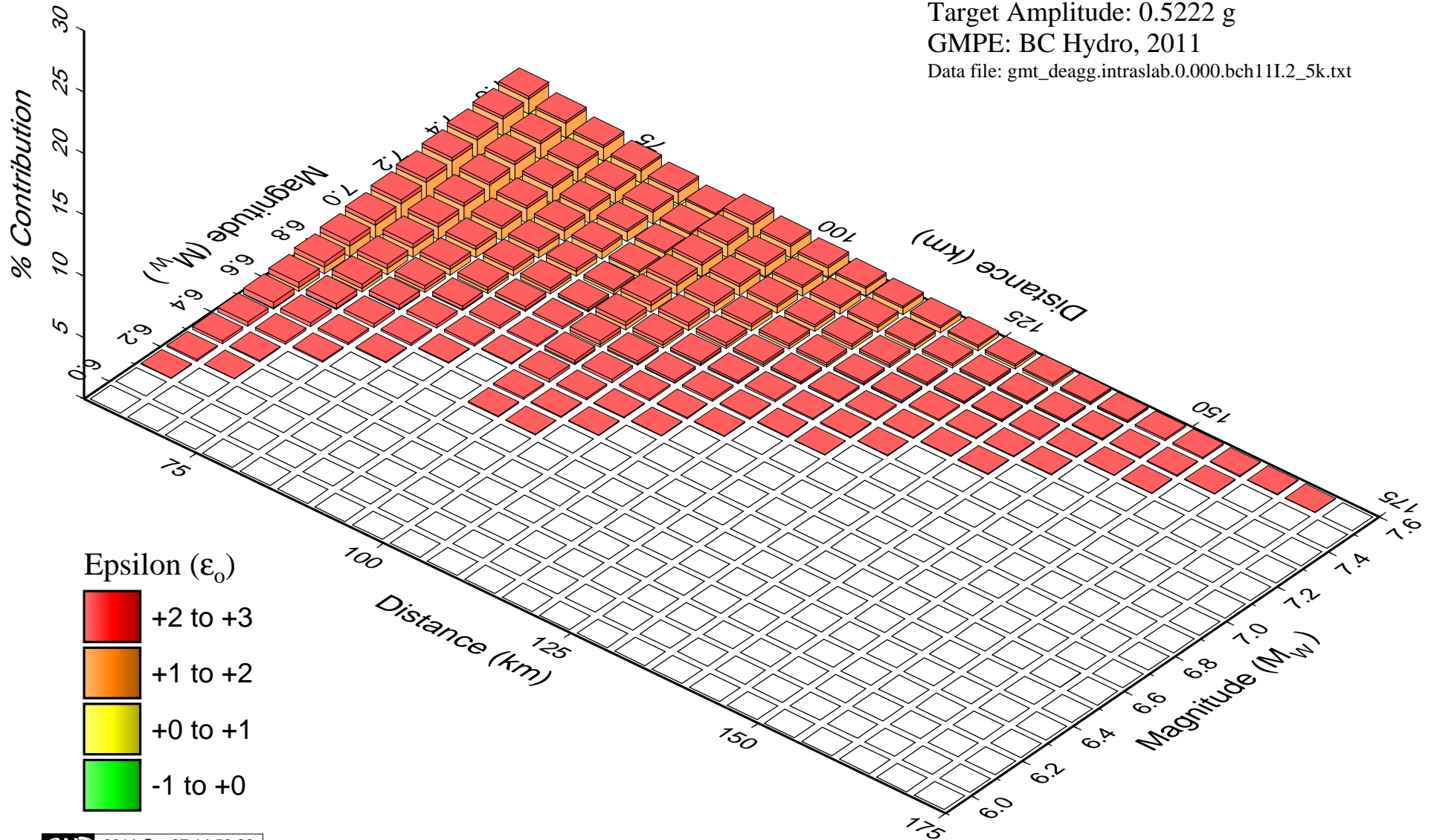
Intraslab

PHA: 2,500 year return period

Target Amplitude: 0.5222 g

GMPE: BC Hydro, 2011

Data file: gmt_deagg.intraslab.0.000.bch11I.2_5k.txt



Watana Dam, AK

Seismic Hazard Deaggregation

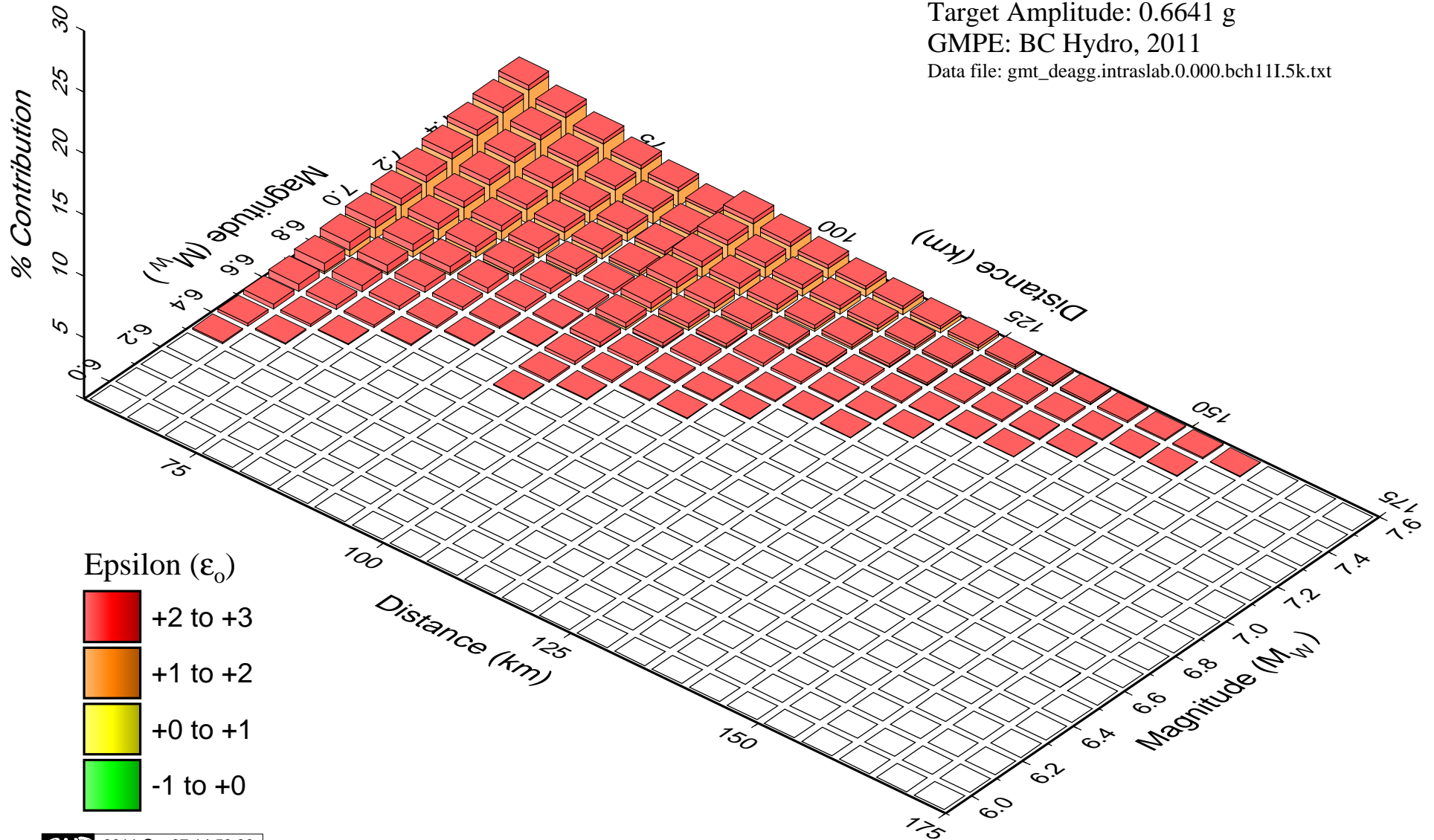
Intraslab

PHA: 5,000 year return period

Target Amplitude: 0.6641 g

GMPE: BC Hydro, 2011

Data file: gmt_deagg.intraslab.0.000.bch11I.5k.txt



Watana Dam, AK

Seismic Hazard Deaggregation

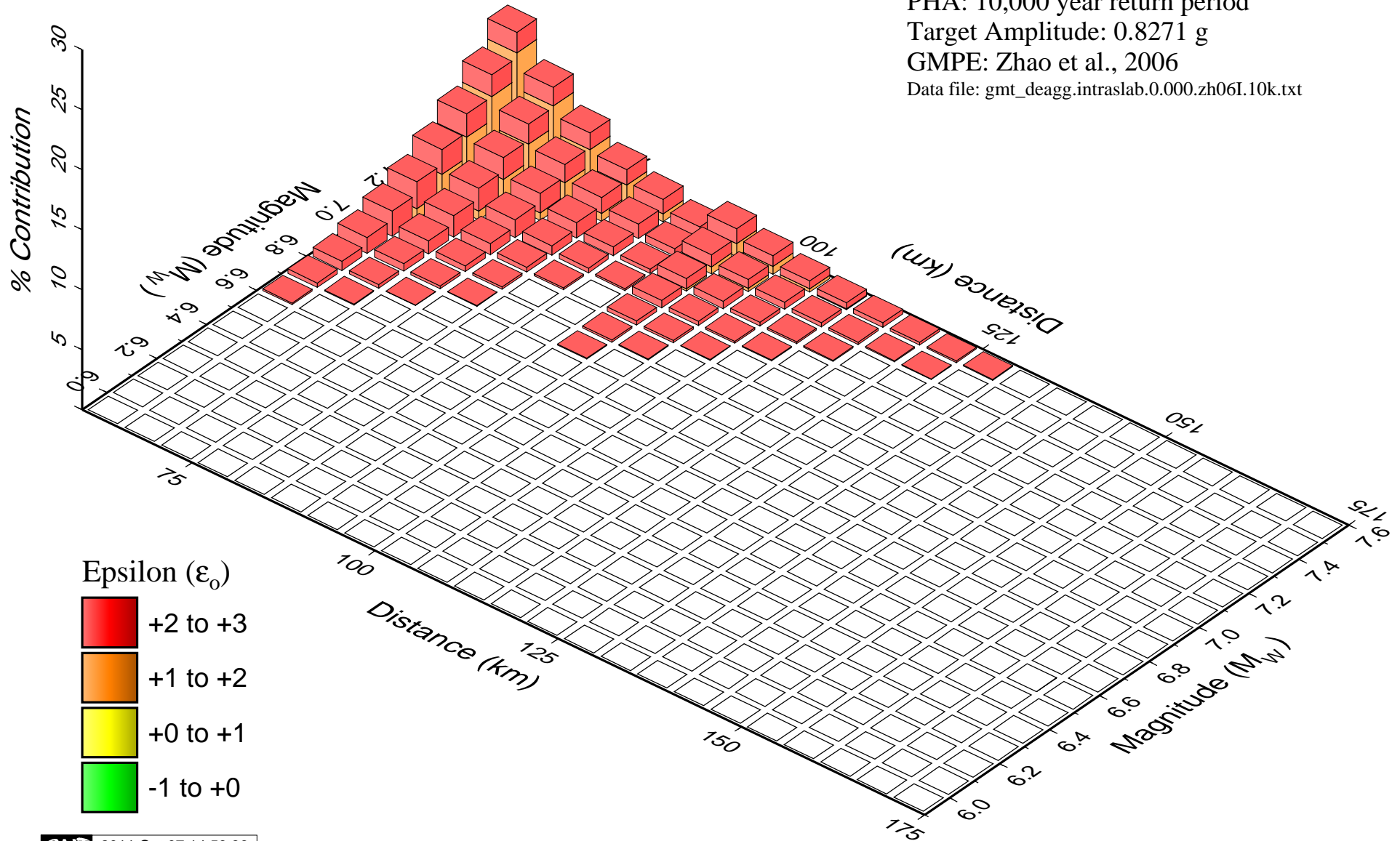
Intraslab

PHA: 10,000 year return period

Target Amplitude: 0.8271 g

GMPE: Zhao et al., 2006

Data file: gmt_deagg.intraslab.0.000.zh06I.10k.txt



Watana Dam, AK

Seismic Hazard Deaggregation

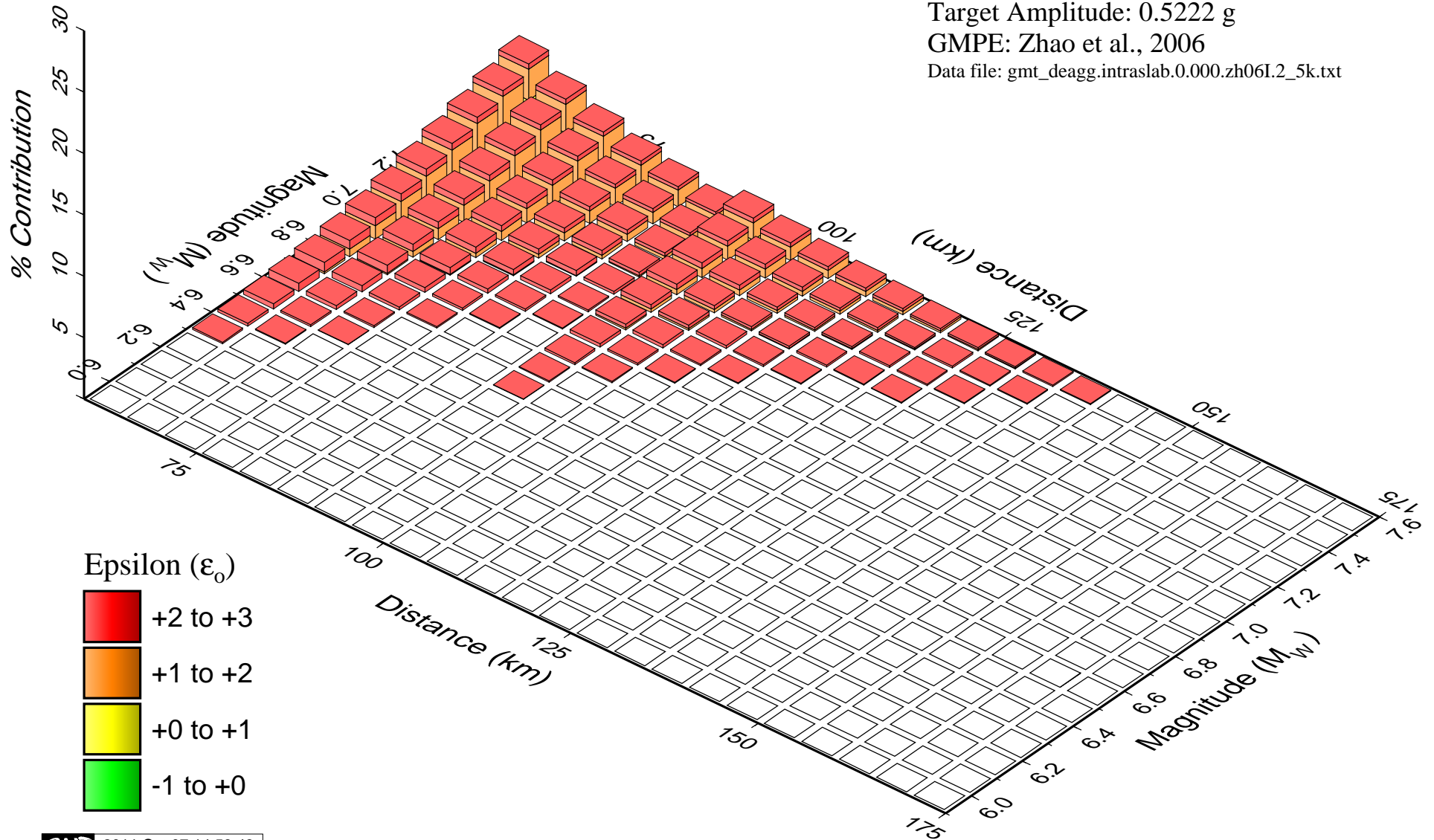
Intraslab

PHA: 2,500 year return period

Target Amplitude: 0.5222 g

GMPE: Zhao et al., 2006

Data file: gmt_deagg.intraslab.0.000.zh06I.2_5k.txt



Watana Dam, AK

Seismic Hazard Deaggregation

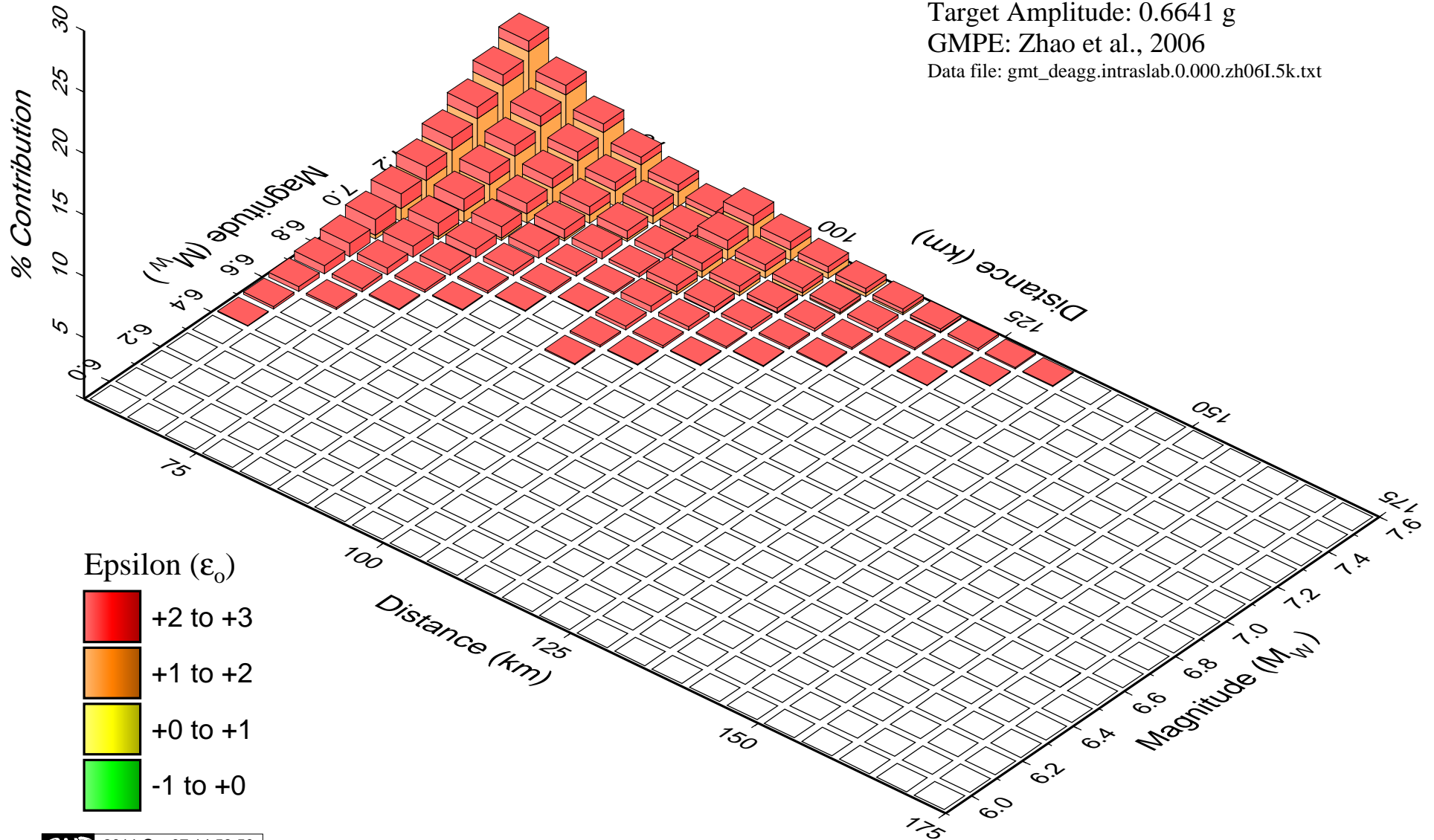
Intraslab

PHA: 5,000 year return period

Target Amplitude: 0.6641 g

GMPE: Zhao et al., 2006

Data file: gmt_deagg.intraslab.0.000.zh06I.5k.txt



Watana Dam, AK

Seismic Hazard Deaggregation

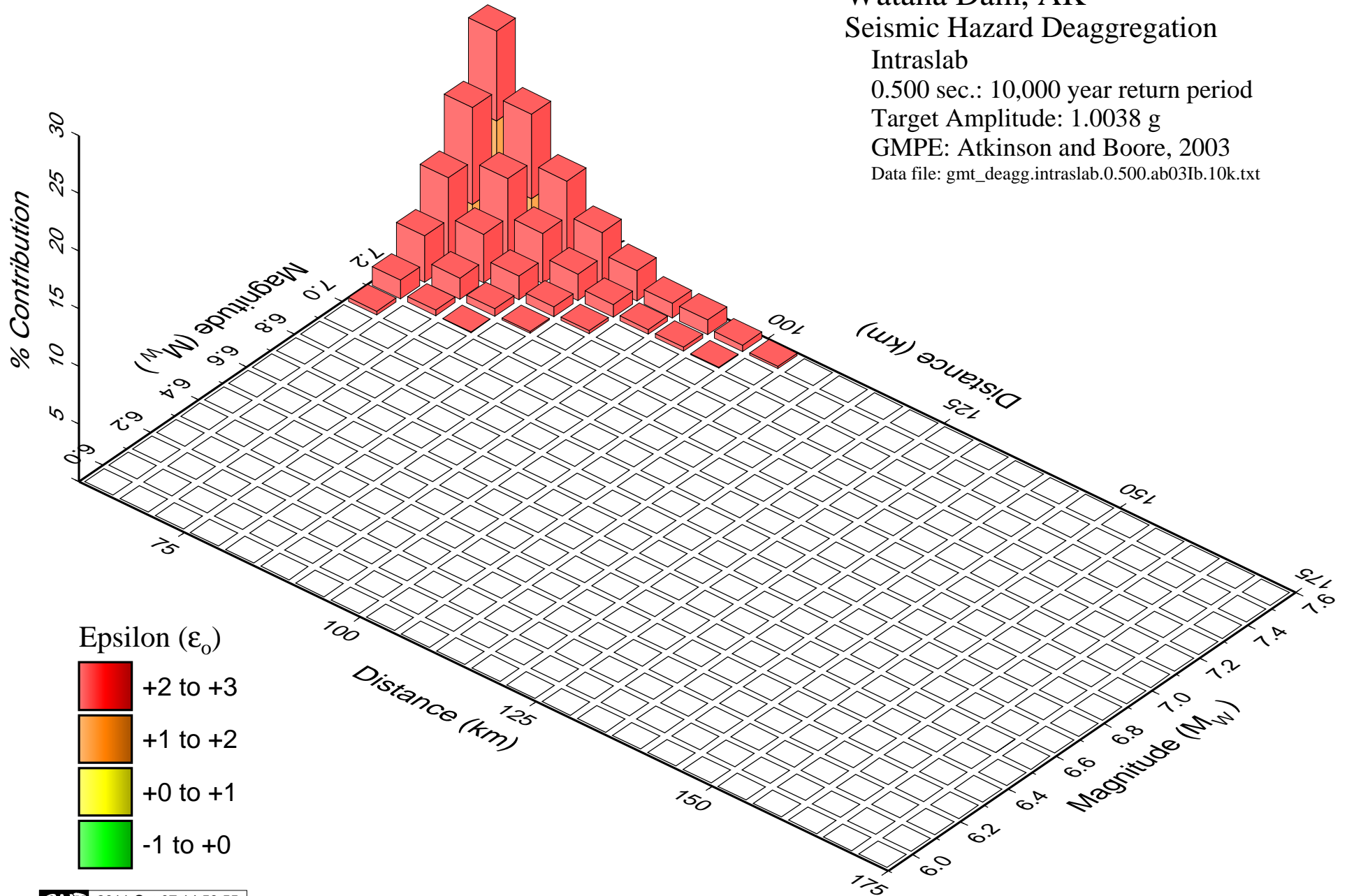
Intraslab

0.500 sec.: 10,000 year return period

Target Amplitude: 1.0038 g

GMPE: Atkinson and Boore, 2003

Data file: gmt_deagg.intraslab.0.500.ab03Ib.10k.txt



Watana Dam, AK

Seismic Hazard Deaggregation

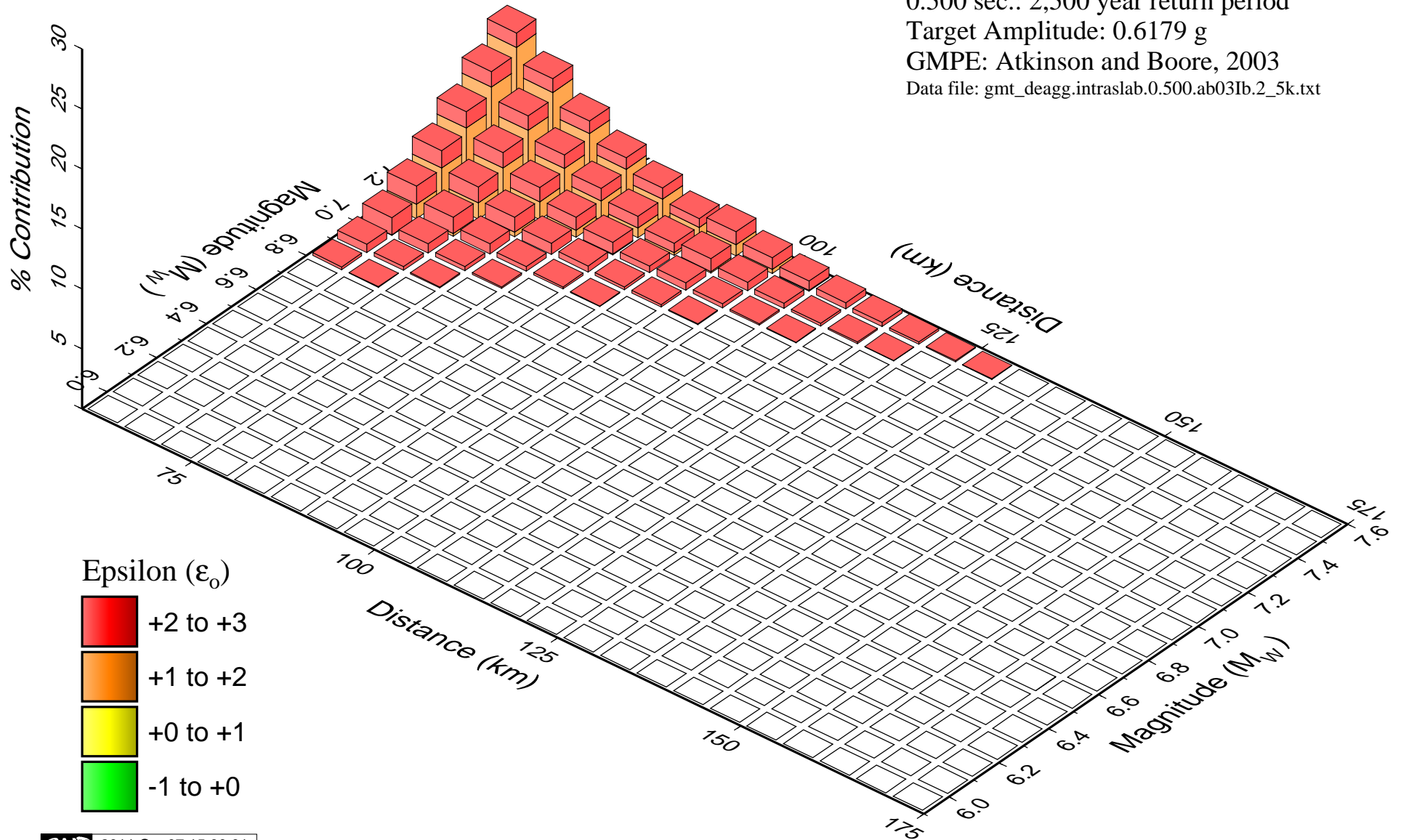
Intraslab

0.500 sec.: 2,500 year return period

Target Amplitude: 0.6179 g

GMPE: Atkinson and Boore, 2003

Data file: gmt_deagg.intraslab.0.500.ab03Ib.2_5k.txt



Watana Dam, AK

Seismic Hazard Deaggregation

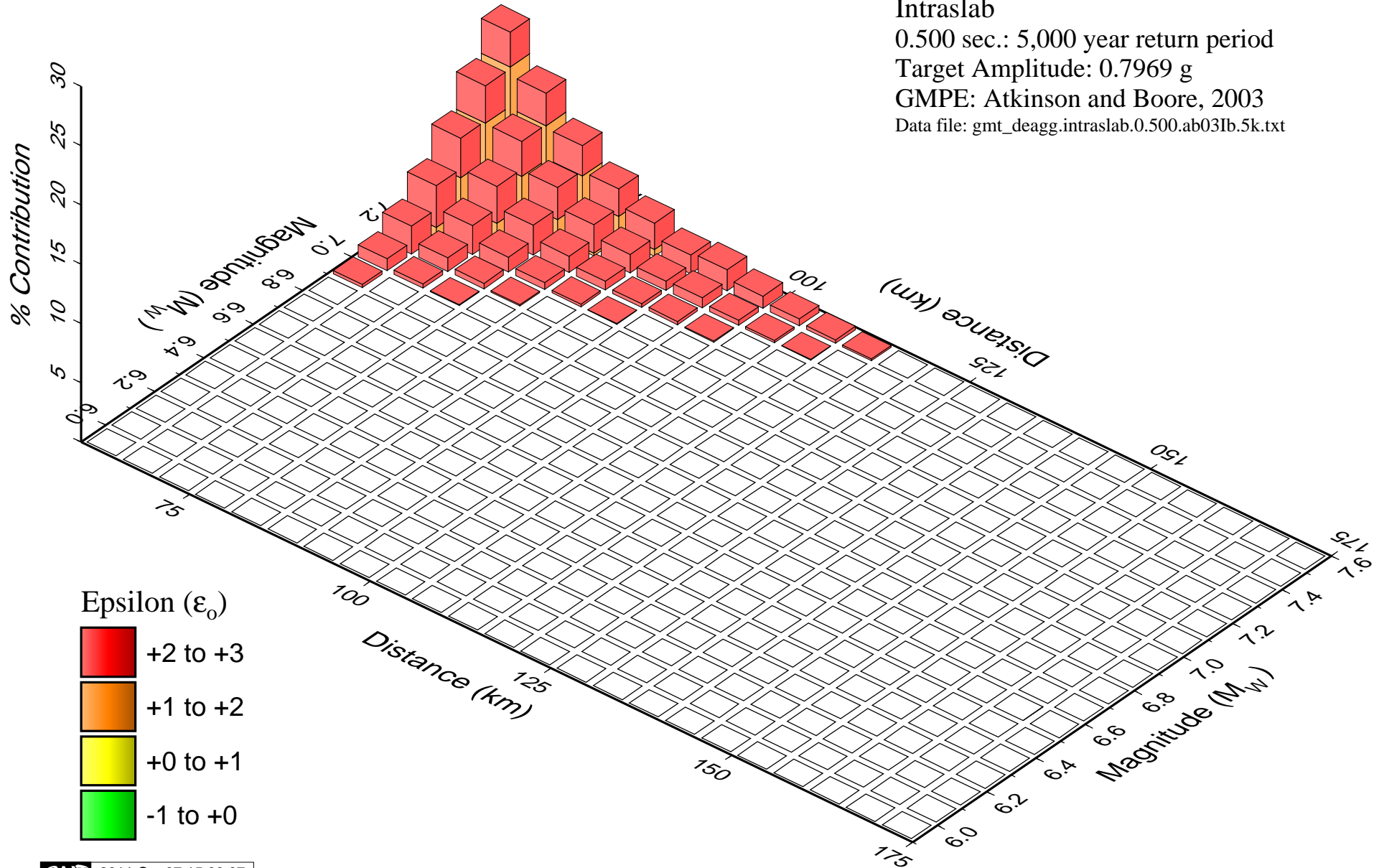
Intraslab

0.500 sec.: 5,000 year return period

Target Amplitude: 0.7969 g

GMPE: Atkinson and Boore, 2003

Data file: gmt_deagg.intraslab.0.500.ab03Ib.5k.txt



Watana Dam, AK

Seismic Hazard Deaggregation

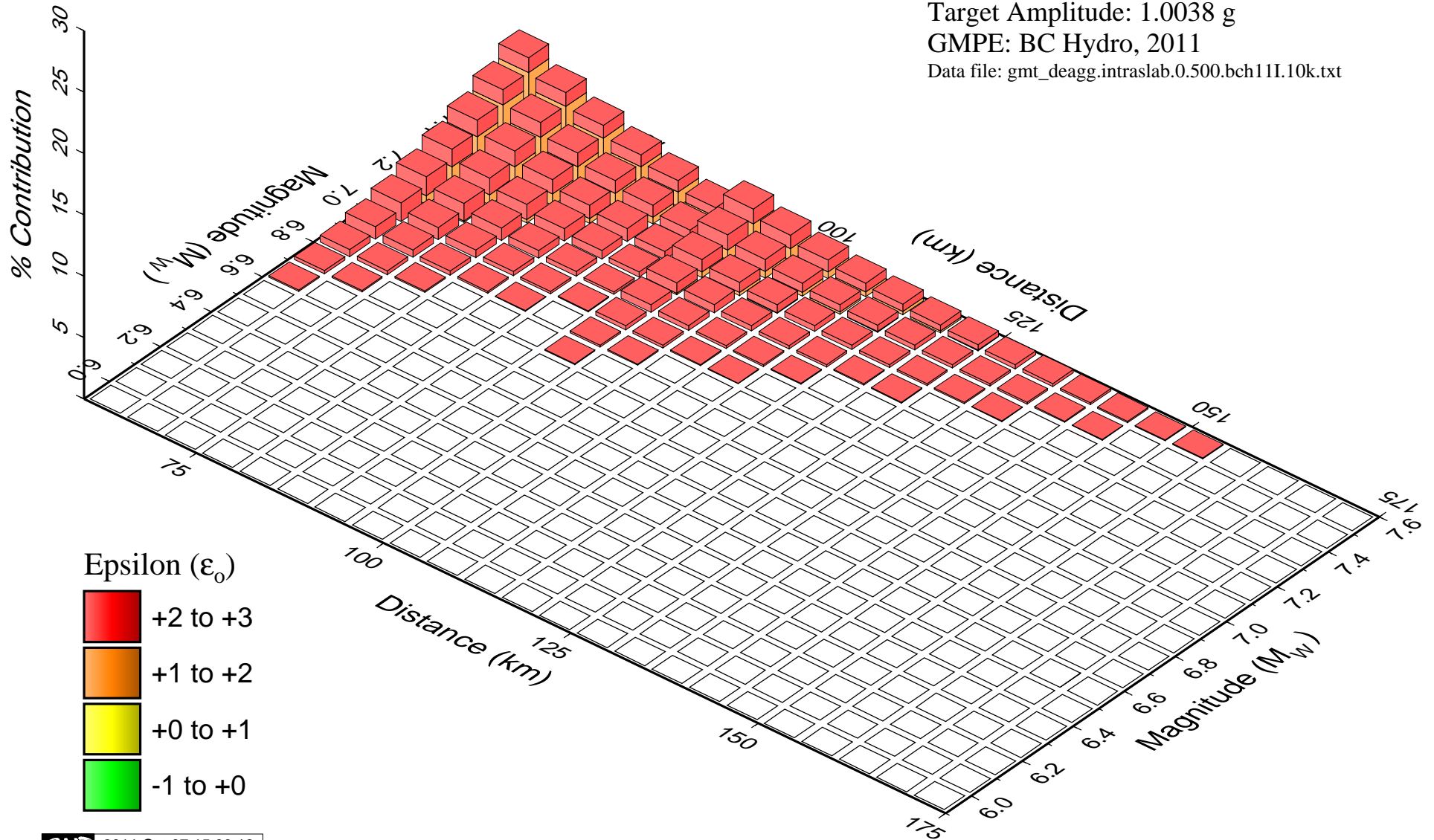
Intraslab

0.500 sec.: 10,000 year return period

Target Amplitude: 1.0038 g

GMPE: BC Hydro, 2011

Data file: gmt_deagg.intraslab.0.500.bch11I.10k.txt



Watana Dam, AK

Seismic Hazard Deaggregation

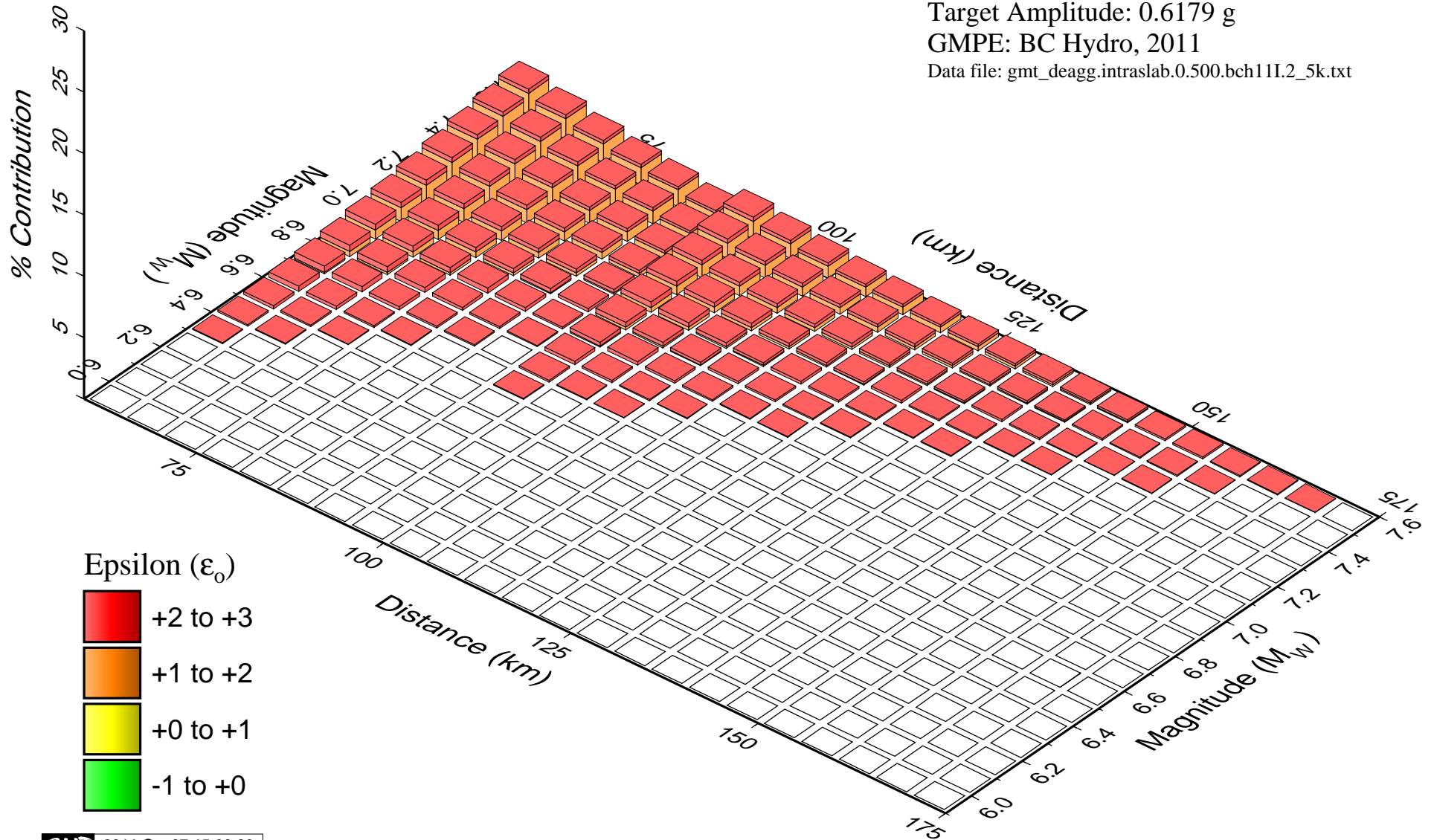
Intraslab

0.500 sec.: 2,500 year return period

Target Amplitude: 0.6179 g

GMPE: BC Hydro, 2011

Data file: gmt_deagg.intraslab.0.500.bch11I.2_5k.txt



Watana Dam, AK

Seismic Hazard Deaggregation

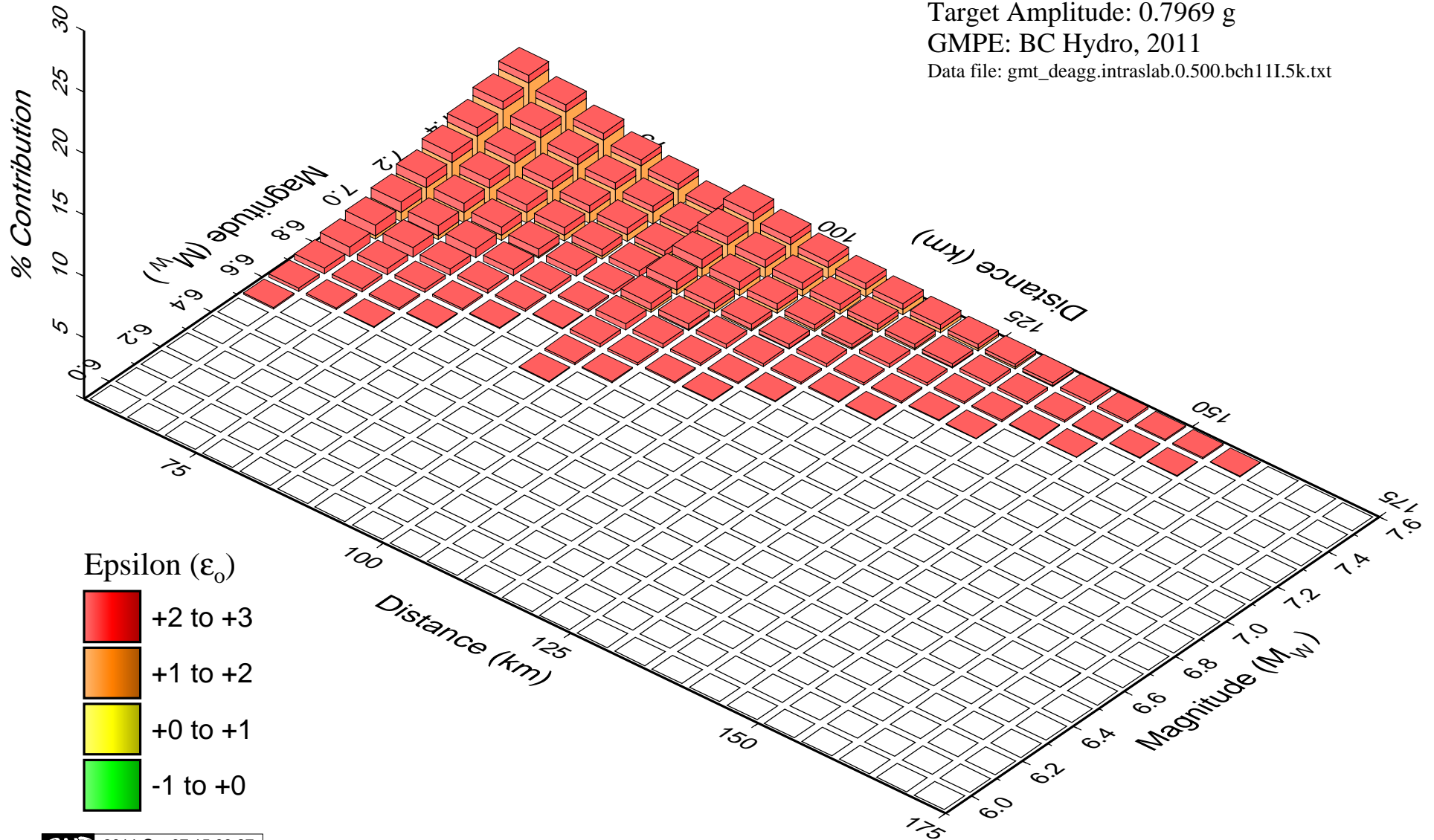
Intraslab

0.500 sec.: 5,000 year return period

Target Amplitude: 0.7969 g

GMPE: BC Hydro, 2011

Data file: gmt_deagg.intraslab.0.500.bch11I.5k.txt



Watana Dam, AK Seismic Hazard Deaggregation

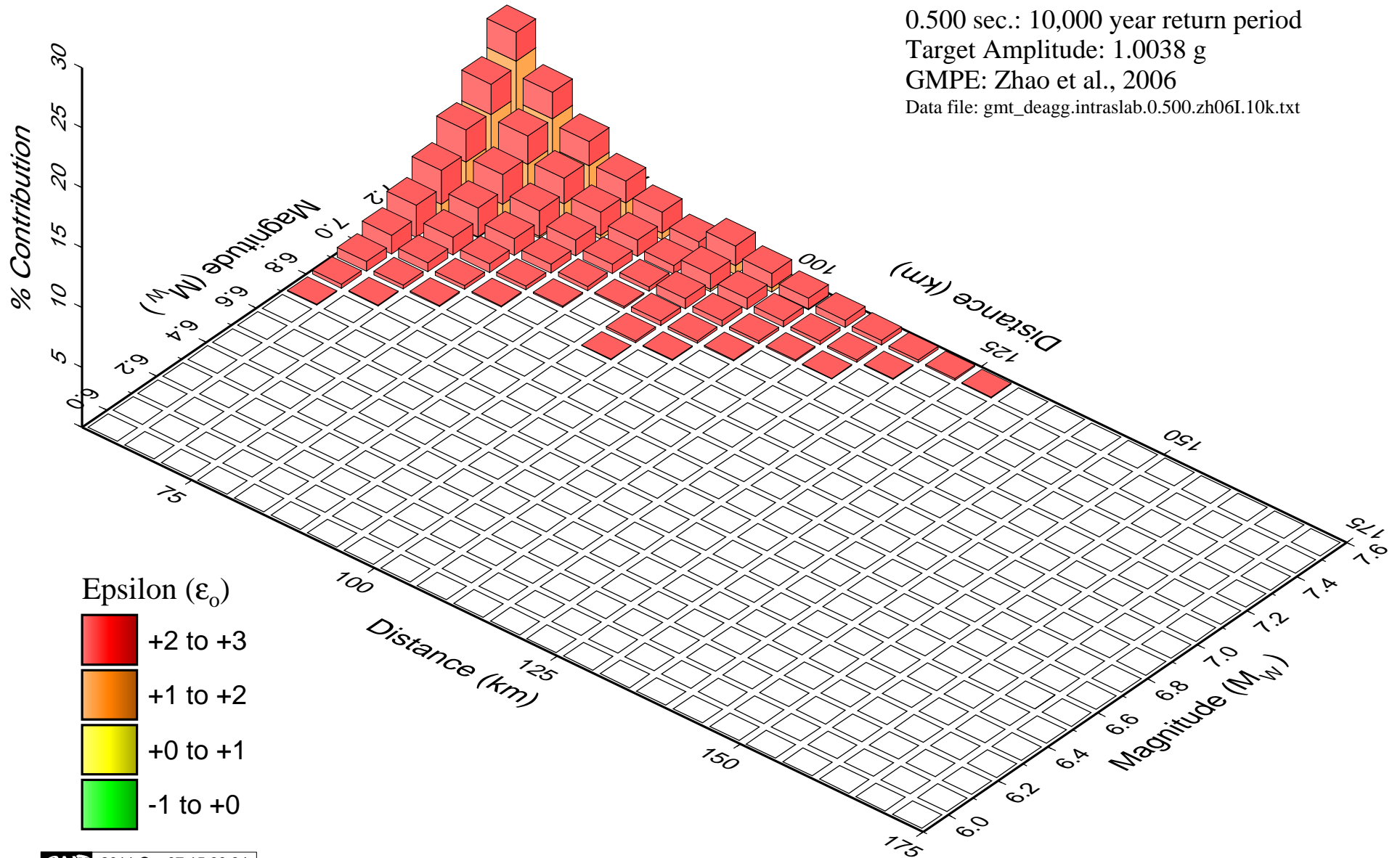
Intraslab

0.500 sec.: 10,000 year return period

Target Amplitude: 1.0038 g

GMPE: Zhao et al., 2006

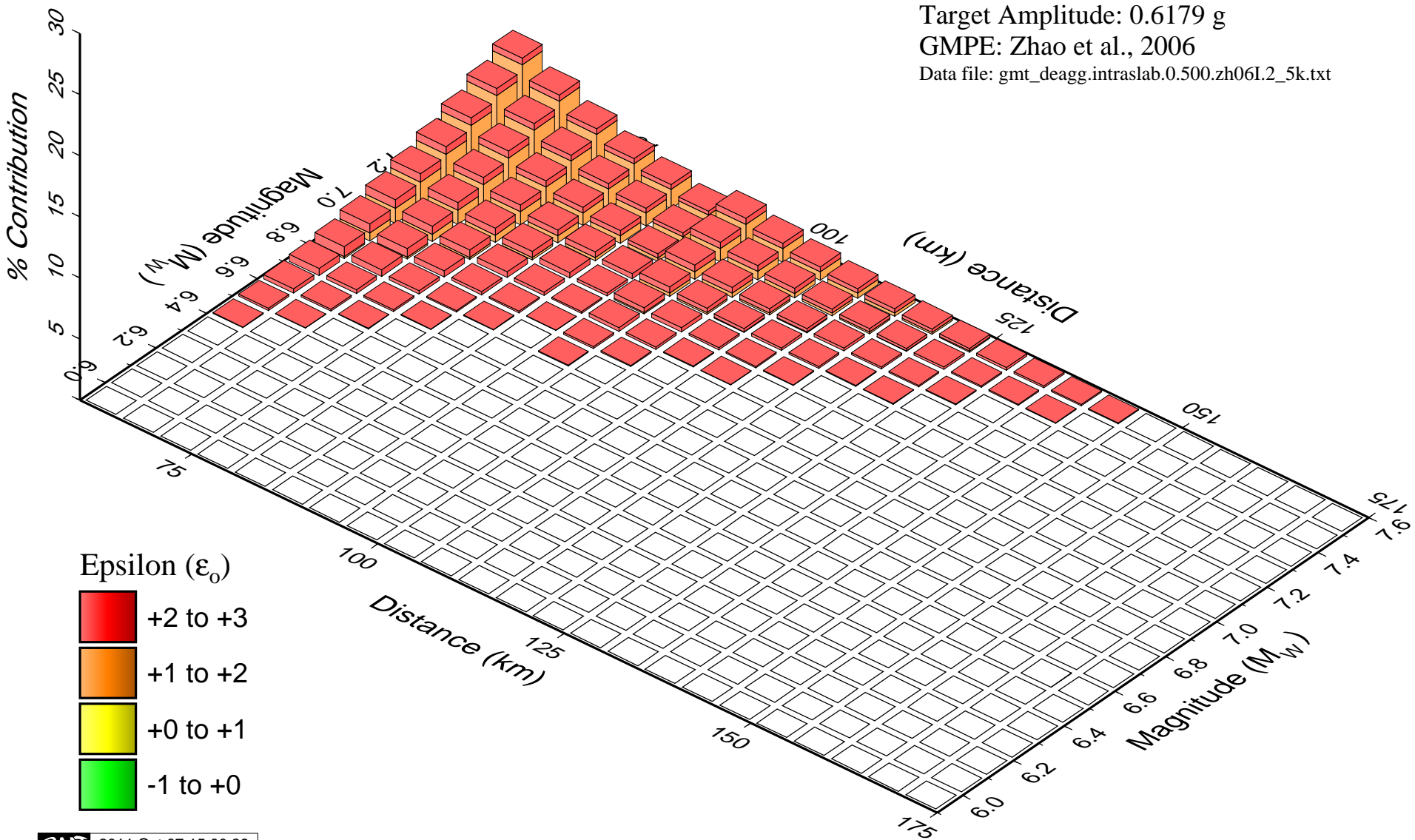
Data file: gmt_deagg.intraslab.0.500.zh06I.10k.txt



Watana Dam, AK

Seismic Hazard Deaggregation

Intraslab
0.500 sec.: 2,500 year return period
Target Amplitude: 0.6179 g
GMPE: Zhao et al., 2006
Data file: gmt_deagg.intraslab.0.500.zh06I.2_5k.txt



Watana Dam, AK

Seismic Hazard Deaggregation

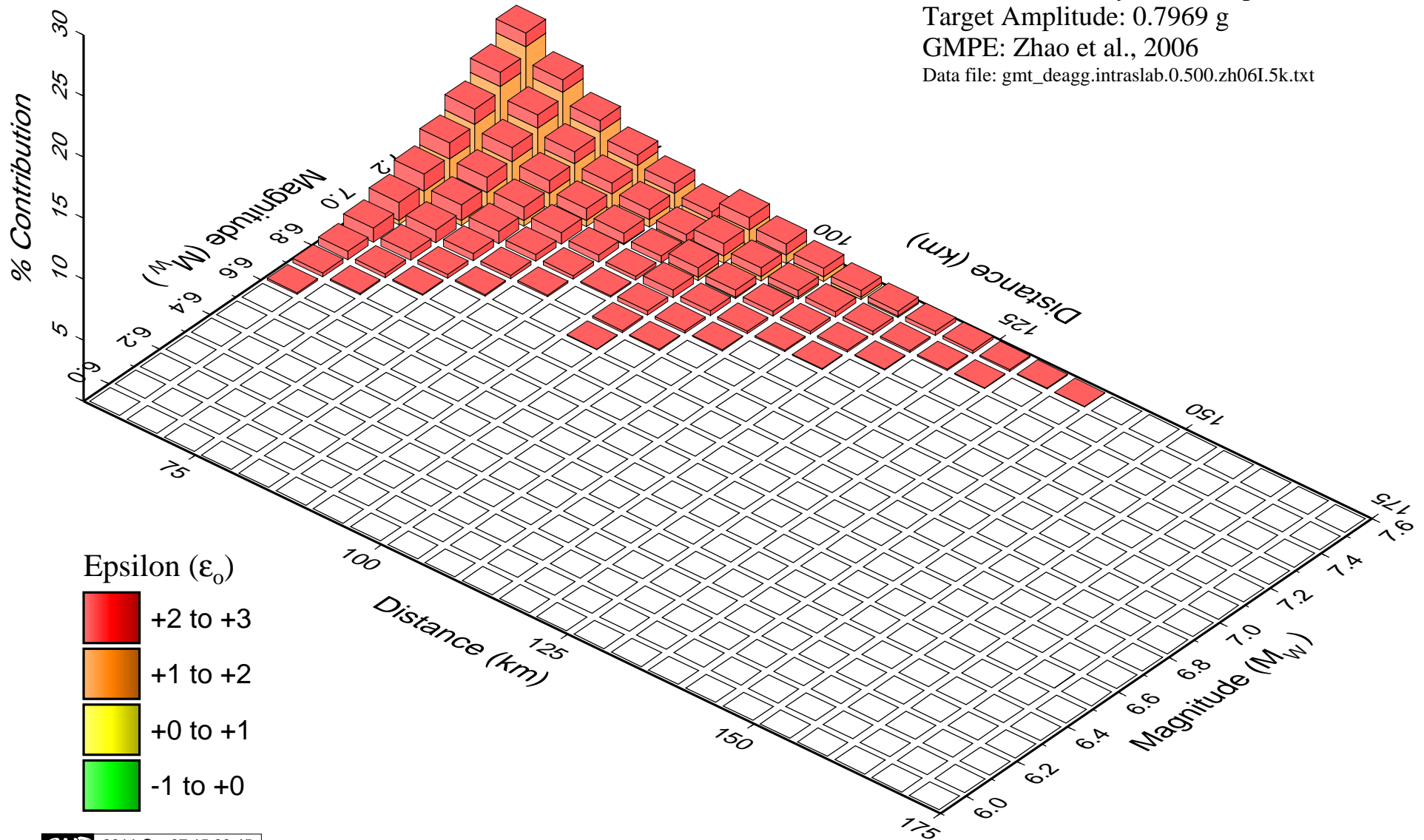
Intraslab

0.500 sec.: 5,000 year return period

Target Amplitude: 0.7969 g

GMPE: Zhao et al., 2006

Data file: gmt_deagg.intraslab.0.500.zh06I.5k.txt



Watana Dam, AK Seismic Hazard Deaggregation

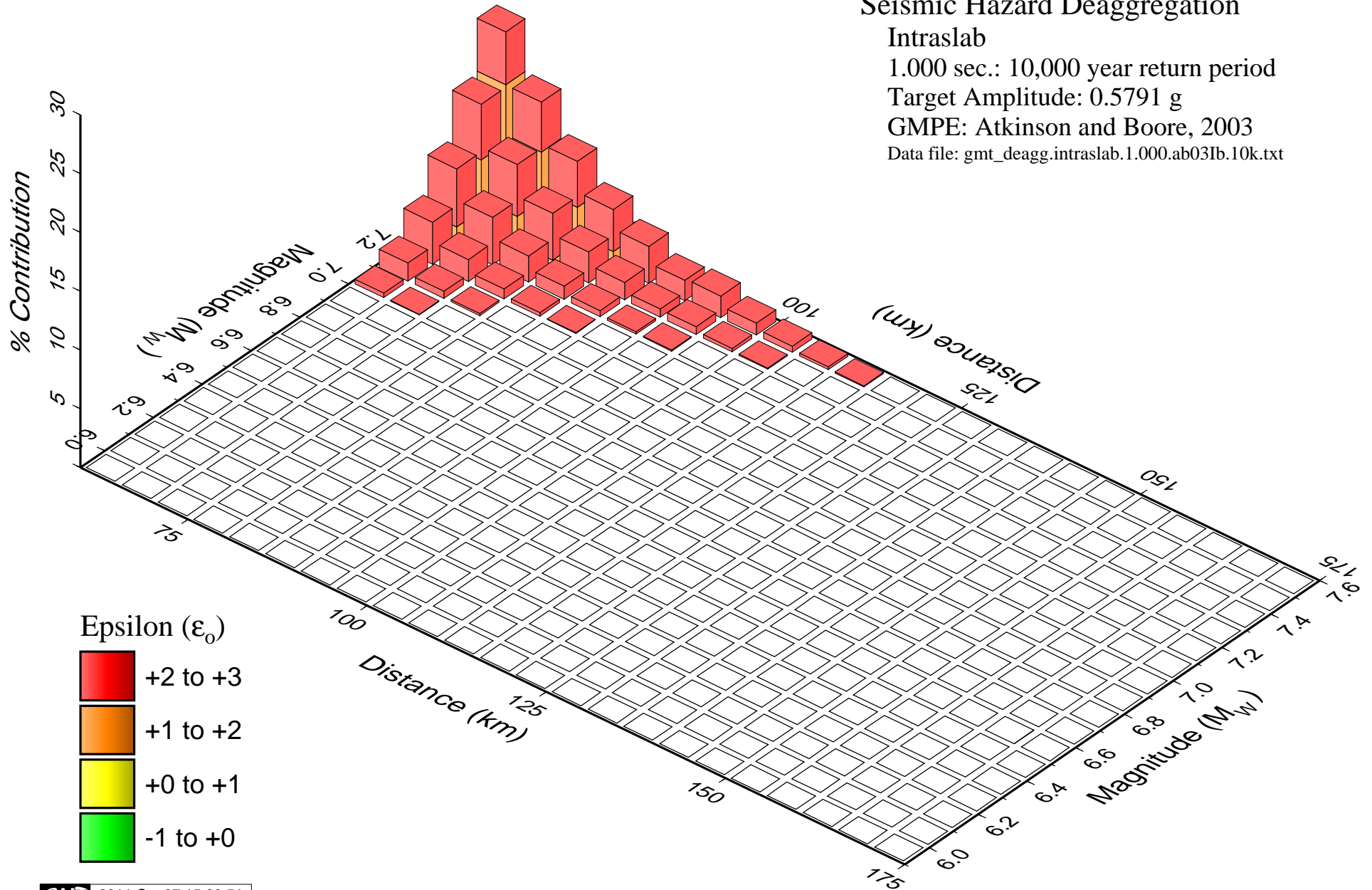
Intraslab

1.000 sec.: 10,000 year return period

Target Amplitude: 0.5791 g

GMPE: Atkinson and Boore, 2003

Data file: gmt_deagg.intraslab.1.000.ab03Ib.10k.txt



Watana Dam, AK

Seismic Hazard Deaggregation

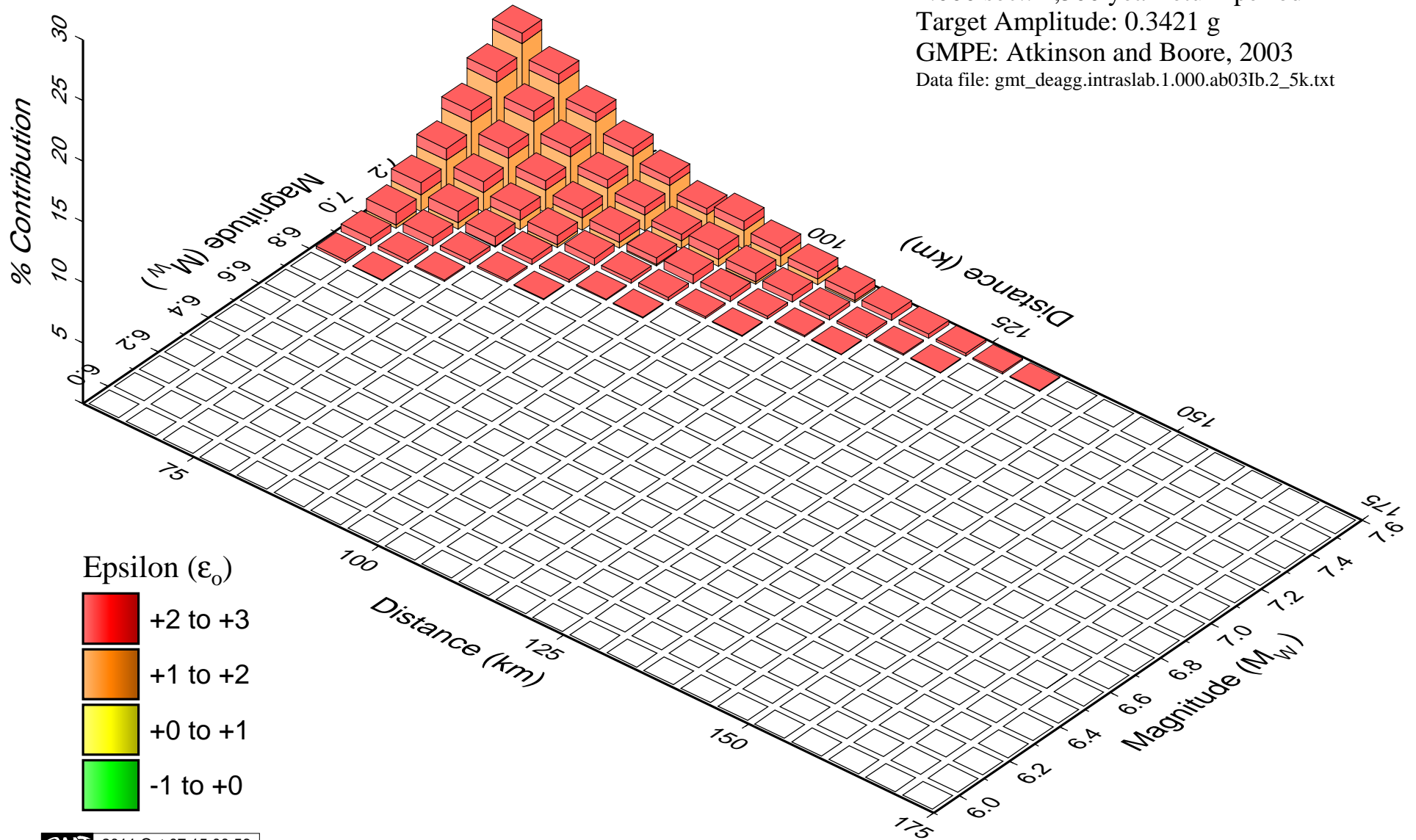
Intraslab

1.000 sec.: 2,500 year return period

Target Amplitude: 0.3421 g

GMPE: Atkinson and Boore, 2003

Data file: gmt_deagg.intraslab.1.000.ab03Ib.2_5k.txt



Watana Dam, AK Seismic Hazard Deaggregation

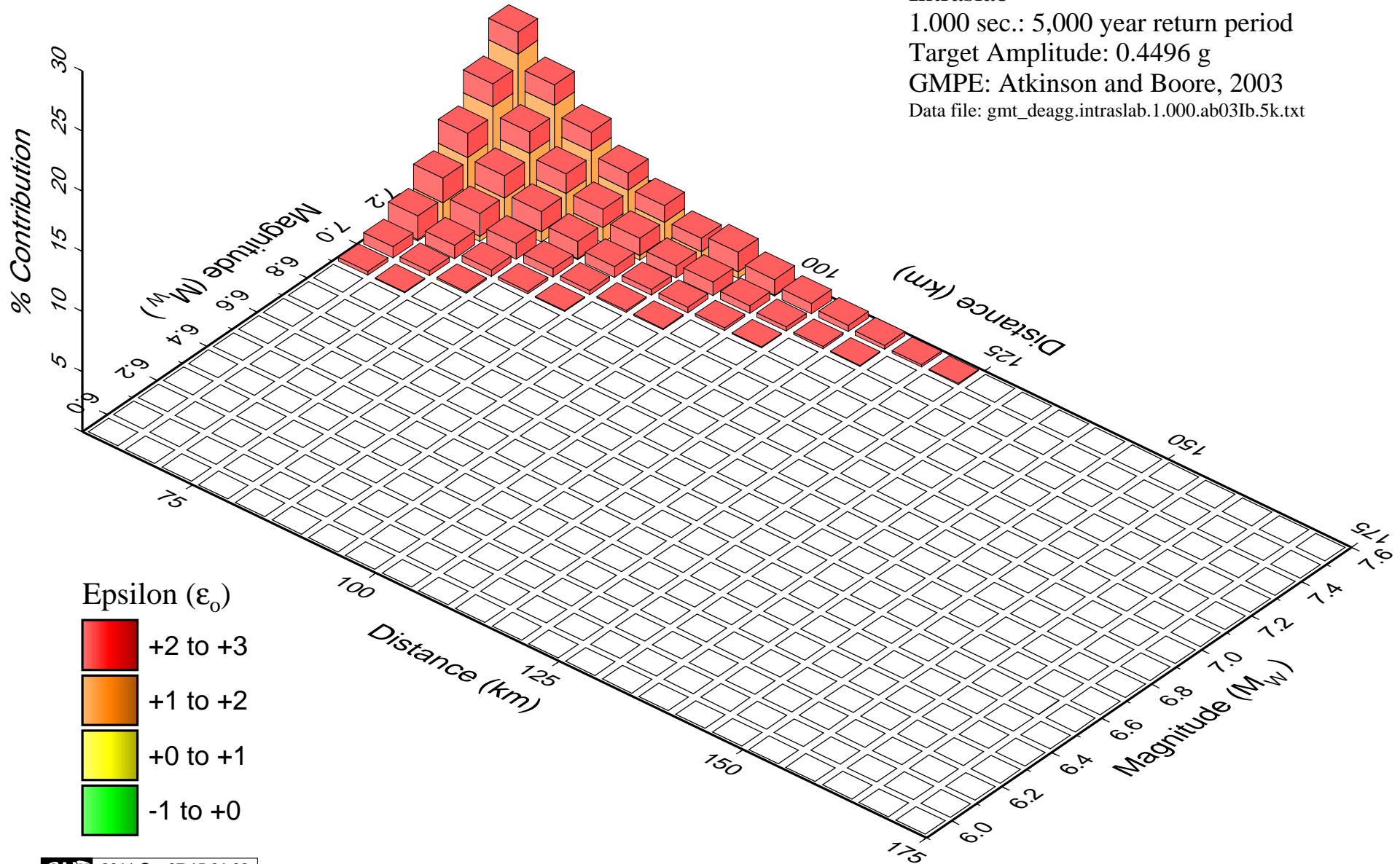
Intraslab

1.000 sec.: 5,000 year return period

Target Amplitude: 0.4496 g

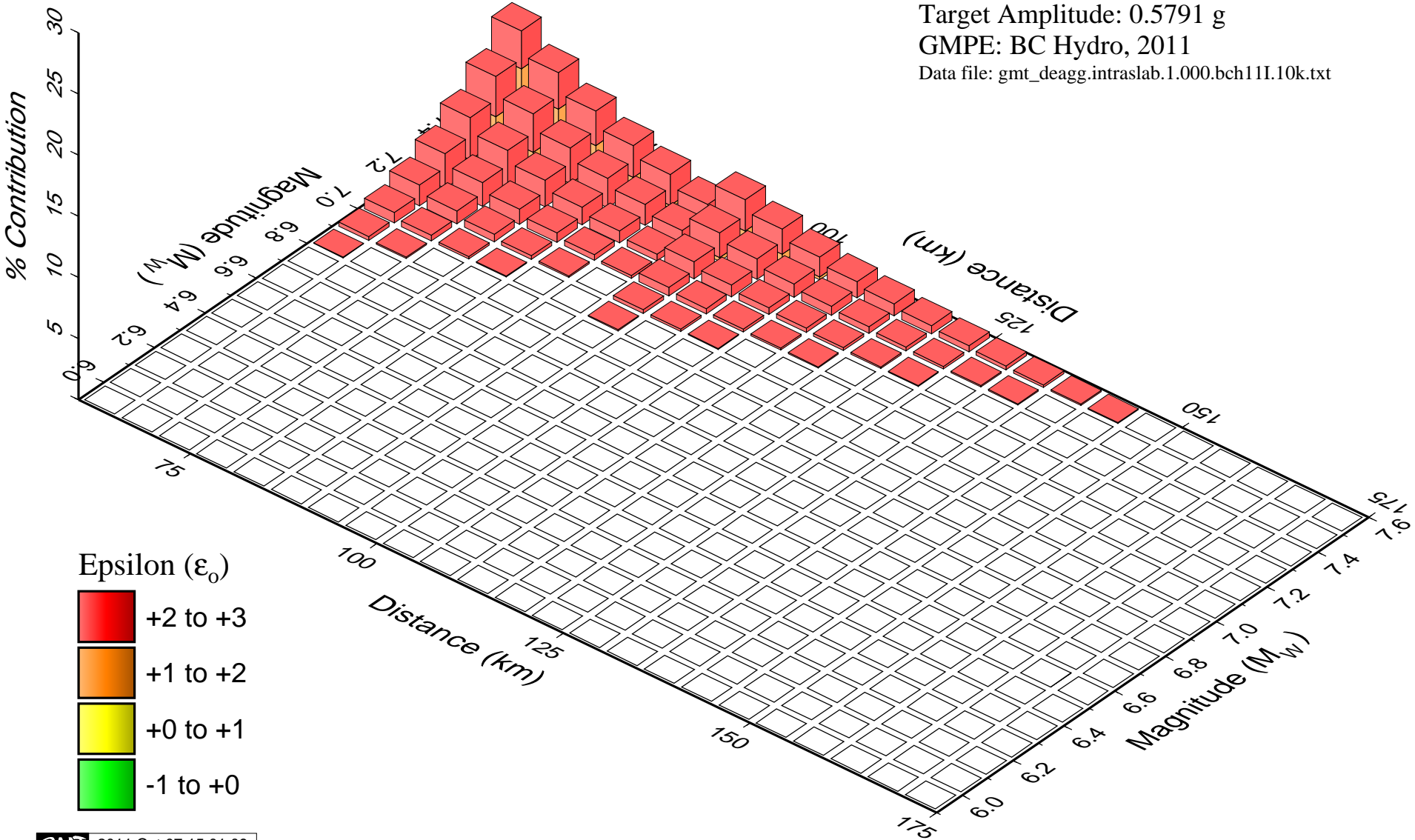
GMPE: Atkinson and Boore, 2003

Data file: gmt_deagg.intraslab.1.000.ab03Ib.5k.txt



Watana Dam, AK Seismic Hazard Deaggregation

Intraslab
1.000 sec.: 10,000 year return period
Target Amplitude: 0.5791 g
GMPE: BC Hydro, 2011
Data file: gmt_deagg.intraslab.1.000.bch11I.10k.txt



Watana Dam, AK Seismic Hazard Deaggregation

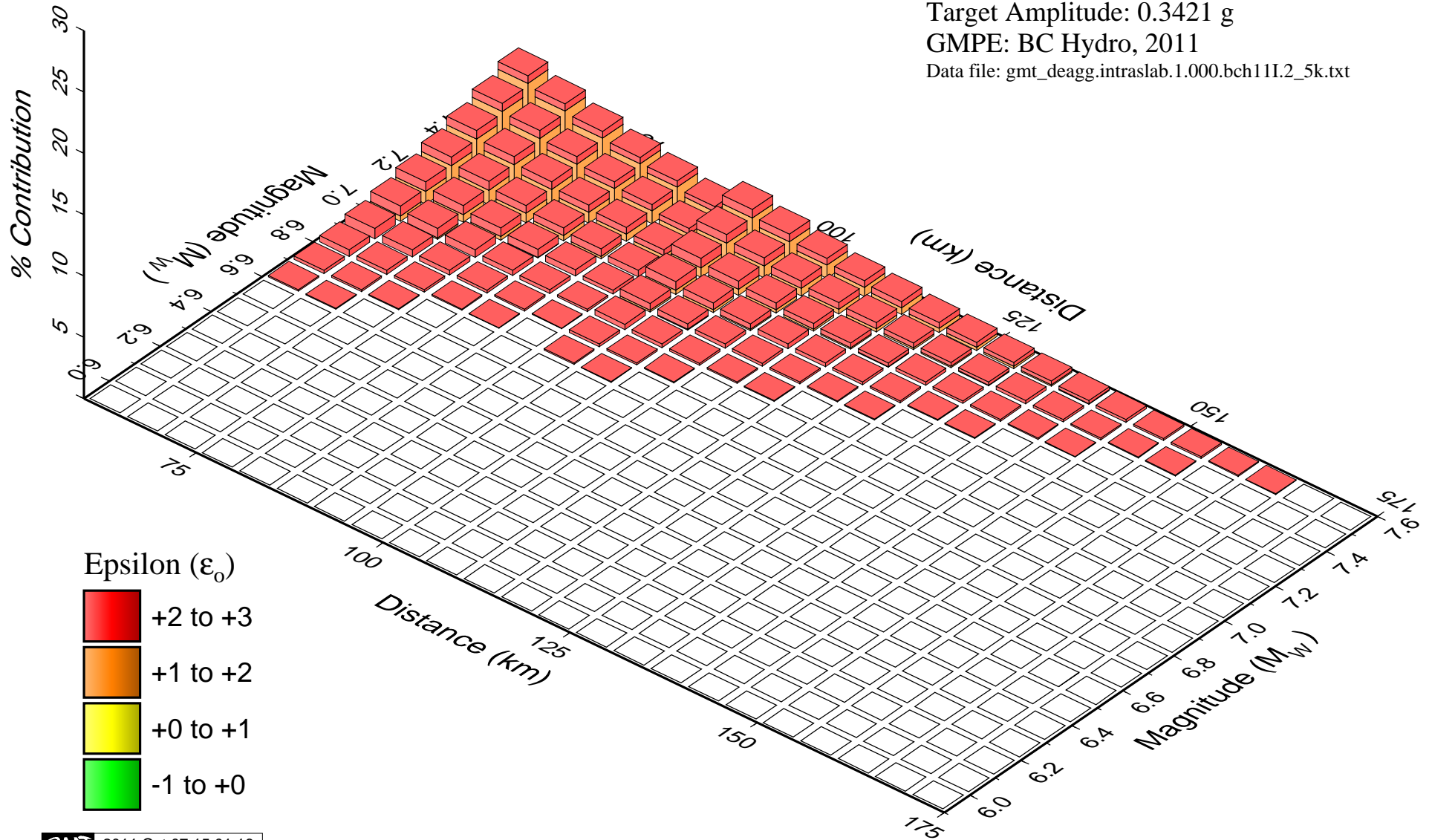
Intraslab

1.000 sec.: 2,500 year return period

Target Amplitude: 0.3421 g

GMPE: BC Hydro, 2011

Data file: gmt_deagg.intraslab.1.000.bch11I.2_5k.txt



Watana Dam, AK

Seismic Hazard Deaggregation

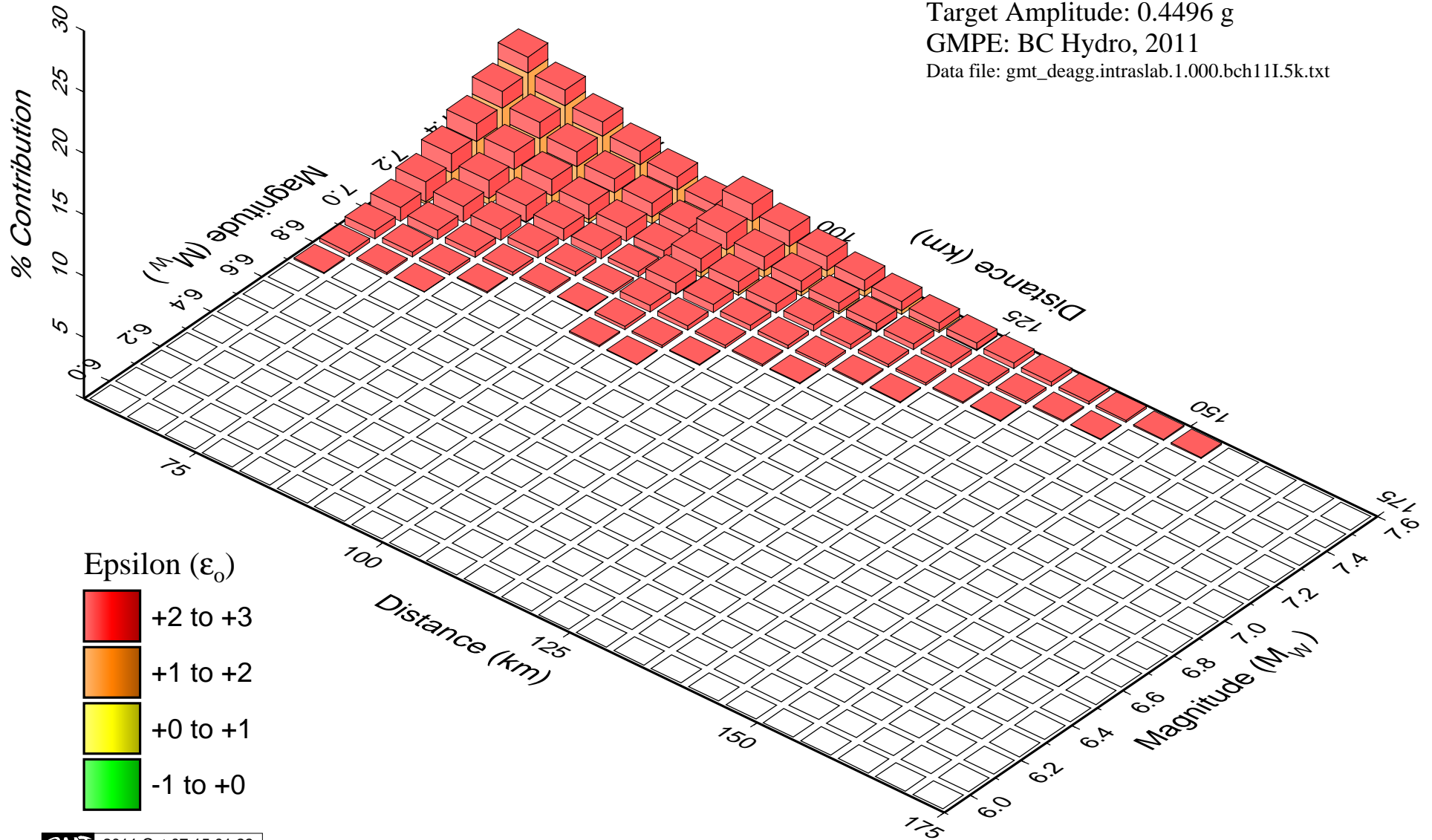
Intraslab

1.000 sec.: 5,000 year return period

Target Amplitude: 0.4496 g

GMPE: BC Hydro, 2011

Data file: gmt_deagg.intraslab.1.000.bch11I.5k.txt



Watana Dam, AK

Seismic Hazard Deaggregation

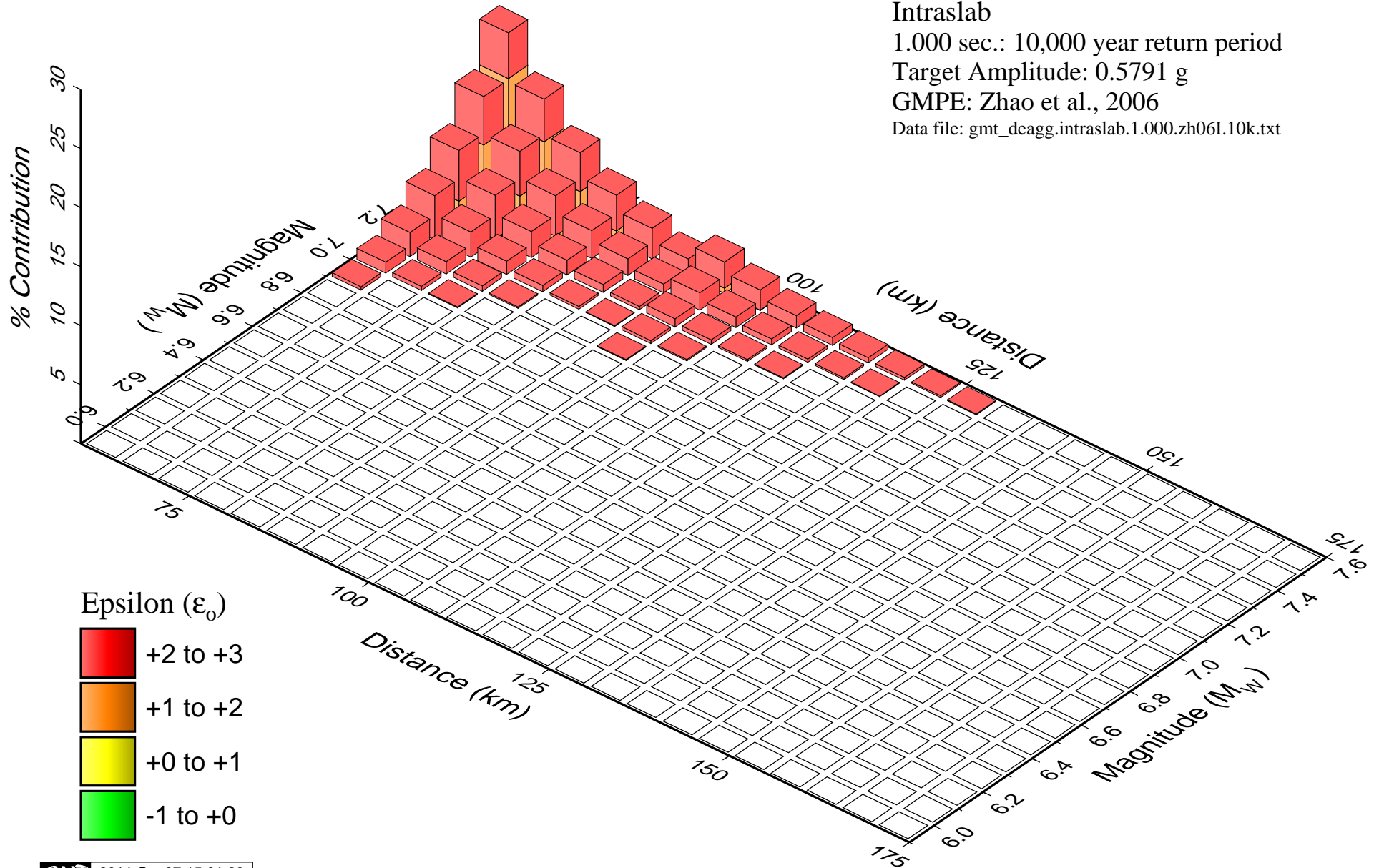
Intraslab

1.000 sec.: 10,000 year return period

Target Amplitude: 0.5791 g

GMPE: Zhao et al., 2006

Data file: gmt_deagg.intraslab.1.000.zh06I.10k.txt



Watana Dam, AK

Seismic Hazard Deaggregation

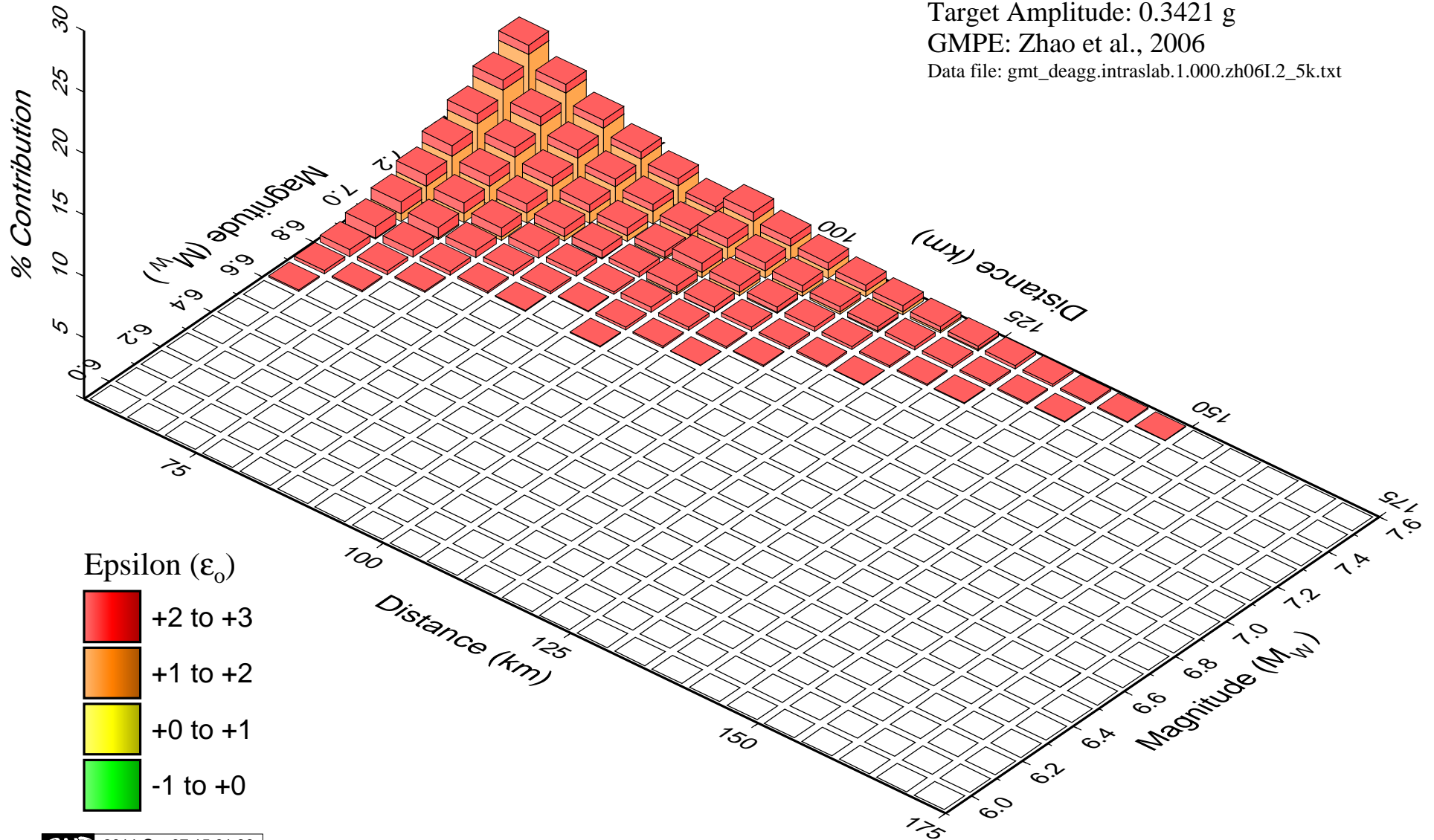
Intraslab

1.000 sec.: 2,500 year return period

Target Amplitude: 0.3421 g

GMPE: Zhao et al., 2006

Data file: gmt_deagg.intraslab.1.000.zh06I.2_5k.txt



Watana Dam, AK

Seismic Hazard Deaggregation

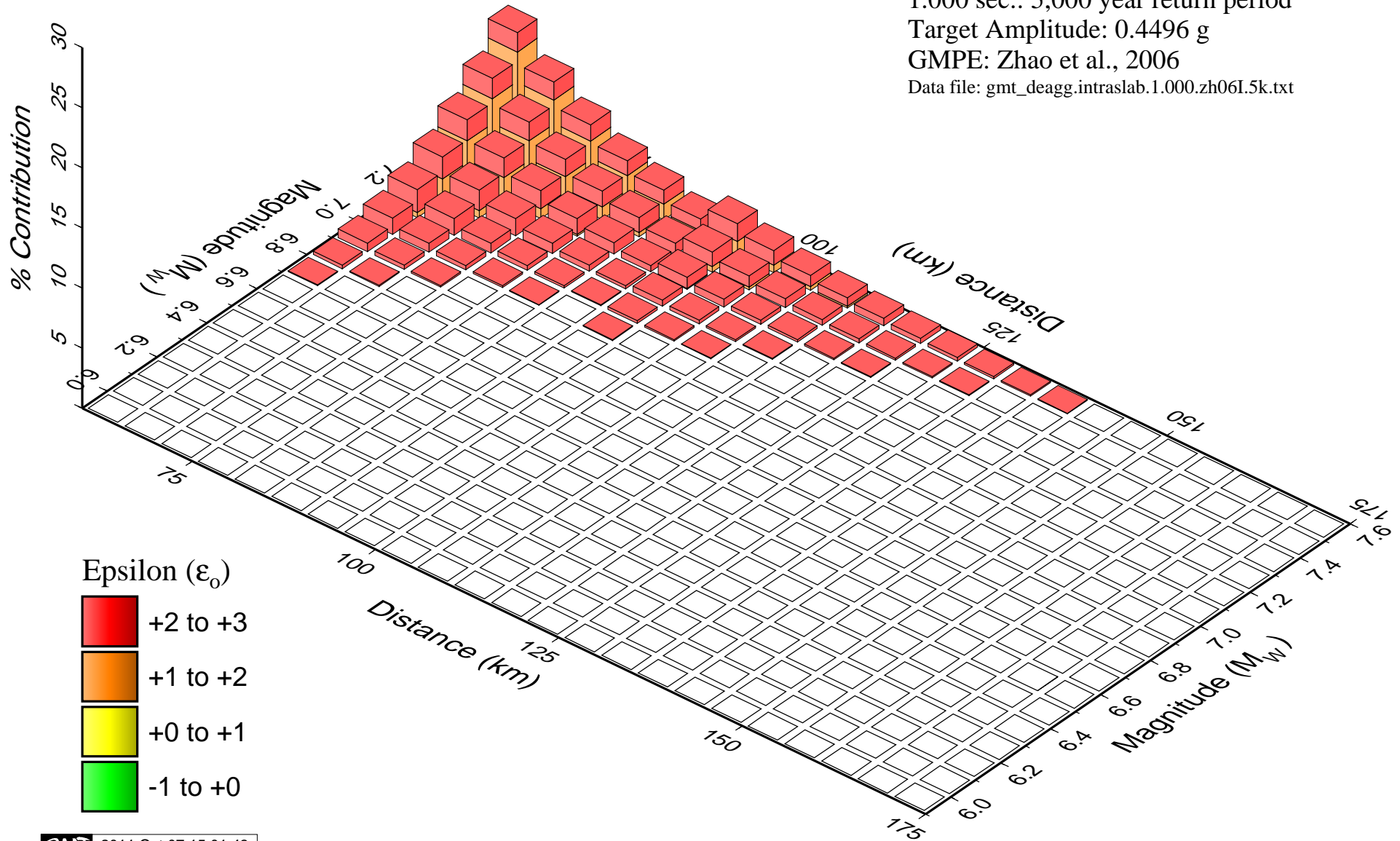
Intraslab

1.000 sec.: 5,000 year return period

Target Amplitude: 0.4496 g

GMPE: Zhao et al., 2006

Data file: gmt_deagg.intraslab.1.000.zh06I.5k.txt



Watana Dam, AK

Seismic Hazard Deaggregation

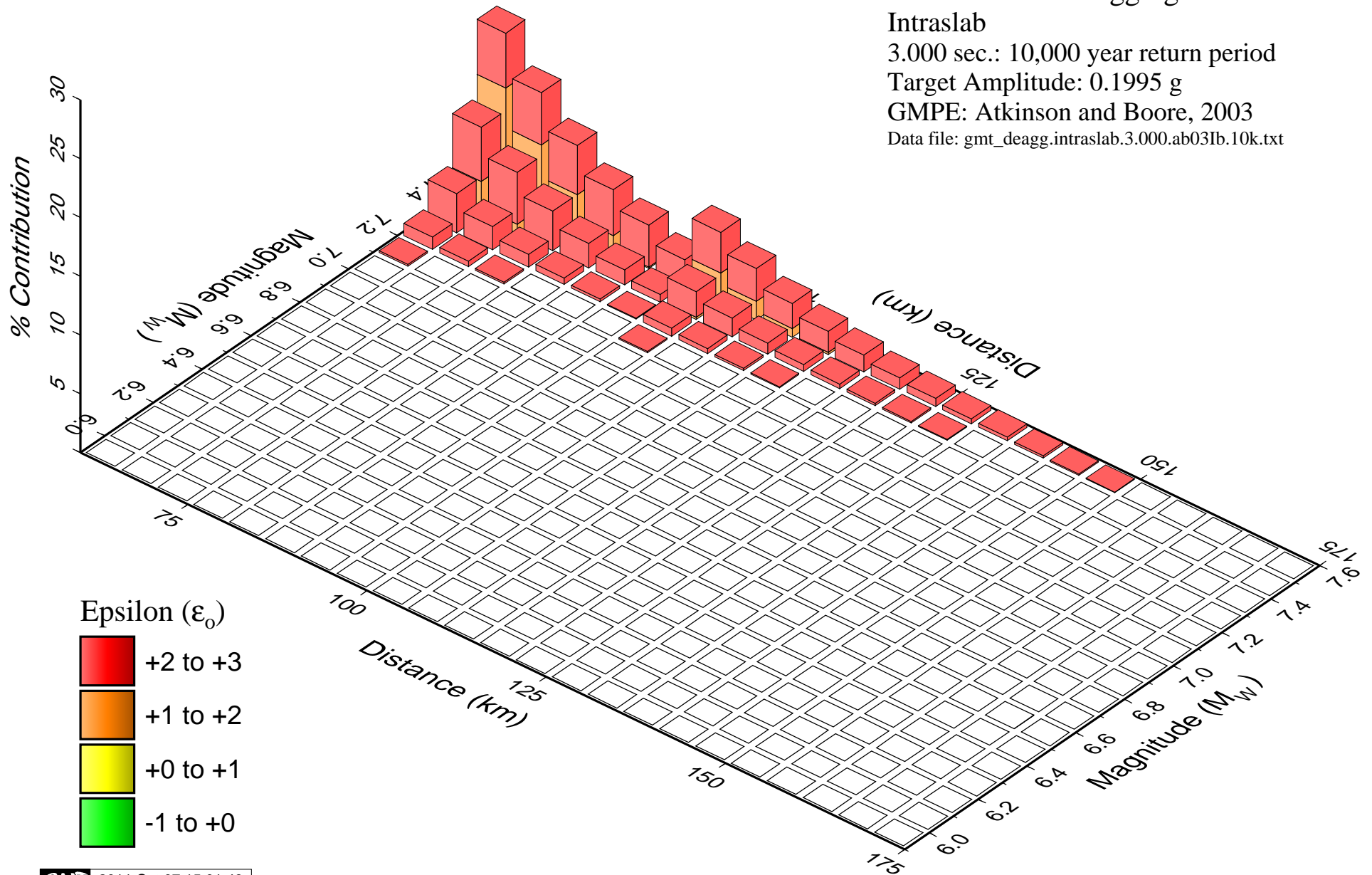
Intraslab

3.000 sec.: 10,000 year return period

Target Amplitude: 0.1995 g

GMPE: Atkinson and Boore, 2003

Data file: gmt_deagg.intraslab.3.000.ab03Ib.10k.txt



Watana Dam, AK

Seismic Hazard Deaggregation

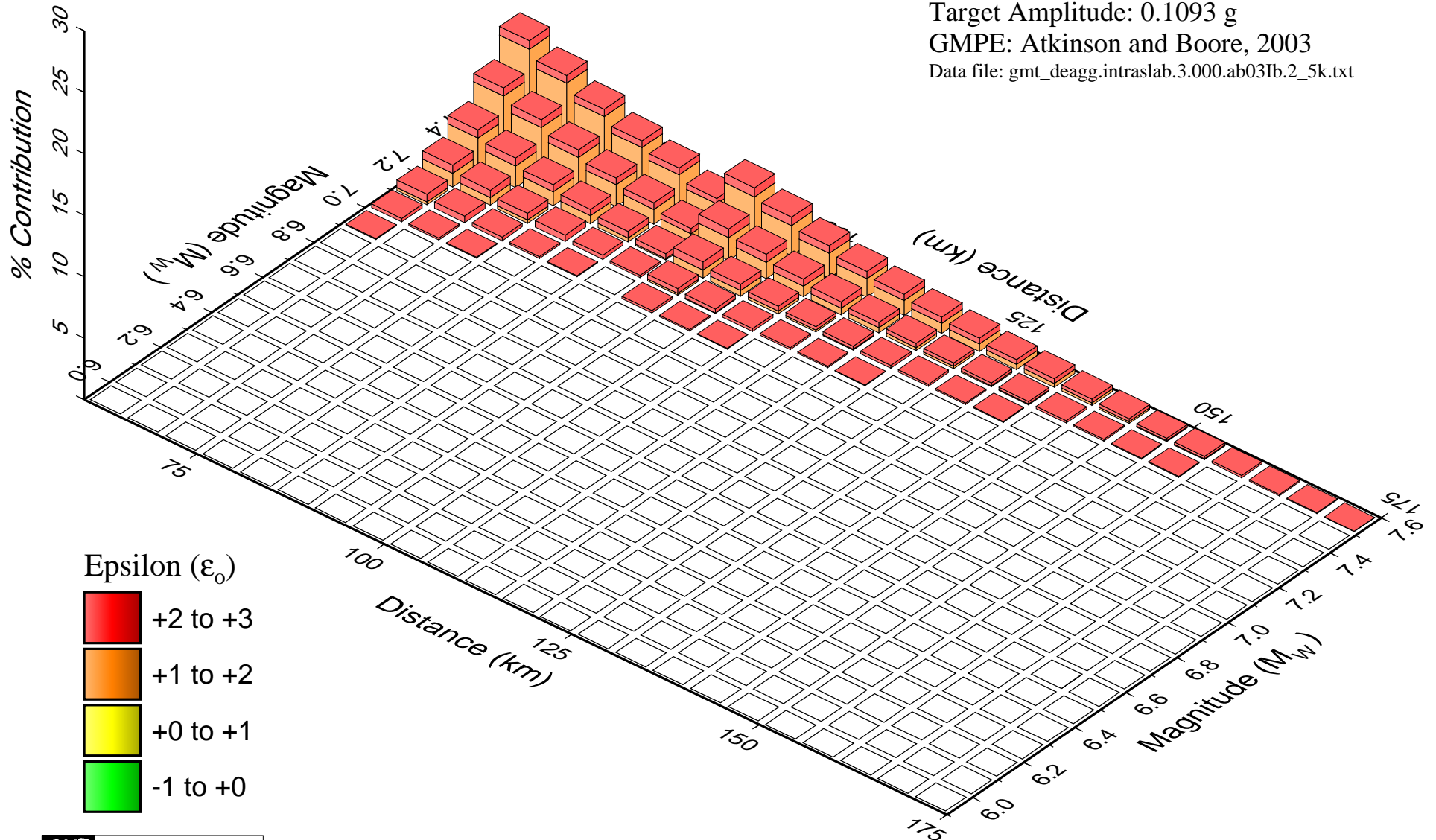
Intraslab

3.000 sec.: 2,500 year return period

Target Amplitude: 0.1093 g

GMPE: Atkinson and Boore, 2003

Data file: gmt_deagg.intraslab.3.000.ab03Ib.2_5k.txt



Watana Dam, AK

Seismic Hazard Deaggregation

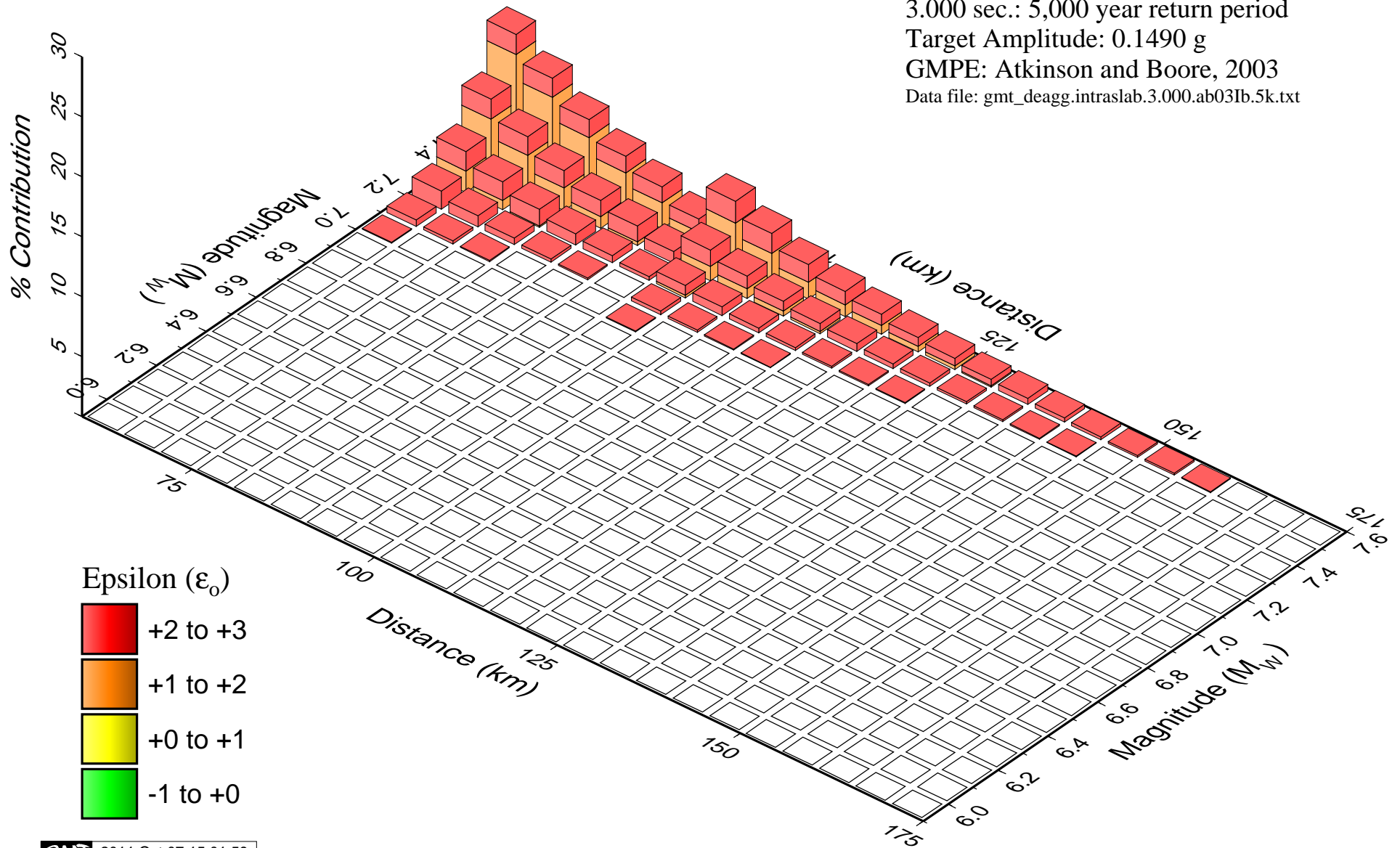
Intraslab

3.000 sec.: 5,000 year return period

Target Amplitude: 0.1490 g

GMPE: Atkinson and Boore, 2003

Data file: gmt_deagg.intraslab.3.000.ab03Ib.5k.txt



Watana Dam, AK Seismic Hazard Deaggregation

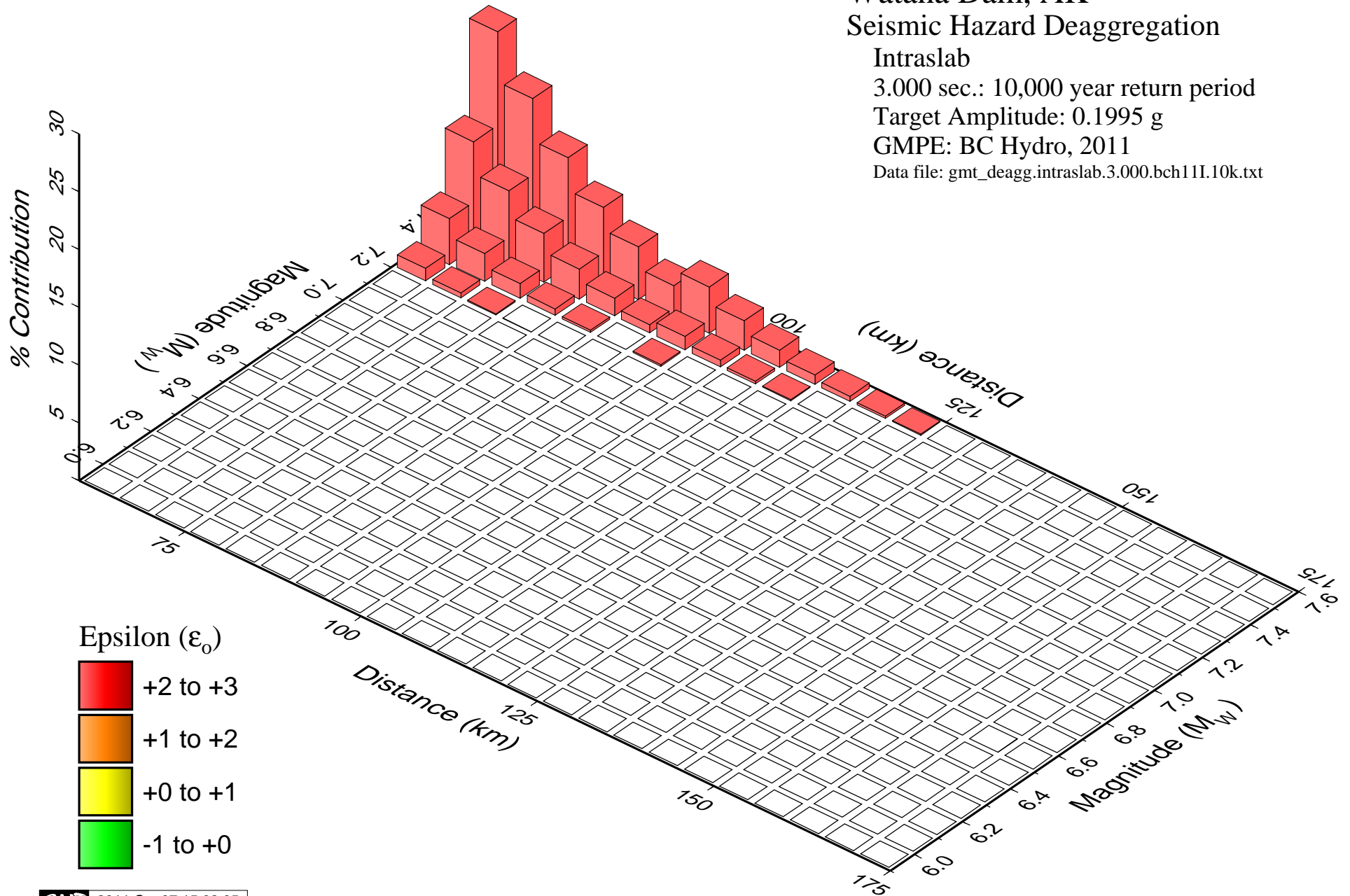
Intraslab

3.000 sec.: 10,000 year return period

Target Amplitude: 0.1995 g

GMPE: BC Hydro, 2011

Data file: gmt_deagg.intraslab.3.000.bch11I.10k.txt



Watana Dam, AK Seismic Hazard Deaggregation

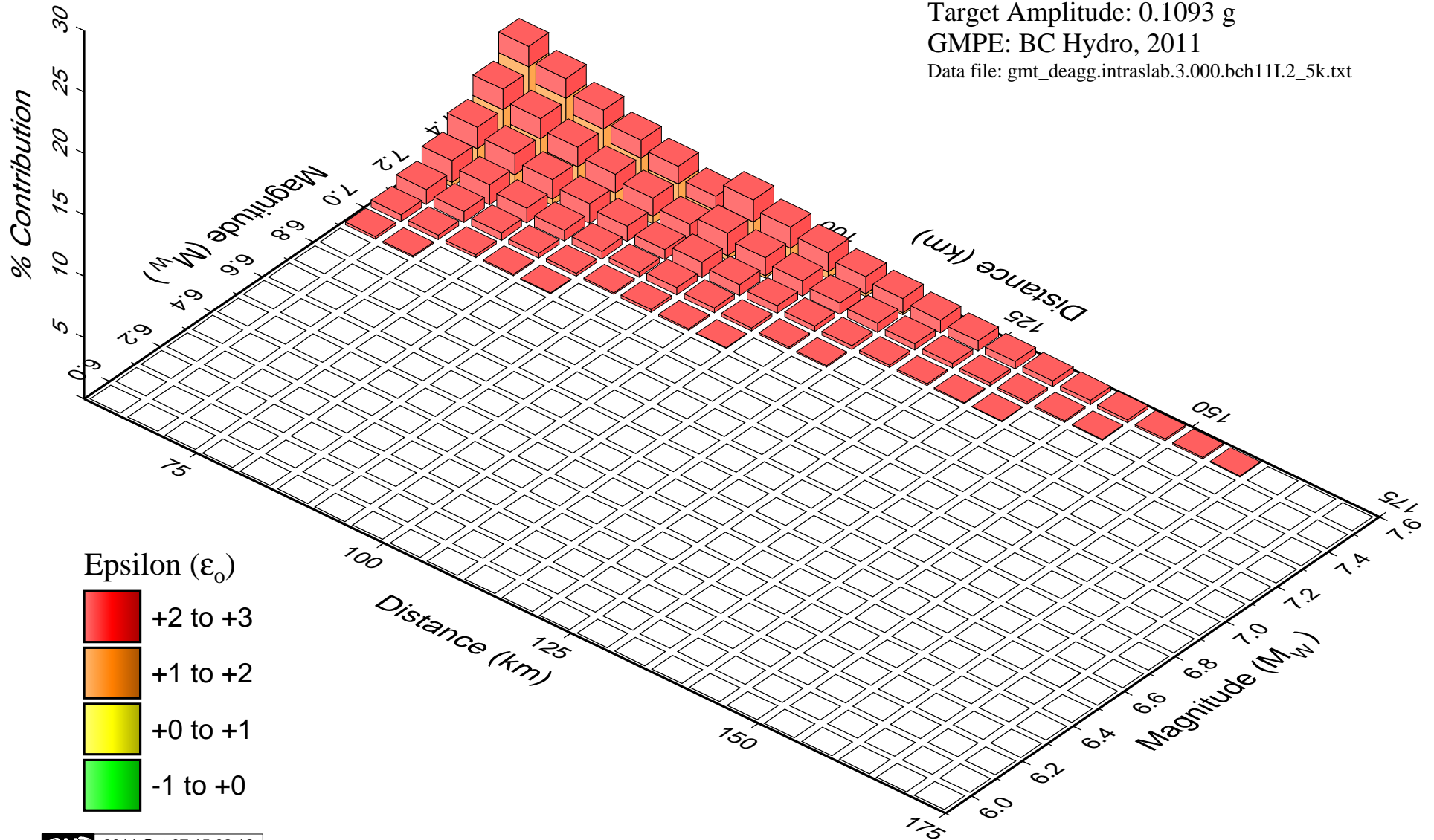
Intraslab

3.000 sec.: 2,500 year return period

Target Amplitude: 0.1093 g

GMPE: BC Hydro, 2011

Data file: gmt_deagg.intraslab.3.000.bch11I.2_5k.txt



Watana Dam, AK

Seismic Hazard Deaggregation

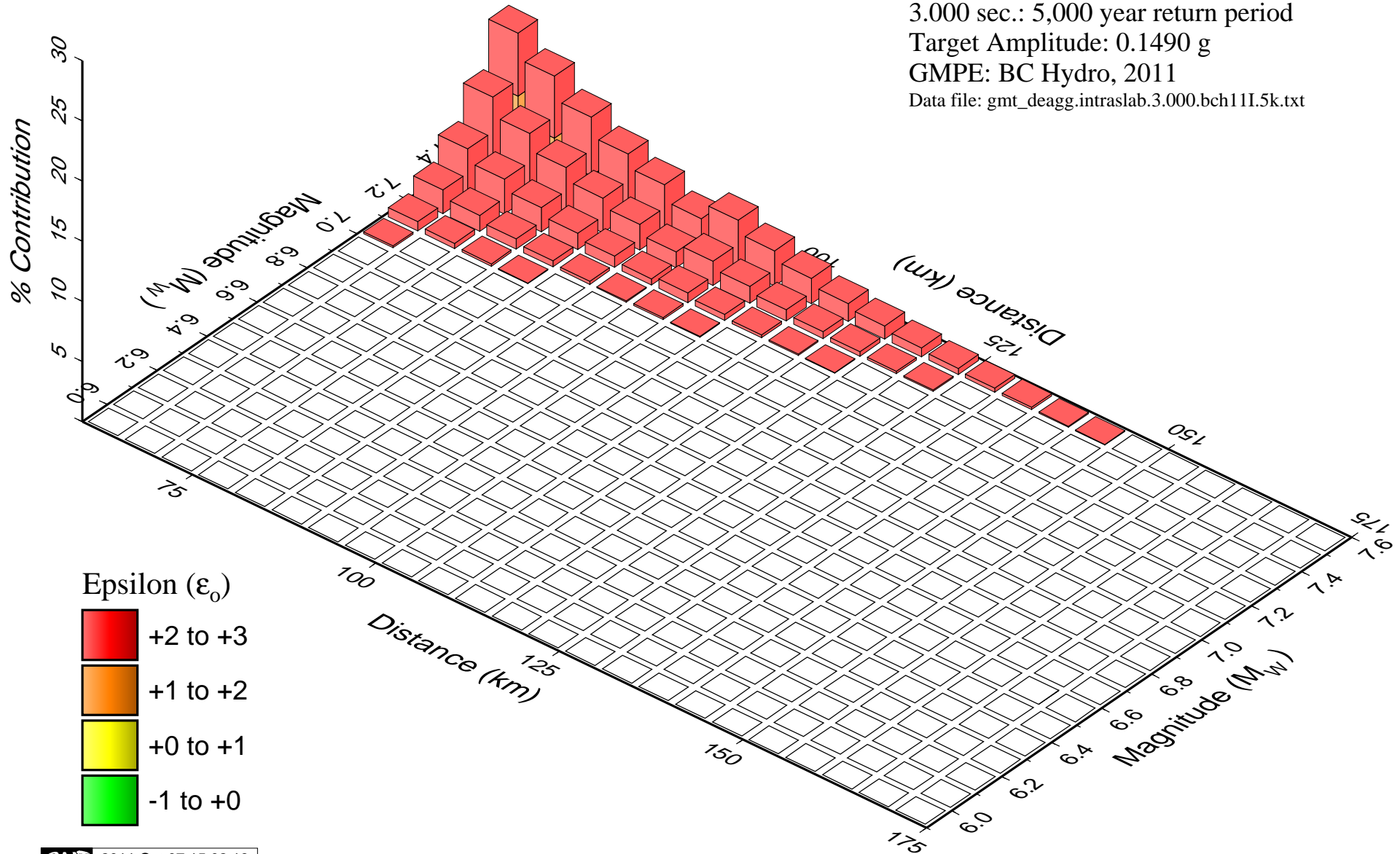
Intraslab

3.000 sec.: 5,000 year return period

Target Amplitude: 0.1490 g

GMPE: BC Hydro, 2011

Data file: gmt_deagg.intraslab.3.000.bch11I.5k.txt



Watana Dam, AK Seismic Hazard Deaggregation

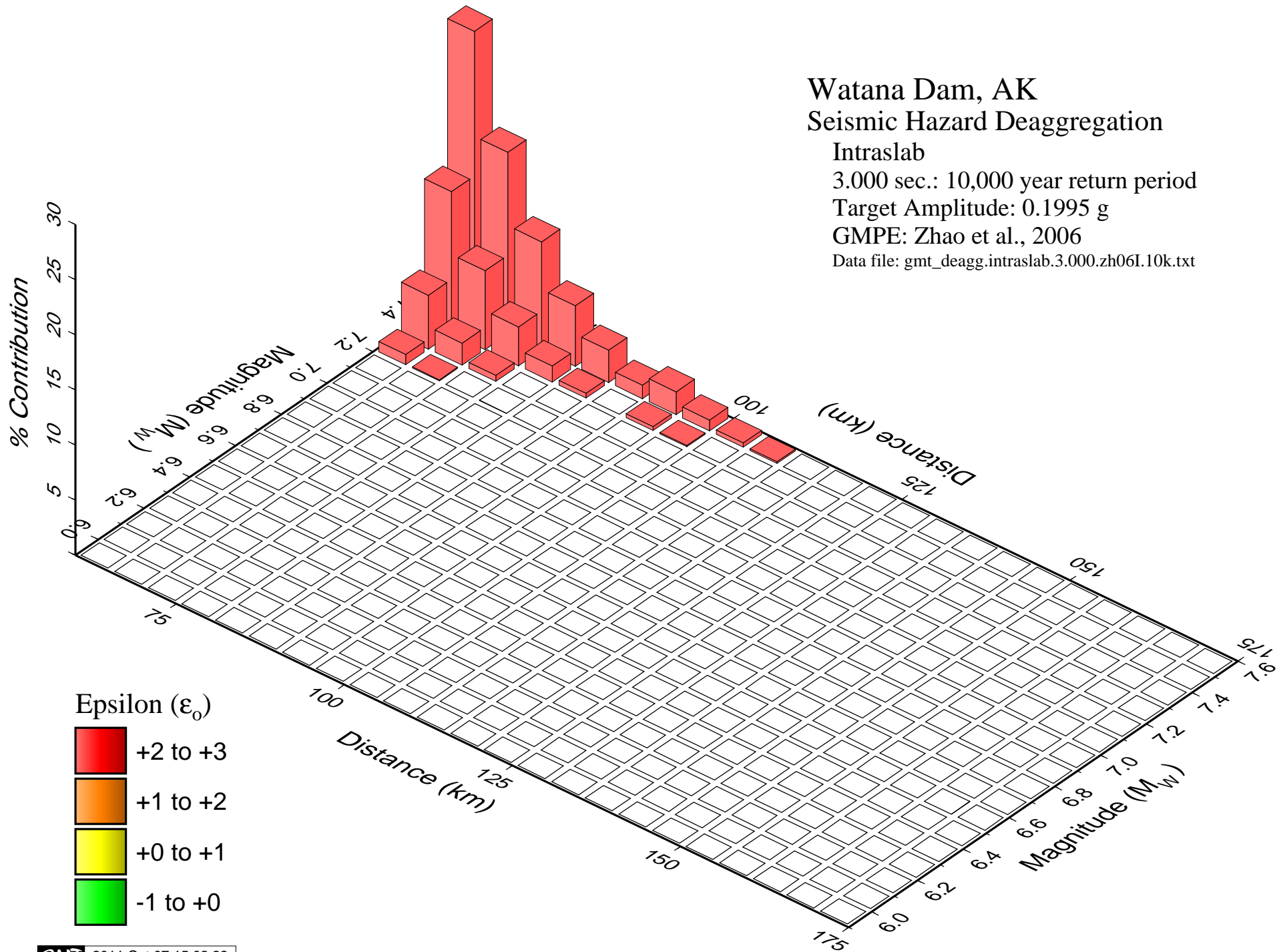
Intraslab

3.000 sec.: 10,000 year return period

Target Amplitude: 0.1995 g

GMPE: Zhao et al., 2006

Data file: gmt_deagg.intraslab.3.000.zh06I.10k.txt



Watana Dam, AK

Seismic Hazard Deaggregation

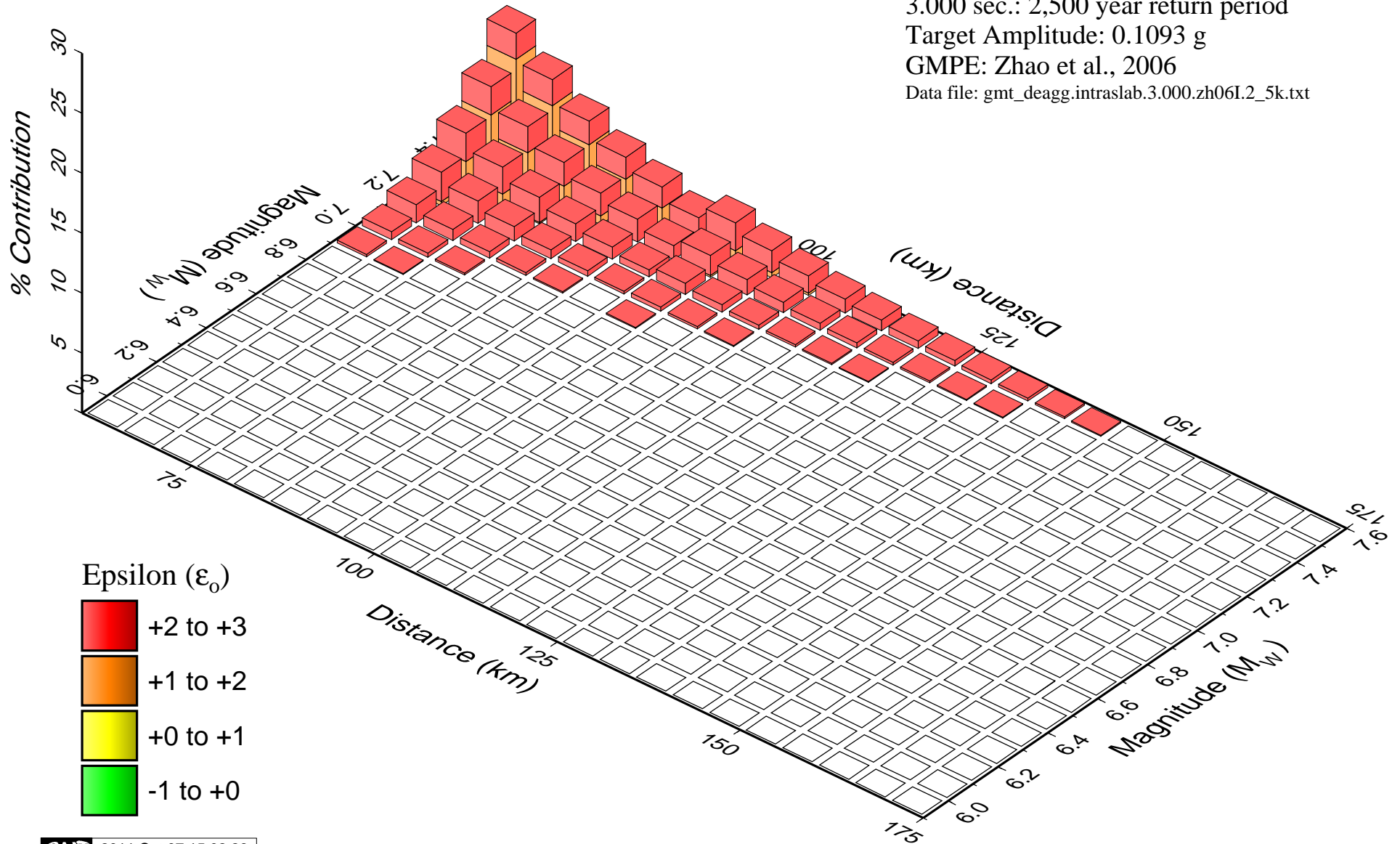
Intraslab

3.000 sec.: 2,500 year return period

Target Amplitude: 0.1093 g

GMPE: Zhao et al., 2006

Data file: gmt_deagg.intraslab.3.000.zh06I.2_5k.txt



Watana Dam, AK

Seismic Hazard Deaggregation

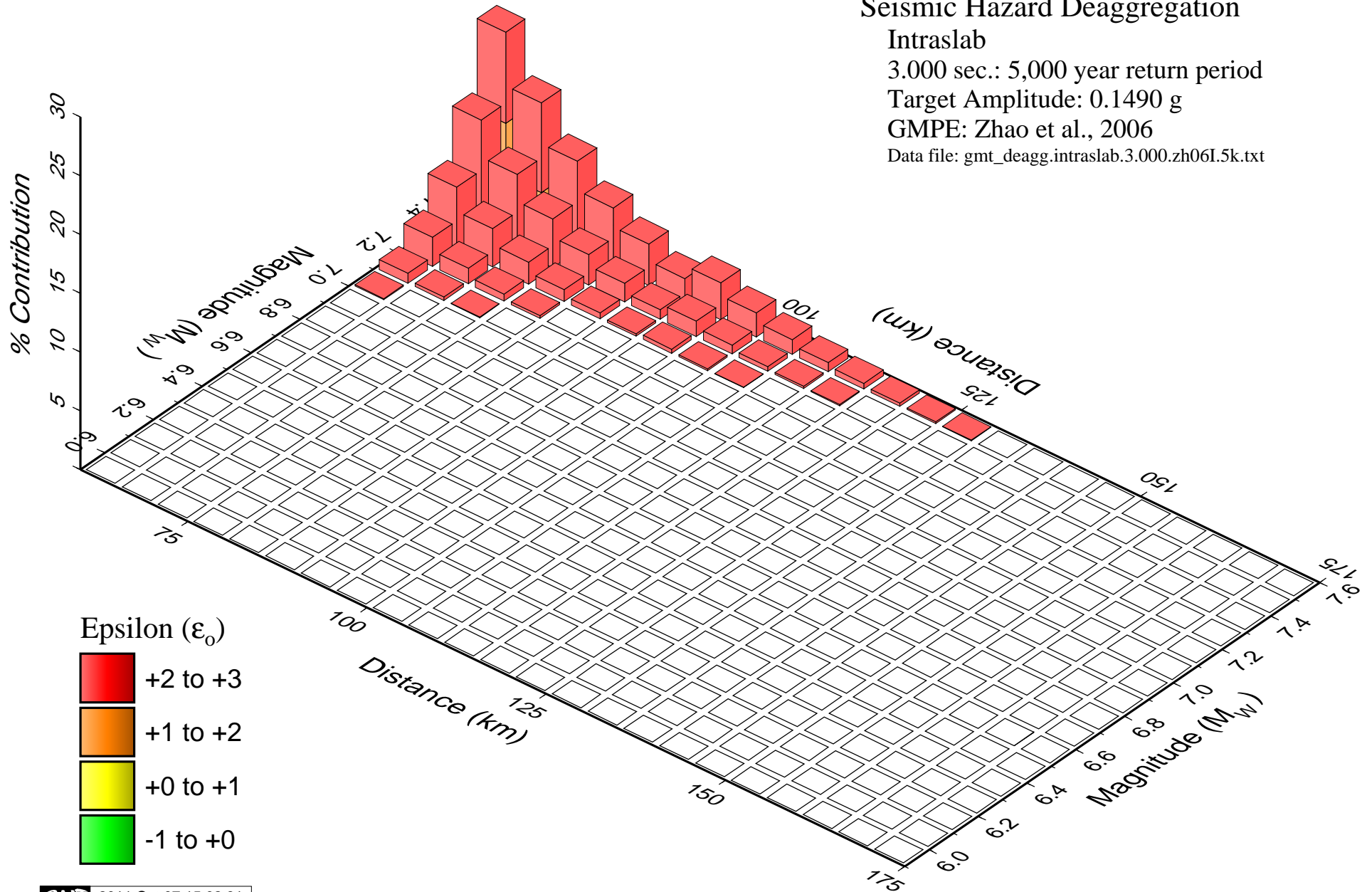
Intraslab

3.000 sec.: 5,000 year return period

Target Amplitude: 0.1490 g

GMPE: Zhao et al., 2006

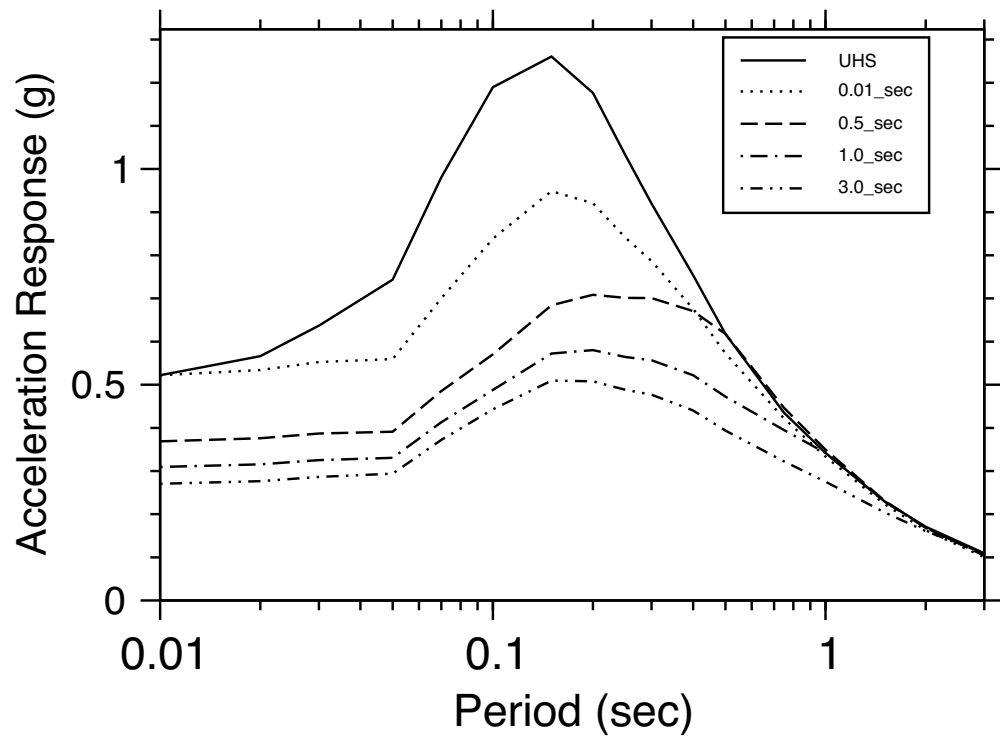
Data file: gmt_deagg.intraslab.3.000.zh06I.5k.txt



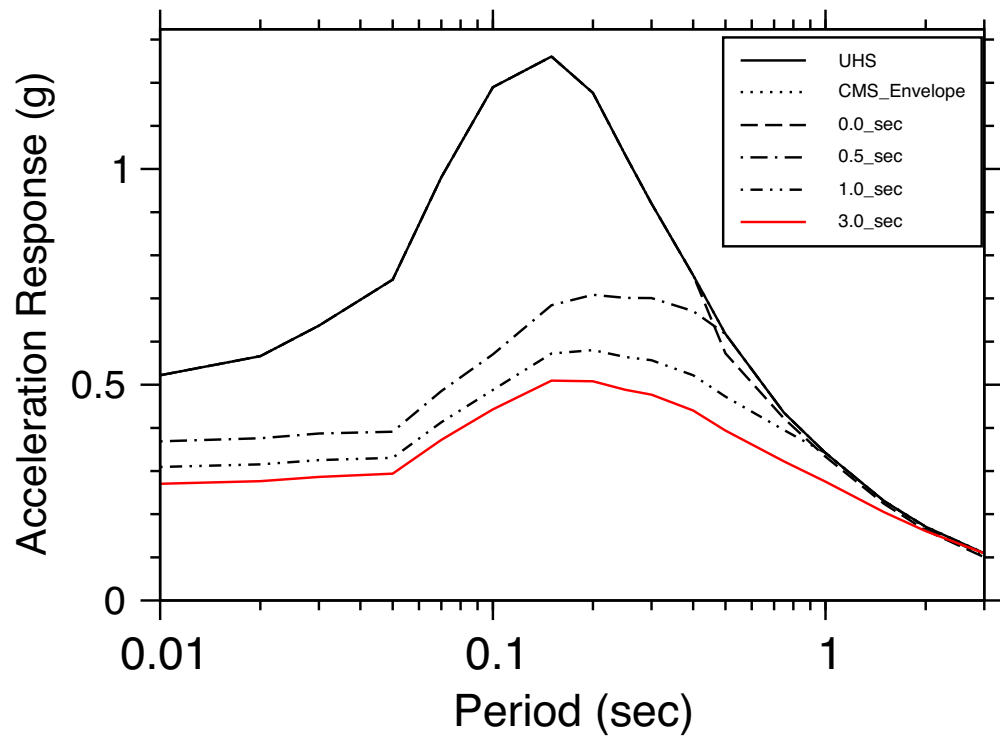
Appendix C – CONDITIONAL MEAN SPECTRA RESULTS

Cover Page

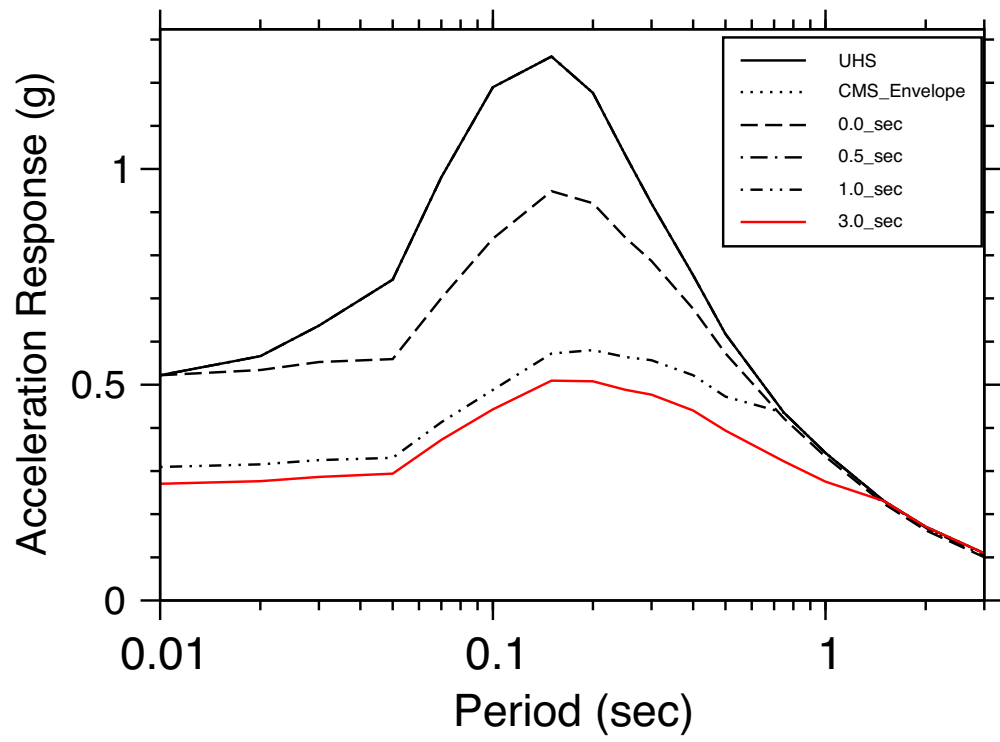
Interface, 2500 yrs



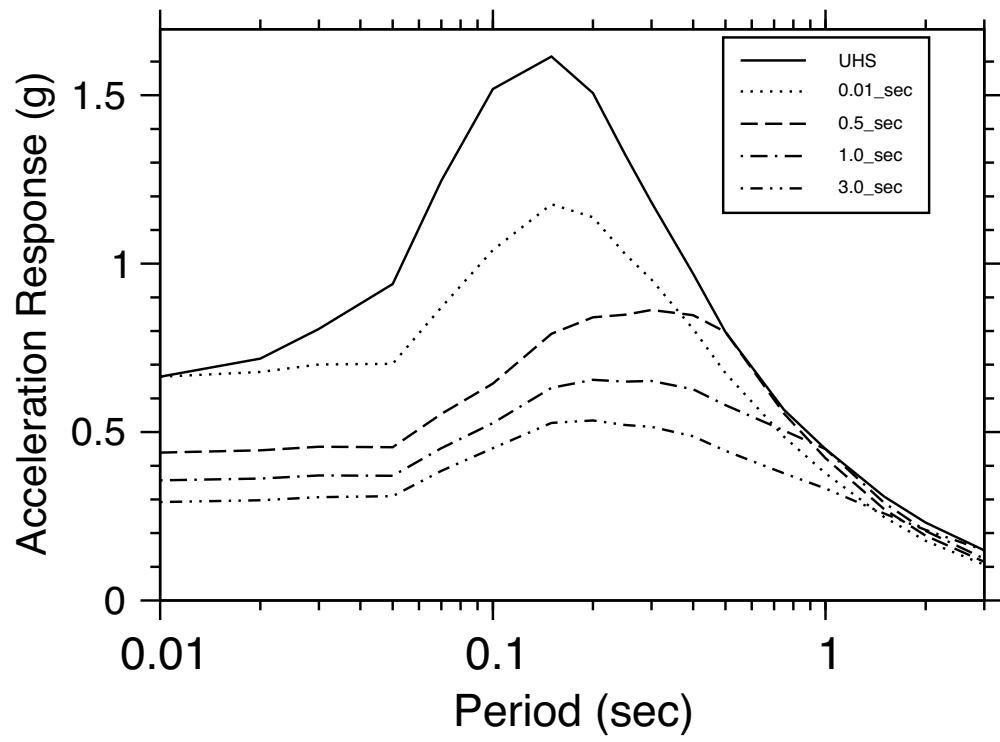
Interface, 2500 yrs



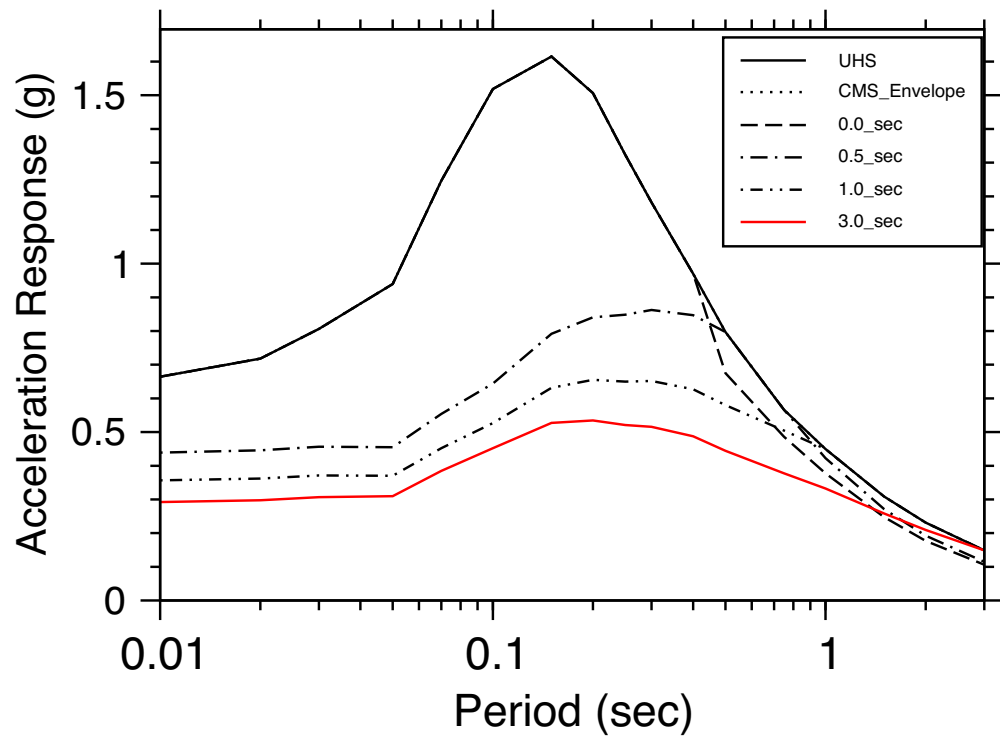
Interface, 2500 yrs



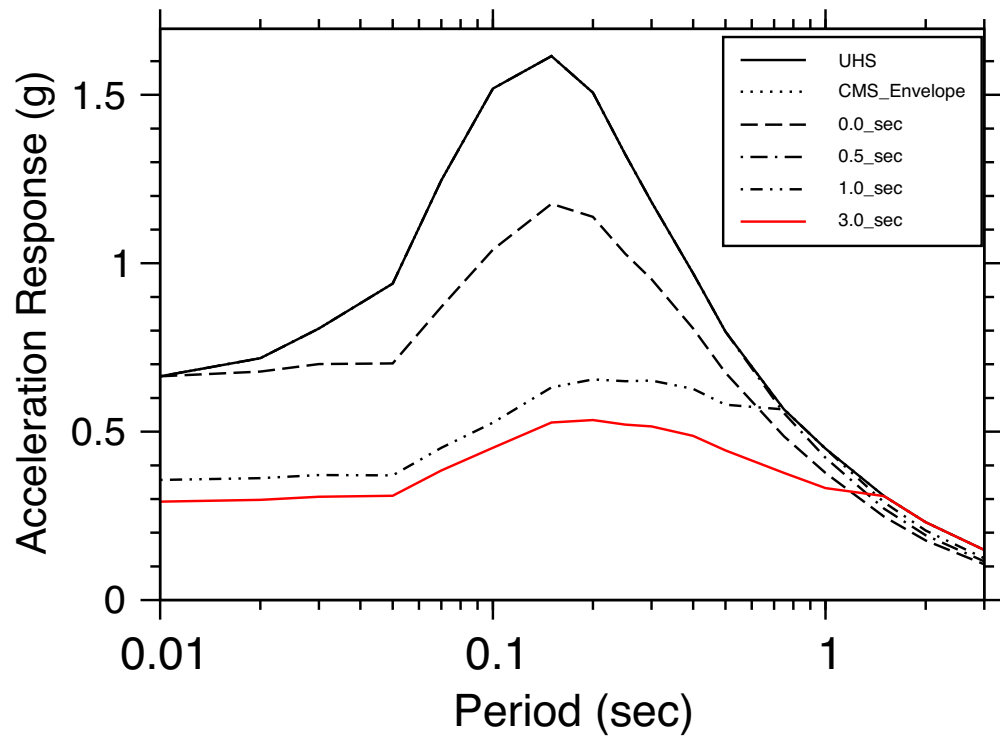
Interface, 5000 yrs



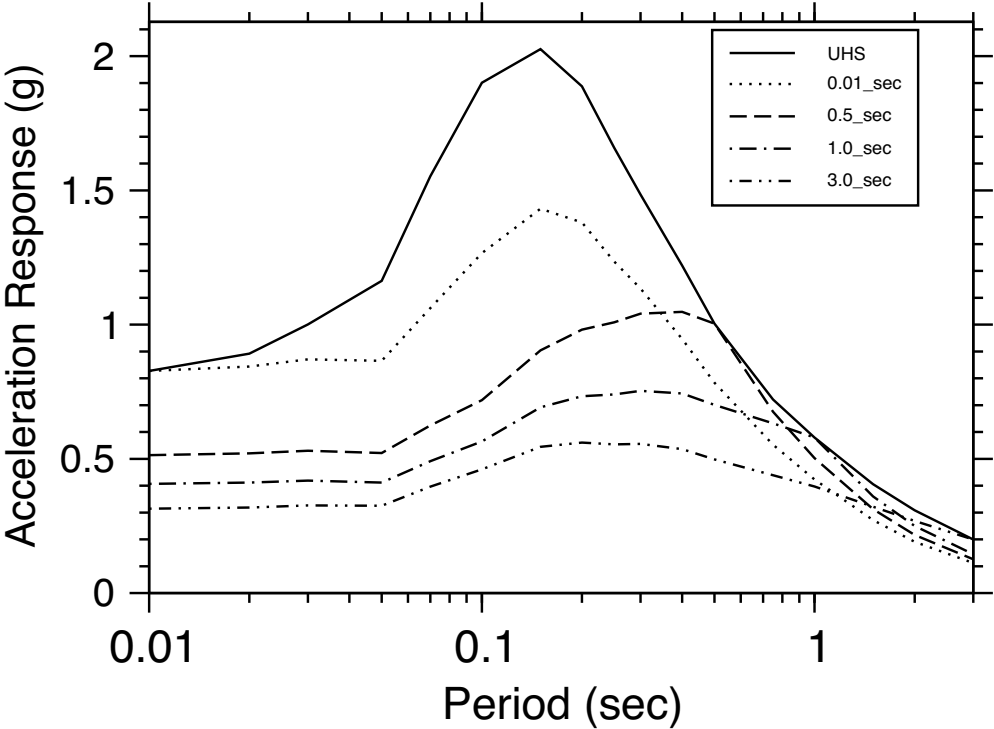
Interface, 5000 yrs



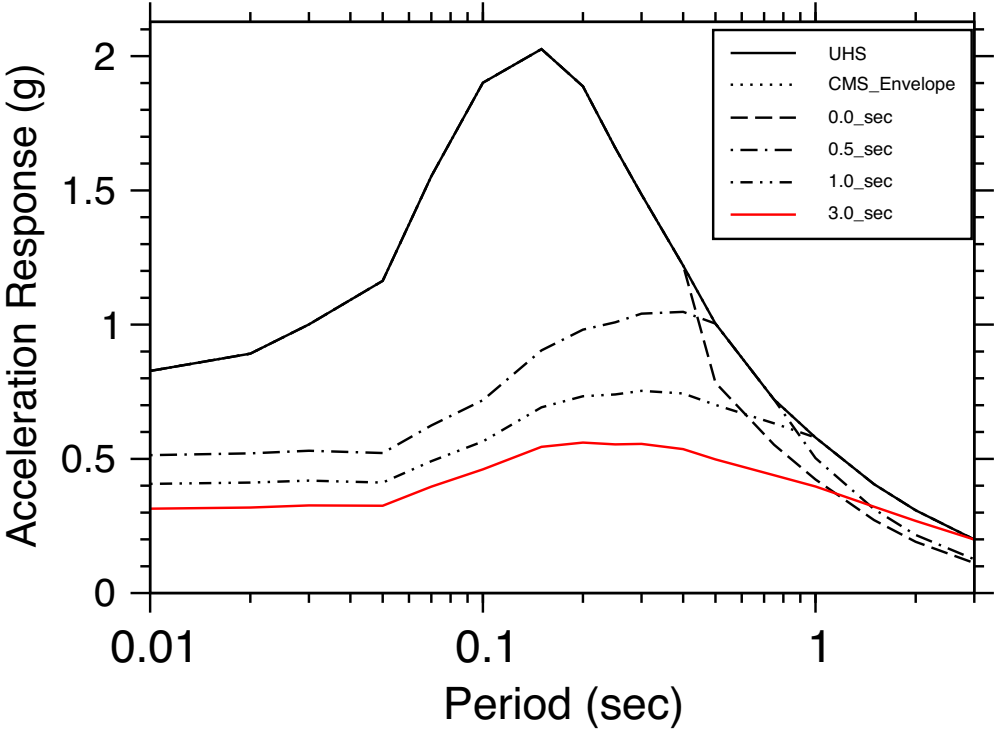
Interface, 5000 yrs



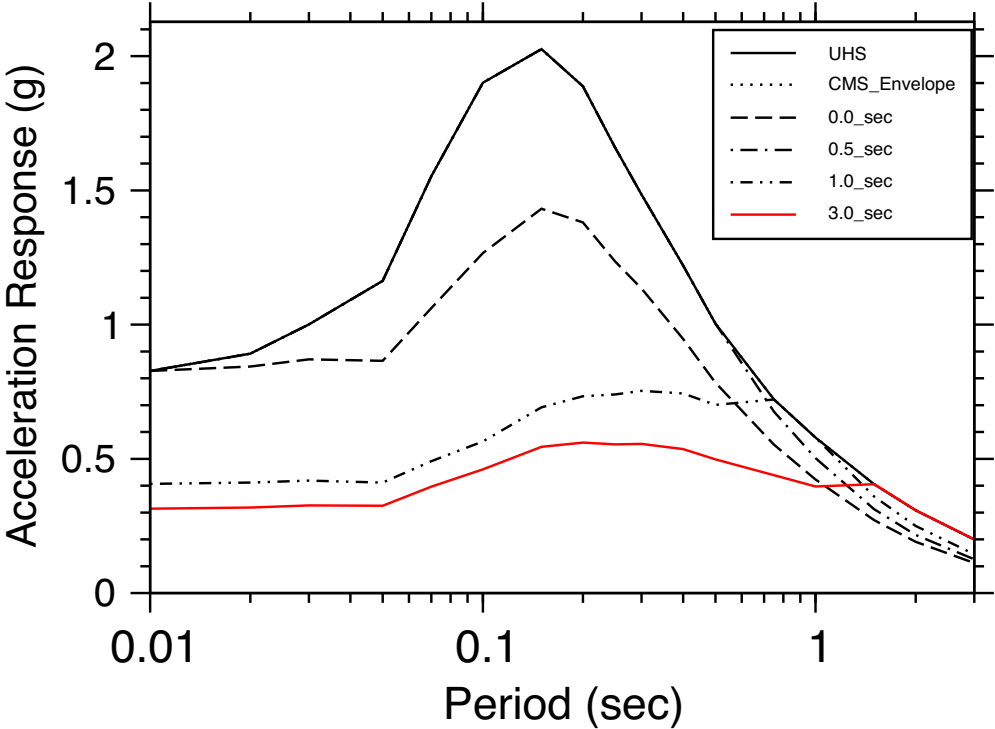
Interface, 10000 yrs



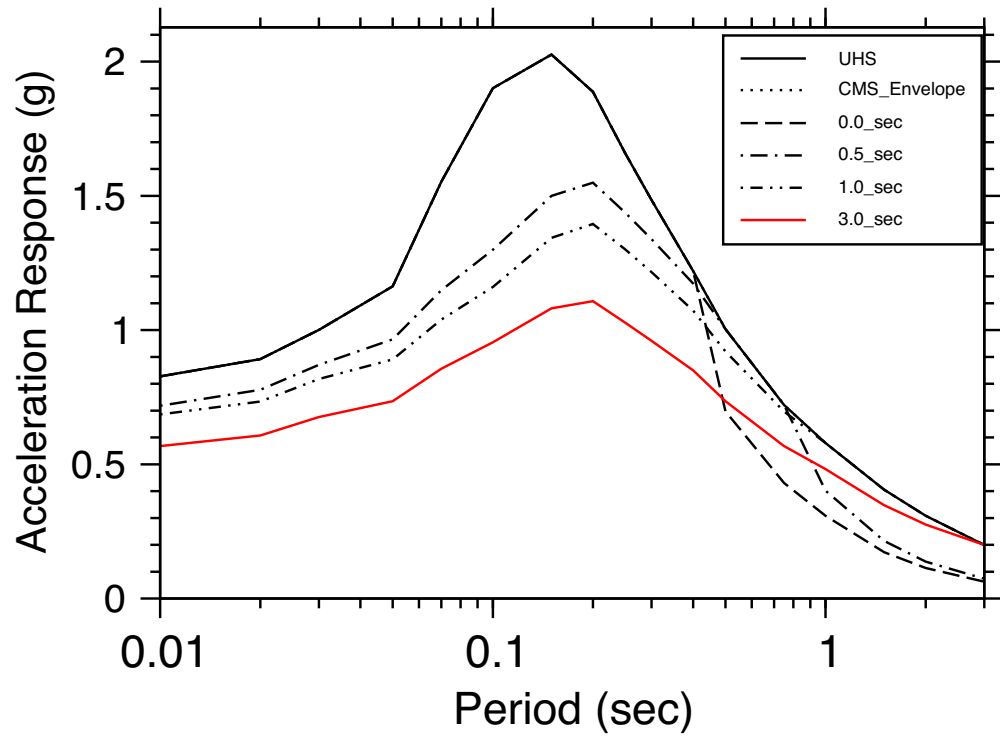
Interface, 10000 yrs



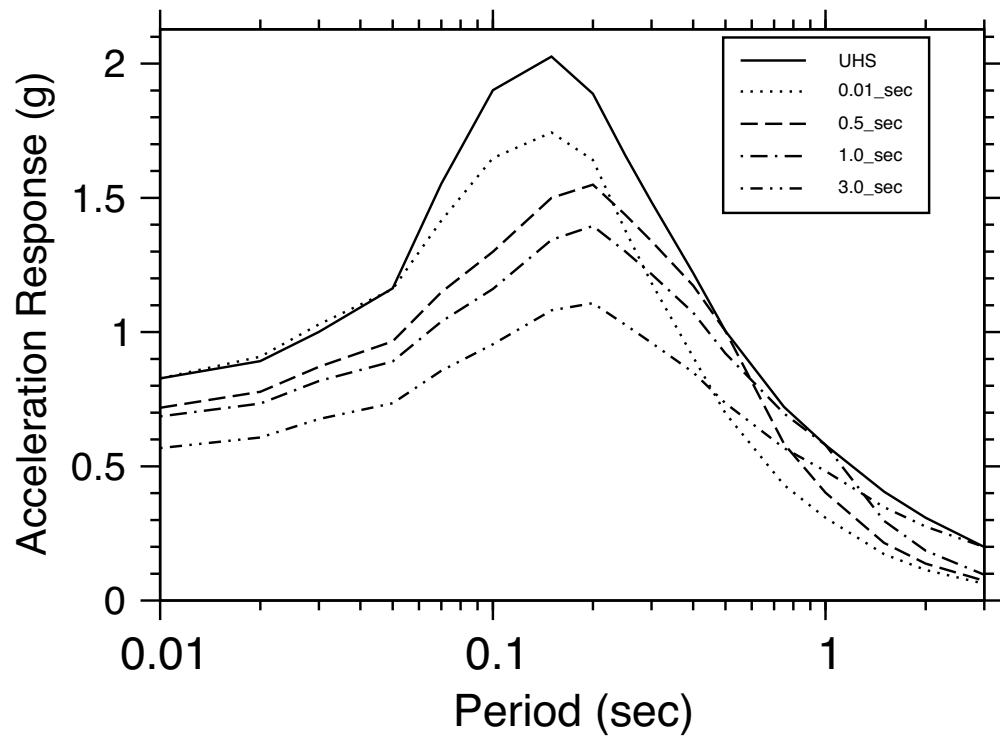
Interface, 10000 yrs



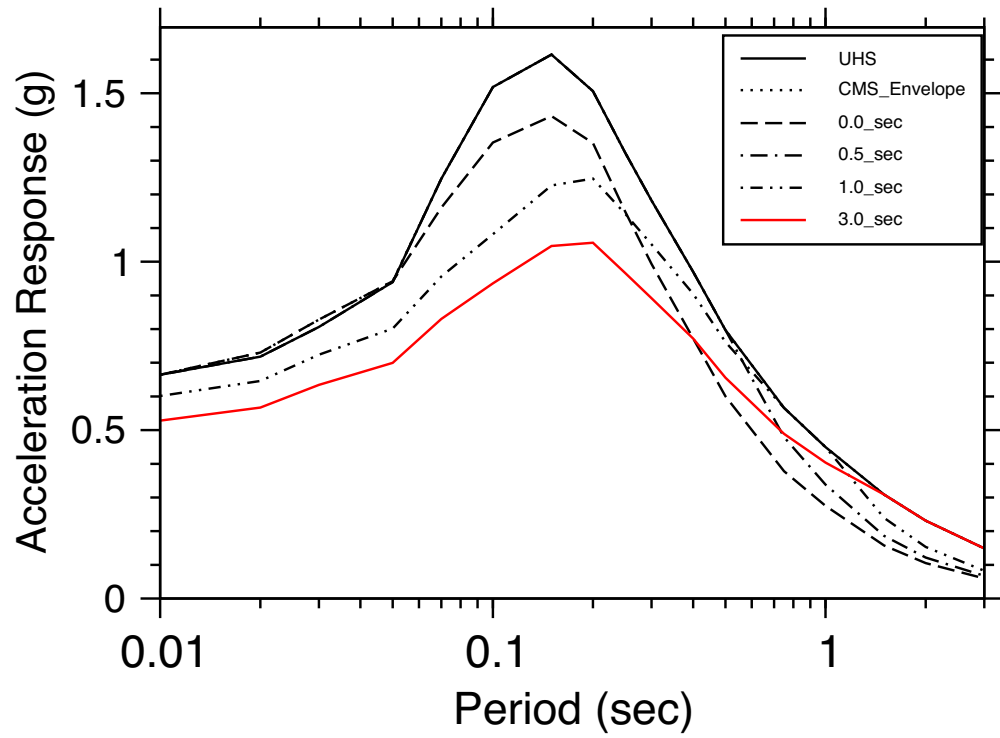
Intraslab, 10000 yrs



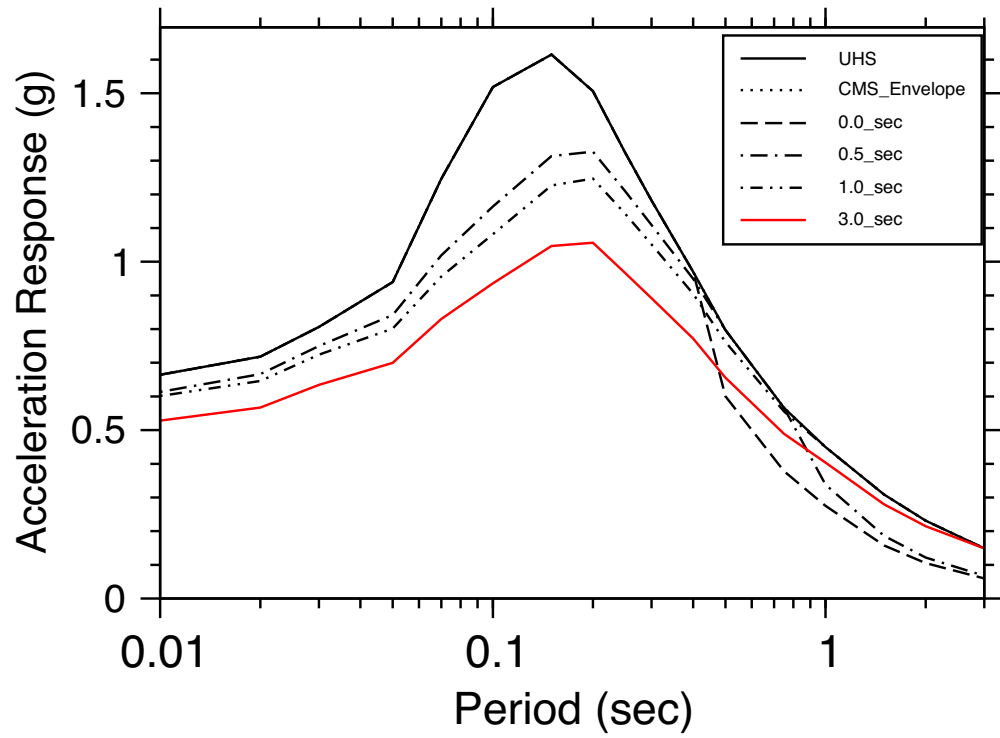
Intraslab, 10000 yrs



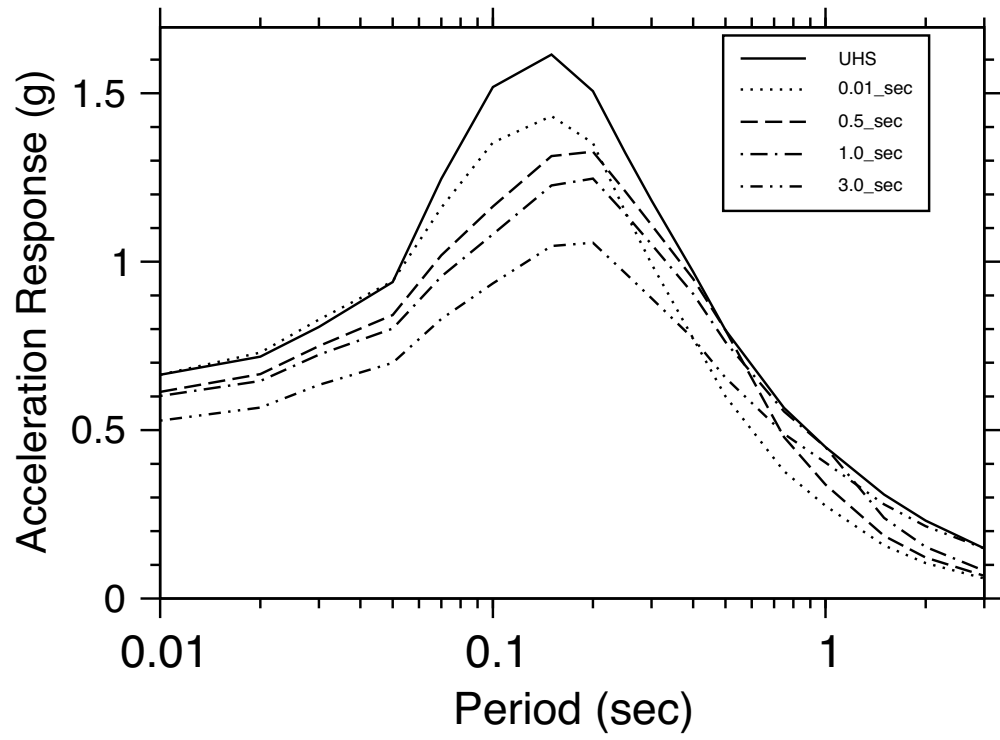
Intraslab, 5000 yrs



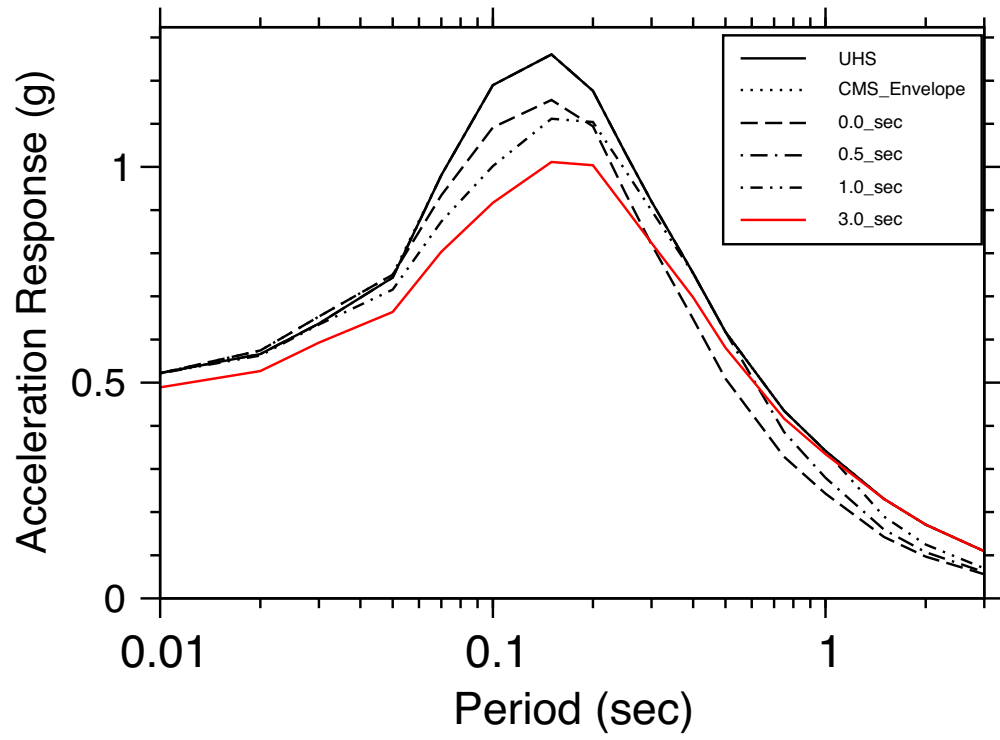
Intraslab, 5000 yrs



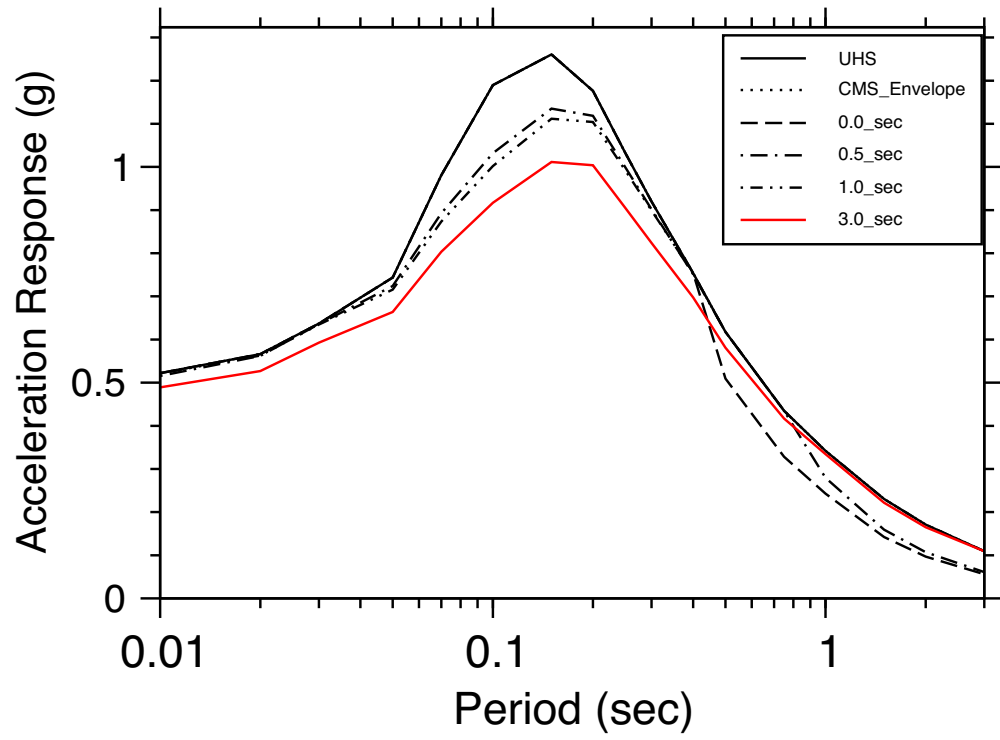
Intraslab, 5000 yrs



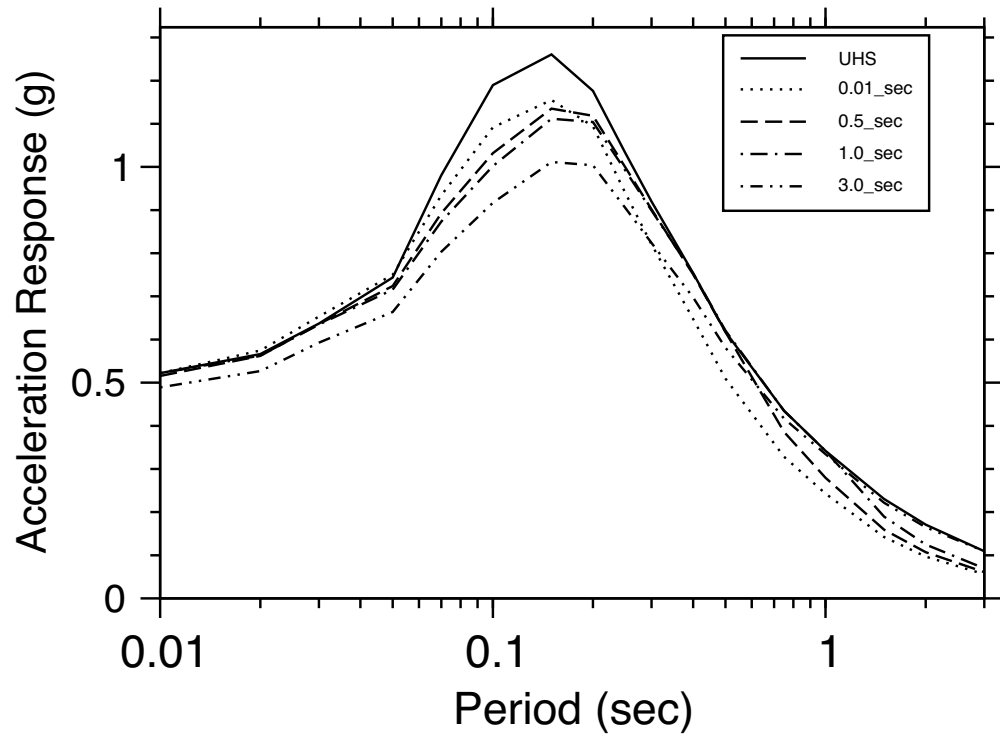
Intraslab, 2500 yrs



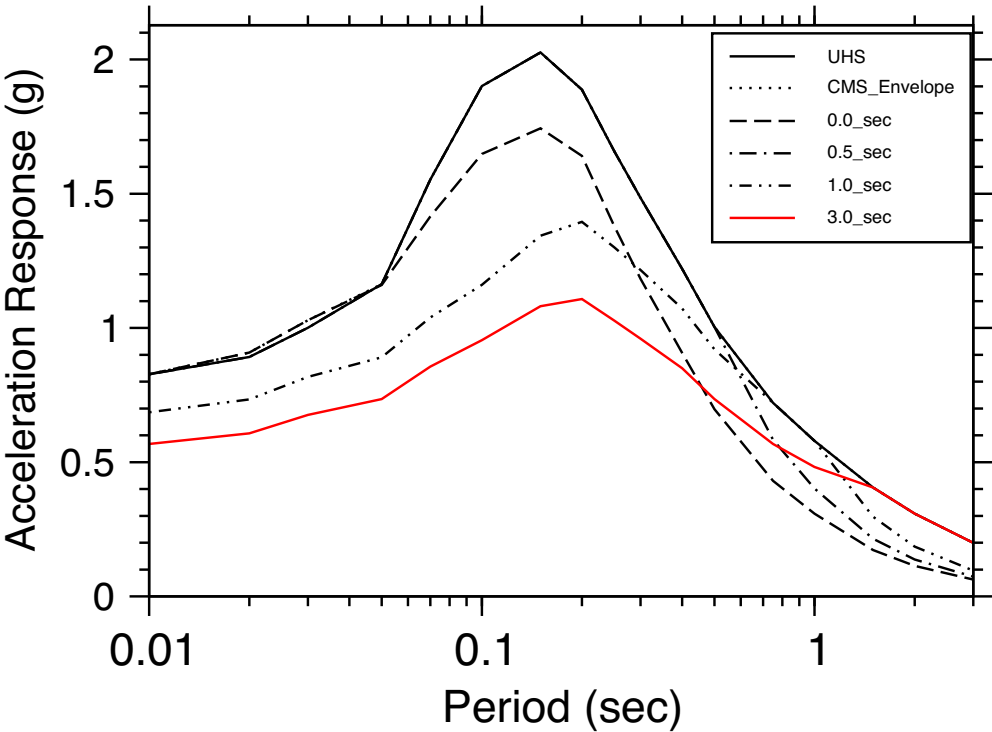
Intraslab, 2500 yrs



Intraslab, 2500 yrs



Intraslab, 10000 yrs



Appendix D – MERCALLI EARTHQUAKE INTENSITY SCALE

Cover Page

Mercalli Earthquake Intensity Scale¹

Value Description of shaking severity

I Not felt

II Felt by people sitting or on upper floors of buildings.

III Felt by almost all indoors. Hanging objects swing. Vibration like passing of light trucks. May not be recognized as an earthquake.

IV Vibration felt like passing of heavy trucks. Stopped cars rock. Hanging objects swing. Windows, dishes, doors rattle. Glasses clink. In the upper range of IV, wooden walls and frames creak.

V Felt outdoors. Sleepers wakened. Liquids disturbed, some spilled. Small unstable objects displaced or upset. Doors swing. Pictures move. Pendulum clocks stop.

VI Felt by all. People walk unsteadily. Many frightened. Windows crack. Dishes, glassware, knickknacks, and books fall off shelves. Pictures off walls. Furniture moved or overturned. Weak plaster, adobe buildings, and some poorly built masonry buildings cracked. Trees and bushes shake visibly.

VII Difficult to stand or walk. Noticed by drivers of cars. Furniture broken. Damage to poorly built masonry buildings. Weak chimneys broken at roof line. Fall of plaster, loose bricks, stones, tiles, cornices, unbraced parapets and porches. Some cracks in better masonry buildings. Waves on ponds.

VIII Steering of cars affected. Extensive damage to unreinforced masonry buildings, including partial collapse. Fall of some masonry walls. Twisting, falling of chimneys and monuments. Wood-frame houses moved on foundations if not bolted; loose partition walls thrown out. Tree branches broken.

¹ Descriptions are shortened from: Richter, C.F., 1958. Elementary Seismology. W.H. Freeman and Company, San Francisco, pp. 135-149; 650-653. <http://quake.abag.ca.gov/shaking/mmi/>

IX General panic. Damage to masonry buildings ranges from collapse to serious damage unless modern design. Wood-frame structures rack, and, if not bolted, shifted off foundations. Underground pipes broken.

X Poorly built structures destroyed with their foundations. Even some well-built wooden structures and bridges heavily damaged and needing replacement. Water thrown on banks of canals, rivers, lakes, etc.

XI Rails bent greatly. Underground pipelines completely out of service.

XII Damage nearly total. Large rock masses displaced. Lines of sight and level distorted. Objects thrown into the air.